Apoptosis as a mechanism in tri-n-butyltin mediated thymocyte cytotoxicity

Mark Raffray

Submitted to the University of London
for examination for the degree of Doctor of Philosophy
1994

Toxicology Department, The School of Pharmacy,
University of London, Brunswick Square,
London WC1N 1AX

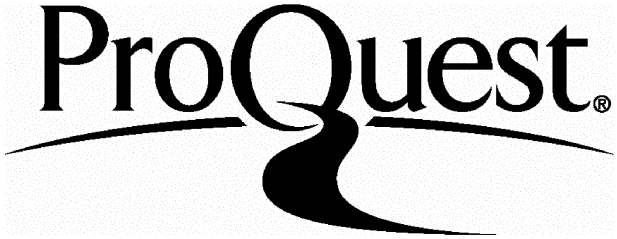

ABSTRACT

Tri-n-butyltin (TBT), an important environmental pollutant, is immunotoxic when administered to experimental animals. Thymic atrophy due to the depletion of cortical thymocytes has been shown to be central to this effect although the mechanism involved is currently undefined. The mode of cell death known as apoptosis has a key role in a number of physiological processes, including the regulation of the developing thymic T lymphocyte repertoire, but can also be triggered in pathological states including toxic injury. This study investigated the effects of bis(tri-n-butyltin) oxide (TBTO) on rat thymocytes and compared these findings to observations with other lymphotoxic model compounds.

Exposure of thymocytes in vitro to low concentrations of TBTO resulted in delayed cell killing which bore many of the morphological and biochemical characteristics of apoptosis. Stereotypical internucleosomal DNA cleavage preceded viability loss and both these processes were inhibited by intracellular Ca^{2+} chelators, zinc, and agents expected to interfere with protein-DNA interactions. At tributyltin treatment levels less than an order of magnitude higher, cytolethality by necrosis supervened.

In contrast to thymocyte apoptosis caused by most other stimuli including glucocorticoids, that mediated by TBTO apparently did not require *de novo* protein synthesis. Thymocytes exposed to TBTO remained able to instigate apoptotic death although their ATP levels were severely depressed, indicating that the process was not dependent on fully conserved cellular energetics function. In common with the microtubule assembly inhibitor nocodazole, tributyltin was very effective in disrupting the cellular microtubule cytoskeleton. Though there was evidence that this effect may have been causal to nocodazole-mediated thymocyte apoptosis, a similar relationship was not apparent for TBTO. Apoptosis caused by TBTO was associated with nuclear hypodiploidy, but no overt disturbance of thymocyte cell cycle parameters occurred.

In vivo studies indicated that thymocyte apoptosis contributed significantly to the cortical thymocyte deletion underlying the thymic involution provoked by administration of TBTO to immature rats.

ACKNOWLEDGEMENTS

This thesis is dedicated to Linda. Her love, patience and encouragement buoyed me up when a planned 'n=3' sometimes developed into 'n=33'. Luckily, her sense of humour outlasted my Invisible Man impersonations.

I am genuinely indebted to the many people who encouraged and assisted me during the course of this work. As a 'part-timer', I must sometimes have seemed a rather furtive figure, which given the nature of the process I was observing, may not have been entirely inappropriate: Now you see me....now you don't! Thanks are due to many people, but especially to the following:

- Dr Gerry Cohen, my supervisor, for having sufficient faith to let me get started in the first place, and particularly for the way he always made time to enthusiastically discuss the latest riveting finding or hot new paper (sadly, these originated mainly from researchers other than myself)
- Particularly to David McCarthy for microscopy sample processing, expert microscopy involvements, and photography
- Adrian Rodgers, whose encyclopaedic technical knowledge opened up new approaches and fixed the 'unfixable'
- Fellow 'partners in crime' Adrian K, Mike, Winston, Jane, Cathy, Andy J, Phil, Michelle, Simon, Ruth, Vitor et al.; I shall miss the scientific 'tea' club on Friday evenings. Surely you can't be serious!
- Professor Andrew Wyllie and Dr Andre Penninks for making the subject area so magnetic during early discussions, and for strategic advice
- Dr. Andreas Kortenkamp for further sage advice, and for not boasting about how much better his electrophoresis kit was than mine!
- Roger Snowden of the MRC Toxicology Unit
- Dr. Alan Crowe of the International Tin Research Institute

- Finally to my parents, Jean and Raff, for their selfless devotion to the education of their three children, and for their wisdom and support whenever storm clouds gathered.

- The ninth visitor is life.
- The tenth visitor
  Is not usually named.

Charles Causley.

"The thymocyte, you see, is a large, ugly mystery to us. If you've ever studied thymocytes you'll know what I mean! We're pretty sure today that the thymocyte exists, and we have a fairly good idea of what it does whenever it's doing whatever it's supposed to be doing. Beyond that, we're really in the dark."

With profuse apologies to Joseph Heller's Catch 22.

CONTENTS

ABBREVIATIONS

A23187	Cation ionophore A23187; calcimycin
ACTH	Adrenocorticotrophic hormone
AO	Acridine orange; 3,6-bis(dimethylamino)acridine hydrochloride
ATA	Aurintricarboxylic acid
ATP	Adenosine triphosphate
BAPTA-AM	1,2-bis(2-aminophenoxy)ethane-N,N,N',N'-tetraacetoxymethyl ester
B cell	Bone marrow derived lymphocyte
bp; kbp	Base pairs; kilobase pairs
$[Ca^{2+}]_i$	Intracellular free calcium ion concentration
CaM	Calmodulin
cAMP	Adenosine 3':5'-cyclic monophosphate
CD	Cluster of differentiation
CsA	Cyclosporin A
CTL	Cytotoxic T lymphocyte
CyH	Cycloheximide
Da, kDa	Dalton, kiloDalton
DAG	1,2-diacylglycerol
DBT/C	Di-n-butyltin/Di-n-butyltin dichloride
DMEM	Dulbecco's modified Eagle's medium
DMSO	Dimethyl sulphoxide
DNase	Deoxyribonuclease
D_V	Cell density (viable)
EDTA	Ethylenediaminetetraacetic acid
EGTA	Ethylene glycol-bis-(β-aminoethyl)-N,N,N',N'-tetraacetic acid
FCCP	Carbonyl cyanide p-(trifluoromethoxy)-phenylhydrazone
FITC	Fluorescein isothiocyanate
FSC	Forward light scatter
GTP	Guanosine triphosphate
h	hour/hours
H33342	Hoescht 33342; 2'-(4-ethoxyphenyl)-5-(4-methyl-1-piperazinyl)-2',5'-bi-1H-benzimidazole trihydrochloride
H33258	Hoescht 33258; 2'-(4-hydroxyphenyl)-5-(4-methyl-1-piperizinyl)-2,5'-bi-1H-benzimidazole trihydrochloride
HEPES	N-(2-hydroxyethyl)piperazine-N'-(2-ethanesulphonic acid)
IC_{50}	Median inhibitory concentration
Ig	Immunoglobulin
IL	Interleukin
InP_3	Inositol 1,4,5-triphosphate

i.v.	Intravenous
K*i*	Inhibitor constant
KH	Krebs Henseleit buffer
MAb	Monoclonal antibody
MHC	Major histocompatibility complex
MPc	Mononuclear phagocyte/phagocytic cell(s)
MPS	Methylprednisolone (hemisuccinate sodium salt)
MT	Microtubule(s)
MTOC	Microtubule organising centre
ND	Not determined
NK	Natural killer
PBS	Phosphate buffered saline
PCA	Perchloric acid
PDBu	Phorbol 12,13-dibutyrate
PKA	Protein kinase A
PKC	Protein kinase C
p.o.	Oral
P_{ow}	Partition coefficient (n-octanol : water)
Quin 2/Quin-2 AM	2-[(2-amino-5-methylphenoxy)methyl]-6-methoxy-8-aminoquinoline; N,N,N',N'-tetraacetoxymethyl ester of Quin-2
RCF	Relative centrifugal field
RPMI-1640	RPMI-1640 medium (*i.q.* Roswell Park Memorial Institute)
RNase	Ribonuclease
SE	Standard error (of the mean)
t½	Half-time
T cell	Thymus-derived lymphocyte
TBE	Tris/borate/EDTA buffer
TBTO	Bis(tri-n-butyltin) oxide
TCA	Trichloroacetic acid
TCDD	2,3,7,8-tetrachlorodibenzo-p-dioxin
TcR	T cell receptor
TE	Tris/EDTA buffer
TEM	Transmission electron microscopy
TF	Transcription factor, e.g. TF-AT (TF-activated T cells)
TGF	Transforming growth factor
T(M/E/P/B/O/Ph)T[C]	Tri(methyl/ethyl/-n-propyl/-n-butyl/-n-octyl/phenyl)tin [chloride]
TNF	Tumour necrosis factor
TPA	12-O-tetradecanoylphorbol-13-acetate
UV	ultraviolet

CHAPTER 1
INTRODUCTION

1.1 INTRODUCTION

1.1.1 Modes of cell death

The first cell death mode to be characterised in detail was necrosis (Majno et al., 1960). Many pathology texts have focused on the morphological identification of necrotic cells by their nuclear pyknosis, karyorrhexis or karyolysis, associated with cytoplasmic eosinophilia, and demarcation of the affected tissue by a zone of acute reactive inflammation (Glaister, 1986). This death mode is primarily invoked not by factors intrinsic to the cell itself, but by traumatic environmental perturbation, which must be severe, leading to rapid incapacitation of key cellular functions (ion regulation, energetics, and biosynthesis) and resulting in collapse of internal homeostasis (Trump and Berezesky, 1984). The ultrastructural appearances of necrosis can be summarised as organelle swelling, membrane breakdown, eventual lysosomal involvement and subsequent cellular disintegration (Trump et al., 1981).

Quite separately, cell death was being considered in the apparently specialised context of vertebrate and invertebrate development by researchers such as Glucksmann (1951) and Saunders (1966). They recognised that cell death in normal tissues during multicellular animal ontogeny was a highly conserved biologically universal phenomenon. Glucksmann classified developmental cell death in terms of its usefulness to the developing organism, and Saunders extended this into the notion that such patterns of cell death are programmed as normal morphogenetic events in development. The concept of 'programmed cell death' (Lockshin and Beaulaton, 1974), also referred to synonomously as 'physiological cell death', emerged from the recognition that an intrinsic, active cellular process was involved, which could be thought of as a program for self-destruction. Studies of developmental death in systems such as the nematode *Caenorhabditis elegans* have shown that gene expression is a vital facet of this form of cell deletion (Ellis et al., 1991).

Kerr (1965) described two morphologically distinct forms of cell death in liver injury following portal vein branch ligation. Patches of confluent necrosis were seen at early stages, whilst over the succeeding period of weeks the periportal parenchyma shrank. During this parenchymal regression hepatocytes were continually deleted on an individual basis by a process which involved rounding up of cells, detachment from their neighbours, and formation of residual bodies often containing condensed chromatin. Their histological form differed from necrotic cells, and no intracellular release of lysosomal enzymes or contingent inflammatory response accompanied this scattered cell death. In 1971, the same author described the ultrastructure of this process, which he named 'shrinkage necrosis', and determined that it was predominantly marked by cellular contraction and fragmentation into membrane-bounded bodies containing crowded but structurally preserved organelles, and condensed nuclear remnants. The term 'apoptosis' * was coined a year later in a

* From the Greek word (αποπτωσισ) meaning dropping off, or falling off of petals from flowers or leaves from trees.

landmark paper by Kerr, Wyllie and Currie (1972). They described this death mode in terms of a basic biological phenomenon of controlled cell deletion, with a complimentary and opposite role to mitosis in the regulation of animal cell populations of vertebrates and invertebrates. In contrast to necrosis, it was postulated that apoptosis was an active process involving an internal biochemical cascade leading to death, and that it occurred naturally. Furthermore, these authors considered it to be of pivotal importance in the regulation of cell numbers in ontogenesis, normal tissue homeostasis, and in abnormal processes including neoplasia and mild extrinsic noxious stimuli. This work formed the basis for an entirely new perspective on cell death, which has subsequently been extended by many investigators (see reviews by Wyllie et al., 1980; Searle et al., 1982; Duvall and Wyllie, 1986; Gerschenson and Rotello, 1992; Raff, 1992; Hickman, 1992). It is now evident that necrosis and apoptosis are totally distinct, and do not form part of a continuum of lethal change (Wyllie et al., 1984b). Except in the case of 'secondary necrosis' as a terminal apoptotic change, there is no essential overlap in morphology (Kerr and Harmon, 1991). The molecular mechanisms underlying apoptosis are the subject of vigorous debate and research, but it is quite clear that it is an active process relying on conserved biochemical pathways, which also serves to distinguish it from necrosis (Arends and Wyllie, 1991; Trump and Berezesky, 1992; Cohen, 1993). However, no single molecular biology characteristic unambiguously defines its appearance in all vertebrate cells. The physiological ancestry of apoptosis also explains why the sequelae of the process differ from necrotic death, since the former must function to remove unwanted cells in the midst of valuable neighbours with little disturbance.

Programmed cell death (developmental cell death) is similar to apoptosis in terms of its cell and molecular biology (Lockshin and Zakeri-Milovanovic, 1984), though recently a case has been made that there are sufficient operational and other differences to require that it be separately defined (Lockshin and Zakeri, 1991) in terms of character and nomenclature from apoptosis (Alles et al., 1991). Whilst this premise remains somewhat controversial, and stems mainly from an operational definition for programmed cell death versus a morphological and biochemical description of apoptosis, the distinction has been adopted throughout this thesis. Table 1.1 outlines some salient characteristics that distinguish programmed cell death, apoptosis and necrosis, which are expanded upon in later sections.

More obscure forms of cell death have been described mainly in terms of histological appearance. 'Dark cell' or 'type B dark cell' death involves metabolically inert single cells that show cytoplasmic electron density, mitochondrial swelling and essentially normal nuclear morphology (Hume, 1987; Wyllie, 1987a). Other death modes, perhaps including ghost cells, colloid bodies and extreme terminal differentiation may also exist, but it is difficult to interpret where these forms lie in the spectrum of reproductive death, metabolic incapacity and lethal change.

Characteristic	Programmed cell death	Apoptosis	Necrosis
Occurrence	Single cells, may involve synchronous waves of PCD	Single cells, normally asynchronous	Groups of contiguous cells in tissues
Causation	Developmental stimuli	Apoptotic factors, loss of trophic stimuli, mild injury	Severe injury
Reversibility	Not after program is initiated ?	Not after morphological changes ?	At early stages (up to 'point of no return')
Biochemical nature	Active, gene expression	Active, gene expression at least for priming events	Homeostasis failure, biosynthesis cessation
RNA/protein synthesis	Death blocked by inhibitors	Death sometimes blocked by inhibitors	Not involved
Nuclear biochemical change	No internucleosomal DNA ladders	High order/internucleosomal DNA cleavage often present as early event	Non-specific degradation of DNA
Ion homeostasis/energetics	Conserved	Conserved	Failure of ion homeostasis, energetics crisis
Morphology	Cellular condensation, fragmentation	Cellular condensation, fragmentation	Lysis
Nucleus	Often early chromatin condensation, nuclear fragmentation	Early chromatin condensation, nuclear fragmentation, nucleolar dispersal	Chromatin flocculation, dissolution when nuclear membrane lost, nucleolus only lost at late stages
Cytoplasm	Contraction	Contraction	Swelling
Membranes	Conserved until late stage	Conserved until late stage	Rupture of organelle and plasma membranes
Mitochondria	Specific wave of autophagocytosis	Structure and function unaffected	High amplitude swelling, flux densities
Lysosomes	Often involved, controlled	Unaffected	Involved, uncontrolled
Fate of cell remnants	Autophagy common	Apoptotic bodies rapidly ingested by macrophages or surrounding cells	Significant persistence, gradual dissolution or engulfment by phagocytes
Reactive inflammation	Absent	Absent	Normally present, neutrophil infiltration

TABLE 1.1 Operational, functional and morphological characteristics of programmed cell death, apoptosis and necrosis.

PCD = programmed cell death. For references see sections 1.1 - 1.3.

1.1.2 Necrosis

To appreciate the distinction between necrotic and apoptotic cell death it is necessary to overview some salient features of the former, though an extensive treatise is beyond the scope of this thesis. Necrosis refers to the morphological and biochemical state most often seen when cells die from severe and sudden injury, such as ischaemia, sustained hyperthermia, complement cytolysis or marked toxicity (Majno et al., 1960). It is sometimes termed 'accidental cell death'. Detailed staging of events in necrosis has been attempted (Trump and Berezesky, 1984), but these essentially resolve into a reversible phase before a 'point of no return', and a subsequent irreversible phase involving total loss of structure and function, i.e. cell death.

The ultrastructural sequence and allied biochemical alterations of necrosis have been intensively studied (the following summarises reviews by Trump et al., 1981, and Trump and Berezesky, 1984; 1992). Early reversible cellular changes following injury include generalised and organellar swelling (hydropic change) as ATP levels fall and plasma membrane ion translocase activity declines; this results in movement of Na^+, K^+, Mg^{2+} and Ca^{2+} down their respective concentration gradients, with concomitant uptake and intracellular redistribution of water. Alternatively plasmalemmal injury can occur directly, as in the case of complement attack. There is cytoplasmic bleb formation probably due to Ca^{2+}-mediated cytoskeletal alterations (Orrenius et al., 1989), chromatin clumping, dilatation of the endoplasmic reticulum, ribosomal dispersal and minor mitochondrial alterations. Biosynthetic activity diminishes with progressive rapidity. The transition across the 'point of no return' is marked by abrupt high amplitude mitochondrial swelling with irretrievable loss of inner membrane function, and the deposition of stereotypic floccular and crystalline matrix densities. A syndrome of terminal changes develops with leakage of damaging lysosomal hydrolases, obvious focal discontinuities in the plasma membrane, total disorganisation of cytoplasmic organelles, nuclear breakdown, karyolysis and cell rupture. There is accompanying rapid digestion of cellular macromolecules as evidenced by increases in free fatty acids, amino acids and inorganic phosphate. Spillage of cellular contents elicits an exudative inflammatory change and infiltrating neutrophils eventually clear the dead cells. Some investigators consider massive Ca^{2+} overload and consequent downstream degradative processes to be fundamental to the initiation and outcome of this mode of cell death (Nicotera et al., 1992). Although uncontrolled cellular entry of Ca^{2+} is clearly important in necrosis, a causal relationship has often been disputed (Lemasters et al., 1987; Hardwick et al., 1992).

Several characteristics provide counterpoints and contrasts with apoptosis (see also Table 1.1). Necrosis invariably results from stimuli causing gross perturbation of the cellular environment and severe cellular injury; there is very little evidence that it has a role in physiologically normal conditions (Wyllie, 1981). As a histological phenomenon it is

normally conspicuous, involving groups of cells and is long-lasting (Hume, 1987). Necrosis does not require genetic control or synthetic activity for its initiation or progression (Arends and Wyllie, 1991), rather it is a failure of homeostasis with cessation of biosynthetic activity. The plasma membrane is an early critical site of damage and dysfunction (Lemasters et al., 1987), pivotal to the cell's progressive loss of ability to translocate ions and osmoregulate, leading to gross swelling and rupture. Many methods used to monitor necrotic death depend on this loss of membrane integrity (Bowen, 1981). Necrotic cells swell rather than shrink, and cytoplasmic blebs do not separate, but either regress or burst. Organelles undergo severe structural and functional alterations coincident with the irreversible phase. The action of degradative enzymes in necrosis is wide-scale and non-specific, e.g. DNA breakdown is random and has no discernible pattern when visualised by gel electrophoresis (Kerr and Harmon, 1991). Due to the involvement of large contiguous regions of cells, inflammation is invariably provoked in necrotic tissue, and is required to ensure effective removal of debris and allow repair. The neighbouring viable cells play essentially no part in this clearance process; which is primarily the function of phagocytic neutrophil polymorphs. As will become clear from the following accounts, the cell biology of apoptosis is radically different from necrosis.

1.1.3 Cardinal operational aspects of apoptosis

Apoptosis represents a death mode capable of selective deletion of cells in the midst of living tissue. It is normally evoked in an asynchronous fashion in single cells and is therefore relatively inconspicuous (Searle et al., 1982). Cell injury is not a prerequisite for activation of the internal cellular death program, since normal mammalian cell proliferation is balanced by cell death via apoptosis (Kerr and Harmon, 1991). In broad terms, the nature and sequence of morphological changes in apoptotic cells, and major facets of its molecular biology show marked consistency in cells of widely differing lineage and different species (Wyllie, 1981; Bursch et al., 1990a). Particularly when considered in parallel with programmed cell death, it has come to be regarded as a phylogenetically ancient process involving a conserved set of genes with equivalent functions (Tomei, 1991). Differential cellular susceptibility to apoptosis commonly relates to pre-priming for this death mode (Arends and Wyllie, 1991), as is seen for thymocytes, spermatogonia or intestinal epithelia. Whereas, when present, selectivity in necrotic killing appears to relate mainly to the locus of action of lethal stimuli.

A central tenet of apoptosis, contrasting with necrosis, is its active biochemical nature. This involves the concepts of maintenance of cellular control over the process, and the participation by the cell in its own death (Cotter et al., 1990; Waring et al., 1991). The control cascade begins at the level of gene regulation (*induction* stages), with subsequent intracellular signal transduction, resulting finally in activation of *effector* mechanisms (Cohen, 1993). Due to their active biochemical nature, almost all forms of programmed

cell death, and many instances of apoptosis involve induced macromolecular synthesis (Bowen and Bowen, 1990), whereas uncontrolled loss of homeostasis and synthetic activity are evident during necrosis. Control of apoptosis at a unitary cellular level provides the opportunity for hierarchical regulation at a tissue level as a normal physiological process (Kerr et al., 1972; Raff, 1992).

Diagnostically significant markers which distinguish apoptosis from necrosis are manifold. Early cardinal nuclear morphological changes (Arends et al., 1990; Oberhammer et al., 1993a), are preceded or paralleled by the degradation of nuclear DNA, in some cases typified by endonucleolytic internucleosomal DNA cleavage, leading to characteristic oligonucleosomal fragment patterns (Wyllie 1980; Skalka et al., 1976). Membrane integrity is maintained until endstage changes, and the functionally intact membranes continue to exclude vital dyes (Bachvaroff et al., 1977; Barry and Eastman, 1993). Cellular shrinkage and density increase (Klassen et al., 1993) differentiate apoptotic death from the hydropic swelling which typifies necrosis. Perhaps even more fundamental idiotypical markers of apoptosis are events commencing with cellular fragmentation into viable apoptotic bodies, and changes in cell surface molecules culminating in phagocytic clearance of residual apoptotic bodies by macrophages or neighbouring cells (Wyllie et al., 1984b).

Unlike necrosis, apoptosis involves an occult stage ranging from minutes to days where cells prepare the machinery for their deletion, though the core of the process proceeds by a rapid sequence of events (Bursch et al., 1992a). Since the objective of apoptosis is controlled cell deletion without undue disturbance, there is no histological persistence reminiscent of necrosis—apoptotic cell remnants are rapidly removed, and reactive inflammation never ensues (Kerr et al., 1987).

Sections 1.2 and 1.3 describe in detail the morphology and molecular biology of apoptosis.

1.1.4 Programmed cell death

Programmed cell death as a descriptor has been used interchangeably and synonomously with apoptosis in considerations of active cell death modes distinct from necrosis. Cellular contraction, chromatin condensation, phagocytosis of cellular remnants, and failure to elicit an inflammatory response are characteristics of apoptotic cells which are commonly associated with death in developmental situations. Therefore, based on ultrastructural observations some investigators have considered it to be morphologically identical (Wyllie et al., 1980), though this has been challenged (Lockshin and Zakeri, 1991), and it is perhaps more appropriate to reserve the term for deliberate deletional death in developmental morphogenesis. For example, during vertebrate nervous system construction three forms of cellular death have been identified (Server and Mobley, 1991). Type 1 involves nuclear collapse with cell fragmentation, and is equivalent to apoptosis.

Type 2 death is characterised by the involvement of numerous autophagic vacuoles in the absence of early overt nuclear change. Cytoplasmic compartment alterations also predominate in type 3 deletion with moderate swelling of organelles, mitochondrial damage, and heterophagocytosis of affected neurones. The morphological changes seen in dying cells in planaria species are also idiomorphically different from apoptosis, with vast vacuoles visible in the nucleus and cytoplasm and early membrane breakdown (Bowen, 1981). Death in the *C.elegans* system is typified by membrane whorling and autophagy present with nuclear condensation, though some non-degenerate cells are 'murdered' by phagocytes (Ellis et al., 1991).

The accumulated knowledge from many studies of programmed cell death have allowed the definition of several broadly applicable features (drawn from reviews by Saunders, 1966; Lockshin and Beaulaton, 1974; Bowen and Bowen, 1990; Lockshin and Zakeri, 1991). It occurs during development of multicellular eukaryotic organisms, and operates on a controlled basis to precise time schedules deleting only select groups of cells. The affected cells require a positive stimulus to engage the self-destruction sequence. In *C.elegans*, the only well understood system, fourteen genes have so far been identified in the genetic pathway, of which the *ced-3* and *ced-4* members seem most pivotal (Yuan et al., 1993). Death is often triggered or prevented by cell-cell signalling via hormones or cytokines (Lockshin and Zakeri-Milovanovic, 1984). Thus it has been shown that 'scheduled' death in embryonic systems can be abrogated by culturing explants of cells predestined for elimination with tissues from a different part of the organism. Activation of the intracellular program requires de novo synthesis of mRNA and protein. There are marked increases in specific and total activities of various acid hydrolases in the dying cells. The process is not necessarily associated with activation of endonucleases, especially those producing the internucleosomal DNA fragmentation often typical of apoptosis. This is borne out by the secondary action of the NUC-1 endonuclease in C.elegans, since *nuc-1* gene mutants still undergo cell death and engulfment but the condensed nuclei are not degraded (Ellis et al., 1991).

It seems probable that the mechanisms involved in developmental cell death are conserved within cells to function in whole or part during later life. What is currently unclear is the degree of overlap with death occurring physiologically in the homeostasis of formed tissues, and accidental apoptotic cell killing. Whether this question resolves into merely a case of semantics, or distinct biological differences awaits future investigations.

1.1.5 The incidence of apoptosis and programmed cell death

The plethora of publications implicating these mechanisms in many physiological or pathological situations, make it impossible to give a complete account of their incidence. The approach taken here is to illustrate major biological systems and processes.

Embryonic development and metamorphosis

Programmed cell death, either focal in nature, or massive synchronised waves, has a vital role in the morphogenesis of tissues and organs, the elimination of phylogenetic vestiges and larval metamorphosis (Saunders, 1966; Lockshin and Beaulaton, 1974; Bowen and Bowen, 1990). In higher mammals, it is involved in formation of intestinal villi and retinal differentiation, the deletion of interdigital webs, and palatal structure fusion (Kerr et al., 1987). Neurogenesis produces about twice as many neurones than are needed by the mature nervous system, and the remainder are eliminated by physiological cell death (Server and Mobley, 1991). As discussed in section 1.1.4, the morphology of this varies from a mode similar to apoptosis, to dissimilar cytopathology patterns. Saunders (1966) and co-workers determined that developmental cell deletion is pivotal to the shaping of the (misnamed) posterior necrotic zone of bird wing buds. For lower organisms, the system of developmental cell death occurring in *C.elegans* is particularly well elucidated (Ellis et al., 1991; Yuan et al., 1993), whereby 131 cells out of a total of 1090 undergo specific coordinated deletion. Fourteen genes, some with mammalian counterparts, have now been identified which function in this death pathway. Many examples of programmed cell death come from investigations of insect and amphibian metamorphosis. In amphibians, thyroxine stimulates cell destruction in striated muscle fibres leading to tail regression, and allowing development of legs (Bowen and Bowen, 1990). The transition from insect pupal stage to ecdysis, e.g. in moths, involves rapid and large-scale programmed cell death under endocrine control in the intersegmental muscles (Lockshin and Beaulaton, 1974). In all the above circumstances, cell deletion occurs at predictable sites and times in development.

Cell turnover in normal adult tissues

Due to its constrained sequelae, apoptosis is ideally suited to the deletion of extraneous cells in normal tissues. Where quantitative data are available for formed adult tissues, the apoptotic and mitotic indices often seem to be approximately matched, suggesting a role for apoptosis in routine physiological regulation of cell number (Wyllie et al., 1980). This death mode has been reported as a spontaneous event under steady state conditions for numerous cell types, either proliferating slowly, such as hepatocytes (Kerr, 1971) or rapidly, e.g. differentiating spermatogonia (Allan et al., 1987) and crypt cells in the small intestine (Potten et al., 1994). In the former situation, cell loss by apoptosis balances cell proliferation. Thus kinetic studies of cell loss in the adrenal cortex indicate that apoptosis is capable of balancing the net mitotic input (Wyllie, 1981). Conversely, where the mitotic index exceeds the deletional index, the excess cell production is directed toward migration or shedding (Kerr and Harmon, 1991). There is evidence that homeostatic regulation of tissue mass is under cyclical control of survival and death factors (Bursch et al., 1992a). Although potentially implicated in natural ageing processes (Goya, 1986), it is not currently known what contribution apoptosis makes to senescence. Cell suicide also provides an efficient mechanism for eliminating potentially harmful cells or those that develop improperly. These phenomena include intrathymic clonal deletion of developing

thymocytes possessing TcR with high avidity for self antigens (MacDonald and Lees, 1990; Swat et al., 1991; see also section 1.4.3); removal of effete neutrophils during inflammatory responses (Savill et al., 1989); and elimination of dysfunctional B cells (Deenen et al., 1990). Raff (1992) suggested that cells deposited in an abnormal location, e.g. keratinocytes shifted into the hypodermis by injury, may also die in this manner, providing an intrinsic monitoring mechanism for tissue integrity.

Endocrine-dependent atrophy and regression of hyperplasia

Tissues that depend on continuous hormonal or mitogenic stimulation undergo involution with extensive cell death when these factors are withdrawn—this is effected by apoptosis (Searle et al., 1982). Thus under either physiological conditions, this process accounts for the cell deletion that accompanies a variety of normal involutional processes that are under endocrine control. These include regression of lactating breast tissue, of the endometrium after oestrus, catagen involution of hair follicles, and ovarian follicular atresia (Kerr et al., 1987). Deprivation of growth factors from dependent cells can also lead to death (Williams et al., 1990). In contrast, apoptosis may be enhanced by hormones, as in glucocorticoid atrophy of lymphoid tissues (Munck and Crabtree, 1981; section 1.5.1). Pathologically originated atrophy can also proceed by apoptosis in various endocrine and non-endocrine tissues. Castration elicits non-necrotic cell death in the ventral prostate due to reduced testosterone levels (Buttyan, 1991). Adrenocorticotrophic hormone withdrawal causes a rapid 9-fold increase in apoptotic index in the rat adrenal cortex (Wyllie et al., 1980). Mild ischaemia produces atrophy that is associated with reduction in cell numbers, but conservation of basic organ architecture, and this occurs via apoptosis (Kerr, 1965). Where pathogenic hyperplasia of a tissue has been produced by extrinsic mitogenic stimulus, following cessation of this stimulus apoptosis ensues to allow reversion of the tissue to normal. Documented examples include regression of hepatocellular hyperplasia caused by tumour promoters such as phenobarbital or synthetic sex steroids (Bursch et al., 1990b; Schulte-Hermann and Bursch, 1990). Notably, these compounds directly inhibit spontaneous cell deletion (Bursch et al., 1986).

Cell death in tumours

Apoptosis occurs spontaneously in virtually all malignant neoplasms (Moore, 1987), in both growing and regressing tumours. Together with more limited contributions from necrosis, exfoliation, and metastasis, it is thought to account for much of the high degree of 'cell loss' (the discrepancy between mitotic proliferative input and actual neoplastic growth) seen in malignant tumours. This is borne out by the prevalence of apoptotic bodies observed in neoplasms with known high cell loss factors, e.g. human basal cell carcinomas (Wyllie, 1985). Morphological observations show that phagocytosis of apoptotic bodies is frequently accomplished in solid tumours by neighbouring tumour cells (Kerr et al., 1972), and that apoptosis is most obvious at the periphery of zones of hypoxic necrosis. Mild ischaemia, infiltration by CTL, other immunologically-mediated killing, and tumour necrosis factor release by macrophages probably contribute to its causation (Bowen and

Bowen, 1990). However, random apoptotic events are very common during neoplasia, presumably as a result of tissue autoregulation controls or genetic programming of individual cells. Apoptosis is pivotal to many other aspects of the biology of neoplasia. It is enhanced in preneoplastic conditions, such as in liver foci and is thought to play a fundamental role in multistage carcinogenesis (Bursch et al., 1992a). In a diethylstilbestrol-dependent hamster kidney tumour the incidence of apoptosis was increased by withdrawal of this oestrogen, and decreased again by retreatment (Schulte-Hermann and Bursch, 1990), demonstrating the importance of non-necrotic cell death in the growth patterns of endocrine-dependent tumours. Therapeutically induced tumour cell killing, including chemotherapy with agents as disparate as alkylating agents and hormonal antagonists promotes apoptosis (Searle et al., 1975; Hickman et al., 1992). Though cancers of haemopoietic or germ cell origin are readily amenable to this approach (largely due to their primed state for apoptosis) epithelial and mesenchymal tumours are much more resistant to drug therapy (Hickman, 1992).

Other disease states

An overview of apoptosis in other disease states is impractical due to the currently fragmentary state of knowledge, but some important phenomena have been observed which suggest that it may be commonplace. Various congenital malformations appear to result from inappropriate levels of apoptosis (Kerr et al., 1987), and enhanced cell death underlies the teratogenic effect of retinoid-induced limb malformation, whereby the zone of programmed cell death in the mammalian apical ectodermal ridge is increased (Bursch et al., 1992a). Viral hepatitis leads to increased prevalence of apoptotic (Councilman) bodies (Searle et al., 1982), and human immunodeficiency virus infection causes apoptotic death and depletion of $CD4^+$ T helper cells (McCabe and Orrenius, 1992).

Immunologically-mediated cell killing

Unlike necrotic lysis produced by antibody-modulated complement lesions, cell mediated immune killing of targets tends to be mainly by apoptosis, although in some cases sufficient injury occurs to produce necrosis, and certain target cells undergo hybrid forms of death (Young and Liu, 1988). The morphological features of apoptosis in target cells killed by cytotoxic lymphocytes are seen in three types of effector response: NK cell attack, CTL lethal hit delivery, and killer (K) cell antibody-dependent cellular cytotoxicity (Christmas and Moore, 1987; Taylor and Cohen, 1992). Effector cells are unharmed during these processes, and several peculiarities distinguish the biochemical events from classical apoptotic patterns, viz. endogenous endonuclease activity is not detectable in targets, high order DNA-nucleoprotein interactions are disrupted separately from DNA fragmentation, and killing occurs independently of *de novo* protein synthesis (Duke, 1991). Examples of this death mode in immune reactions thought to be induced by CTL include graft versus host disease, rejection of pig liver allografts, dermal lichen planus reactions, fixed drug eruptions, and killing of neoplastic or virally infected cells (Wyllie et al., 1980; Duvall and Wyllie, 1986; Duke, 1991). Certain forms of chronic hepatitis of drug or viral aetiology,

and biliary cirrhosis involving focal apoptosis may also result by cell mediated immunity (Searle et al., 1982). Control of lytic virus infections by CTL, with viral particle containment in apoptotic bodies rather than release by cell lysis, may be effective means to halt such infections. Lymphotoxins secreted by lymphocytes also induce morphological changes involving cell fragmentation similar to CTL effectors (Russell et al., 1972), together with internucleosomal DNA fragmentation (Young and Liu, 1988)

Non-specific pathological stimuli

A variety of non-specific pathological stimuli activate apoptosis when injury thresholds or cellular repair capacity is exceeded. Moderate levels of ionising radiation, including X-irradiation and γ-rays, elicit this response in proliferating cell populations, e.g. intestinal crypt cells (Ijiri, 1989; Potten et al., 1994) and spermatogonia (Allan et al., 1987), where stem cells appear to be particularly sensitive. When given equivalent treatments, non-proliferating cells such as those found in lymphoid tissues die in a similar manner (Skalka et al., 1976; Umansky et al., 1981), normally during interphase. In these cases radiosensitivity lethality (as opposed to repair) seems to correlate with either the risk attendant with mutational fixation, such as is the case with germ cells, or where clonal expansion of dysfunctional cells would be especially dangerous, e.g. lymphocytes. Non-ionising radiation like UV-B increases apoptosis in the skin (Hume, 1987) and other cell types (Lennon et al., 1991; Deeg and Bazar, 1991). Thermal stress via hyperthermia (Dyson et al., 1986; Sellins and Cohen, 1991a) or hypothermia (Perotti et al., 1990; Nagle et al., 1990) can also engage this death mode, though the mechanisms involved remain obscure. More pronounced injury with all these agents leads to necrotic death (Lennon et al., 1991; Dyson et al., 1986).

Toxicant injury

Unscheduled apoptosis has now been implicated in a number of instances of toxic injury (McCabe et al., 1992; Corcoran and Ray, 1992; Lennon et al., 1991). Examples include direct killing of hepatocytes after in vivo administration of cycloheximide (Ledda-Columbano et al., 1992), and indirect apoptotic death of liver parenchymal cells after dimethylnitrosamine-induced injury of hepatic endothelia (Pritchard and Butler, 1989).

Due to their primed state for apoptosis, thymocytes are readily killed by various environmental toxicants including thioacetamide (Barker and Smuckler, 1973), dimethylbenzanthracene (Burchiel et al., 1992), and TCDD (McConkey et al., 1988a); though the relevance of this to in vivo immunotoxicity requires further study. Intestinal crypt cells are similarly vulnerable to alkylating or radiomimetic agents (Ijiri, 1989). Whilst poorly explored to date, it is likely that lower organisms can also respond in a similar fashion to toxic insult (Batel et al., 1993). Two broad principles seem to relate to apoptosis produced by toxic agents and other pathological stimuli (Wyllie, 1987b). Firstly, apoptosis is induced by injurious stimuli of lesser amplitude than those which cause necrosis in the same cells, and secondly, this killing occurs more readily in

populations which have a intrinsically high turnover due to physiological apoptosis.

1.1.6 The significance of apoptosis

Apoptosis theory developed over the last 20 years has challenged conceptual thinking in all aspects of cell biology, including pathology, immunology, developmental biology, carcinogenesis, and of late, toxicology. Due to the broad applicability of apoptosis, cell death can no longer be considered solely in the specialised terms of the catastrophic failure of homeostasis that typifies necrosis, or developmental cell loss. Now it seems plausible that apoptosis is the pre-eminent form of cell death, and that necrosis is considerably rarer than was thought a decade ago, only being relevant in circumstances of gross injury.

Some of the advantages of apoptosis have already been alluded to. These include high selectivity, and ability to 'pick off' unwanted or damaged cells in the midst of normal neighbours, since internal cellular controls determine its activation and it is unaccompanied by generalised reactions like inflammation. Aside from linkage with active surveillance modes such as cell mediated immunity, apoptosis has a more important passive role. For instance, the absence of intercellular survival factors may ensure the euthanasia of inappropriately located cells (Raff, 1992). Also in general terms, there is a clear biological host advantage in the elimination of cells with genomic damage subsequently leading to mutational fixation. After severe injury, this will be accomplished by necrosis, but dealing with low level DNA damage represents a more difficult problem for organisms, and the engagement of apoptotic cell death under such circumstances appears to be a widespread evolutionary development. It thereby ensures the deletion of cells insufficiently injured to be metabolically non-viable but having potentially compromised genomic integrity; a mechanism which has been described as a 'triage' process in eukaryotic cells (Tomei, 1991). In teleological terms, this is especially true of injured lymphocytes, where it may be too dangerous for the host to allow these cells to attempt potentially faulty repair, with the attendant risks of autoimmune response development or leukaemia.

Within disease processes, the treatment of currently intractable major human cancers is one of the foremost challenges for the application of emergent knowledge on the biology of apoptosis. Antitumour drug development has reached a plateau short of desired effectiveness and selectivity (Dive and Hickman, 1991), and focus has shifted onto manipulation of intrinsic death pathways as a means of preventing the clonal expansion of neoplastic cells, or killing established tumours. Thus manipulation of apoptotic mechanisms is viewed as a major current research sector (Douglas, 1994). This includes gene therapy to correct tumour-suppressor gene mutation or dysfunction; specific antibodies to apoptosis triggering receptors, e.g. anti-APO-1 (Krammer et al., 1991); and immunotoxins bearing apoptosis-inducing ligands. The great significance of apoptosis in immune system development and immunological phenomena is now also evident. A recent

model of CD4 T cell loss in human immunodeficiency virus-positive patients involves CD4 cross-linking by a complex of viral gp120 antigen and antibody, and subsequent altered disposition toward apoptotic deletion rather than activation (Groux et al., 1992; Cohen, 1993). Obvious directions for therapeutic manipulation of apoptosis, including drug reversal of the altered T cell state, arise from these findings. Whether apoptosis has a central role in human autoimmune states such as multiple sclerosis and systemic lupus erythematosus is presently unclear, but recent observations of defective T cell negative selection in mice suffering from autoimmune syndromes (Watanabe-Fukunaga et al., 1992) are particularly noteworthy.

As a final exemplification, mechanistic toxicology has previously dwelt on necrotic or other end-points to toxic injury (Timbrell, 1991), with scant or no reference to apoptosis. However, recent reviews in the toxicological literature have recognised the significance of non-necrotic death in chemically-mediated injury (Bursch et al., 1992b; Fawthrop et al., 1991; McConkey et al., 1992). This is timely, since the historical preoccupation with severe acute toxicity has been supplanted by interest in more subtle adverse effects such as immunotoxicity, chemical carcinogenesis and developmental toxicity. Emergent work suggests that apoptosis is inextricably linked with certain low level toxic insults, and the scope of this subject area must be destined to grow.

1.2 MORPHOLOGICAL CHARACTERISTICS OF APOPTOSIS

The morphological descriptions detailed hereafter are derived from studies of apoptosis in many tissues resulting from a multitude of initiating stimuli. Some generalisations are unavoidable, and it should be noted that variations do occur between various systems of apoptosis in parameters such as the relative conspicuousness of the respective nuclear and cytoplasmic alterations, minor sequence variations, and temporal heterogeneity. For example, phagocytosis of apoptotic bodies does not normally occur in ex vivo suspension cultures of non-transformed cells (Kerr et al., 1987). Programmed cell death occurring during development shares many architectural similarities with apoptosis (Lockshin and Zakeri, 1991), though subtle differences exist between the two which are mentioned in section 1.1.4. In broad terms, the morphological changes of apoptosis occur in 3 consecutive phases (Kerr et al., 1972; Wyllie et al., 1980; Searle et al., 1982; Arends and Wyllie, 1991): (i) intracellular alterations in cytoplasmic and nuclear compartments; (ii) formation of apoptotic bodies; (iii) degenerative changes commonly associated with apoptotic body phagocytosis and elimination. Each of these phases contain events of diagnostic relevance to discrimination of apoptosis, which will be highlighted, as will key alterations in cellular functional status. Figure 1.1 summarises the cardinal morphological events of apoptosis resolvable at the ultrastructural level, and their typical sequence.

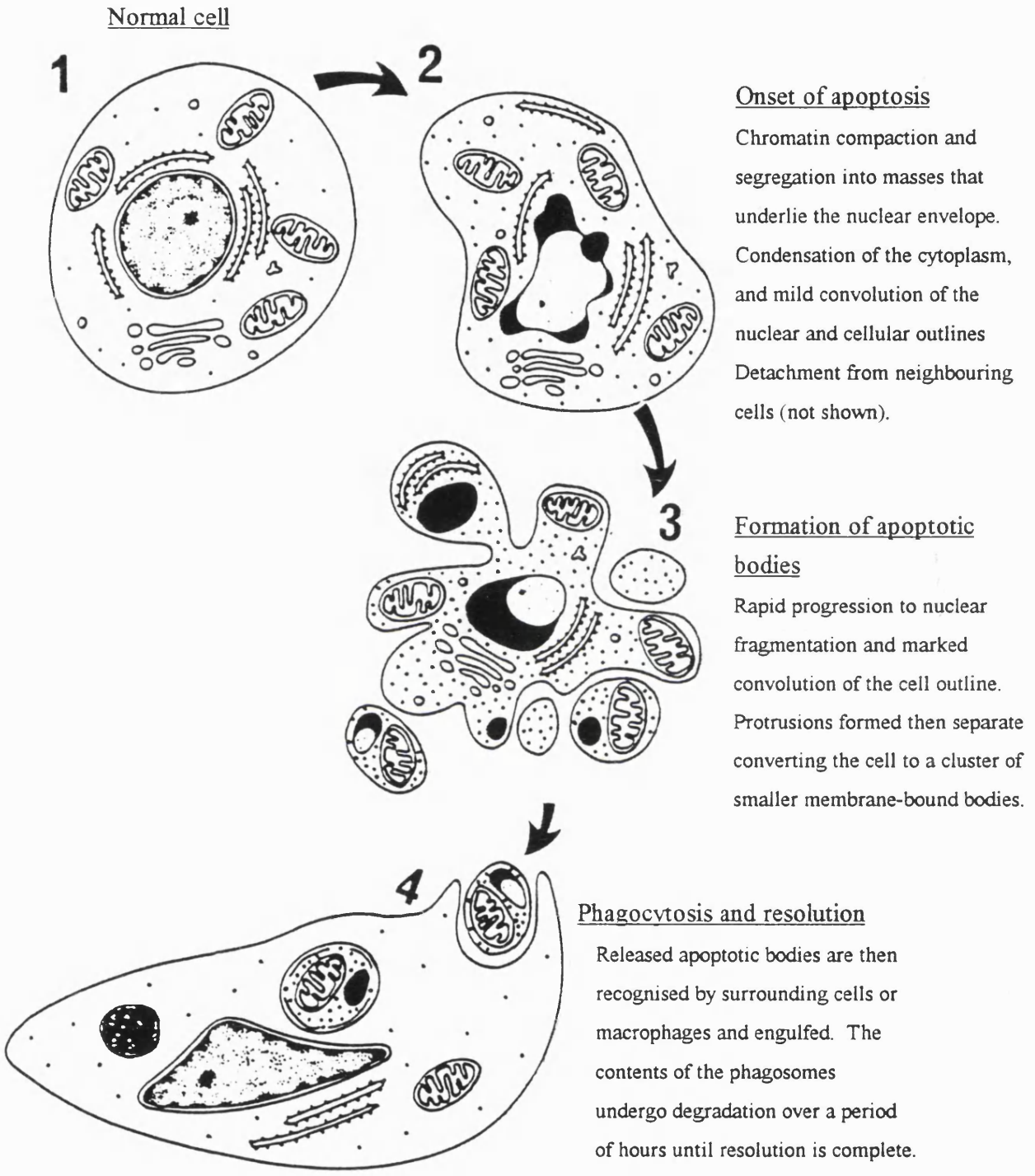

FIGURE 1.1 The morphological features of apoptosis.
Stylised diagram showing the key cellular changes and their approximate sequence (adapted from Kerr and Harmon, 1991).

1.2.1 Phase 1; early intracellular changes

After the initial apoptotic stimulus there is a delay before the first morphological signs appear, which corresponds with the commencement of various biochemical cascades (Wyllie, 1985); this interval differs depending on the cell type involved and also the triggering event, and can last from a few minutes to several days. The earliest definitive changes discernible at the ultrastructural level are firstly nuclear chromatin redistribution and condensation, and secondly, cytoplasmic contraction (Kerr et al., 1972; Wyllie et al., 1980; Searle et al., 1982; Kerr and Harmon, 1991; Anilkumar et al., 1992). In apoptotic thymocyte cultures, it is possible to identify 'preapoptotic' cells exhibiting aggregation of heterochromatin, but not frank chromatin condensation (Cohen et al., 1993), though the latter rapidly ensues. A similar progression may be applicable to other cell types, but in any event, chromatin undergoes marked compaction into sharply circumscribed, uniformly dense, granular masses which abut onto the nuclear envelope. In cells in which the proportion of euchromatin was originally high, these aggregates may be widely separated (e.g. see Boe et al., 1991), whereas in cells with smaller more hyperchromatic nuclei, the peripheral aggregates often form crescentic hemilunar caps or alternatively toroids, viz. continuous circumferential zones (Wyllie, 1986). Thus the latter patterns are often seen in cells such as lymphocytes (Galili et al., 1982; Wyllie and Morris; 1982). In either case, normal nuclear chromatin structure is altered; this is of diagnostic significance, and with care can be identified even at the light microscope level (Searle et al., 1982; Raffray and Cohen, 1991). Together with a reduction in nuclear size, there is a tendency for the centrinuclear region to become more electron-lucent, and in some cells there may also be slight convolution of the nuclear outline. Nuclear pores are normally lost next to condensed chromatin, though they may persist adjacent to euchromatin. Nucleolar change is also an early prominent alteration, leading to eventual disintegration of this nuclear subcompartment (Arends et al., 1990). Ribonucleoprotein particles disperse first, often leaving the RNA fibrillar centre visible in a osmiolucent furrow adjacent to condensed chromatin.

Necrosis superficially shares with apoptosis the characteristics of nuclear pyknosis and karyorrhexis, but the patterns of nuclear change occurring at the ultrastructural level and their temporal appearance are quite dissimilar (Kerr and Harmon, 1991; Duvall and Wyllie, 1986; Wyllie et al., 1984a; Ojcius et al., 1991; Hotz et al., 1992). During necrosis, chromatin clumping is a secondary process, which may initially be due to intracellular pH reduction (Trump and Berezesky, 1984). It leads to a flocculated appearance, with in many cases reasonable preservation of the regional heterochromatin and euchromatin spatial organisation. Compared to apoptotic chromatin condensation patterns, the hyperchromatic areas of necrotic nuclei are more diffuse, exhibit greater density variation and possess less sharply demarcated edges. Nucleolar structures tend to be conserved in necrosis (prior to terminal dissolution of the nucleus), though they may be enlarged.

Concomitant with the initial nuclear alterations of apoptosis, there are changes affecting the cytoplasmic compartment and the cell surface (Kerr et al, 1987; Wyllie, 1986; Galili et al., 1982; Arends and Wyllie, 1991). The cytoplasm begins to condense as evidenced by volume reduction (Wyllie, 1987a), and the cell surface develops a smooth contour with associated loss of specialised surface structures such as microvilli and cell-cell contact junction complexes. In solid tissues, affected cells separate from their neighbours at about this point, and in adherent cultures there is detachment from substrata (Wyllie et al., 1980). Epithelial cell intermediate filament desmosomal attachments break down (Bursch et al. 1990a). Progression of cytoplasmic contraction then results in a marked stereotypical crowding of organelles, especially in metabolically active cells like hepatocytes. For instance, aggregates of mitochondria and lysosomes (Pritchard and Butler, 1989), and sometimes semi-crystalline arrays of ribosomes have been reported. Though compacted and disordered, the organelles retain their structural and functional integrity (Kerr et al., 1972), e.g. in contrast to necrosis, high amplitude swelling of mitochondria and flux density formation does not occur (Searle et al., 1975), and cell membranes continue to exclude vital dyes like trypan blue and nigrosine (Wyllie, 1987b). Dilation of golgi and smooth endoplasmic reticulum elements results in the appearance of translucent cytoplasmic vacuoles, the more peripheral of which fuse with the cell membrane. Fusion of these dilated cisternae, when visualised by scanning electron microscopy presents as a blistered or cratered appearance of the cell surface (Morris et al., 1984; Galili et al., 1982). Cytoskeleton changes also occur with contraction of nuclear intermediate filaments (Bursch et al. 1990a), possible rearrangement of microtubules (Allen, 1987), and the formation of aberrant bundles of putative cytoskeletal elements in the cytoplasm (Wyllie et al., 1984a), which commonly run parallel to the cell surface. The timecourse of the cellular condensation stage is rapid, with completion occurring within a few minutes (Wyllie, 1985). In hepatocytes regressing after hyperplasia it has been determined to be in the order of 30 minutes (Bursch et al., 1992a).

The nuclear and cytoplasmic components of initial apoptotic processes can be dissociated. Thus anucleate cytoplasts exposed to apoptotic stimuli still exhibit characteristic cytoplasmic changes (Jacobson et al., 1994).

1.2.2 Phase 2; apoptotic body formation

The beginning of the second phase, which may overlap with the first (Arends and Wyllie, 1991), is characterised by simultaneously more extreme convolution of the nuclear outline with bizarre invaginations, and increasingly pronounced focal cell surface protrusions (Robertson et al., 1978; Wyllie et al., 1980; Allen, 1987; Kerr et al., 1987). Nuclear fragmentation occurs with dissociation of this organelle into spherical fragments of densely granular material, some with double membranes, whilst others have no discernible membranal structures. The surface protuberances separate, and after plasmalemmal

resealing the cell is quickly converted into a cluster of smaller, ovoid or round, membrane-bounded *apoptotic bodies* of varying sizes. This nuclear and cytoplasmic fragmentation and resultant apoptotic body formation is especially idiomorphic of apoptosis (Wyllie et al., 1980; Hume, 1987; Cotter et al., 1992), and although the residual cell bodies are often obscured by subsequent phagocytosis, with careful interpretation, they are recognisable by light microscopy. However, these bodies are rather inconspicuous when demonstrated by standard histological preparations; all that is visible is rounded small hyperchromatic nuclear remnants surrounded by a thin rim of eosinophilic cytoplasm.

The extent of nuclear fragmentation and cellular budding varies with cell type and tends to be restricted in cell types with a high nucleocytoplasmic ratio (Kerr et al., 1987), e.g. thymocytes. Apoptotic body content is dependent on the cellular constituents immediately proximate to protrusions as they form, i.e. some contain mainly nuclear remnants whereas others are anucleate, or possess only an array of intact cytoplasmic organelles (Kerr et al., 1972). Therefore the number, size and composition of apoptotic bodies derived from individual cells, even from a homogenous population, may differ widely (Searle et al., 1975). Phase contrast and microcinematography studies show that this core phase of violent cellular contortion (zeiosis) and budding off of apoptotic bodies is accomplished within several minutes (Kerr and Harmon, 1991; Matter, 1979). In tissues, the membrane-bounded bodies are dispersed in the intercellular tissue spaces (Griffiths et al., 1987; Ledda-Columbano et al., 1992). The smaller ones tend to disperse from the site of formation, and in organs such as the liver (Pritchard and Butler, 1989) or adrenal cortex are often seen in the spaces between the parenchymal and sinusoidal cells. In the case of glandular lining epithelia they may be shed into the lumen (Kerr et al., 1987). Where they occur in suspension, for example in ascites tumours or cultured cells (Searle et al., 1975; Galili et al., 1982), apoptotic bodies are rapidly dispersed into the surrounding milieu. But as described in section 1.2.3, by far the most common fate for apoptotic bodies is phagocytosis by surrounding cells.

It should be stressed that lysosomal rupture plays no part in the changes occurring during the first two phases of apoptosis. Lysosomes together with most other cytoplasmic organelles remain intact (Searle et al., 1982; Kerr and Harmon, 1991). Pipan and Sterle (1979) showed that acid hydrolase (e.g. acid phosphatase) activity, in newly generated apoptotic bodies remained localised within their lysosomes. The absence of demonstrable hydrolase activity at this stage contrasts with autophagic cell destruction (Bowen, 1981). It is only after phagocytosis that lysosomal digestion occurs, with the requisite enzymes being supplied, at least initially, by the engulfing cell (section 1.2.3). As mentioned previously, at the stage where apoptotic bodies are formed, basal cellular functions are largely conserved, together with viability markers (Wyllie, 1985). However, apoptotic bodies exhibit barely perceptible rates of macromolecular synthesis (Wyllie and Morris,

1982), and after 1-2 hours begin to lose the capability for volume homeostasis, and allow ingress of vital dyes. This marks the onset of less specific morphological changes including cytoplasmic swelling, sometimes termed 'secondary necrosis' (Wyllie, 1985).

1.2.3 Phase 3; phagocytosis and resolution

The third phase of apoptosis, constitutes progressive degeneration of residual nuclear and cytoplasmic structures. On formation in tissues, apoptotic bodies are normally immediately recognised and phagocytosed (Kerr et al., 1972; Wyllie et al., 1980; Wyllie, 1985; Anilkumar, 1992). Some are ingested by cells of the mononuclear phagocyte system, i.e. tissue macrophages, but many may be taken up by adjacent epithelial cells. In glandular tissues, intraepithelial macrophages are prominently involved. Phagocytosis of apoptotic bodies by tumour cells appears to the commonest removal method where they form during neoplasia, particularly in carcinomata where the cells phagocytose more avidly than tissue macrophages. Irrespective of the identity of the engulfing cell, the process of digestion of apoptotic bodies contained in heterophagic phagosomes commences after fusion with primary or secondary lysosomes, from which hydrolytic enzymes are acquired. Histochemical studies have shown the presence of acid phosphatase (Bowen and Bowen, 1990), but other hydrolases such as cathepsins and proteases are also thought to be involved. The phagocytosed bodies then go through morphological changes reminiscent of necrosis of whole cells, such that the process has been termed 'secondary necrosis'. Eventually all apoptotic body internal organelle and membrane structure is lost, and the last visible hallmarks are the presence of amorphous remnants in secondary lysosomes.

Recognition of apoptotic bodies and their phagocytosis by surrounding cells or tissue macrophages; is a cardinal feature of apoptosis (Wyllie, 1987a). Histologically defined examples include 'tingible body macrophages' in lymphoid germinal centres where dying lymphocytes are engulfed (Searle et al., 1982); apoptotic thymocyte removal in the thymus (Smith et al., 1989); resolution of Councilman bodies in the liver (Kerr, 1971); 'melanosis coli' (Arends and Wyllie, 1991) typified by accumulation of mononuclear phagocytes laden with cell remnants in the lamina propria of mucosal cells; keratinocyte engulfed 'sunburn cells' in the epidermis (Hume, 1987).

Free-floating apoptotic bodies liberated from tissues or present in cultures undergo spontaneous degeneration typified by generalised swelling, increased permeability to vital dyes, and membrane rupture (Galili et al., 1982; Robertson et al., 1978). After protracted incubation in suspension cultures (typically from 4-6 hours onwards) a significant proportion of apoptotic bodies undergo these more marked endstage degenerative changes (Robertson et al., 1978). Neutrophils are not involved in the removal of apoptotic bodies, and irrespective of the incidence of apoptosis in a tissue, no reactive inflammatory response ensues (Wyllie, 1981). Thus the components of apoptotic cells are essentially repackaged

without leakage of any chemotactic inflammatory components into the extracellular spaces. This is important, and is a distinctive difference from necrosis (where for example cellular enzymes are released to a significant extent) since it allows resolution of apoptosis without disruption of tissue architecture. After phagocytosis, adjacent cells close up leaving no sign of the deletional event.

Due to the asynchronous appearance of apoptotic bodies and the methodological difficulties implicit in kinetics measurements, the timecourse of phase 3 is rather poorly characterised in most systems. The process in rat liver is relatively rapid, taking an average of 3 hours from completion of cellular fragmentation to final resolution of phagosomes (Bursch et al., 1990a; 1990b; 1992a); which equates to a half-time of about 2 hours. Synchronised regression of adrenal cortical cells after ACTH withdrawal is slower, since the histological persistence of apoptotic bodies has been estimated at between 12 to 18 hours (Wyllie et al., 1980). A half-time of 4-9 hours is quoted as a typical range (Wyllie, 1985), and the kinetics of tumour cell apoptosis and secondary necrosis of cultured cells are of a similar order (Moore, 1987; Robertson et al., 1978).

1.3 THE MOLECULAR BIOLOGY OF APOPTOSIS

Detail of the molecular biology of apoptosis is steadily emerging, but remains incomplete, and therefore it is currently impossible to give an integrated overview. Several researchers (e.g. Wyllie, 1992; Fesus et al., 1991) have defined the various biochemical features as being involved in either *initiation/regulation* or *effector* processes. Though somewhat arbitrary, this is a convenient operational classification and has been adopted here. A further key distinction discussed by Arends and Wyllie (1991) is that two classes of event, *priming* and *triggering* are required for apoptosis. Some cells types, such as rodent cortical thymocytes, normally contain a high proportion of primed cells carrying most or all of the required effector proteins, whereas others, for instance, hepatocytes do not (though they may subsequently shift character during events such as hyperplasia). Only primed cells undergo apoptosis after triggering. Though priming is subject to specific gene level control, once the cell is primed the apoptotic triggering stimuli may be highly specific (Gerschenson and Rotello, 1992), e.g. hormones, or non-specific, e.g. mild injury. Considerable evidence has been presented that primed cells are the most vulnerable to both physiological or pathological apoptosis (Arends and Wyllie, 1991), and differential sensitivity therefore exists between apparently closely related cell types like cortical and medullary T cells, or differentiated intestinal crypt cells and the stem cells at the crypt base (Potten et al., 1994). Apoptosis and programmed cell death are active processes with organised and regulated biochemical processes, which in general terms include gene expression, intracellular signal transduction, macromolecular synthesis, energy metabolism, functional biomembranes and cell interaction (Cotter et al., 1990; Bursch et al., 1990a; Lockshin and Zakeri, 1991).

1.3.1 Regulation of apoptosis: gene level events

The concept of cell death via a 'death program' has arisen mainly from consideration of examples of programmed cell death, and stated simply, involves the triggered expression of one or more genes, the products of which effect an active biochemical cascade and eventual cytolethality. It has been pointed out that gene-directed cell death may also take the form of pre-existent gene expression so as to leave a cell type primed for apoptosis (Arends and Wyllie, 1991; Tomei, 1991). In such circumstances a full or partial array of apoptosis-linked gene products may be present and be held in check by signal transduction controls, e.g. $[Ca^{2+}]_i$ status, or a requirement for modification prior to activation. An example of one such gene product is the constitutive Ca^{2+}/Mg^{2+}-dependent endonuclease found in thymus derived lymphocytes, and certain other cells.

The genetic basis of programmed cell death in the nematode *C.elegans* has been elucidated by Horvitz and associates (reviewed in Ellis et al., 1991) using mutants with defective putative cell death genes. During *C.elegans* development *ced* (cell death abnormal) genes regulate 131 distinct single cell death events. Two permissive genes, *ced-3* and *ced-4* are presumed to encode or enable cytotoxic gene products and promote these programmed cell deaths; mutations that inactivate either gene result in the survival of almost all cells that normally die. The *ced-9* gene protects cells from programmed cell death, probably by antagonising the activity of *ced-3* and *ced-4* (Hengartner et al., 1992), since mutations at this locus cause embryolethality. Other loci affect specific cell death: *egl-1* causes death of neurones and *her-1* may function as an associated hormone messenger; ces-1 and ces-2 (cell death specification) also respectively promote, or negatively regulate pharyngeal cell death. A total of seven genes (*ced-1*, *ced-2*, *ced-5*, *ced-6*, *ced-7*, *ced-8*, *ced-10*) control the recognition and phagocytosis of dying cells in *C.elegans*, whilst degradation of engulfed effete cell DNA is effected by the *nuc-1* endonuclease. Vertebrate counterparts of the *C.elegans* gene array, which are involved in apoptosis, are now beginning to be identified. The mammalian oncogene *bcl-2*, discussed below, has a close functional similarity with *ced-9*, and the CED-3 protein (a cysteine protease) is homologous to human and murine interleukin-1-β-converting enzyme (Yuan et al., 1993). Apoptosis activation by the latter can be suppressed by the *crmA* or *bcl-2* genes (Miura et al., 1993).

In mammalian systems, several regulatory genes which influence cellular susceptibility to apoptosis are now known; most have previously been identified as oncogenes or oncosuppressor genes. The activity of *c-myc* is commonly of central importance, since it determines whether cells undergo proliferation or apoptosis. For example, Evan et al. (1992) showed that immortalised Rat-1 fibroblasts respond to growth factors by *c-myc*-dependent proliferation, and upon removal of growth factor they revert to a non-proliferating state. In cells genetically modified to constitutively express *c-myc* the absence of growth factor propels a high proportion of these cells into apoptosis. The effect of

c-myc expression on cell status has been summarised by Wyllie (1992): (i) *c-myc* off, growth factors absent - growth arrest; (ii) *c-myc* on, growth factors present - proliferation; (iii) *c-myc* on, growth factors absent - apoptosis. Thus in addition to its role in regulating proliferation, by engaging apoptosis *c-myc* may safeguard against aberrant cell growth in the absence of appropriate cytokine signalling. Equivalent findings have been reported in mesenchymal, myeloid and T cells, but *c-myc* expression in apoptosis does not appear to be universally applicable, as CEM-C7A cells do not conform to this model when apoptosing after dexamethasone exposure (Wood et al., 1994). Indeed apparently diametrically opposite findings link *c-myc* down-regulation to apoptosis in other cells. Multiple tumour suppressor (*MTS1*) appears to act as a 'gate-keeper' for *c-myc*, preventing its action by blocking signal transduction from cell surface receptors for cytokines via an inhibitor of cyclin-dependent kinase 4 (Kamb et al., 1994). This keeps *c-myc* switched off, thereby promoting apoptosis in this case. Kamb et al. found that *MTS1* was missing in certain cell lines derived from human tumours. A gene linked to cell death subsequent to terminal differentiation, *c-fos*, becomes upregulated during apoptosis of serum-deprived transformed fibroblasts, in a manner reminiscent of *c-myc* (Smeyne et al., 1993).

The anti-oncogene *p53* is implicated in DNA damage recognition and apoptosis initiation (Lane, 1993), and functions as a sentinel or surveillance gene. For instance, *p53* expression in the small intestine is highly elevated shortly after irradiation and precedes resultant apoptosis (Potten et al., 1994), though it is quiescent in normal cells. This mechanism may be exquisitely sensitive, since a single DNA-damaging event in the genome of certain crypt cells is sufficient to trigger the death program. The involvement of *p53* in detecting injury rather than in normal development is borne out by the finding that thymocytes from *p53* knock-out mice apoptose normally in response to TcR activation or glucocorticoids, but are extraordinarily resistant to induction of this process by ionising radiation (Lowe et al., 1993). Small and large intestine epithelia are rendered radioresistant in *p53* null mice (Merritt et al., 1994), but normal *p53* expression is higher in the former tissue, a fact of probable significance to its differentially lower susceptibility to carcinogenesis. The mode of operation of *p53* involves halting cell proliferation in G_1 phase to allow repair, or if this is impossible, diversion into apoptosis. Under these circumstances linked *WAF1 / CIP1* expression has been implicated in down-regulation of the crucial cyclin-dependent kinase Cdk2 (Eldeiry et al., 1993; Harper et al., 1993)

Several lines of evidence indicate that the proto-oncogene *bcl-2* represents an anti-apoptosis control which can rescue cells from a high turnover mode into a population expansion state. Hockenbery et al. (1990) characterised the Bcl-2 protein as a integral inner mitochondrial membrane component and demonstrated that over-expression of *bcl-2* blocks the apoptotic death of a pro-B-lymphocyte cell line when deprived of IL-3. In fact, similar over-expression of *bcl-2* spares several haemopoietic cell lines from death following

growth factor withdrawal, and upregulation of *bcl-2* in transgenic mice promotes tumourigenesis (Korsmeyer, 1992). It has also been suggested that *bcl-2* could be a new and discrete molecular level determinant of tumour cell resistance to cytotoxic treatments (Fisher et al., 1993). When *bcl-2* expression is redirected from medullary to cortical thymocytes in transgenic mice, $CD4^+CD8^+$ cells become refractory to normal apoptotic stimuli like glucocorticoids, irradiation, ionophores and anti-CD3 antibodies (Sentman et al., 1991; Strasser et al., 1991). However, clonal deletion of autoreactive cells is delayed (Strasser et al., 1991) but not operationally impaired (Sentman et al., 1991) in this system, suggesting that multiple death pathways exist. T cell selection in the thymus probably involves salvation of mature cells by *bcl-2*-dependent processes (Korsmeyer, 1992). In addition, control of *bcl-2* gene expression within the peripheral antigen-primed activated $CD45RO^+$ cell population may be a key factor in the balance between death and survival (Akbar et al., 1993), and hence underpin management of T cell memory and clonal expansion. Regulation of apoptosis by *bcl-2* also appears important in mammalian systems where tissue homeostasis is effected by cell death, i.e. *bcl-2* expression occurs in progenitor and stem cells which must be highly conserved for proliferative integrity. The mechanism by which this gene represses apoptosis is still being elucidated, but the recent finding that it is associated with intracellular sites of free radical formation, including the endoplasmic reticula and nucleus, as well as mitochondria (Hockenbery et al., 1993) seems important. It was found that bcl-2 protein protected cells from oxidative species injury after dexamethasone treatment. They concluded that the sustained lipid peroxidation seen after apoptotic stimuli may be implicated in signal transduction or direct damage, and that *bcl-2* expression blocks this cascade without affecting free radical formation *per se*. In common with growth factors, bcl-2 can prevent cytoplasmic apoptotic changes in anucleate cytoplasts indicating that nuclear function need not be involved (Jacobson et al., 1994).

Aside from cytokine cell survival promotion, other death repressor genes apart from *bcl-2* must exist, e.g. suppression of apoptosis in the mid-crypt region of the small intestine does not involve *bcl-2* (Potten et al., 1994). Upregulation of *ras* oncogenes may an alternative device (Wyllie, 1992), as considerable endogenous endonuclease activity exists in Rat-1 fibroblasts when *c-myc* is constitutively transcribed, but is absent when mutated Ha-*ras* is expressed at high levels. Coincident with inhibition of *ras* expression, apoptosis in rat chloroleukemia cells involves activation of the long interspersed repetitive DNA (*L1Rn*) transposon-like element common to all mammalian cells (Servomaa and Rytomaa, 1988).

Several models of gene regulation in apoptosis arising either from tissue homeostasis requirements or cell injury have been devised—Fig. 1.2 is a scheme recently devised by Potten and colleagues (1994). However, a generally applicable framework for how these regulatory genes influence the susceptibility of cells to apoptosis has yet to be constructed, especially in terms of their 'cross-talk'.

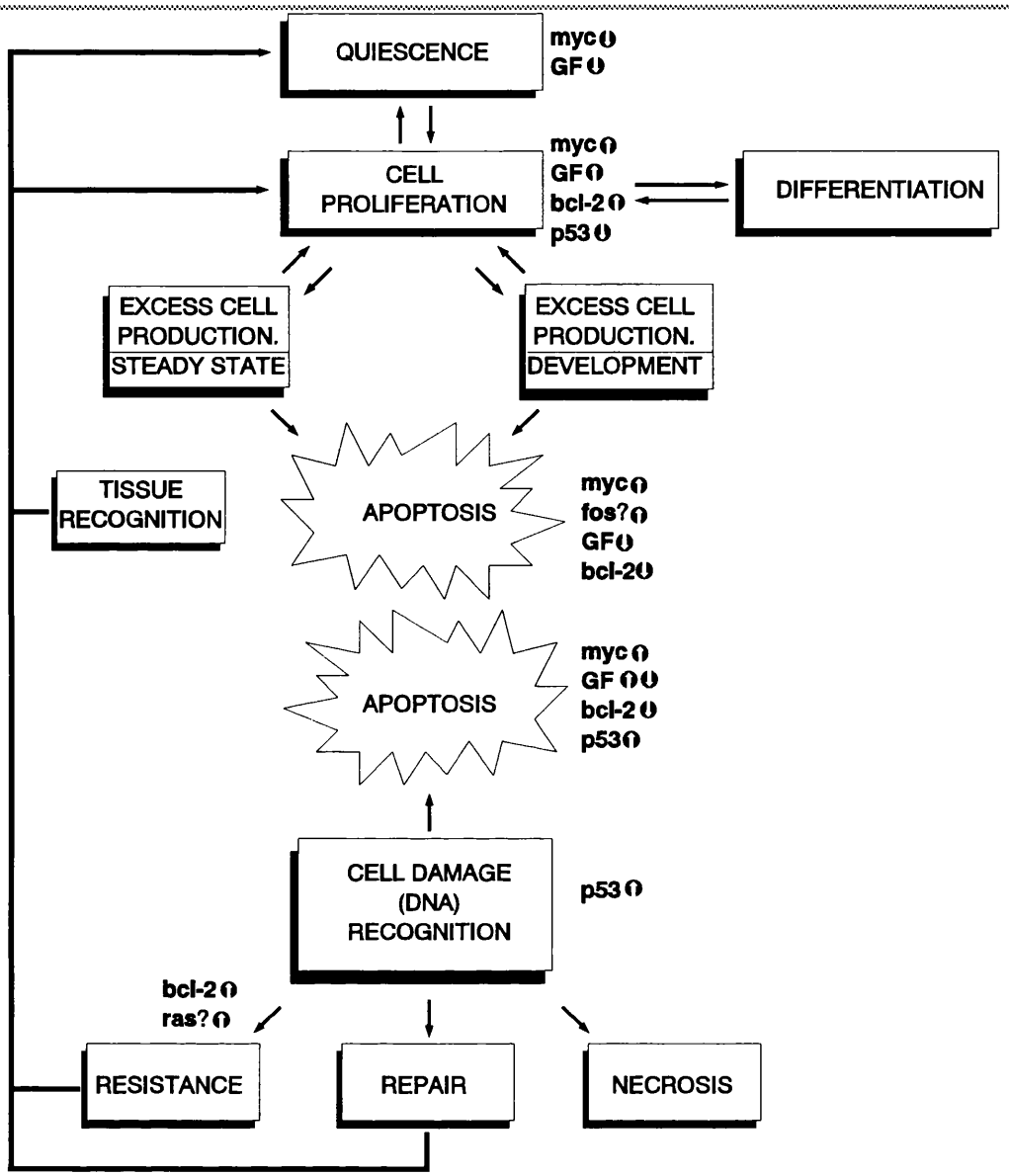

FIGURE 1.2 Gene regulation of apoptosis in tissue homeostasis and cell injury. (↑) and (↓) signify up- or down-regulation of gene expression, respectively. Adapted from Potten et al., 1994.

1.3.2 Signal transduction

This section broadly considers primary and secondary signalling events; for detail on signal transduction processes of relevance to the rodent thymocyte model see section 1.4.3 (T cell apoptosis) and chapter 4. Specific receptor-linked interactions and the influence of 'apoptotic factors' and 'survival factors' represent early phenomena of importance in the regulation of developmental cell death and apoptosis (Fesus et al., 1991). Several cell surface molecules when triggered by their ligand or antibody are able to transduce a death signal; amongst these are the Fas (APO-1) antigen, surface immunoglobins, the TcR and tumour necrosis factor (TNF) receptor. The Fas antigen is a cell surface protein, structurally homologous with TNF and nerve growth factor receptors, that initiates apoptosis in various tissues including the thymus. Mice carrying the lymphoproliferative

(*lpr*) mutation have Fas antigen gene defects, and develop an autoimmune syndrome involving accumulation of $CD4^-CD8^-$ immature thymocytes (Wanatabe-Fukunaga et al., 1992), suggesting a role for Fas in T cell negative selection. The *gld* gene encodes the Fas receptor ligand, and it may be significant that constitutive TNF synthesis occurs in the thymus (Giroir et al., 1992). The human cell APO-1 molecule is an identical cell surface receptor present on B and T cells and certain tumours, which when engaged activates apoptotic death (Krammer et al., 1991); tumour cell resistance to death correlates with degree of APO-1 expression. Russell et al. (1991) found that in T cells the TcR coupling to the death program is open during maturation, but is closed in host-tolerant mature cells until they encounter antigen. Hence the receptor is involved in clonal restriction during negative selection and also termination of T cell proliferation after resolution of antigenic challenge. In contrast, other receptors, e.g. CD28 in T cells, suppress apoptosis and promote proliferation (Groux et al., 1992).

A number of 'apoptotic factors' such as Mullerian inhibiting substance, TNF-α, TGF-β bind to cell surface receptors (Fesus et al., 1991). For example, TGF-β inhibits proliferation and induces apoptosis in hepatocytes and cultured endometrial cells (Gerschenson and Rotello, 1992; Bursch et al. 1990a), and TNF-α binding activates several second messenger pathways including some that ultimately result in apoptotic killing (Larrick and Wright, 1990). Other messengers require internalisation and often act via receptors which translocate to the nucleus. Thus in lymphoid cells possessing a glucocorticoid receptor, engagement by glucocorticoids causes irreversible commitment to apoptosis, and the intracellular thyroxine receptor mediates tadpole tail regression (Bowen and Bowen, 1990). Conversely, a number of cytokine growth factors induce proliferation and also act to suppress apoptosis, since their removal from dependent cells causes death rather than simply non-proliferation. Colony stimulating factors like IL-3 (granulocyte-macrophage colony stimulating factor) promote myeloid cell survival (Williams et al., 1990); IL-2 has similar effects in IL-2 dependent CTL clones (Duke, 1991; Nieto and Lopez-Rivas, 1989); IL-4 and IL-2 may prevent distinct T helper cell subset death induced by endogenous glucocorticoids (Zubiaga et al., 1992); and erythropoietin retards apoptosis in normoblasts (Koury and Bondurant, 1990). Raff (1992) postulated that cell-cell signalling is a general mechanism fundamental to survival, and that competition for survival factors is vital to cellular selection and tissue homeostasis. Apoptosis also develops following loss of trophic hormonal or tissue mitogen signals, e.g. in the adrenal cortex after ACTH withdrawal (Wyllie et al., 1980), or in liver cell hyperplasia regression after removal of phenobarbital or cyproterone (Bursch et al., 1992b).

Only fragmentary understanding exists of the intracellular signal pathways which initiate apoptosis via actions upstream of effector elements. However, Ca^{2+} flux generation appears to be a common feature in many instances (Waring et al., 1991), involving both

intracellular mobilisation and extracellular ingress. Though it is clear that Ca^{2+} overload can activate apoptotic endonucleases (Nicotera et al., 1990; see also 1.3.5), few studies to date have distinguished between Ca^{2+}-linked signal transduction in apoptosis and Ca^{2+}-dependent effector enzyme activation. Unlike the loss of homeostasis typified by necrosis, elevations in $[Ca^{2+}]_i$ during apoptosis are: (i) moderate in degree; (ii) controlled; (iii) persistent; (iv) observed to precede or accompany the appearance of apoptotic markers such as internucleosomal cleavage (McCabe and Orrenius, 1992; McConkey et al., 1989a). Much evidence stems from experiments in the thymocyte model of apoptosis; intracellular Ca^{2+} levels increase in cells dying after exposure to glucocorticoids (McConkey et al., 1989b), anti-CD3 antibody (McConkey et al., 1989c) or irradiation (Zhivotovsky et al., 1993). This process can also be activated by cation ionophores (Wyllie et al., 1984a; Smith et al., 1989) and inhibited by use of intracellular Ca^{2+} chelation or extracellular depletion (Boobis et al., 1989; Kerr and Harmon, 1991). In CTL delivering their lethal hit, $[Ca^{2+}]_i$ rises by several hundred nM followed by greater increases in target cells undergoing apoptosis (Poenie et al., 1987; Duke, 1991), and NK cells also induce a similar rapid increase in targets (McConkey et al., 1990d). Examples of Ca^{2+}-dependent apoptosis in other systems are numerous and include the triggering effect of extracellular Ca^{2+} ingress in prostatic epithelium (Kyprianou et al., 1988), menadione-stimulated DNA fragmentation in hepatocytes (McConkey et al., 1988a), and cold-shock killing of synovial cells (Perotti et al., 1990). Calcium-mediated signal transduction may be important in developmental cell death, as suggested by the presence of Ca^{2+}-binding domains on the ced-4 protein of *C.elegans* (Ellis et al., 1991). In some cases Ca^{2+} signalling is effected by receptor mediated processes involving specific agonists. Thus RU486 antagonises glucocorticoid-induced Ca^{2+} elevations (McConkey et al., 1989b), and the aryl hydrocarbon (Ah) receptor appears to be involved in similar TCDD-mediated effects (McConkey et al., 1988a). Other stimuli, such as TBT (see chapter 4), can direct modulate $[Ca^{2+}]_i$. In terms of linkage to apoptotic effector mechanisms, plasmalemmal and nuclear Ca^{2+}-transport systems have been described (McConkey et al., 1989b; Jones et al., 1989), and local transients in the nucleus appear important, e.g. TNF-α increases adenocarcinoma cell intranuclear Ca^{2+} to 800nM (Bellomo et al., 1992), and this cation accumulates in the nucleus of apoptotic hepatocytes after paracetamol treatment (Shen et al., 1992).

However, neither Ca^{2+}-linked signal transduction or Ca^{2+}-stimulated endonuclease action is necessarily axiomatic of apoptosis. There are situations where DNA degradation in apoptotic cells requires Ca^{2+}, but signal transients are not involved (McConkey et al., 1990a; Zhivotovsky et al., 1993). Furthermore, CEM-C7 lymphocytes (Alnemri and Litwack, 1989) or activated T cells (Deeg and Bazar, 1991) are not protected by EGTA from internucleosomal cleavage induced by glucocorticoid or irradiation, respectively. Ionophore-induced apoptosis in HL-60 cells is completely dissociated from increased $[Ca^{2+}]_i$ (Barry and Eastman, 1992), and in excitable cells, calcium elevations may actually

be required to suppress apoptosis (Martin and Johnson, 1991).

From the above and section 1.1.2, it will be evident that there is a clear distinction between the role of Ca^{2+} fluxes in apoptotic and necrotic death modes. In the more controlled situation of apoptosis, modulations via physiologically relevant Ca^{2+} signalling pathways often lead to activation of a very restricted set of apoptotic effector mechanisms, whereas necrosis involves disruption of organelle and cellular Ca^{2+} homeostasis as a secondary degenerative process activating a cascade of calcium-dependent degradative enzymes.

Calcium signalling in apoptosis may be transduced via calmodulin-dependent pathways, since inhibitors like calmidazolium are often protective in lymphoid and non-lymphoid cells (McConkey et al., 1989b; Zheng et al., 1991; Perotti et al., 1990; 1991). Other second messengers may also be important in regulating death programs. Raised inositol triphosphate levels precede gliotoxin-stimulated DNA degradation in macrophages (Waring, 1990), and IP_3 and DAG are important secondary signals to Ca^{2+} and PKC pathways in T cell activation (McConkey and Orrenius, 1991). Exciting new findings using cyclosporin A as an inhibitor of calcineurin A in T cell hybridomas, indicate that this phosphatase is a critical signalling molecule coupling TcR stimulation with activation-induced cell killing (Fruman et al., 1992), and suggest that T cell apoptosis is partly dependent on Ca^{2+} due to the obligate requirement of calcineurin for this cation and calmodulin. Cyclic nucleotide levels are often elevated in cells undergoing apoptosis (Lockshin and Zakeri-Milovanovic, 1984), and stimulation of PKA by cAMP has been shown to induce apoptosis (McConkey et al., 1990a; 1993). This has led to the postulate that, in T cells at least, this pathway is important to endonuclease activation and cell death (McConkey et al., 1990c). Phorbol esters which are potent activators of PKC, appear to inhibit apoptosis induced by various agents in disparate cell types such as fibroblasts (Tomei, 1991), adenocarcinoma and synovial cells (Perotti et al., 1991), T cell hybridomas (Iseki et al., 1991), and thymocytes (McConkey et al., 1989c; 1989d). However, contradictory reports exist where PKC stimulation by phorbol esters increases the incidence of apoptosis in thymocytes (Kizaki et al., 1989; Migliorati et al., 1992) and other cell types (Boe et al., 1991). Given that $[Ca^{2+}]_i$ elevations are apparent during both apoptosis and mitogen-stimulated proliferation, additional signals must determine which path the cell will take. Whilst PKC signalling has been proposed as such a switch (McConkey and Orrenius, 1991), doubts remain as to the validity of this notion.

Post translational modification of nuclear proteins, chromatin conformation state and cellular ATP and NAD levels can all be modulated by the enzyme poly(ADP-ribose) polymerase (Gaal et al., 1987), and it is possible that it could be involved in distal signal transduction pathways in apoptosis (Hickman, 1992). As might be expected, activation of poly(ADP-ribose) polymerase has been implicated in non-necrotic cell death in

circumstances where toxicant-induced DNA strand breaks occur (Shimizu et al., 1990), and also during DNA degradation in glucocorticoid-mediated lymphoid cell apoptosis (Wielckens and Delfs, 1986) and CTL cytolysis (Duke and Sellins, 1989). However, there is meagre evidence to suggest that it plays a pivotal role during apoptosis. Findings relating to lymphoid cells are detailed in section 4.1.1.

1.3.3 Macromolecular synthesis

Due to space limitations the following seeks only to examine key themes and illustrate them with relevant examples; section 5.1.1 provides further development in the specific context of thymocyte apoptosis, and 1.3.1 considers gene expression during apoptosis. The possible involvement of macromolecular synthesis in non-necrotic cell death was first raised during early reviews of programmed cell death (Lockshin and Beaulaton, 1974) and apoptosis (Kerr et al., 1972). Ample evidence has now accumulated that *de novo* mRNA and protein synthesis have an early and pivotal role in developmental cell death. Degeneration of insect pupal intersegmental muscles and tadpole tail involution feature among numerous examples (Lockshin and Beaulaton, 1974; Bowen and Bowen, 1990). In both cases, the transcriptional and translational inhibitors actinomycin D and cycloheximide block cell death. Upregulation of several RNA transcripts has been matched to two distinct waves of cell death in insect homologous muscles; similar patterns of new protein synthesis are detectable in involuting labial glands; and burst synthesis of mRNAs occurs during planarian worm physiological cell death (Lockshin and Zakeri, 1991; Bowen and Bowen, 1990). The latter reviewers also noted that the process of rat palatal cell death during histiogenesis is dependent on protein synthesis.

Other than programmed cell death, a unifying feature of many early studies of a variety of pathophysiological stimuli and cell types was the apparent dependence of the apoptotic process on the maintenance of *de novo* protein synthesis for at least a limited period following the triggering event. This conclusion stemmed from indirect evidence relating to the protection afforded by transcriptional and translational inhibitors such as actinomycin D, emetine, puromycin and cycloheximide. Examples often cited include the prevention of DNA fragmentation and viability loss by these inhibitors in rodent thymocytes exposed in vitro to glucocorticoids (Cohen and Duke, 1984), cation ionophores (Wyllie et al., 1984a) or γ-irradiation (Pechatnikov et al., 1986). Thus in the study by Wyllie and co-workers (1984a) MPS-stimulated chromatin cleavage was inhibited in a dose-dependent manner by either actinomycin D or cycloheximide, whilst removal of reversible RNA synthesis blockade caused by 5,6-dichloro-1-β-ribofuranosylbenzimidazole allowed irradiated cells to proceed to fragment their DNA (Sellins and Cohen, 1987). Equivalent protection has been described in a diverse circumstances, including apoptosis caused by: glucocorticoids in lymphocytic leukemia cells (Galili et al., 1982); hypothermia in chinese hamster ovary cells (Nagle et al., 1990); activation-induced T cell death (Shi et al., 1990); glutamate treatment

of neurones (Kure et al., 1991); exposure of thymoma cells to exogenous ATP (Zheng et al., 1991); and prostatic epithelium involution due to testosterone withdrawal (Buttyan, 1991). As has been pointed out (Collins et al., 1991), the effect loci of most transcriptional and translational inhibitors is complex and not limited solely to macromolecular synthesis. In addition, at the levels feasible in studies of apoptosis, their inhibition of transcription or translation is rarely complete (Wyllie et al., 1984a; McConkey et al., 1989a).

Attempts have been made in some systems to detect new protein expression, but identification and characterisation of limited numbers of new protein moieties is methodologically complex, and complicated by apoptotic events such as chromatin changes which may release nuclear proteins (Alnemri and Litwack, 1989). Again, the rodent cortical thymocyte model of apoptosis is perhaps most studied. Glucocorticoids induce a small number of proteins in thymocytes (Voris and Young, 1981) which appear in synchrony with apoptosis, and subtractive hybridisation studies have shown the transcription of two death-associated mRNAs, RP-2 and RP-8, in irradiated cells (Owens et al., 1991). Although induction of thymocyte endonucleases by glucocorticoids has been claimed (Compton et al., 1987), the same group later concluded that the NUC18 enzyme originally described was in fact constitutively present as an inactive complex of higher molecular weight which was activated in apoptotic cells (Gaido and Cidlowski, 1991). A variety of poorly characterised new proteins appear during the acute phase of ventral prostatic epithelium involution, as do *c-fos*, *c-myc* and heat shock protein 70 transcripts (Buttyan, 1991). On balance, it is still unclear whether the aforementioned macromolecular synthesis requirements relate to initiator or effector mechanisms, e.g. signal transduction protein synthesis in the former case, or endonuclease production in the latter.

The tenet of obligate macromolecular synthesis dependency in apoptosis is challenged by growing number of reports in which inhibitors of macromolecular synthesis have proven to be ineffective. These include certain immunologically mediated instances of cell killing such as that produced by TNF-α and cytotoxic effector T and NK cells (Goldstein et al., 1991; Duke, 1991; Sellins and Cohen, 1991b); death of CEM lymphoblastic leukemia cells after novobiocin treatment (Alnemri and Litwack, 1990); apoptosis in HL-60 cultures following exposure to etoposide (Kaufmann, 1989); hepatocyte apoptosis caused by protein phosphatase inhibitors (Boe et al., 1991) and T blast and macrophage killing by gliotoxin (Waring, 1990). Moreover, potent inhibitors of protein or RNA synthesis may themselves initiate apoptosis as has been shown in the case of diphtheria toxin (Chang et al., 1989), ricin (Waring, 1990; Griffiths et al., 1987), puromycin or emetine (Vedeckis and Bradshaw, 1983), and most notably cycloheximide (Kaufmann, 1989; Collins et al., 1991; Ledda-Columbano et al., 1992) and actinomycin D (Martin et al., 1990). Such data involve disparate cell systems and agents, and no entirely satisfactory explanation for this paradigm exists. An integrated postulate has been devised by Cohen (1993), whereby apoptotic

death is classified into three types: (i) inductive mechanisms (protein synthesis required); (ii) transduction mechanisms, e.g. CTL lethal hit delivery (protein synthesis not required); (iii) release mechanisms (where interruption of protein synthesis initiates apoptosis). As a more extreme viewpoint, Raff and colleagues (Jacobson et al., 1994) focus on the ability of programmed cell death to commonly occur in the absence of *de novo* protein synthesis, and postulate that the effector proteins are constitutively expressed in most, or all mammalian cells. They favour the possibility that RNA and protein production are required for regulation of the death program rather than for synthesis of effector components. As discussed further in Chapter 5, new findings threaten even the validity of the dogma linked to the thymocyte model, since it appears that these cells have more than one apoptotic pathway which variously function in a manner dependent, or independent, of protein synthesis (Migliorati et al., 1992).

TRPM-2 (SGP-2) protein is formed in large amounts during regression of many tissues (Buttyan, 1991), though its function is unclear. Transglutaminases are terminal phase apoptotic effector proteins (Fesus et al., 1989); their action is described in section 1.3.6. Several other enzyme activities have been implicated in the destruction of apoptotic cells during hormone-dependent tissue regression (Bursch et al. 1990a); cytoskeletal-directed proteases and collagenases feature amongst these enzymes, but it is not known whether they are newly synthesised or upregulated by signal transduction events.

The question arises as to the functional relevance of macromolecular synthesis in regulating programmed cell death and apoptosis. A requirement for protein synthesis could relate to:

The production of effector enzymes. Unequivocal evidence for *de novo* synthesis of apoptotic endonucleases has rarely been established, but it is known that nucleases are constitutively present in some cell types, e.g. cortical thymocytes, whilst in others they must be induced prior to apoptosis. Thus in the latter case, when human and murine lymphoid cell lines undergo toxicant-mediated cell death, the extractable Ca^{2+}/Mg^{2+}-endonuclease activity rises from low levels and peaks coincidently with the onset of chromatin cleavage (Wyllie et al., 1986, Giannakis et al., 1991). Though autolytic lysosomal hydrolase action is increased in many forms of programmed cell death (Bowen and Bowen, 1990), it is not considered to be of causal significance in the spectrum of early morphological changes (Lockshin and Zakeri, 1991).

Resynthesis of effector proteins in rapid turnover. It has been suggested that protein synthesis dependency relates to rapid endonuclease turnover (Nikonova et al., 1982; 1993; McConkey et al., 1990b), but a basis for the general applicability of this theory is lacking.

Proteins involved in signal transduction. Thymocytes synthesise a heat-labile factor which elevates $[Ca^{2+}]_i$ (McConkey et al., 1989b), and the death program engaged by γ-irradiated thymocytes probably involves the production of signal transduction proteins, since

macromolecular synthesis inhibition prevents antecedent Ca^{2+} flux and subsequent apoptosis (Gabai et al., 1990; Zhivotovsky et al., 1993). The *C. elegans* cell death gene *ced-4* produces a Ca^{2+}-binding protein, and the allied *ced-3* gene product, a cysteine protease homologous to interleukin-1-β-converting enzyme has serine residue motifs equivalent to known phosphorylation sites (Ellis et al., 1991; Yuan et al., 1993). Since neither protein is thought to function as an endonuclease, the *C. elegans* programmed cell death system may be dependent on the early synthesis of signal transduction proteins.

Regulation of DNA conformation. One or more nucleoproteins may be formed capable of altering chromatin structural constraints, and hence nuclease susceptibility. Alternatively, the extent of DNA methylation could be altered by induced methylases—susceptibility to endonuclease attack can be governed by the degree of DNA methylation (Lockshin and Zakeri-Milovanovic, 1984). Evidence for such mechanisms is currently circumstantial.

Mediation of cell cycle-linked events. There is circumstantial evidence that protein synthesis may be instrumental in allowing certain injured cells to progress through the cell cycle and before proliferative arrest and apoptosis (Eastman, 1990; Wood et al., 1994). Under these conditions synthetic processes associated with the G_2/M interface seem to be particularly crucial in determining reprogramming from proliferation to death.

Control of effector mechanisms. A scheme devised by Gerschenson and Rotello (1992) could account for the paradoxical activation of apoptosis in some circumstances by transcriptional and translational inhibitors. Short-lived apoptotic repressor proteins might be continually synthesised in some cells; this model allows for the possibility that repressor and inducer proteins could coexist. Bcl-2 is a possible candidate in such a role. Others have alluded to the possibility of similar 'survival factors' (Fesus et al., 1991), but whilst empirically appealing, direct experimental support for these ideas is currently meagre.

Metabolic integrity maintenance. It has been hypothesised that protein synthesis inhibition *per se* could actuate apoptosis due to loss of proteins critical to cell metabolism. Though there is no data to suggest that suppression of transcriptional and translational activity is immediately toxic to thymocytes, the typical inhibitors used, e.g. actinomycin D rarely completely abolish synthetic activity, so this has been incompletely tested in this model. However, extended incubation with cycloheximide does elevate thymocyte apoptosis (Sellins and Cohen, 1987; Dr S Chow, personal communication). In other cell types, the extent of protein synthesis depression by these inhibitors does not correlate well with the incidence of apoptosis (Martin et al., 1990; Chang et al., 1989; Bicknell et al., 1994).

1.3.4 Chromatin organisation: relationship to DNA degradation in apoptosis

Eukaryotic DNA possesses at least 4 subchromosomal levels of organisation: (i) nucleotide sequence (primary); (ii) double stranded DNA helix (secondary); (iii) DNA supercoiling (tertiary); (iv) supercoiled domains (quarternary). The last two levels of topology have been referred to as 'superstructure' or 'high-order' organisation (Lipetz et al., 1982; Alberts

et al., 1989). As shown in Fig. 1.3, high-order chromatin is thought to consist of DNA wound around *nucleosomes*, packed by histone H1 into a *solenoid* which forms the *30 nm fibre*; this is then organised as 50 kbp *loops*, further into 300 kbp *rosettes* (200-300 nm fibre), then *coils*, and finally *chromatids*.

Fig. 1.3 also shows how, at the lowest level, the nucleosomal organisation governs DNA accessibility to the neutral Ca^{2+}/Mg^{2+}-dependent endonuclease widely implicated as an effector enzyme of apoptosis (see 1.3.5). High-order chromatin structures may also govern nucleolytic processes in apoptosis. It has been suggested that breakdown of chromatin, with loss of supercoiling and formation of individual 25-30 nm fibre elements is important in some instances of apoptosis (Tomei, 1991), and initial high-order cleavage which finally proceeds to internucleosomal degradation has been demonstrated in systems including liver cells and thymocytes (Filipski et al., 1990). Changes in nucleoprotein interactions may modify DNA superstructure, and thereby indirectly affect constraints on nuclease attack. For example, phosphorylation of H1 by histone kinases like $p34^{cdc2}$ is key to chromatin condensation (Darzynkiewicz, 1986; Eastman, 1990) and conversely nucleoprotein phosphatases mediate relaxation (Darzynkiewicz, 1986); though untested, it has been suggested that apoptosis and mitosis pathways may share some common elements (Eastman, 1990). It is interesting that certain inhibitors of apoptosis, e.g. Zn^{2+} inhibit nucleoprotein dephosphorylation (Tanphaichitr and Chalkley, 1976). Most findings suggest that histone proteolysis is unimportant to actuation of apoptosis (Umansky et al., 1981; Kyprianou et al., 1988; Arends et al. 1990). In thymocytes, the role of chromatin decondensation is disputed (Nikonova et al., 1982), but there is evidence in similar systems that non-supercoiled transcriptionally active DNA is preferentially cleaved by endonucleases (Vanderbilt et al., 1982). Certain cations, and in particular polyamines, charge-stabilise DNA and promote high-order packing (Widom and Baldwin, 1980)—exogenous polyamines inhibit endonuclease action, whereas polyamine depletion stimulates apoptosis (Brune et al., 1991). Topoisomerase II is a major non-histone nuclear protein, which relaxes supercoiled DNA conformations during replication and transcription (Liu, 1989). This function derives from a unique ability to permit double-strand DNA passage linked to ATP-dependent transient DNA cleavage and subsequent religation. It appears to bind preferentially to nucleosome-depleted regions of chromatin loop domains (Adachi et al., 1989). High order DNA cleavage due to topoisomerase II-directed agents can lead to apoptosis (Walker et al., 1991; Kaufmann, 1989), and it is possible that it could have a more general role in apoptotic effector processes (see next section).

1.3.5 Nuclear enzyme involvement

As previously outlined, a common, but not universal, biochemical hallmark of apoptosis is a characteristic internucleosomal degradation of genomic DNA. Independent studies during the 1970's showed that mammalian cells exposed to lethal stimuli could fragment their

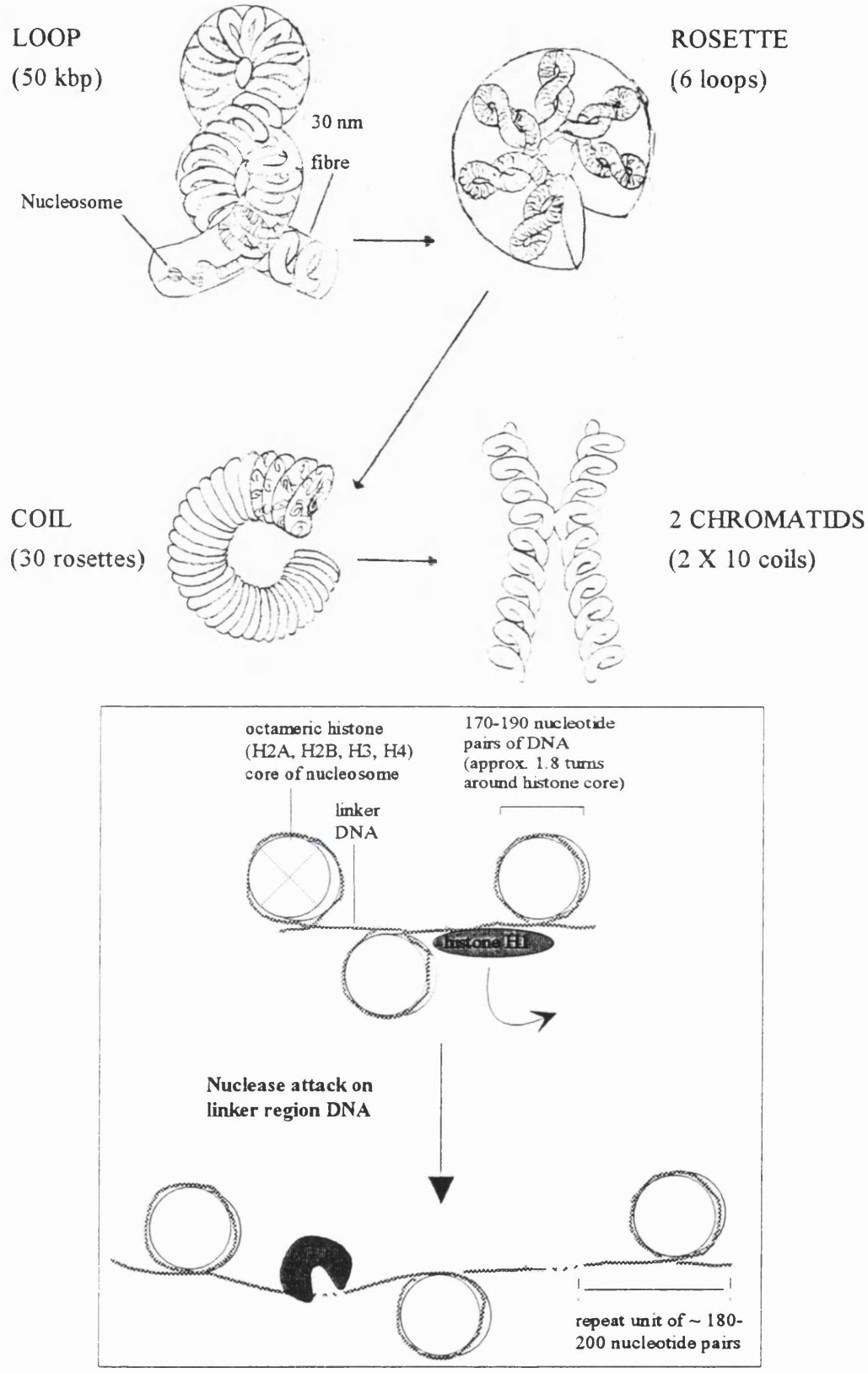

FIGURE 1.3 Organisation of eukaryotic DNA into high-order chromatin structures. Adapted from Filipski et al., 1990. The inset depicts the nucleosomal organisation of DNA (shown partially decondensed for clarity), and indicates the basis of endonuclease-mediated internucleosomal DNA cleavage; an important biochemical apoptotic marker.

DNA by an endonucleolytic process (Skalka et al., 1976; Williams et al., 1974), and that divergent cell types, including lymphocytes and liver cells, contained an endogenous endonuclease activity which preferentially cleaved DNA in hypersusceptible regions between nucleosomes (Hewish and Burgoyne, 1973; Bachvaroff et al., 1977). These workers determined that the activity was dependent on the presence of Ca^{2+} and Mg^{2+}, and its cleavage products appeared indistinguishable from those arising from brief digestions of chromatin with micrococcal nuclease. Following linkage of glucocorticoid-induced apoptotic nuclear changes to a prototypic thymocyte endonuclease (Wyllie, 1980), numerous studies have shown similar associations relating to many cell types and pathophysiological apoptotic stimuli (see reviews by Arends and Wyllie, 1991; Umansky, 1991; Compton 1992; McConkey et al., 1992). Internucleosomal DNA scission during apoptosis has been described in phylogenetically wide-ranging circumstances, from various higher vertebrate systems (Gerschenson and Rotello, 1992) to simpler organisms such as marine sponges (Batel et al., 1993), and from stem cells (Manes and Menzel, 1982) to terminally differentiated cells, e.g. neurones (Kure et al., 1991).

The nature and biochemical character of this enzyme is widely debated, but it is evident that similar moieties exist in a wide range of cells (Table 1.2). The rodent thymocyte endonuclease involved with internucleosomal DNA cleavage has been most studied, in whole cells exposed to apoptotic stimuli, and in isolated nuclei autodigestion experiments (Table 1.2). Several features have been consistently described. It produces double-stranded cleavage products which are multiples of 180-200 bp, i.e. correspond to integer mono- and oligonucleosomal chromatin DNA fragments, forming a stereotypical DNA ladder when resolved by neutral gel electrophoresis (Umansky et al., 1981; Kyprianou et al. 1988). The enzyme is associated with the nucleus and is not lysosomal in origin (Nikonova et al., 1993; Wyllie et al., 1984b). It has an obligate requirement for Ca^{2+} and Mg^{2+}, and is activated by millimolar levels of these cations (Hewish and Burgoyne 1973; Vanderbilt et al., 1982; Compton 1991), though submicromolar concentrations can be stimulatory in some instances (Jones et al., 1989), and it is strongly inhibited by zinc (Cohen and Duke, 1984; Giannakis et al., 1991). The cleavage products possess 3'-OH termini (Umansky, 1991; Nikonova et al., 1993), and optimum activity is observed at neutral pH (Table 1.2). Chromatin proteolysis is not a component of its action (Arends et al., 1990; Tomei, 1991). Its activity is upregulated in apoptotic cells (Nikonova et al., 1982; Compton and Cidlowski, 1986). In many instances (Waring et al., 1991), but not invariably (Alnemri and Litwack, 1990), protein synthesis inhibitors can block its activation.

Partial or full purifications of nucleases putatively involved in apoptotic internucleosomal cleavage have been achieved (Table 1.3). The majority seem to be Ca^{2+}/Mg^{2+}-dependent with neutral pH optima, but there are acidic endonucleases lacking an obligate requirement for these cations (Nikonova et al., 1993; Barry and Eastman, 1992; 1993). The latter team

Source[1]	pH optimum[2]	Modulators[3]	Other properties/comments[4]	Reference
a) lymphoid cells				
Mouse B cells, T cells	neutral*	$Ca^{2+}(+)/Mg^{2+}(+)$	MNase ≡	Bachvaroff et al., 1977
Rat thymocytes	i. neutral ii. acidic	i. $Ca^{2+}(+)/Mg^{2+}(+)$, TTI(–) ii. $Ca^{2+}(\sim)/Mg^{2+}(\sim)$	i. γ-irradiation activated; half-life 1-2 h	Nikonova et al., 1982
Mouse thymocytes	neutral*	$Ca^{2+}(+)/Mg^{2+}(+)$, TTI(–), $Zn^{2+}(-)$	similar activity found in mature T cells	Cohen and Duke, 1984
Rat thymocytes	neutral*	GC-activated	ds; ss nicks/gaps absent; MNase ≡	Arends et al., 1990
Chicken thymocytes	neutral*	$Ca^{2+}(+)/Mg^{2+}(+)$, $Zn^{2+}(-)$	GC-activated	Compton, 1991; 1992
Rat thymocytes	neutral*	*see below*	GC-activated; 200 and (late) 10-11 bp products detectable	Vanderbilt et al., 1982
CTLL-2 T cell clone	neutral*	$Ca^{2+}(+)/Mg^{2+}(+)$, $Zn^{2+}(-)$, $Na^{+}(-)$		Nieto and Lopez-Rivaz, 1989
CLL cells, rat splenocytes	neutral*	$Ca^{2+}(+)/Mg^{2+}(+)$, $Zn^{2+}(-)$, TTI(–)		Giannakis et al., 1991
CEM-C7 cells	neutral*	$Ca^{2+}(\sim)$, TTI(~)	ds; 3'-hydroxyl/5'-phosphoryl termini	Alnemri and Litwack, 1990
Rodent thymocytes	neutral*	$Ca^{2+}(+)/Mg^{2+}(+)$	GC-activated; ss nicks; minor 10 bp fragments; DNase I ≡	Peitsch et al., 1993a; 1993b
b) non-lymphoid cells				
Rat/hen liver, chick oviducts, immature erythrocytes	neutral*	$Ca^{2+}(+/-)$, $Mg^{2+}(+/-)$, univalent cations or polyamines(+/–)	biphasic concentration-dependent cation effect; 200 and 10-11 bp products detectable	Vanderbilt et al., 1982
Rat prostate	neutral*	$Ca^{2+}(+)/Mg^{2+}(+)$		Kyprianou et al., 1988
Rat liver	neutral*	$Ca^{2+}(+)/Mg^{2+}(+)$,ATP(+),$NAD^{+}(+)$	submicromolar range cation activation	Jones et al., 1989
Rat liver, kidney	neutral*	$Ca^{2+}(+)/Mg^{2+}(+)$, $Zn^{2+}(-)$	low activity in lung, heart, brain, testis	Giannakis et al., 1991
HL-60 cells, Chinese hamster ovary cells	acidic	$Ca^{2+}(\sim)/Mg^{2+}(\sim)$, $Zn^{2+}(\sim)$, $OH^{+}(+)$ ATA(~)	characterised as DNase II	Barry and Eastman, 1992; 1993

TABLE 1.2 Characteristics of endonuclease activities mediating internucleosomal DNA cleavage in: (a) lymphoid, or (b) non-lymphoid cells.

[1] All endonuclease activities were associated with cell nuclei; CLL = chronic lymphocytic leukemia [2] (*) indicates that profile was not investigated although appreciable activity existed at neutral pH. [3] (+), (–) and (~) respectively indicate stimulation, inhibition or no effect on DNA cleavage; TTI = transcription or translation inhibitor(s). [4] ds; ss = double stranded or single stranded scission, respectively; MNase = micrococcal nuclease; ≡ DNA cleavage profile equivalence; GC = glucocorticoid.

Source[1]	M.W. (kDa)	pH optimum	Modulators[2]	Other properties/ comments	Reference
Rat thymocytes, S49 lymphoma cells	18-25 active > 100 inactive	7.0-8.5	Ca^{2+}(+), Zn^{2+}(–), ATA(–)	i. pI 8.5 (basic protein) ii. descriptor NUC-18	Gaido and Cidlowski, 1991 Caron-Leslie et al., 1991
Rat thymocytes	100-130	neutral	Ca^{2+}/Mg^{2+}(+)	i. acidic protein ii. possible homology with topoisomerase II sub-unit?	Wyllie et al., 1988 Arends and Wyllie, 1991
Rat thymocytes	i. 36-45 ii. 37 iii. 22	i. 6.0/8.0* ii. 5.5-6.0 iii. 6.0-7.5	Mn^{2+}(+), Ca^{2+}/Mg^{2+}(~), Ca^{2+}/Mg^{2+}(~) Mn^{2+}(+), Ca^{2+}/Mg^{2+}(+)	i. loosely bound to nucleus ii. 5'-OH termini; DNase II like iii. in rapid turnover?	Nikonova et al., 1993
Mouse thymocytes	65	7.0-8.0	Ca^{2+}(+), Mg^{2+}(+), Zn^{2+}(–)		Dykes et al., 1987
Human splenocytes, thymocytes, placenta	22-26	8.0	Ca^{2+}(+),Mg^{2+}(+), Zn^{2+}(–), ATA(–)	i. also inhibited by spermine ii. labile enzyme	Ribeiro and Carson, 1993
Rat hepatocytes	27-34	7.4-7.6	Ca^{2+}, Mg^{2+}(+)		Orrenius, personal communication
CHO cells	28-38	5.0	Ca^{2+}(~), Mg^{2+}(~) Zn^{2+}(~)	Homologous with DNase II	Barry and Eastman, 1993

TABLE 1.3 Properties of some purified endonucleases implicated in apoptosis.

[1] All endonucleases were purified from cell nuclei; CHO = chinese hamster ovary. [2] (+), (–) and (~) respectively indicate stimulation, inhibition or no effect on activity. * two pH maxima of 6.0-6.5, and 7.5-8.0, respectively.

1978; Alnemri and Litwack, 1989).

New evidence has implicated another enzyme activity distinct from the above endonuclease in the initial stages of apoptosis. Due to chromatin periodicity (see 1.3.4), digestion of hepatocyte nuclei DNA, or the DNA of thymocytes exposed to A23187 or topoisomerase II-directed agents , proceeds in a stepwise fashion with formation of ≧ 300 kbp, and then 50 kbp fragments (Filipski et al., 1990). The 50 kbp cleavage parallels the first appearance of apoptotic markers and, together with subsequent internucleosomal degradation, but unlike high-order cleavage (700 or 300 kbp), it is dependent on macromolecular synthesis (Walker et al., 1991). Further support for a multistage endonucleolytic process arises from the finding that Zn^{2+} blockade of glucocorticoid-mediated thymocyte apoptosis, whilst arresting internucleosomal fragmentation, does not prevent early chromatin condensation (Cohen et al., 1992) due to the appearance of high molecular weight DNA fragments (Brown et al., 1993). Formation of ≧ 700, 200-250, or 30-50 kbp products were shown to be Mg^{2+}-dependent, the interstage sequential digestion to 30-50 kbp was Mg^{2+}-dependent and Ca^{2+}-facilitated, whilst only the final internucleosomal degradation obligately required both Ca^{2+} and Mg^{2+} (Sun and Cohen, 1994; Cain et al., 1994). These data relate to both thymocyte and hepatocyte systems, and suggest that at least two distinct enzymic processes occur in these cells. The appearance of 300 kbp and then 50 kbp fragments may represent chromatin rosette breakdown with progressive detachment of chromatin loop domains from their anchoring points on the nuclear matrix.

Hepatocyte apoptosis caused by TGF-β1 does not involve oligonucleosomal DNA fragmentation (Oberhammer et al., 1993a). Similar findings have been reported in epithelia (Boe et al., 1991), and other non-lymphoid cell types (Tomei, 1991), which brings into serious doubt the universality of this phenomenon as a biochemical marker of apoptosis. Studies to test this theory (Oberhammer et al., 1993b) have shown that whilst 300 and/or 50 kbp high-order DNA degradation was common to most of the cells examined, and was coincident with morphological apoptotic indicators (e.g. chromatin condensation), internucleosomal cleavage was not invariably present. Similar differences may explain the cell type dependency of internucleosomal degradation in CTL target cells (Duke, 1991; Sellins and Cohen, 1991b). These observations do not detract from the importance of internucleosomal cleavage in the production of marked nuclear chromatin condensation in some cells. For example, this DNA degradation pattern is not detected in thymocytes separated at a transitional apoptotic stage, which exhibit only slight aggregation of heterochromatin, though it appears to be causally related to subsequent gross chromatin compaction (Cohen et al., 1993).

In summary, endonuclease-mediated internucleosomal DNA cleavage in apoptosis, when evident, is an endstage event, though in affected cells it is a common precursor of cell

death. Internucleosomal DNA cleavage is most commonly associated with apoptosis of haemopoietic cells, especially lymphoid lineage, and can be present in non-lymphoid systems, but certain endothelial and epithelial cells do not degrade their genome in this manner. High-order chromatin degradation is an important and consistent feature in several model systems of apoptosis. The enzymes involved in both process are poorly characterised at this time.

1.3.6 Other aspects of the molecular biology of apoptosis

Many examples of apoptosis involve terminally differentiated cells in phase G_0 of the cell cycle, but this is not always the case, and some death-committed cells transit through the cycle before dying by apoptosis (Bursch et al. 1990a). Two forms of apoptosis were observed in Chinese hamster ovary cells injured by cisplatin (Barry et al., 1990); at high drug levels rapid DNA degradation was followed by death, whereas at lower concentrations apoptosis was delayed until cells negotiated the cell cycle to arrest at G_2/M phase. The yeast RAD9 gene provides a cell cycle 'checkpoint' to assess cellular damage, and the search for mammalian homologues is being progressed (Hickman, 1992). Eastman (1990) postulated that mitosis and apoptosis might share similar signal transduction elements and that lethal mitosis could be a form of apoptosis; cell cycle alterations could represent a common type of damage providing an initiating sequence for altruistic cell suicide (Dive and Hickman, 1991).

Abrupt cellular volume reduction has long been recognised as a cardinal identifier for apoptosis (Wyllie, 1987a), and until recently a single stepwise increase in buoyant density was thought to occur (Wyllie and Morris, 1982). The underlying biochemical processes remain obscure but may be brought about by transport of water and ions into migrating endoplasmic reticular cisternae (Arends and Wyllie, 1991). Alternatively, it has been suggested that inhibition of a $Na^+/K^+/Cl^-$ cotransporter could be involved (Wilcock et al., 1988). Studies of radiation-induced thymocyte apoptosis have shown that the volume reduction occurs in two discrete stages (Klassen et al., 1993), and the lost fluid is thought mainly to be water.

The swift engulfment of apoptotic bodies results from recognition of new molecular structures on the surface of the dying cell (Wyllie et al., 1984b; Fesus et al., 1991). Apoptotic thymocytes probably express a glycan determinant rich in exposed N-acetylglucosamine residues, since macrophage binding in vitro can be blocked by this monosaccharide or its dimer, N,N'-diacetylchitobiose (Duvall et al., 1985). The vitronectin receptor (a β3 integrin) of human macrophages is responsible for binding to apoptotic neutrophils via a thrombospondin heterodimer bridge (Savill et al., 1989; 1990). Three general recognition mechanisms, which may function either independently or in concert, are currently known (Dr J Savill, personal communication): (i) interactions with lectin

molecules on phagocytic cells; (ii) formation of thrombospondin linkages; (iii) recognition by phosphatidylserine receptors. In thymocytes, the process apparently involves loss of terminal glycoprotein sugar residues, e.g. sialic acid; N-acetylneuraminic acid (Morris et al., 1984), thus exposing previously cryptic carbohydrate moieties which can then interact with lectin-like macrophage receptors. Alternatively, recognition could be due to exposure of incompletely synthesised glycoproteins upon eversion of endoplasmic reticulum or golgi vesicles at the cell surface (Wyllie, 1987a).

Apoptotic bodies contain highly cross-linked protein scaffolds due to the action of the ubiquitous Ca^{2+}-dependent tissue transglutaminase found in mammalian cells (Fesus et al., 1991). For example, apoptotic hepatocytes become insoluble in detergents and resistant to chaotropic agents due to the formation of ε-(γ-glutamyl)lysine and N^1, N^8-bis(γ-glutamyl)spermidine protein cross-linkages (Fesus et al., 1989). Expression and activation of tissue transglutaminase is therefore a common endstage event of apoptosis in various systems including tumour cells, and correlates with the apoptotic index (Piacentini et al., 1991). It is likely that this process is a safety device to prevent loss of the cellular contents from dying cells.

Very little is known about the inevitable cytoskeletal changes that occur during apoptosis (see also section 5.1.2). The major microtubule, microfilament and intermediate filament components of the cytoskeleton are linked together via bridging molecules like tropomyosin or α-actin (Alberts et al., 1989) to form a coordinated microtrabecular network. This in turn has physical and biochemical connections with other cellular components, e.g. biomembranes and organelles, and intracellular signalling pathways including those employing Ca^{2+} and nucleotides. Since apoptosis is such a dynamic process the cytoskeleton surely plays a key part in its progression. Terminally injured cells treated with microfilament inhibitors cannot form apoptotic bodies (Cotter et al., 1992) which strongly suggests that microfilaments are involved in this process. The altered tubulin expression that occurs during apoptosis (Strickland et al., 1992) may implicate microtubules in shape changes such as apoptotic body budding and nuclear invagination.

1.4 T LYMPHOCYTE ONTOGENY AND APOPTOSIS

1.4.1 The thymus; thymocytes and T cells

The following is a synthesis of material from reviews by Ritter and Crispe (1992), Revillard (1990), Alberts et al. (1989) and Taylor and Cohen (1992). Though much of this knowledge derives from rodent studies, there is acceptance of its broad applicability to other systems including that of humans.

The role of the vertebrate thymus as a primary lymphoid organ, is to provide the appropriate environment to allow cells of T lymphocyte lineage to generate their antigen

receptor repertoire, and hence achieve immunocompetence, and at a population level to become major histocompatibility complex (MHC) restricted and tolerant to self. Implicit within this system are the intrathymic processes of T cell development, selection, proliferation and maturation, which culminate in cell exit from the thymus to form the peripheral circulating mature T cell pools central to cell mediated immune function. Though the thymus is most important in fetal and neonatal life when the T cell complement is established, and it undergoes partial involution in adult animals, its structure and function are conserved which may represent a low grade T lymphocyte maintenance capability.

In mammals, the thymus is a bilobed organ located in the anterior aspect of the thoracic cavity proximate to the heart. At the histological level, three main thymic areas can be distinguished: (i) the subcapsular region underlying the connective tissue capsule; (ii) the highly cellular cortex; (iii) the less densely packed central medulla which is separated from the cortex by a distinct cortico-medullary junction. Two major cell groups are evident, viz. the lymphoid and stromal cell populations. Thymic T lymphocytes (thymocytes) are the most numerous cell type; approximately 5% of these are large dividing blast forms located in the subcapsular region, whereas the majority (80-85%) of predominantly non-dividing thymocytes reside in the cortex, with the remaining 10% located in the medulla. Stromal cells provide the thymic support microenvironment for thymocytes. A heterogeneous family of epithelial cells comprised of six sub-types form the major component, and most engage in cell-cell interactions with developing thymocytes, or in the case of those in the medulla, secrete trophic thymic hormones. Type 2 epithelia, the thymic nurse cells, envelop pockets of thymocytes. Concentric whorls of epithelial cells (Hassall's corpuscles) of uncertain function are characteristic medullary features. Macrophages and dendritic cells (interdigitating cells) are the other major stromal types. Cortical macrophages show the highest activity levels, and in the immature thymus most contain engulfed thymocyte apoptotic bodies, whereas the cortico-medullary and medullary sub-types are more quiescent. Macrophage-mitotic lymphocyte rosettes indicate that macrophage interaction also plays a part in control of thymocyte proliferation. Functional aspects of the thymic microenvironment are poorly understood at present, but are thought to comprise of direct cell-cell interactions, and also the production of cytokines (particularly stimulatory interleukins) and thymic polypeptide hormones, e.g. thymulin and thymosin, which influence T cell maturation.

Thymocyte progenitors (haemopoietic stem cells) derived from the bone marrow or foetal liver, are attracted by chemotactic factors from thymic epithelia, and enter the thymus where they are thought to be committed to T cell lineage. Aspects of thymocyte ontogeny and differentiation are dealt with in section 1.4.2. T cells develop into different subpopulations which can be distinguished by their phenotypic cell surface glycoprotein molecules, often referred to by the cluster of differentiation (CD) marker classification.

Some mature T cells are $CD4^+$, which predominantly represent helper cells that secrete cytokines to activate other T cells, B cells or macrophages, though a smaller cytotoxic subset also exists. The rest express instead $CD8^+$, and are mainly cytotoxic cells (CTL). In contrast, about 85% of thymocytes express both markers and these $CD4^+CD8^+$ predominate in the cortex, together with about 2-4% $CD4^-CD8^-$ cells. The remainder, are medullary cells approximating to the mature phenotypes. Two types of specific antigen receptors (TcR), which are membrane-bound heterodimeric polypeptides, are expressed on distinct subsets of mature T cells. Most bear $\alpha\beta$ TcR, whilst a minor population of cytotoxic T cells that resemble NK cells (not MHC restricted and less specific killer properties) carry $\gamma\delta$ receptors. The TcR is associated with an invariant CD3 complex comprised of five polypeptide chains; γ, δ, ε, ζ and η, which serves to transduce the signal produced by TcR interaction by means of tyrosine kinase and phospholipase C linkage. A continuum of TcR expression is evident in thymocytes paralleling their developmental station, through null to low, and then high TcR levels.

1.4.2 Thymocyte maturation (ontogeny)

During intrathymic development thymocytes undergo three major events. Initially, the specificity of individual cells is determined by rearrangement of β then α TcR chain genes, followed by surface expression of the receptor (Ritter and Crispe, 1992). Then thymocytes are subjected to separate positive and negative selection processes (Blackman et al., 1990) designed to ensure that firstly, only cells whose TcR-CD3 complex fits a self MHC complex are allowed to mature (MHC restriction), and secondly, that cells possessing TcR with too high an avidity for self antigens (autoreactives) are clonally deleted (negative selection).

Thymocyte maturation actually represents a continuum of cell differentiation to endstage mature T cells, but it can be followed as a sequence of phenotypically distinguishable subsets. In addition to TcR$\alpha\beta$-CD3, the adhesion molecules CD4 and CD8, which bind to class II and I MHC molecules (Blackman et al., 1990), respectively, have principally been used to characterise the course of this differentiation. The process is highly complex, and remains incompletely understood; but recent studies in foetal rodents (e.g. Scollay et al., 1988; Kampinga and Aspinall, 1990) have allowed the development of an outline schema (summarised in Fig. 1.4). After thymic acquisition of lymphocyte stem cells ($CD3^-TcR^-CD4^-CD8^-$), these progenitors develop via CD44, Thy-1, CD2 bearing cells into the $CD4^-CD8^-$ (double negative) subset. Approximately half the $CD4^-CD8^-$ population express the early CD2 marker (Kampinga and Aspinall, 1990) capable of interacting with the LFA-3 ligand on thymic epithelial cells, which probably provides a proliferative stimulus. Double negative cells differentiate into $CD4^+CD8^+$ (double positive) thymocytes, via a transient TcR-low-positive $CD4^-CD8^+$ stage (Scollay et al., 1988), and possibly also from an immature $CD4^+CD8^-$ subpopulation. In the rat, these precursor $CD4^-CD8^+$ cells can be

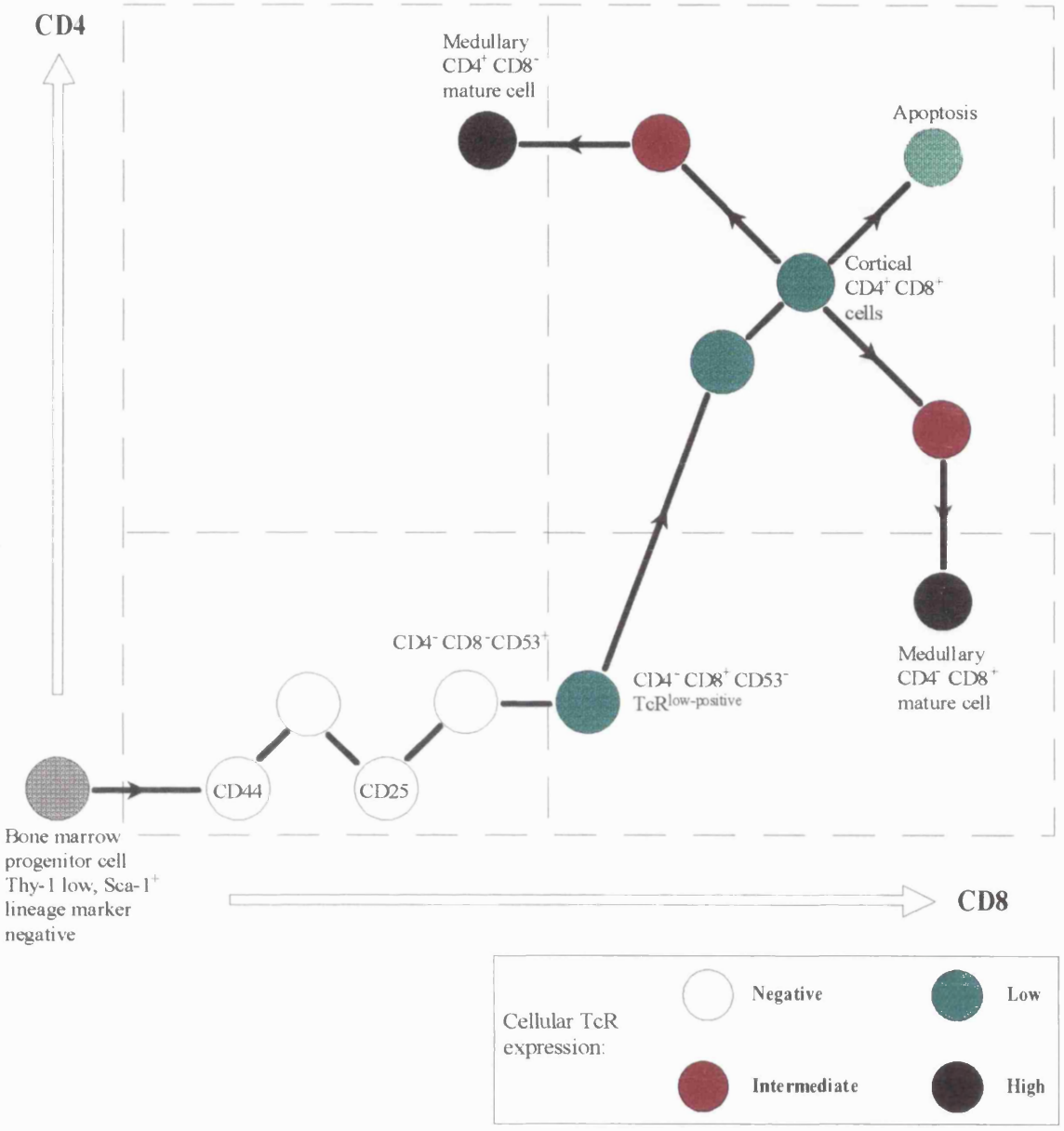

FIGURE 1.4 The developmental differentiation pathway of rodent thymocytes.
The depicted sequence is considerably simplified, and shows only principal CD molecule and TcR expression. Some minor thymocyte subpopulations have been excluded.

distinguished from their mature medullary counterparts by the absence of the CD53 (OX-44) molecule (Patterson et al., 1987). Double positive cells, which as mentioned previously account for the majority of all thymocytes, either survive the intrathymic selection processes and become mature functionally competent $TcR^+CD4^+CD8^-$ or $TcR^+CD4^-CD8^+$ cells, or else they die by apoptosis (Scollay et al., 1988; Rothenberg, 1990). When these phenotypic changes occur in the foetus, the size of the thymus markedly increases, e.g. in the mouse from 1000 cells at day 13 of gestation to 10 million cells at day 18-19 (Ritter and Crispe, 1992); in adult animals cell differentiation and maturation is accomplished in 3-4 days.

The cortical epithelium plays a critical part in the positive selection of MHC-restricted T cells (Ritter and Crispe, 1992) via the TcR, MHC and CD4 or CD8 molecules. However, the identity of the components responsible for inducing negative selection and clonal deletion remains unclear; bone marrow-derived antigen presenting cells apparently possess this capability, but are not solely responsible (Blackman et al., 1990), and medullary epithelial cells, or possibly even any cell bearing the appropriate combination of antigen and self-MHC may be involved. Interdigitating cells are thought to play a crucial role in thymocyte interactions at MHC level, $ED1^+/ED2^+$ intrathymic macrophages are involved in acceleration of thymocyte maturation and proliferation, whilst $ED1^+/ED2^-$ macrophages phagocytose dying thymocytes (Kampinga and Aspinall, 1990).

1.4.3 Aspects of thymocyte negative selection and T cell apoptosis

Maturation of mammalian thymocytes depends on their avoidance of two types of deletional death by apoptosis. One form is negative selection during tolerance development, i.e. the removal of cells whose TcR reacts too strongly with self (Kisielow et al., 1988); the other is death by default, due to failure of selection of cells with defective TcR or receptors inappropriate for binding MHC structures (Blackman et al., 1990). The random TcR gene recombination germline which forms the diverse repertoire of TcR positively selected to recognise antigen plus self MHC, clearly includes many autoreactive receptors which must be eliminated to prevent disastrous autoimmune consequences for the host. Studies of weanling mice have shown that 50 million cells, mainly of cortical phenotype, die each day (Rothenberg, 1990), and possibly as few as 1% of the thymocyte pool emigrates to the periphery as mature cells (Scollay et al., 1988). In vivo (Kisielow et al., 1988) and organ culture (Smith et al., 1989) investigations have implicated the immature $CD4^+CD8^+$ cells as the main target population for elimination. This is in keeping with their apparently highly primed state for apoptosis triggered by various pathophysiological agents (McConkey et al., 1989c), and their susceptibility to death triggered by interaction with intra- or even extrathymic antigen presenting cells provided the latter carry appropriate antigen and MHC molecules (Swat et al., 1991). However, apoptosis can be induced in other immature subsets, such as autoreactive transitional

$CD4^+CD8^-$ thymocytes (MacDonald and Lees, 1990), and also more primitive $CD4^-CD8^-$ cells (Smith et al., 1989), suggesting that a death pathway is open for a considerable proportion of cortical development. Under such physiological circumstances, the apoptotic program seems to be primarily modulated via CD3/TcR, hence antibodies to CD4 or Thy 1, or stimulation of incompletely formed TcR do not initiate death (Smith et al., 1989). It has also been suggested that autoreactive thymocytes could be deleted by stromal cell interaction with the Fas antigen on their surface (Watanabe-Fukunaga et al., 1992).

Though the αβTcR determines both positive and negative selection, as well as T cell activation in the periphery, the manner in which this unchanging receptor can produce such dramatically different responses is just starting to be understood. A key pathway in T lymphocyte apoptosis and activation is mediated by transient, moderate elevations in $[Ca^{2+}]_i$ (McConkey and Orrenius, 1991). Immature TcR bearing thymocytes appear to exist in two forms (Marrack et al., 1989; Finkel et al., 1991); in the first, receptor engagement does not increase $[Ca^{2+}]_i$ and consequently antigen binding does not lead to apoptosis. At another, probably later stage, receptor binding leads to Ca^{2+} flux and death. The nondeletable and deletable pools appear to differ in the extent of the coupling between their TcR αβ polypeptides and the signal-transducing CD3 complex (Marrack et al., 1989). This is borne out by the finding that TcR engagement kills a similar proportion of cells to the number able to mobilise Ca^{2+} after such a stimulus (Finkel et al., 1991); ligation of CD3 bypasses the need for αβTcR coupling and hence kills many more cortical cells. The looser form of coupling may be more permissive of MHC binding, and therefore useful during preceding positive selection processes. In another model, presently lacking adequate substantiation, additional signals delivered by accessory cells are postulated to activate PKC-modulated events and thereby salvage thymocytes from TcR-induced, Ca^{2+}-mediated apoptosis (McConkey et al., 1990c).

Activation control of the endogenous apoptosis program is not limited to intrathymic development. Calcium ionophores, alone or with phorbol esters, strongly induce apoptosis in immature T lymphocytes (Kizaki et al., 1989; Iseki et al., 1991), whereas mature T cells are resistant to apoptotic death (McConkey et al., 1989c), and in the latter case the combination actually acts as a co-mitogen (Truneh et al., 1985). Similarly, appropriate presentation of antigen, and accessory cell cytokines, to mature T cells in the periphery allows TcR engagement with phospholipase C activation, phosphoinositide hydrolysis, InP_3 and DAG formation, resultant Ca^{2+} mobilisation and PKC activation, and downstream signalling leading to cellular proliferation and lymphokine secretion. However, following primary antigenic stimulation, the link between the TcR and the death program is re-established in mature T cells (Russell et al., 1991). This suggests that the apoptotic program is conserved, albeit latently, in fully differentiated peripheral T cells, with obvious homeostatic implications. The reason why increased $[Ca^{2+}]_i$ alone produces apoptosis in

cortical thymocytes, but anergy in unstimulated peripheral T cells (McConkey and Orrenius, 1991) is not well defined. Mature T cells possess activatible constitutive endonuclease activity (Cohen and Duke, 1984; McCabe et al., 1993), and therefore supplementary signal transduction controls may check its actuation in this situation. It is notable that Bcl-2, a repressor of apoptotic death (see 1.3.1), is present in surviving medullary thymocytes, but absent in the cortical cells subject to massive clonal deletion (Korsmeyer, 1992).

Akbar and colleagues (1993) have suggested that Bcl-2 has a pivotal role in mature T cell homeostasis. Antigen primed $CD4^+$ and $CD8^+$ cells of $CD45^+RO^+$ phenotype express low levels of Bcl-2 compared to their quiescent $CD45^+RA^+$ counterparts, and hence the former are prone to apoptosis. Two benefits potentially accrue from such a mechanism. Firstly, unwanted effector cells that are activated and clonally expanded could be removed after cessation of antigenic threat. Secondly, low grade apoptosis of memory cells balanced by proliferation would allow dynamic regeneration of these key T cells from freshly stimulated precursors; stromal cell interactions may also spare a proportion of primed $CD45^+RO^+$ T lymphocytes. Akbar et al. point out that these suggestions are consistent with recent findings on T cell lifespan and kinetics. From other work, it appears that *bcl-2* and the *Fas/Apo-1* genes may have reciprocal roles in lymphocyte survival after activation, although other pathways, e.g. IL-2 signalling must also be involved.

In summary, apoptosis during negative selection represents a mechanism for cell deletion without disruption of the surrounding milieu and the finely balanced process of T cell immunocompetence development. There is also growing evidence to implicate control of the endogenous T cell death pathway as a homeostatic device in post-developmental life.

1.5 CYTOTOXIC MODEL COMPOUNDS

Several cytotoxic compounds served as reference positive controls in the investigations described in this thesis. They included (i) methyl prednisolone, a glucocorticoid hormone possessing specific lymphotoxicity; (ii) A23187, a divalent cation ionophore toxic to a variety of cells and capable of inducing lymphocytolysis; and (iii) nocodazole, a microtubule disrupting agent with activity against most interphase and mitotic cells. Many previous reports implicate the first two agents in the activation of thymocyte or mature T cell apoptosis, and nocodazole has also recently been recognised as an activator of apoptotic cell killing. Chemical structures for these substances are depicted in Figure 1.5, and brief commentaries on aspects of the biological activity are given below.

1.5.1 Glucocorticoids

Glucocorticoids are steroid hormones synthesised by the zona fasciculata of the adrenal cortex. Corticosterone is the principal natural glucocorticoid of rats, mice and rabbits,

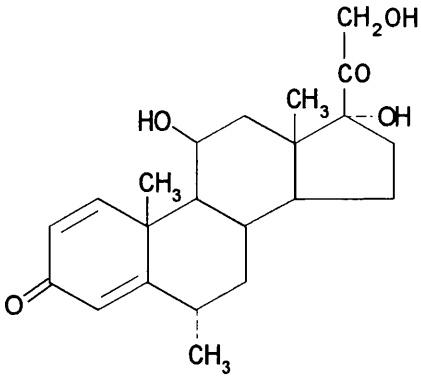

Methylprednisolone; 11,17,21-trihydroxy-6-methyl-
-1,4-pregnadiene-3,20-dione (CAS no. 83-42-2; hemisuccinate salt 2375-03-3)

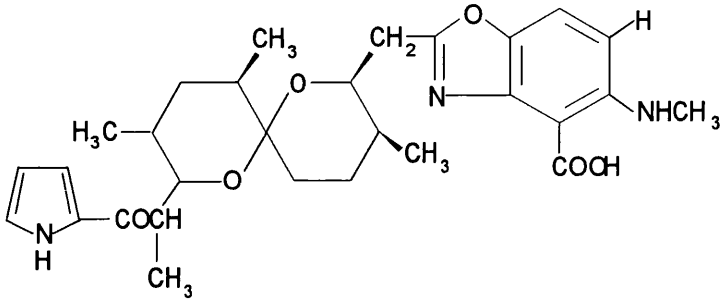

Calcimycin; Calcium ionophore A23187 free acid (CAS no. 52665-69-7)

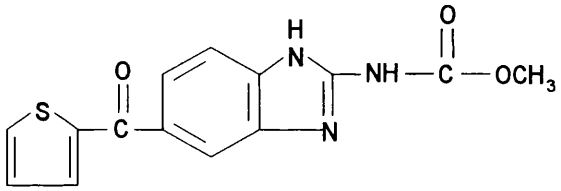

Nocodazole; Janssen Pharma R17934;
Methyl [5-(thienylcarbonyl)-1H-benzimidazol-2-yl] carbamate (CAS no. 31430-18-9)

FIGURE 1.5 Chemical structures of lymphotoxic reference compounds.

whilst the counterpart in primates and guinea pigs is cortisol (hydrocortisone), and there are numerous synthetic glucocorticoids, e.g. dexamethasone and methylprednisolone, which all have comparable activity in qualitative terms. After diffusion through cell plasma membranes they bind tightly, but reversibly, to specific cytosolic receptor proteins, and upon translocation to the nucleus this complex upregulates transcription of a small number of genes, the *primary response*, followed by secondary gene expression and protein formation (Alberts et al., 1989). The DNA binding domain of the receptor is masked by heat shock protein 90 until hormone interaction causes its dissociation (Bowen and Bowen, 1990). Glucocorticoids have pleiotropic effects in mammalian cells at nanomolar concentrations, but in lymphoid cells they are antiproliferative, suppress immune effector processes, and cause cytolethality (reviewed in Munck and Crabtree, 1981). Morphology changes stereotypic of apoptosis were noted by early investigators of glucocorticoid-induced lymphoid cell death (Kerr et al., 1972; Robertson et al., 1978). It is now

recognised that these hormones activate apoptosis in thymocytes, immunoactivated T lymphocytes, and lymphomas and leukemias of T cell origin (Umansky et al., 1981; Wyllie and Morris, 1982; Galili et al., 1982; Vedeckis and Bradshaw, 1983; Bansal et al., 1991). Cell killing by glucocorticoids requires intracellular receptor binding and activation; competitive antagonists, e.g. RU486, prevent apoptotic DNA degradation (Compton et al., 1987), and lymphoma cell mutants lacking a functional receptor do not undergo apoptosis (Wyllie et al., 1984a; Caron-Leslie et al., 1991).

Rodent cortical thymocytes are acutely sensitive to killing by glucocorticoids, in vivo (Compton and Cidlowski, 1986) and in vitro (Morris et al., 1984). The process is dependent on Ca^{2+}/Mg^{2+} and protein synthesis (Kaiser and Edelman, 1977; McConkey et al., 1989b), and involves rapid internucleosomal DNA cleavage, that precedes eventual viability loss (Schwartzman and Cidlowski, 1991). Glucocorticoid exposure results in burst rate *de novo* synthesis of a few proteins (Voris and Young, 1981), and it has been claimed that some of these correspond to expression of a 'death gene',.whose product is an endonuclease (Compton et al., 1987). However, this has been a matter of dispute (Alnemri and Litwack, 1989) and counter-claim (Gaido and Cidlowski, 1991). The latter investigators characterised a protein (NUC18) from apoptotic glucocorticoid-treated cells with properties closely corresponding to a putative constitutive endonuclease activity responsible for internucleosomal cleavage of thymocyte genomic DNA. Thymocyte apoptosis is of pathophysiological relevance in vivo, since stress-induced glucocorticoid release in rodents via the pituitary-adrenal axis results in rapid cortical thymocyte depletion and thymic involution (Munck and Crabtree, 1981), whilst adrenalectomy results in thymic hypertrophy.

1.5.2 Divalent cation ionophores

A23187 (calcimycin), a polyether carboxylate antibiotic derived from *Streptomyces chartreusensis*, has been extensively used as a divalent cation ionophore in biological systems (Pressman, 1976), particularly in respect of Ca^{2+} transport. It is highly selective for divalent over univalent ions, and forms a two molecule complex which greatly facilitates cation entry through biomembranes. The following order of specificity has been observed for A23187: $Mn^{2+} >> Ca^{2+} > Mg^{2+} >> Sr^{2+} > Ba^{2+}$, and the relative binding affinities have been calculated as: Mn^{2+} 210.0, Ca^{2+} 2.6, Mg^{2+} 1.0 (Calbiochem, 1990). It may also bind other cations e.g. Cu^{2+}, Fe^{2+} and Zn^{2+}.

A23187 has been widely used to manipulate cellular Ca^{2+} levels, and Ca^{2+}-dependent processes, especially in the context of cell proliferation. This ionophore, used in tandem with PKC activators, acts as a mitogenic stimulus in T lymphocytes (Truneh et al., 1985). Alternatively, in the presence of extracellular Ca^{2+}, A23187 and its analogues can be

cytotoxic to many cells (Farber, 1990; Nicotera et al., 1986; Hardwick et al., 1992), and necrosis thus caused is probably directly attributable to markedly increased $[Ca^{2+}]_i$. A23187 also causes Ca^{2+}-dependent lymphocytolysis (Kaiser and Edelman, 1977; 1978; Durant et al., 1980). At low concentrations of ionophore the death mode involved in thymocyte killing has been characterised as apoptosis, since internucleosomal cleavage occurs and the process is dependent on protein synthesis (Wyllie et al., 1984a; McConkey et al., 1989a). Though mature T cells exhibit an equivalent elevation in $[Ca^{2+}]_i$ after exposure, they are relatively resistant to A23187-activated apoptotic killing (McConkey et al., 1989c; Kizaki et al., 1989). Non-lymphoid cell types can also be killed via apoptosis induced by this agent (Lennon et al., 1991). The impact of other divalent cation carriage by A23187 on thymocyte apoptosis is currently uninvestigated.

1.5.3 Microtubule disrupting agents

Mammalian cell microtubule (MT) arrays are highly dynamic, and are functionally dependent on their assembly and disassembly kinetics (Alberts et al., 1989). The action of MT-directed compounds can broadly be classed into: (i) polymerisation inhibitors with a specific tubulin binding site (e.g. colchicine, colcemid and nocodazole); (ii) inducers of paracrystalline tubulin aggregates (e.g. vinblastine and vincristine); (iii) and tubulin polymer stabilisers (e.g. taxol). They have a pronounced anti-mitotic action, and recently it has been recognised that some MT-disruptors have the ability to initiate apoptosis (Cotter et al., 1990). The role of the cytoskeleton in apoptosis is discussed further in section 5.1.2. Several questions remain to be answered regarding the cytotoxicity of these compounds. Firstly, it is not clear whether the toxicant-induced collapse of the MT cytoskeleton is a causal event in apoptosis. In addition, the differential capability of MT-disrupting agents to cause cytolethality either by apoptosis or necrosis is not well established. Lastly, associations exist between the major cytoskeletal elements, and agents thought to be specific for MT, e.g. colchicine, can also cause changes in microfilament and intermediate filament distribution (Sager et al., 1984)—the significance of these effects is unclear.

Bisbenzimidazole carbamates typified by nocodazole are useful antimicrotubular agents since their action is fully reversible, unlike that of colchicine. Nocodazole binds specifically to tubulin (K_i of 9.5×10^{-6} M), causing rapid MT disassembly, increases in the intracellular tubulin monomer pool, and decreased tubulin synthesis (Syversen et al., 1984). Its binding is reversible and competes with that of colchicine (Horwitz et al., 1986). There are indications that it is more specific than colchicine, colcemid, or vinca alkaloids (De Brabander et al., 1976). Unlike the latter agents, few studies exist on the mechanisms of nocodazole cytolethality. However, apoptosis is activated in the promyelocytic HL-60 cell line when exposed to relatively high concentrations of nocodazole (Martin and Cotter, 1990).

1.6 TRIORGANOTINS

1.6.1 Chemistry, physicochemical properties and applications

Organotins are compounds that contain at least one covalent carbon-tin bond. The subgroups essentially consist of mono-, di-, tri- and tetrasubstituted members; $RSnX_3$, R_2SnX_2, R_3SnX or R_4Sn, respectively, where R is an alkyl or aryl group and X is an anionic substituent. Although tin may exist in either the Sn^{2+} or Sn^{4+} oxidation state, almost all organotins have a tetravalent structure. All the alkyltins described in this work contain unbranched, saturated hydrocarbon side-chains (n-alkyltins). In terms of economic importance and environmental exposure, the di- and triorganotins are the most important—the structure of the principal compounds is shown in Fig. 1.6.

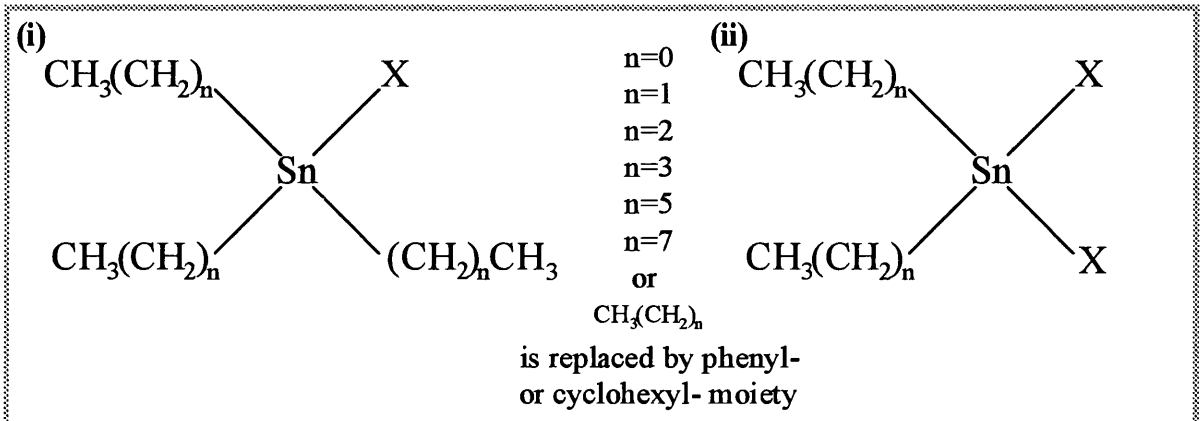

FIGURE 1.6 The chemical structure of (i) tri- and (ii) diorganotin compounds.
Sn = the central tin atom in the 4+ oxidation state, X = a singly charged anion or organic group; commonly chloride, bromide, fluoride, oxide, hydroxide, carboxylate or thiolate. For the structure of bis(tri-n-butyltin) oxide [TBTO] see Fig. 3.1.

Solubility data for organotins are incomplete. Their solubility in water at ambient temperatures ranges from 5-50 mg/l and is dependent on pH, temperature and ions present in solution. For TBTO, values of 0.7-7 mg/l (20°, pH 5-7) are cited for distilled water, whereas in salt water 8-10 mg/l is typical (IPCS, 1990). In solution under physiological conditions, TBT is thought to exist as three primary species (hydroxide, chloride and carbonate) in equilibrium. The view is widely held that at the level of cellular interaction, anionic moieties attached to the tin atom are not of prime importance (Byington et al., 1974) since the organotins will exist either as cations (TBT^+, DBT^{2+}), as the salts mentioned above, or be bound to cell macromolecules (Maguire, 1987; Penninks et al., 1990). The octanol/water partition coefficients (log P_{ow}) of a number of triorganotins are known (Wulf and Byington, 1975), and range from 0.3 for TMTC to 4.1 for TPhTC. At 25° the value for TBTC is 3.1, whereas for TBTO it is between 3.2-3.8 for distilled water, and 3.5 in sea water. The vapour pressure of TBT compounds is very low (approximately 1×10^{-3} Pa at 20°), and loss from aqueous solutions is correspondingly minimal. TBTO binds strongly to particulate matter; the published absorption coefficients span from 110 to 55 000 (IPCS, 1990). Space constraints permit mention of only a few aspects of chemical behaviour pertinent to their biological activity. It has been concluded that, in contrast to

the diorganotins, triorganotins possess low thiol reactivity (Boyer, 1989). Other contrary reports (Byington et al., 1974; Marinovich et al., 1990a) suggest that some interaction with protein thiol groups may occur. Interaction with DNA and RNA has also been stated to be minimal (Aldridge and Street, 1964), though this is incompletely investigated.

After the first systematic explorations of organotin chemistry in the 1950s, particularly by Van der Kerk and co-workers (Van der Kerk and Luijten, 1954), the commercial use of organotins rapidly expanded. The annual world production rose from a total of 50 tons in 1950 to 25 000 tons in 1975 (Van der Kerk, 1976), and was 35 000 tons in 1986 (Maguire, 1987). Trisubstituted compounds, especially TPT, TBT and TPhT, have primary applications as industrial biocides, since they demonstrate high fungicidal, antibacterial and molluscicidal properties. TBT, and in particular TBTO, has been extensively employed for wood preservation, in marine antifouling coatings, and as a slimicide. Antifouling marine paints function partially by continuous slow release of TBT into the water proximate to the protected hull, and it has been calculated that a single tanker-sized ship could release up to 280 g of organotin per day (Schrantz, 1990). Due to concerns over environmental impact and toxicity (see 1.6.3-1.6.5) some of these uses are now restricted or being phased out. However, recent production of TBTO has been considerable, with the USA alone manufacturing 4 100 tonnes per annum in 1986, and at one stage 215 biocidal formulations containing TBT were approved in the United Kingdom under the Control of Pesticides regulations (MAFF/HSE database for 1988). In 1980 the WHO suggested that TBTO and TPhT compounds might prove useful for the control of the schistosoma parasite vectors, which prompted detailed investigations of the mammalian toxicity of TBTO (Krajnc et al., 1984; Vos et al., 1990; Krowke et al., 1986).

1.6.2 The growing problem of sub-mammalian ecotoxicity

During the last decade, the possible environmental hazard of triorganotin compounds has become a matter of major concern. TBT levels in water, sediments and biota in harbours, estuaries and marinas have increased in parallel with the use of organotin antifouling paints. In addition, ecotoxicity studies showed that TBT exposure produced pronounced toxicity in a range of organisms. The effects included shell malformations in bivalves; imposex changes in gastropods; early developmental abnormalities in amphipod, mussel and fish larvae; and gross systemic toxicity and pathological abnormalities in mature marine fish (reviewed in IPCS, 1990; Maguire, 1987). Acute mortality was noted at TBT concentrations of 0.1-5 ppb for zooplankton (Hall and Pinkney, 1985), whereas water analytic data indicated that in some areas TBT and DBT levels reached as high as 60 ppb generally, and up to 2.6 ppm in the surface microlayer. Developmental toxicity occurred in the most sensitive oyster species at 50 ng l^{-1} TBT. By the early 1980s, a decline in productivity of the French and English oyster fisheries was noticed, and regulatory action ensued to control the problem. Most countries have now taken steps to ban TBT

preparations on small boats (< 25 m), though its use continues on larger vessels. Lipophilic compounds such as TBTO are a concern due to bioaccumulation within the food chain (bioconcentration factors varying between 100-30 000 have been reported).

1.6.3 Mammalian toxicity of the trisubstituted organotins

For organotins as a whole, their toxicity decreases from tri- to monoorganotins. Tetraorgano- compounds closely resemble the triorganotins, though their effects are delayed in onset—it has been suggested that this is due to preceding metabolic dealkylation (Snoeij, 1987). In broad terms, the acute toxicity of triorganotins is inversely proportional to the n-alkyl chain length, such that TMT and TET are the most toxic. TPT and TBT, along with TPhT, exhibit similar effect specificity and potency, whilst trioctyltin compounds are essentially non-toxic. Variation in the anionic substituent usually has little influence, and for TBT homologues this is borne out by their acute toxicity indices (Table 1.4).

In rodents and other experimental species, the principal target system of TMT and TET is the nervous system. TMT is a potent and persistent neurotoxicant causing a number of effects including tremor, hyperexcitability, aggression, convulsions and death (Barnes and Stoner, 1958). Neuronal necrosis in specific areas of the CNS occurs in rats given low oral doses (Bouldin et al., 1981); the hippocampus and pyriform nucleus being particularly affected. Other CNS areas and neurotransmitter levels are also affected (reviewed in Snoeij et al., 1987), and occupationally exposed humans exhibit psychomotor disturbances. In contrast, TET compounds produce interstitial oedema of the white matter of the brain and spinal cord (Leow et al., 1979), with myelin involvement and resultant behavioural abnormalities and neurological dysfunction. A tragic contamination of the medicinal diethyltin preparation Stalinon with triethyltin caused a mass poisoning in man involving fatal cerebral oedema (Alajouaine et al., 1958). However, the precise mechanism of TMT

TBT(X)	LD_{50} (mg/kg)	LD_{50} (mmol TBT/kg)
fluoride	94	0.30
chloride	122	0.38
oxide	127; 87[1]	0.42; 0.29[1]
benzoate	99; 203[1]	0.24; 0.49[1]
linoleate	190	0.34
naphthenate	224	0.37
di-n-butyltin dichloride	219; 126; 112-182	
tetra-n-butyltin	>4000	

TABLE 1.4 Acute oral toxicity of some tri-n-butyltins in the rat: comparison with other model organotins.

Adapted from Henschler, 1991; Snoeij, 1987, and RTECS, 1993. [1] Separate experiments.

or TET action is unknown. Neurotoxicity does not usually result from oral administration of higher trisubstituted homologues, though it is possible that the lethality observed after i.v. administration of TPT or TBT (Snoeij, 1987) may involve such an effect.

The predominant effects of TPT and TBT centre on the immune system (see section 1.6.5). Injury of the liver and bile duct have been noted in rodents and dogs after oral administration of TBT compounds (Barnes and Stoner, 1958; Krajnc et al., 1984; IPCS, 1990). The principal lesion is inflammation and hyperplasia of the bile duct, but hepatocellular necrosis has also been described, and it is likely that local bioconcentration due to biliary excretion of TBT or DBT metabolites is responsible.

Scant data is available on genotoxicity and carcinogenicity except in the case of TBTO. Mutagenicity was absent in bacterial or yeast point and frameshift mutation detection systems, as were chromosomal aberrations, clastogenic or dominant lethal activity (IPCS, 1990). A recent, as yet, unconfirmed report indicated that several organotin compounds, including TBTC and TBTO, were direct-acting mutagens in a modified *S. typhimurium* mutagenicity assay (Hamasaki et al., 1993). In vitro investigations have shown that organotins such as TMT, TBT and TPhT may be capable of inducing aneuploidy (Jensen et al., 1991). Increases in endocrine organ tumours observed in long-term feeding studies with TBTO in the rat were evident only at levels that caused immunosuppression and endocrinological disturbances, and were considered to be of questionable significance (Wester et al., 1990). In vivo, TBTO does not cause embryotoxicity at sub-maternally toxic doses; however, low concentrations (50 nM) introduced into ex vivo mouse limb bud cultures interfered with morphogenetic differentiation (Krowke et al., 1986).

1.6.4 Effects of triorganotin compounds on lymphoid tissues and functions

Due to their differential selective effects on the thymus and cell mediated immunity, the immunotoxicity of some triorganotin compounds, and their corresponding disubstituted homologues, has been extensively studied and reviewed (Penninks et al., 1990; Boyer 1989; Vos and Penninks, 1987; Penninks et al., 1991). Comparative assessments of structure activity relationships for induction of thymic atrophy (see Table 1.5), and comprehensive profiles of the functional immunotoxic effects of certain triorganotins now exist (Table 1.6). The following text focuses on trialkyltins, and in particular TBT compounds. Consideration of dialkyltin thymotoxicity is included in Chapter 6 due to the metabolic and mechanistic interrelationships that exist between these organotin subgroups.

The first report that triorganotins could cause adverse effects on the lymphopoietic system came from short-term studies conducted by Verschuuren et al. (1966) in young rats and guinea-pigs using triphenyltin derivatives. They observed that low dietary levels produced atrophy of the thymus and spleen which correlated with decreased numbers of lymphocytes

Compound	Relative activity	Compound	Relative activity	Compound	Relative activity
Triorganotins		*Diorganotins*		*Monoalkyltins*	
Trimethyltin chloride	–	Dimethyltin dichloride	–		
Triethyltin chloride	–	Diethyltin dichloride	+	Mono-n-butyltin trichloride	–
Tri-n-propyltin chloride	++	Di-n-propyltin dichloride	++	Mono-n-octyltin trichloride	–
Tri-n-butyltin chloride	+++	Di-n-butyltin dichloride	+++		
Bis(tri-n-butyltin) oxide*	+++				
Tri-n-hexyltin chloride	+	Di-n-hexyltin dichloride	++	*Tetraalkyltins*	
Tri-n-octyltin chloride	–	Di-n-octyltin dichloride	+++	Tetra-n-octyltin	–
		Di-n-dodecyltin dibromide	–		
Triphenyltin chloride	++	Diphenyltin dichloride	+		

TABLE 1.5 Structure-activity relationships of the thymolytic activity of various organotin compounds.

Rankings are derived from the findings of 2 week studies in weanling rats in which equivalent doses were administered by the oral route (except * - interpolated from a 4 week comparative study on TBTO and TBTC). Effect ranking (percentage thymic weight reduction): – no effect; + <25%; ++ 25-50%; +++ >50%. References: Seinen et al., 1977a; Seinen and Penninks, 1979; Snoeij et al., 1985; Penninks et al., 1991; Bressa et al., 1991.

Immune system parameter	Effect*	Method	Reference
Cell mediated immunity			
Delayed type hypersensitivity to tuberculin and ovalbumin	↓	in vivo	Vos et al., 1984a
Resistance to Trichinella spiralis	↓	in vivo	Vos et al., 1984a; 1990
Mixed lymphocyte reaction	↓	ex vivo	Smialowicz et al., 1989
Blast transformation of thymocytes and T splenocytes by PHA[1] and ConA[2]	↓	ex vivo	Vos et al., 1984a; 1990; Smialowicz et al., 1989
Humoral immunity			
Thymus-dependent IgG response to sheep red blood cells	↓	in vivo	Vos et al., 1984a
Thymus-dependent IgG/IgM response to ovalbumin and T. spiralis	–	in vivo	Vos et al., 1984a; 1990
Blast transformation of B splenocytes cells by PWM[3] and LPS[4]	–	ex vivo	Vos et al., 1984a
Non-specific resistance			
Splenic clearance of *Listeria monocytogenes*	↓	in vivo	Vos et al., 1984a; 1990 Verdier et al., 1991
Phagocytosis and killing of *L. monocytogenes* by peritoneal and splenic macrophages	–	ex vivo	Vos et al., 1984a
NK activity of spleen cells	↓	ex vivo	Vos et al., 1984a; 1990; Smialowicz et al., 1989

TABLE 1.6 The effects of TBT compounds on various immune functions of the rat.
Ex vivo tests were performed on isolates from animals previously treated with TBTO. Footnotes: *↓ immunosuppressive effect, – no effect; [1]phytohaemagglutinin; [2]concanavalin A; [3]poke weed mitogen; [4]lipopolysaccharide from *E. coli*.

in the blood, and concluded that triphenyltin was a potential immunosuppressive agent. Subsequently the same group demonstrated functional immune deficits and lymphoid cell depletion in guinea-pigs given 15 ppm TPhT acetate in the diet for up to 104 days (Verschuuren et al., 1970). Reduced spleen weights were noted in juvenile Swiss male mice fed approximately 150 ppm TBTO for 7 days, though thymic weights were not determined (Ishaaya et al., 1976). Mature animals were less sensitive, and certain other aryl substituted organotins including TPhTC were considerably less immunotoxic to mice. Thymic atrophy was an important central finding in weanling rats fed 50 or 150 ppm TBTC in the diet for 2 weeks, whilst TOTC was inactive and TMTC and TETC were neurotoxic (Seinen and Penninks, 1979). Funahashi et al. (1980) showed that TBTO given to rats by gavage in olive oil at 13 or 26 mg/kg/day (five days a week) resulted in a marked, dose-dependent reduction in absolute and relative thymus weight; this effect was not seen with 3 mg/kg/day for 13 weeks. A concurrent diminution in spleen weights was also evident at the two highest dose levels. The accompanying findings of depressed animal growth, adrenal hypertrophy and elevated serum cortisol concentrations complicate the interpretation of this study, since the existence of stress-related effects on the lymphoid tissues cannot be excluded.

Large scale investigations of the immunotoxicity of TBTO to rats were conducted in the mid-1980's in the Netherlands by groups led by Professor J.G. Vos. They reported the effects of feeding diets containing TBTO at 0, 5, 20, 80, 320 ppm (approximately equivalent to 0, 0.5, 2, 8 or 32 mg/kg/day, based on food consumption data) to young Wistar rats for 4 weeks (Krajnc et al., 1984). Absolute and relative thymus weights were significantly reduced in both males and females at the two highest levels, and also in males only at 20 ppm. Coincident reductions in spleen weight were recorded for both sexes at 320 ppm and for males that received 80 ppm, and an effect on mesenteric lymph node weights was also apparent in rats fed 320 ppm TBTO. Attendant histopathological effects included a dose-related depletion of cortical thymocytes and of splenic and mesenteric lymph node T cells. Mean white blood cell counts were also depressed, due to a reduction in lymphocyte numbers, in the 80 (males only) and 320 ppm groups. Signs of systemic toxicity were apparent at the top two dietary levels, including diminished bodyweight gain, food intake and water consumption. Parallel investigations (Vos et al., 1984a) showed that the reduced lymphoid organ weights seen at 80 or 320 ppm were associated with a time-dependent (3, 8 and 20 days exposure) progressive reduction in thymus and spleen cell count and viability, and in bone marrow cellularity. After 9 weeks treatment with 20 or 80 ppm TBTO, splenic T cells were reduced, but no disturbance of the ratio of T helper to T non-helper subsets was found. Mesenteric lymph nodes atrophy was dose-related and occurred in all animals fed 320 ppm; both the size and cellularity of the paracortex and medulla of lymph nodes were reduced, as well as follicle size and number. B cell areas were also affected with fewer follicles present and inconspicuous germinal centres.

In 2 week feeding studies in male weanling rats with TBTC at 0, 15, 50, 100 and 150 ppm (Snoeij et al., 1985), severe dose-dependent reduction in thymus and spleen weight occurred at or above 50 ppm. TPTC and TPhTC caused qualitatively similar effects. Thymic atrophy seen with TBTC, was equally apparent in adrenalectomised and sham-operated rats, and completely reversed within one week of treatment cessation. Cortical thymocytes depletion, resulting in indistinct cortico-medullary junctions was the principal histopathological finding. A one month feeding trial conducted with older male Wistar rats (Bressa et al., 1991) demonstrated similarly severe, but reversible, cortical thymocyte depletion in animals treated with 5 or 25 ppm of commercial or pure TBTO, or TBTC, though the latter two compounds were most active. By a novel technique involving administration of a single dose of 75 mg/kg TBTO to rats followed by transplantation of the maximally involuted thymuses to untreated animals, it has been shown that recovery to normal thymic architecture occurs by 20 days after toxicant insult (Van Loveren et al., 1991). This underlines the ready reversibility of TBT-mediated thymic atrophy.

In long-term studies weaned rats were exposed to diets containing 0, 0.5, 5 or 50 ppm TBTO (equivalent to 0, 0.025, 0.25 or 2.5 mg/kg/day, based on actual food consumption measurements) for up to 2 years (Wester et al., 1990; Vos et al., 1990). A slight but significant reduction in thymic weight was observed at the highest dietary level after 4.5 months, though spleen weight was unaffected. After one year thymic atrophy was no longer evident; this was suggested to be due to masking by physiological thymic involution in ageing animals. Exposure to 5 or 50 ppm TBTO for 6 or 18 months depressed the relative count of T lymphocytes, in mesenteric lymph nodes; calculated per whole node, the absolute numbers of T cells at 50 ppm were diminished by 50% versus control (Vos et al., 1990). Lymphocytopenia was evident from 3-24 months for both sexes at the high dose level. In order to assess the effects of TBTO on aged rats, 1 year-old animals were fed 0, 0.5, 5 or 50 ppm for 5 months. In common with the weanling rats, a reduction in thymus weight was evident at the end of treatment with 50 ppm.

It will be evident from the previous discussion that in rodent species, males generally appear to be more sensitive than females. This has been particularly shown to be true of rats exposed to TBTO for short periods (Krajnc et al., 1984; Verdier et al., 1991). In terms of structure-activity relationship, the degree of trialkyltin-induced thymic atrophy appears to be strongly related to the length of the alkyl chain (Table 1.5). The lower homologues, TMTC and TETC are very neurotoxic and this precludes their assessment. The intermediate chain length members, TPTC and TBTC exhibit the most marked effects, whereas higher homologues such as THTC and TOTC are either slightly active, or do not cause thymic involution. TPhTC, which has a P_{ow} value similar to TBT, shows equivalent activity. An interesting correspondence exists between the thymolytic potency of these compounds in vivo and their in vitro cytotoxicity (see 3.1.3; Snoeij, 1987). At present, the

precise mechanisms underlying the in vivo activity profile of triorganotins are unclear, but these probably include differences in absorption, metabolism and water-lipid distribution. Dialkyltin compounds producing the severest effects on the thymus span alkyl chain carbon-numbers C3-C8 (Table 1.5).

Vos et al. (1984a) also investigated the effect of TBTO number of immune system parameters in the rat. TBTO treatment increased serum IgM and decreased IgG levels. Investigations of functional immune status indicated that a number of adverse effects occurred (this data is summarised in Table 1.6). Cell mediated immunity was strongly impaired after 6 weeks exposure to 20 or 80 ppm TBTO, as evidenced by reduced delayed hypersensitivity reactions to tuberculin and ovalbumin, poorer resistance to Trichinella spiralis infection, and lowered T cell mitogenic responsiveness. The suppressed B cell-mediated IgG response to sheep erythrocytes seen in treated rats may also have been due to reduced regulatory T cell numbers. In terms of non-specific resistance, treatment at 20 or 80 ppm also impaired the mononuclear phagocyte system clearance of *Listeria monocytogenes*. With respect to natural cell-mediated cytotoxicity, TBTO reduced the activity of natural killer (NK) cells in the spleen and cytotoxic macrophages obtained from the peritoneal cavity. TBTC had similar inhibitory effects on murine NK cell activity in vivo (10 ppm for 1 week) and in vitro (0.01 ppm) which has been ascribed to interference with effector cell binding to targets (Ghoneum et al., 1990). Short-term feeding of TPhT hydroxide to 3-4 week-old Wistar rats, produced a broadly similar cell mediated immune dysfunction (Vos et al., 1984b), though splenic clearance of bacteria and phagocyte actions were unaltered. To assess immunosuppressive effects following long-term exposure to TBTO, functional studies were performed after 4-6 and 15-17 months in a later investigation by Vos et al. (1990). Resistance to T. spiralis infection was significantly lower with 5 or 50 ppm TBTO at both timepoints. Clearance of *L. monocytogenes*, a marker of non-specific immunity, was impaired at the higher level only. The most sensitive parameter appeared to be splenic NK activity, which was reduced in all treated groups by 16 months. Humoral immunity was not severely affected, though elevations in serum IgM and IgA, and lowered IgG concentrations were reported (Wester et al., 1990). Vos and co-workers observed that when TBTO feeding was started at an advanced age (1 year-old rats) less conspicuous functional deficits occurred. They concluded that the immune system of mature animals was less sensitive, though it should be noted that doses on a bodyweight basis were lower relative to the study in weanlings. Data from Smialowicz et al. (1989) suggests that TBT is most effective in producing immunosuppression when administered in early post-natal life.

Limited information is available in the literature regarding the effects of trisubstituted organotins on lymphoid organs in different animal species. Snoeij (1987) concluded that mice were much less sensitive than rats. Repeated TBTC intake at relatively high dietary

levels (in the range of 150-200 ppm) appears to be necessary to elicit thymic atrophy (Kempston et al., 1993). The absence of TBT-induced effects on murine lymphoid organs upon oral administration at dose levels devoid of general toxicity, has been suggested to be due to differences in absorption, hepatic blood flow or cytochrome P_{450} metabolism. Guinea-pigs seem to be susceptible, but organotins disturb essential gut bacteria in this species causing gross systemic disturbances. In beagle dogs given variable doses of TBTO (0.5-10 mg/kg/day), effects included thymic atrophy and lymphocyte depletion of thymus, spleen and lymph nodes (IPCS, 1990). Japanese quail are remarkably resistant to TBT immunotoxicity (Penninks et al., 1990). Since TBT compounds reduce thymus weights even in freshwater guppies (IPCS, 1990), they may have immunotoxic effects in a wide range of species.

In summary, the most sensitive parameter of TBT compound toxicity appears to be their effect on lymphoid organs, primarily involving thymic atrophy, and immune function (particularly in respect of cell mediated immunity). During a recent safety factor assessment of TBTO as an environmental contaminant in the human food chain (Penninks, 1993), similar conclusions were reached, and it was judged that tolerable daily intakes of 5 or 0.25 μg/kg/day were appropriate to safeguard against lymphoid toxicity and immune dysfunction, respectively.

1.7 SCOPE OF THIS THESIS

The principle objectives of the work described in this thesis were to:

- investigate whether the immunotoxic environmental pollutant TBT was capable of activating apoptosis in ex vivo thymocytes derived from immature rats.
- probe the cellular mechanisms involved in TBT cytotoxicity, and relate these to apoptosis activated by several positive control compounds including a synthetic glucocorticoid (MPS); a microtubule-disrupting agent (nocodazole); and a divalent cation ionophore (A23187).
- assess the relevance of any in vitro findings to the thymus-directed immunotoxicity of TBT compounds in vivo.

CHAPTER 2
MATERIALS AND METHODS

2.1.1 PREPARATION OF THYMOCYTES

Apart from thymic explant culture, the principle technique used for in vitro study of thymocytes has been primary culture of single cell suspensions. Isolation procedures rely upon the fact that the thymus of young animals has a very high lymphoid to stromal cell ratio, and also on the relative ease by which the lymphoid cell compartments can be dissociated to give monodisperse thymocyte preparations. Contamination by other cell types can be minimised by simple expedients, e.g. avoidance of excessive bleeding during organ excision; careful dissection to remove extraneous connective tissue and parathymic lymph nodes; and surface washes of the thymus prior to processing. Organ disruption can be achieved by mechanical means and satisfactory cellular recovery can be made without the use of enzyme digestion.

As the majority of thymocytes possess relatively low metabolic activity, very high cell viabilities are routinely achievable if all isolation procedures are conducted at 4°. Simple buffered salt solutions are adequate for initial manipulations, but need to be replaced by complex media containing growth factors for longer term culture. Based on a CO_2 gassing system, the buffer system of choice is normally sodium hydrogen carbonate-based, although HEPES may also be used for short term culture. Lymphocytes tend to be intolerant of prolonged culture in phosphate, HEPES or PIPES buffer systems (Moore and Woods, 1976). There are few other absolute requirements, although thymocytes are known to be susceptible to osmotic shock and shear forces, therefore due regard must be paid to media tonicity and to gentle handling during the preparation of cell suspensions (Hunt, 1987).

2.1.2 Rationale for thymocyte derivation

Much of the accumulated knowledge on the physiology and pathology of processes involving thymic lymphocytes has been derived from work with rodent species, particularly rats and mice. Throughout these studies, immature male Wistar rats obtained from the breeding colony at the School of Pharmacy, were used as the source of thymic material. To avoid the confounding effects of age-related thymus involution, and allow direct comparison with the results of other investigators, the age range of the animals used was restricted to 4-7 weeks. The maximum yield of thymocytes from this rat strain is high, typically in the region of 10^9 cells per animal. Animals were group housed in rooms maintained at 20±3°C with a relative humidity of 45-65%, under a 12 h constant light/dark cycle. Drinking water and diet were provided *ad libitum*. Whenever possible litter mates were used within an experimental set.

2.1.3 Materials

DMEM, penicillin/streptomycin mixture and heat-inactivated FCS were purchased from Flow ICN Biomedicals (Irvine, Scotland). RPMI-1640 and trypan blue were from Sigma Chemical Co. Ltd (Poole, England). Other reagents were from BDH Ltd (Poole, England).

2.1.4 Isolation media

A slight modification of unsupplemented Krebs Henseleit buffered salt solution (KH) formula (Krebs and Henseleit, 1932) was used:

	g/l
Sodium chloride (NaCl)	6.900
Potassium chloride (KCl)	0.350
Potassium dihydrogen phosphate (KH_2PO_4)	0.162
Magnesium sulphate heptahydrate ($MgSO_4.7H_2O$)	0.147
Calcium chloride dihydrate ($CaCl_2.2H_2O$)	0.190
Sodium hydrogen carbonate ($NaHCO_3$)	2.100

A solution containing all salt components except the sodium hydrogen carbonate was gassed for 10 minutes with carbogen (5% CO_2 / 95% O_2) immediately prior to use. After addition of sodium hydrogen carbonate, the pH of the solution was measured and adjusted as necessary to 7.4. The osmolality of the resulting buffer had a calculated value of 295 mOsm/kg H_2O. Prior to use, this isolation medium was sterilised by filtration through a 0.2 μm disposable filter assembly and then cooled to 4° on ice.

2.1.5 Incubation media

Two incubation media, DMEM and RPMI-1640, were employed during these studies. Both were supplemented before use with FCS 10% (v/v), that had been heat inactivated (to denature complement components). The pH was then adjusted as necessary to 7.4 using sterile solutions, and media were cooled to 4°, and used without pre-gassing.

1) RPMI-1640 medium

A standard sterile preformulated liquid RPMI-1640 as developed by Moore and co-workers (Moore and Woods, 1976) was used, containing L-glutamine and a sodium hydrogen carbonate buffer system. Formulation details and physico-chemical characteristics, as provided by the supplier, are given as an Appendix.

2) Dulbecco's modified Eagle's medium (DMEM)

A modification of the original DMEM recipe which incorporated 4.5 g/l D-glucose, L-glutamine, and sodium hydrogen carbonate, obtained as a preformulated sterile liquid, was employed. Formulation details and physico-chemical characteristics, as provided by the supplier, are given as an Appendix.

2.1.6 Ancillary solutions

Dulbecco's phosphate-buffered saline (PBS):

	g/l
Sodium chloride (NaCl)	8.00
Potassium chloride (KCl)	0.20
Sodium hydrogen phosphate (Na_2HPO_4)	1.15
Potassium dihydrogen phosphate (KH_2PO_4)	0.20

The pH of the prepared solution was consistent at 7.5.

2.1.7 Preparation of thymocyte suspensions

An outline of the methodology employed is shown schematically in Fig. 2.1. Aseptic technique was maintained by the use of γ-irradiated tissue culture disposable plasticware, sterilisation of equipment by autoclaving or soaking in 70% ethanol, and the use of a laminar air-flow hood with a submicron particulate filtration system.

Two glass containers were each filled with 3-5 ml KH isolation medium and held on ice. A McIlwain tissue chopper (Mickle Laboratories; Gomshall, England) was fitted with a pre-sterilised cutting blade and two polypropylene tissue placement discs.

Prior to sacrifice, animals were kept in a quiet environment to avoid the imposition of stressful stimuli, and were initially anaesthetised with diethyl ether in situ within their holding cage. Each rat was then deeply anaesthetised and subjected to cervical dislocation. The ventral body surface was soaked with 70% ethanol, and an initial incision made through the skin from the sub-sternal thoracic region to below the lower jaw. Two longitudinal cuts were made along each side of the ribcage and laterally along the line of the diaphragm, such that the thoracic cavity could be exposed. The thymus was identified, freed of connective tissue, and carefully excised, ensuring that parathymic lymph nodes were not incorporated, and that contamination by blood was minimised. The thymus was placed in one lot of KH, washed by gentle agitation, transferred to fresh KH and allowed to cool for about 1-2 minutes. After transfer to a tissue placement disc, it was rapidly cross-sliced using a McIlwain tissue chopper and then dispersed back into isolation medium. Disaggregation of the resulting tissue fragments was achieved by expressing them through a 100 mesh nylon sieve (approximately 0.15 mm openings), and the resulting crude suspension was filtered through three layers of gauze to remove debris and cell clumps.

In preliminary experiments, the cell suspension was then centrifuged at low speed (800-1000 rpm) for 5 minutes in a bench centrifuge (Denley BR401 refrigerated centrifuge; Denley Instruments, Billinghurst, England), the supernatant was aspirated and discarded, and the cells were washed once by resuspension in KH. As this step did not significantly improve the quality of the preparation but did result in losses in total cell yield, it was subsequently omitted from the procedure.

2.1.8 Cell count

The thymocyte suspension was diluted with 20-30 ml of incubation medium and the exact volume recorded. An aliquot of 20 μl was removed after gentle agitation to ensure reflux and then diluted with 80 μl of a 0.4% trypan blue solution in PBS (Ca^{2+} and Mg^{2+} free). A coverslip was moistened on two edges and placed onto a haemocytometer (improved Neubauer; Weber Scientific International Ltd, Teddington, England) and the mixed sample

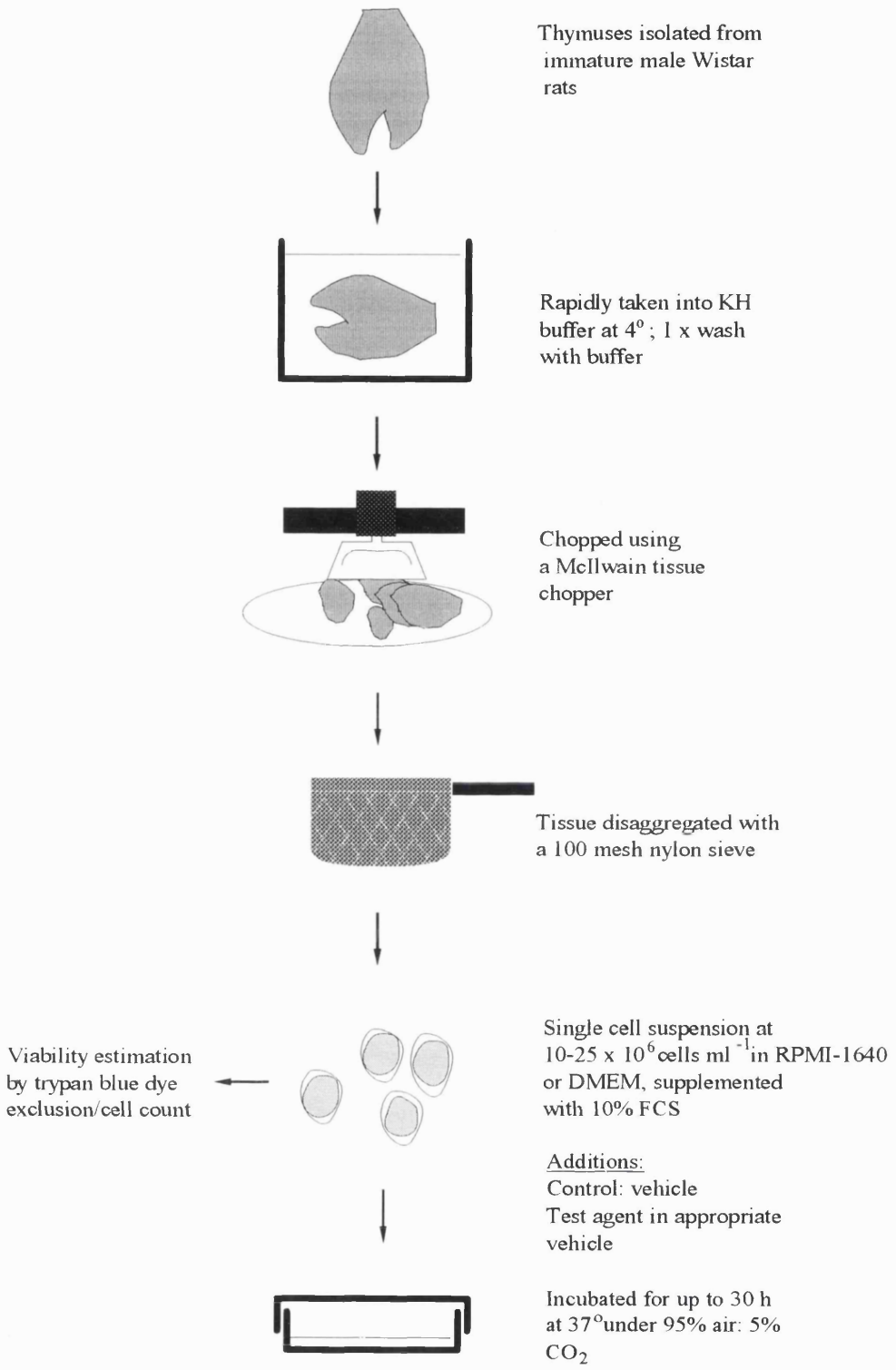

FIGURE 2.1 Schematic representation of ex vivo thymocyte isolation and incubation technique.

was placed under the slip and allowed to settle for 1 minute. This preparation was assessed using a light microscope (x 400 total magnification) to ensure the cells were essentially a monodisperse population, and the total number of viable cells within 1 or 2 minor squares of the haemocytometer central grid were counted (Fig. 2.2). This represents a known volume, and therefore the number of cells per ml^{-1} can be estimated. Counts were made in triplicate on a minimum of 200 cells and the mean value obtained was used for the purpose of calculation. The cell suspension was diluted with incubation buffer to 10-25 x 10^6 cells ml^{-1} and the cell count repeated. During initial studies, the accuracy of this procedure was verified by use of a Coulter Counter D (Coulter Electronics Ltd., Luton, England) electronic particle counter.

2.1.9 Primary cell culture

Incubations were conducted in vented 3.5, 5 or 10 cm diameter polystyrene cell culture dishes, or 1.5 cm multiwell plates (Cel-Cult; Bibby Sterilin Ltd, Stone, England). To ensure the standardisation of cell density, prepared cell suspensions were maintained under constant gentle agitation during removal and delivery of the required volumes into the dishes. Plating depth was kept within a consistent limited range during all experiments via a dispensed volume/plate diameter ratio of 1 ml cm^{-1}. Initial cell density was always 10-25 x 10^6 cells ml^{-1}. Cultures were maintained for up to 30 h in an Flow Laboratories CO_2 Incubator 220 (Flow ICN; Irvine, Scotland) at $37^{o}\pm2\%$, under a humidified atmosphere of 5% CO_2 : 95% air. For culture durations in excess of 8 h, 25 I.U. ml^{-1} penicillin and 25 μg ml^{-1} streptomycin was added to the medium; this treatment was determined have no effect on viability or indices of apoptosis over typical study timeframes.

Prior to the removal of aliquots of cell suspension, the cells were always refluxed back into suspension by swirling for approximately 20 seconds, followed by gentle mixing using a wide bore pipette.

2.2.1 VIABILITY (DYE EXCLUSION)

A number of techniques, with disparate end-points, have been utilised to determine cellular viability and its reciprocal, cell death. These include assessment of clonogenicity; metabolic status e.g. DNA synthesis or ATP levels; or the release of intracellular components such as ^{51}Cr-labelled proteins or marker enzymes (Bowen, 1981). Vital dye exclusion, employing stains such as trypan blue, eosin Y, or nigrosin is a useful approach. This parameter reflects the integrity of the plasma membrane and is based on the assumption that viable cells will continue to exclude the dye for some time after its addition. It has the advantages of speed, ease of application, reproducibility in trained hands, and also gives limited information on cellular morphology. Drawbacks to the technique principally relate to the difficulty in differentiating between altered plasma membrane permeability and cell death, its inherent subjectivity and rather poor statistical precision, and the absence of a theoretical

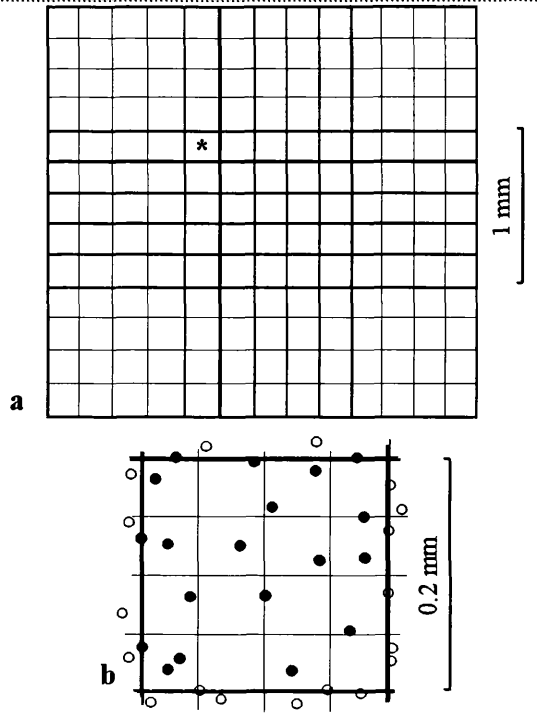

FIGURE 2.2 Standard haemocytometer grid (improved Neubauer).
The central region of the grid (represented in *a*) is the area used for the estimation of cell number, and forms a standard chamber depth of 0.1 mm when a coverslip is correctly positioned over it. One sub-unit square (*, represented in *b*) has sides of 0.2 mm; area 0.04 mm^2. Multiplying the number of cells visible in one sub-unit square (excluding cells designated as open circles) by 25 gives the total count for the central region of *a*. This value is multiplied by 10^4, and corrected as appropriate for any dilution factor, to obtain the final cell count per ml (cm^3) of suspension. The optimal cell concentration for accurate counting is 10^7 ml^{-1}, but the acceptable range is 2 x 10^5 to 4 x 10^7.

basis for correlation with other viability markers. Vital dye exclusion cannot readily distinguish normal cells from those in the early stages of apoptosis (see section 1.2).

2.2.2 Materials

Trypan blue was purchased from Sigma Chemical Co. Ltd (Poole, England). All other reagents were from BDH Ltd (Poole, England).

2.2.3 Preparation of samples and determination of viability

An aliquot of cell suspension was removed and mixed with an appropriate volume of 0.4% trypan blue solution (in PBS) to give an optimal cell density in the region of 10^7 ml^{-1}. A coverslip was placed onto a Neubauer haemocytometer and after gentle mixing the sample was introduced into one half of the counting zone of the slide. The cells were allowed to settle for 1 minute, but were counted within 3 minutes to avoid non-specific dye inclusion into viable cells. Counts were performed using a light microscope (total magnification x 400) on a minimum of 100 cells per sample. Using the grid of the haemocytometer as a fixed reference, viable (clear) and dead (blue stained) cells were enumerated.

2.2.4 Calculation of viability

Viability, as assessed by dye exclusion, is reported as a percentage derived from the following calculation:

$$\text{Percentage viability} = \frac{\text{viable cells}}{\text{total cells}} \times 100$$

2.3 CELL COUNTS

During incubations, cell counts were performed by an equivalent procedure to that described in section 2.1.8. Determinations were made on 50 µl aliquots of cell suspension after gentle admixture with an equal volume of trypan blue solution. Total cells within the prescribed haemocytometer fields were counted, i.e. both viable and non-viable.

2.4.1 MORPHOLOGICAL STUDIES (LIGHT MICROSCOPY)

Direct observation of morphological changes remains a valuable technique in the study of cell injury. The methods described in this section were used in conjunction with vital dye exclusion assessments of viability. One approach involved assessment of fixed thymocyte sections, whilst the other method depended on fluorochrome staining of unfixed cell nuclei.

2.4.1.1 Resin embedded thymocyte sections

This was the routine method used for the evaluation of cell morphology, and quantitation of the incidence of apoptosis. Although the preparative phase was time-consuming, the technique itself conferred significant advantages in respect of the preservation and ease of visualisation of cytopathological changes. It was therefore selected in preference to alternatives such as fixed cytospin preparations.

2.4.1.2 Materials

Glutaraldehyde (TEM grade), sodium dimethylarsonate (sodium cacodylate), toluidine blue (Gurr microscopy stain), sodium tetraborate and XAM mountant were obtained from BDH Ltd (Poole, England). Araldite CY 212 epoxy resin, dodecynyl succinate anhydride and n-benzyldimethylamine were from Agar Scientific Ltd (Stansted, England).

2.4.1.3 Preparation of samples

A solution containing 2.5% glutaraldehyde in 0.1 M sodium dimethylarsonate buffer was prepared, and the pH adjusted to 7.4. Prior to use, this fixative was cooled to 4° and 1.4-1.6 ml was placed into a 2 ml Eppendorf tube (Safe Lock; Eppendorf-Netheler-Hinz GmbH, Hamburg, Germany) on ice. A 0.4-0.6 ml aliquot of cell suspension was removed and added to the tube, and the cells were allowed to fix in suspension for approximately 1 h. The sample was then spun down at low speed (800 rpm for 15 minutes; calculated RCF 170 x *g*) in a Denley BR 401 refrigerated centrifuge. Whole cells were essentially absent from the resulting supernatant. Samples were stored at 4° prior to processing.

2.4.1.4 Sample processing and staining

The supernatant was removed, the cell pellet resuspended in 0.1M sodium dimethylarsonate buffer, pH 7.4, centrifuged at 1000 rpm for 15 minutes and the final supernatant discarded. After a standard dehydration regimen using graded concentrations of methanol followed by acetone washes, the pellet was infiltrated for 18 h with a catalysed epoxy resin system (Araldite CY 212, 1 volume: dodecynyl succinate anhydride, 1 volume: n-benzyldimethylamine, 0.04 volume). The resin block was fully cured by heating to 60° for 18-24 h.

Semi-thin sections (0.5 μm thickness) were cut using a Reichert Om U3 microtome (C. Reichert, Wien, Austria) and transferred to degreased glass microscope slides. The sections were stained for approximately 2 minutes at 60°, using 1% toluidine blue in an aqueous solution of 50% ethanol containing 1% sodium tetraborate. After washing the sections were allowed to air-dry and then mounted beneath a glass coverslip using XAM.

2.4.1.5 Evaluation and counting procedures

Resin embedded thymocyte sections were viewed at high magnification by light microscopy. Toluidine blue, a cationic dye, was selected since it interacts with anionic nucleic acids more avidly than with other cellular structures (Bancroft and Cook, 1984). In addition, it can penetrate epoxy resin sections without the need for permeabilisation (Robinson and Gray, 1990). The differential orthochromatic staining produced by toluidine blue gave good definition of nuclear features. Due to their high nuclear to cytoplasmic ratio and relative lack of cytoplasmic features, thymocytes were evaluated primarily on the basis of nuclear morphology. Cells that exhibited a uniform condensation of nuclear chromatin, without a discernible flocculation pattern, were classified as being apoptotic. For the purposes of quantification, a minimum of 600 consecutive cells were scored in contiguous fields of view. Apoptotic bodies judged to be obviously associated with a single cell were scored as a unitary event, but all others were excluded from the estimation. Erythrocytes and non-lymphoid cells occasionally visualised in the preparations were also excluded. Since cells in the immediate periphery of the sections had a tendency to be very hyperchromatic, counts were not performed in this region.

2.4.1.6 Calculation of the incidence of apoptosis

The proportion of cells classified as apoptotic, on the basis of morphological assessment, is reported as a percentage derived from the following calculation:

$$\text{Percentage apoptotic cells} = \frac{\text{cells with condensed chromatin}}{\text{total cells}} \times 100$$

2.4.2.1 Fluorescence microscopy

The marked chromatin condensation that occurs during apoptosis represents a phenomenon

which can be exploited to identify apoptotic cells, even in their unfixed state, by differential DNA staining using interactive fluorochromes (Hotz et al., 1992). Acridine orange (AO) has been used as a nucleic acid stain principally due to its propensity to act as an intercalator (Rigler, 1969). AO will interact electrostatically with cellular polyanions, therefore to ensure preferential staining of nucleic acids it is necessary to either maintain a low molar ratio of AO per binding site, or to include excess cations (e.g. Na^+ or Mg^{2+}) to compete for anionic sites (Traganos et al., 1977). The stacking reaction of AO on single stranded RNA can be differentiated by the red metachromasia produced.

2.4.2.2 Materials

3,6-bis(dimethylamino)acridine hydrochloride (acridine orange; AO) was sourced from Aldrich Chemical Co. Ltd (Gillingham, England).

2.4.2.3 Sample preparation and visualisation

A stock solution of AO (100 μg ml^{-1}) in 0.9% NaCl was prepared and stored refrigerated. At the requisite timepoints, a 95 μl aliquot of thymocyte suspension was admixed with 5 μl of dye solution (final AO concentration approximately 15 μM). After incubation for 3 minutes at room temperature, a drop of this mixture was placed on a microscope slide, covered with a glass slip and the cells allowed to settle for 1 minute. Visualisation was by epifluorescence using a Nikon Microphot FXA microscope (Nikon Corporation, Tokyo, Japan) with a filter set configured for FITC. Putative apoptotic chromatin structures were distinguished by their differential high yellow-green fluorescence, and quantitative estimations were performed on a minimum of 200 cells in contiguous fields. Photomicrography was with Ektachrom 35 mm ASA 50 colour film (Kodak; Hemel Hempstead, England).

2.4.2.4 Calculation of the incidence of apoptosis

The proportion of cells classified as apoptotic, on the basis of fluorescent nuclear staining character, is reported as a percentage derived from the following calculation:

$$\text{Percentage apoptotic cells} = \frac{\text{cells with highly fluorescent inclusions}}{\text{total cells}} \times 100$$

2.5.1 MORPHOLOGICAL STUDIES (ELECTRON MICROSCOPY)

In studies of cell death, light microscopy is normally adequate to resolve major cytopathological changes and is well suited to quantification of the number of affected cells. However, considerable additional information can be obtained at the ultrastructural level even on gross alterations such as nuclear pyknosis and karyorrhexis. A number of investigators have previously used transmission mode electron microscopy (TEM) to visualise and classify many morphological markers associated with necrosis and apoptosis (Wyllie et al., 1980; section 1.2); therefore TEM has considerable utility in this field.

2.5.2 Materials

In addition to the items detailed in section 2.4.1.2, osmium tetroxide, uranyl acetate, lead acetate and trisodium citrate were sourced from BDH Ltd (Poole, England). Copper TEM grids (400 mesh, 3.05 mm diameter) were from Agar Scientific Ltd (Stansted, England).

2.5.3 Preparation of samples

Cell samples were fixed as described in section 2.4.1.3.

2.5.4 Sample processing

The supernatant was removed, the cell pellet resuspended in 0.1 M sodium dimethylarsonate buffer, pH 7.4, centrifuged at 1000 rpm for 15 minutes and the final supernatant discarded. The pellet was subjected to post-fixation for a period of 30 minutes in 0.25% osmium tetroxide dissolved in 0.1 M sodium dimethylarsonate buffer, pH 7.4. Dehydration was effected by a single immersion in 70% methanol (15 minutes duration), followed by three immersions in 100% methanol (each of 20-30 minutes). After washing twice in acetone, the pellet was blocked into epoxy resin as described in section 2.4.1.4.

Ultra-thin sections (visual silver/gold interference; nominal 80-100 nm thickness) were prepared by ultramicrotomy using a Reichert Om U3 microtome (C. Reichert, Wien, Austria). These were transferred to copper TEM grids previously sequentially cleaned with surfactant, ethanol and acetone. Uranyl acetate was prepared as a saturated solution in methanol. Lead citrate (Reynolds) was formed in situ from a reaction mixture of lead acetate, trisodium citrate and NaOH; solutions were filtered prior to use. Sections were stained en bloc with uranyl acetate for 3 minutes, washed with methanol, stained with lead citrate for an equivalent period, washed twice with distilled water, and dried.

2.5.5 Evaluation and photomicrography

Sample grids were viewed with a Philips 201 transmission electron microscope. Photomicrographs were obtained on TMAX black and white film (Kodak, Hemel Hempstead, England) using an integral 35 mm camera.

2.6.1 DNA FRAGMENTATION (COLORIMETRIC METHOD)

This method is a minor modification of that described by Wyllie (Wyllie, 1980; Wyllie and Morris, 1982) and depends on hypotonic cell lysis, followed by differential centrifugation to separate low molecular weight chromatin products from uncleaved chromatin. Quantitation of relative DNA content is then performed by a colorimetric technique utilising a reaction with diphenylamine (Burton, 1956). The chromophore produced is thought to be a reaction product between diphenylamine and deoxyribose linked to purine nucleotides in DNA. This DNA fragmentation assay, or close variants, have been used in many studies of the chromatin cleavage that occurs during apoptosis (see section 1.3.5),

and is of particular use in cell types, such as thymocytes, where detection sensitivity is not paramount as a significant proportion of cells can be expected to be apoptotic. Advantages of the technique over alternate methodologies for the estimation of DNA fragmentation include; its ease of application, inherent reproducibility; the absence of artefactual damage seen with radiolabelling methods; and the avoidance of complex DNA purification. However, it should be noted that the DNA fragmentation values obtained may deviate from an exactly linear correlation with the actual number of apoptotic cells in a sample.

2.6.2 Materials

Tris, EDTA, Triton X-100 and calf thymus DNA were obtained from Sigma Chemical Co. Ltd (Poole, England). Trichloroacetic acid, perchloric acid, diphenylamine, acetic acid, sulphuric acid and acetaldehyde were from BDH Ltd (Poole, England).

2.6.3 Differential centrifugation

Aliquots of cell suspension containing a minimum of 20 x 10^6 thymocytes were placed into pre-autoclaved 62 x 17 mm polycarbonate centrifuge tubes (MSE Scientific Instruments Ltd, Crawley, England) and spun at 4° to pellet the cells (1000 rpm for 10 minutes). The medium was aspirated and ice-cold hypotonic lysis buffer; 5 mM Tris, 20 mM EDTA, 0.5% (v/v) Triton X-100 (pH 8.0) added to a volume equivalent of 1 ml per 15 x 10^6 cells. After being held on ice for a standard duration of 30 minutes to allow cell lysis to occur, the tubes were loaded into a pre-cooled MFT 70.10 35° angle rotor (MSE Scientific Instruments Ltd) and centrifuged at 16 000 rpm for 20 minutes at 4° in a MSE Europa 50 M ultracentrifuge (MSE Scientific Instruments Ltd). The RCF corresponding to the radius at the median sample position in the rotor was calculated to be 27 000 x *g*. Supernatants were removed into glass sample tubes, and the pellet resuspended in 10 mM Tris/1 mM EDTA, pH 8.0 using a volume equivalent to that of the lysis buffer.

2.6.4 Assay

The method used was essentially that devised by Burton (Burton, 1956) and is described in overview. A stock solution of calf thymus DNA was prepared in 10% TCA by heating to 90° for 15 minutes, this was then serially diluted with TE buffer to the concentrations required for the standard curve (normally 0-200 μg ml^{-1} including at least 8 standard points, in duplicate). Diphenylamine reagent was freshly prepared for each assay by adding 1 g diphenylamine per 100 ml acetic acid, together with 8 mg acetaldehyde. TCA-precipitable material derived from samples was hydrolysed at 90° by addition of 5% TCA. Samples and standards were then made to 0.5 M PCA, mixed with 2 volumes of diphenylamine reagent and incubated at 30° overnight to achieve maximal colour development. After cooling, the extinction value at 600 nm was determined using a Shimadzu MPS 2000 spectrophotometer (Shimadzu Corp., Kyoto, Japan). Initial estimates of the DNA content of cell lysates versus the total DNA content of equivalent supernatant

and pellet fractions (see 2.6.3), indicated that recovery values exceeded 85%.

2.6.5 Calculation of results

The extinction values obtained with the standards were averaged, plotted against the respective DNA concentration, and a linear regression calculation performed. The DNA concentration in the experimental samples was interpolated with reference to the standard curve produced. DNA fragmentation is expressed as the percentage of total DNA that resisted sedimentation at 27 000 x *g*. This was calculated with reference to the DNA content of the supernatant (fragmented DNA; $DNA_{supernatant}$) and pellet (unfragmented DNA; DNA_{pellet}) fractions as follows:

$$\text{DNA fragmentation (\%)} = \frac{DNA_{supernatant}}{DNA_{supernatant} + DNA_{pellet}} \times 100$$

2.7.1 DNA (FLUORIMETRIC METHOD)

This microfluorimetric method is based on the use of the bisbenzimidazole compound H33258, which at low concentrations, and at neutral pH, binds to DNA in a highly specific manner. Fluorochrome binding is accompanied by a shift in the fluorescence emission maximum and a marked increase in quantum yield (Stokke and Steen, 1985).

2.7.2 Materials

H33258 was obtained from Novabiochem UK Ltd (Nottingham, England). Tris, EDTA and calf thymus DNA were from Sigma Chemical Co. Ltd (Poole, England).

2.7.3 Preparation of samples

Samples were diluted (at least tenfold) to appropriate concentrations with buffer; 10 mM Tris, 1 mM EDTA, pH 8.0 (TE) and divided to provide internal triplicates for estimation.

2.7.4 Standards

A 0.2 mg ml^{-1} solution of calf thymus DNA was prepared in TE and stored at 4°. Before use, this was further diluted to 50 μg ml^{-1}, the extinction value at 260 nm determined to ensure the concentration integrity of this reference solution, and a final stock made at 10 μg ml^{-1} in TE. A standard curve of 0-6 μg ml^{-1} DNA was then constructed in triplicate. The standards were subsequently treated in the same manner as the experimental samples.

2.7.5 Assay

H33258 was prepared as a stock solution (150 μM) in distilled water and kept protected from light at -20°; this solution remained stable for at least 3 months. Prior to use, the molar extinction coefficient of the fluorochrome solution was checked for correspondence with an expected value of 4.2×10^4 M^{-1} cm^{-1} at 338 nm, and stock H33258 was diluted in TE to a working solution concentration of 1.5 μM. An 0.5 ml aliquot of this was added

the sample, or standard, and incubated in the dark at room temperature for a standard time of 10 minutes. After transfer to a glass microcuvette, fluorescence measurements were conducted with a LS-3B spectrofluorimeter (Perkin-Elmer, Beaconsfield, England), at excitation and emission wavelengths of 350 and 455 nm, respectively. Initial studies demonstrated that low amounts of Triton X-100 and SDS present in some experimental samples did not modify the fluorescence characteristics within the sensitivity limit of the assay, which was in accordance with previously published data (Brunk et al., 1979).

2.7.6 Calculation of results

Fluorescence values obtained with the standards were averaged for each triplicate set, plotted against the respective DNA concentration, and a linear regression calculation performed. The amount of DNA in the experimental samples was interpolated with reference to the standard curve produced, and an appropriate dilution factor was applied to yield the final concentration.

2.8.1 GEL ELECTROPHORESIS

Gel electrophoresis is an important technique in the characterisation and analysis of DNA species. The neutral agarose gel electrophoresis procedures described herein are based on established norms (Maniatis et al., 1989; Sealey and Southern, 1990). Unwanted DNase activity subsequent to cell lysis was minimised by the use of EDTA in buffers and sample loading solutions. A Tris-borate system was selected as the electrophoresis running buffer due to its superior buffering capacity over Tris-acetate or Tris-phosphate. Periodic checks during electrophoresis confirmed that the pH of the buffer remained constant without a requirement for recirculation or replenishment. The mobility of DNA fragments was calibrated against a commercially available molecular weight standard consisting of a integer multiple series of 123 bp DNA fragments, spanning a size range of 123-4182 bp.

2.8.2 Materials

Tris, EDTA, Ficoll (type 70), ethidium bromide and RNase A (from bovine pancreas; declared activity 88 Kunitz units mg^{-1} solid) were obtained from Sigma Chemical Co. Ltd (Poole, England). Sodium dodecyl sulphate (SDS) was from Koch Light Ltd (Colnbrook, England). 123 bp DNA ladder was from Bethesda Research Laboratories Life Technologies Inc. (Uxbridge, England). Phenol, chloroform, agarose (Electran 10; electroendosmosis value < -0.02), boric acid, glycerol, bromophenol blue and all other reagents were sourced from BDH Ltd (Poole, England).

2.8.3 Preparation of samples

A known volume of the supernatant or buffer containing solubilised pellet from the differential centrifugation technique described in section 2.6.3 was placed in 62 x 17 mm polycarbonate centrifuge tubes (MSE Scientific Instruments Ltd, Crawley, England) and

5 M NaCl (0.1 volume) added, followed by excess absolute ethanol (2 volumes). The chromatin was allowed to precipitate overnight at -20° and recovered by centrifugation (10 000 rpm for 10 minutes; calculated RCF 10 000 x *g*) in a Europa 50 M centrifuge (MSE Scientific Instruments Ltd; Crawley, England). The supernatant was removed and the pellet air-dried prior to addition of 0.5-0.8 ml 10 mM Tris/ 1 mM EDTA, pH 7.5 (TE buffer) and SDS to 0.5%, and the tube very gently agitated on a rocker platform until all suspended matter had dissolved.

After solubilisation, the sample was transferred to a 2 ml Eppendorf tube (Safe Lock; Eppendorf-Netheler-Hinz GmbH, Hamburg, Germany), extracted with an equal volume of a TE-buffered saturated phenol solution (80% phenol), and the phases separated using a microcentrifuge (13 500 rpm for 5 minutes). The aqueous phase was then sequentially extracted with 1:1 phenol: chloroform and chloroform alone (utilising equivalent centrifugation steps), the final supernatant removed, 0.1 volume 5 M NaCl and 2 volumes absolute ethanol added, and the sample was held for 18-24 h at -20°. Precipitated DNA was spun down in a microcentrifuge (13 500 rpm for 10 minutes; calculated RCF 11 000 x *g*), the supernatant discarded, and the pellet dried under vacuum for 2 h to remove all traces of ethanol. The pellet was solubilised in 50-100 µl TE prior to addition of stock RNase A solution (5 mg ml^{-1}), which had previously been boiled for 20 minutes to denature DNase contaminants, to give a final enzyme concentration of 300 µg ml^{-1}. After 2 h at 20° the sample was loaded for electrophoresis, or frozen at -80° until required.

2.8.4 Apparatus

An Atto Corporation (Tokyo, Japan) AE-6110 horizontal submarine slab gel electrophoresis system was used for the agarose gel separation of DNA samples. This consisted of an acrylic electrophoresis chamber with buffer reservoirs, platinum anodic and cathodic electrodes, and a gel tray. A SJ-1082 power supply (Atto Corporation) capable of constant output in the ranges 2-100 mA/10-500 V (D.C.) was connected to the AE-6110 unit. An external timer with a timeframe of 0-24 h was connected to actuate and deactuate the power supply as required.

2.8.5 Electrophoresis

Agarose (1.5-1.8%) was dissolved to complete homogeneity in 89 mM Tris/ 89 mM boric acid/ 2 mM EDTA, pH 8.0 (TBE) by means of constant stirring on a hotplate. The solution was cooled to 50° and rapidly poured into a tape-sealed gel tray to achieve a final gel thickness in the range 3.5 - 5 mm, and a well-former used to fashion 15 sample wells. After complete cooling, the wells were rinsed to remove traces of unset agarose, the gel transferred to the electrophoresis unit and TBE added until the gel was covered to an approximate depth of 1 mm. Equilibration was achieved by 'pre-running' the gel in the electrophoresis unit at 10 mA for 15 minutes.

Where required, the concentration of DNA in experimental samples was determined according to the method described in section 2.7 in order to optimise loading conditions. DNA samples in TE were admixed with 5 µl of a viscous solution consisting of 50 mM NaCl, 25 mM EDTA, 1% Ficoll, 50% glycerol, 0.1% SDS, containing a trace of bromophenol blue. Loaded sample volumes were standardised for each electrophoretic separation, and were related to gel thickness (and therefore well volume) at 5 µl sample per mm gel thickness. The admixture was held at 4° to increase viscosity and then dispensed by careful displacement layering into the gel sample wells. When required, 5 µl of 123 bp calibration standard 0.5 mg ml^{-1} in 10 mM Tris-HCl/ 50 mM NaCl/ 0.1 mM EDTA, pH 7.5 was loaded into an adjacent well after mixing with an equal volume of loading solution.

Electrophoresis was performed using a constant current in the range 12-16 mA for up to 16 h. In the majority of experiments, electrophoresis was for 6-8 h which normally equated to a dyefront migration distance of 5.5-8 cm from the origin. Under the conditions detailed above, a reference current setting of 16 mA was equivalent to a constant voltage of approximately 3.5 V cm^{-1}.

2.8.6 Visualisation and photography

On completion of electrophoresis the gel was immersed in 1 µg ml^{-1} ethidium bromide and held in the dark for 30 minutes. Where necessary, gels were destained with 1 mM $MgCl_2$ for up to 15 minutes to improve the contrast between fluorescent DNA bands and the background. The DNA bands were visualised by transillumination with 302 nm UV-irradiation using a TM 20 transilluminator (Ultra Violet Light Products, Cambridge, England). Photography was by transmitted light onto 35 mm black and white film (TMAX 100; Kodak, Hemel Hempstead, England) using a Wratten 22A yellow filter assembly.

Where accurate estimation of fragment sizes was required, the photographic image was scanned by video processing to obtain a density profile on an expanded scale (PC_Image analysis software; Foster Findlay Associates Ltd, Newcastle, England) The resulting digitised greyscale values were then processed using a commercial data handling software package (Fig.P; Biosoft Ltd, Cambridge, England).

2.9.1 PROTEIN SYNTHESIS

The rate of protein synthesis within thymocytes was determined by measurement of the rate of incorporation of radiolabelled amino acid, [^{3}H]-leucine, into acid-precipitable protein material.

2.9.2 Materials

L-[4,5-^{3}H]-Leucine, of stated specific activity 45 Ci/mmol and 99.7% radiochemical purity, was obtained from Amersham International plc (Rickmansworth, England). Aquasol

scintillation liquid was from E.I. Dupont Nemours NEN (Stevenage, England), and PCA and TCA from BDH Ltd (Poole, England).

2.9.3 Assay

At the required timepoint, [^{3}H]-leucine was added to give a final concentration in the incubation medium of 1 μCi ml^{-1}. In some experiments the radiolabel was added immediately prior to the test compounds, or as an alternative procedure, it was introduced 60 minutes before the test compounds.

Quadruplicate samples of cell suspension (each equivalent to 5 x 10^6 thymocytes) were removed and placed into disposable plastic test tubes (75 x 12 mm) after 10, 30, 60, 120 and 360 minutes of incubation. In studies where cells had been prelabelled with [^{3}H]-leucine, an additional sample timepoint was incorporated (0 minutes) coincident with introduction of the test compounds. Tubes were spun in a refrigerated bench centrifuge (Denley BR401) for 3 minutes at 1000 rpm, the medium aspirated and 1.0 ml 0.5 M PCA added. The contents of each tube were vortex-mixed, and after standing for 10 minutes at 4°, the sediment was spun down by centrifugation (10 minutes at 3000 rpm). The supernatant was removed and the protein pellet was washed three times with 2 ml aliquots of 10% TCA by repeated resuspension and centrifugation (10 minutes at 3000 rpm).

After discarding the final TCA wash, 0.25 ml 1 M NaOH was added and the pellet was resuspended by vortex-mixing. Following an overnight interval to allow digestion of protein, an equal volume of 1 M HCl was added for neutralisation. Beta vials were filled with 4 ml of Aquasol, and the digests added. After thorough mixing (two rolling mixes at 5 minute intervals) the vials were stored for 24 h at 4° to allow any chemiluminescence to decline to acceptable levels. The samples were counted in a LKB 1216 Rackbeta scintillation counter (LKB, Milton Keynes, England). An internal calibration standard based on Aquasol scintillant was employed; the sample counting time was 5 minutes.

2.9.4 Calculation of results

The radiolabel incorporated into acid-precipitable material, in terms of disintegrations min^{-1} (dpm), was plotted against length of incubation. The results were standardised to reference the dpm equivalents for 10^6 cells.

2.10.1 ATP

Spectrophotometric and fluorimetric assays are available for measuring ATP levels, but none are sufficiently sensitive for the determination of the amount found in a practical number of thymocytes, especially if ATP depletion is expected. Bioluminescence techniques, allied to a sensitive photon detection system, can be as accurate as other methodologies but are orders of magnitude more sensitive (10^{-15} M is achievable).

This method uses a crude luciferase/luciferin extract from firefly lanterns which produces light in the presence of ATP according to the following reaction scheme:

$$\text{LUCIFERASE (E)} + \text{LUCIFERIN } (LH_2) + \text{ATP} \rightarrow E.LH_2AMP + PPi$$
$$E.LH_2AMP + O_2 \rightarrow E + CO_2 + \text{AMP} + \text{OXYLUCIFERIN} + \text{LIGHT}$$

Since the number of photons liberated is proportional to the amount of ATP present (one photon is produced for each reactant ATP molecule consumed) suitable amplification allows a photon detection system to be calibrated for the estimation of cellular ATP levels (Lemasters and Hackenbrock, 1978). The reaction is extremely rapid, and therefore it is necessary to partially inhibit the luciferase by the addition of arsenate ions to the incubation. EDTA is added to ensure inactivation of cellular phosphatases. The linear range of the assay is 10^{-12} to 10^{-6} M ATP.

2.10.2 Materials

ATP, EDTA and firefly lantern extract were from Sigma Chemical Co. Ltd (Poole, England), and potassium dihydrogen orthophosphate, magnesium sulphate heptahydrate, disodium hydrogen arsenate heptahydrate, and TCA were from BDH Ltd (Poole, England).

2.10.3 Preparation of samples

Triplicate aliquots of cell suspension (each equivalent to 3 x 10^6 thymocytes) were taken 0, 15, 30, 60, 120, 240 and 360 minutes after introduction of test compounds, placed into disposable plastic test tubes (75 x 12 mm) and spun in a refrigerated (4°) bench centrifuge for 5 minutes at 1000 rpm. The medium was aspirated from each tube, 1.0 ml 1 M TCA/10 mM EDTA was added and the contents vortex-mixed for 5 seconds. After leaving to stand for 10 minutes at 4°, to allow complete precipitation, the sample was processed or stored at -80° (ATP is stable for up to 14 days under the latter conditions).

2.10.4 Standards

Thymocytes contain approximately 4-6 nmoles ATP per 10^7 cells and therefore extraction of 3 x 10^6 cells into 1 ml of TCA gave a concentration of 1.2-1.8 μM ATP. In order to cover this range of values, a standard curve of 0-4 μM ATP was constructed. After dilution, the standards were treated in the same manner as the experimental samples.

2.10.5 Instrumentation

A photomultiplier (PM) tube (Cat. No. 9863B98/350; red sensitive), control unit and forced-air cooling system constitute the Photon Detection System MkII (Thorn EMI Ltd, Ruislip, England). A cooling system enables the PM tube to be operated at a temperature of -25° which markedly reduces spurious background counts (with cooling, this system routinely gives a background of 3-7 counts s^{-1}). The control unit contains the power supply and the PM controller. Samples are placed into a compartment adapted for the purpose; the sample holder is surrounded on one side by a hemifocal reflector unit whilst

the other side is located close to the window of the PM tube. The system was controlled during the assay by a proprietary computer program supplied with the unit (Thorn EMI). After a counting time of 10 seconds per sample, the number of counts s^{-1} was calculated and the background count obtained prior to the start of measurement was subtracted to give a corrected final value.

2.10.6 Assay

The assay was carried out in plastic disposable test tubes (75 x 12 mm) to avoid the possibility of variance in photon transmission due to differences in the thickness of glass tubes. A buffer system; 80 mM $MgSO_4.7H_2O$, 10 mM KH_2PO_4 and 100 mM $Na_2HAsO_4.7H_2O$, was freshly mixed on the day of use and the pH adjusted to 7.4. The firefly lantern extract was supplied as a powder, containing buffer, in 10 ml vials and the contents of one a vial were resuspended in 5 ml of UHQ water. After thorough mixing, the insoluble fraction was sedimented by centrifugation (5 minutes at 1000 rpm) and the supernatant was used as the source of luciferase/luciferin. Although stable in its dried form, the luciferase was found to rapidly lose activity in solution even when stored frozen at -20°, and therefore it was always freshly prepared and held on ice prior to use. 2 ml of buffer was pipetted into each plastic tube and 0.02 ml of sample, or standard, was added. The reaction was initiated by the addition of 0.1 ml of the lantern extract solution and the contents of the tube were rapidly vortex-mixed. Light emission from the sample is not constant; there is a short lag phase leading to maximal light production followed by a slow lengthy decay phase. Therefore the length of the interval between lantern extract addition and the measurement of the sample was standardised to an optimal timing of 15 seconds.

2.10.7 Calculation of results

A linear regression program was used to compute the relationship between the bioluminescence values (counts s^{-1}) and the respective ATP concentrations (nmoles ml^{-1}) for the range of standards. After interpolation from this standard curve, the values for experimental samples were standardised with respect to the original cell number in the sample (nmoles per 10^7 cells).

2.11.1 FLOW CYTOMETRY/CYTOFLUOROGRAPHY

Flow cytofluorography is a relatively new technique that has been applied to population analysis of parameters such as viability, cell cycle status and cellular phenotype. In addition, useful information can be acquired on the morphometric character of monodisperse cell suspensions from forward light scatter (FSC) measurement of cell size, and 90° light scatter to probe internal cellular structure. Multiparameter flow cytometry has the advantage of event quantitation without averaging the result over a potentially heterogeneous cell population, and its relatively high analysis throughput confers advantages over single cell level, labour intensive techniques such as immunocytochemistry.

The DNA histogram/cell cycle analysis method described is based on modifications of techniques originally devised for fluorochrome assessment of cell cycle kinetics parameters (Crissman et al., 1975; Telford et al., 1991). Since analysis is best achieved after treatment of cells to reduce the amount of cytoplasm adjacent to stained nuclei (Thornthwaite et al., 1980), a hypotonic staining solution containing a low concentration of non-ionic surfactant was employed.

2.11.2 Materials

Ethidium bromide, Triton X-100, trisodium citrate and ribonuclease A were obtained from Sigma Chemical Co. Ltd (Poole, England). Phosphate-buffered saline was prepared as detailed in section 2.1.6.

2.11.3 Preparation of samples

Aliquots of approximately 5 x 10^6 thymocytes were pipetted into 70% ethanol (pre-cooled to -20°), mixed by vigorous swirling to avoid agglutination, and allowed to fix at 4°. In studies with test agents, the sample times were standardised to 0, 1, 2, 4, 6, 8 and 24 h after incubation commencement. During initial experiments, the dispersion was evaluated by phase contrast microscopy and found to consist mainly of single cells. After centrifugation at 1000 x *g* for 10 minutes the cell pellet was resuspended in 4 ml PBS, vortex-mixed for 10 seconds, and allowed to equilibrate for 10 minutes. After centrifugation the supernatant was removed, 2 ml of hypotonic fluorochrome solution; 3.5 mM trisodium citrate/ 0.1% (v/v) Triton X-100/ 50 μg ml^{-1} ethidium bromide was added, the cell pellet resuspended and vortex mixed for 10 seconds. RNase A, that had previously been boiled for 20 minutes, was added to give a final concentration of 250 μg ml^{-1}, and the sample incubated for 1 h in the dark at ambient temperature; this treatment was designed to prevent fluorescence being detected as a result of ethidium bromide interaction with RNA.

2.11.4 Instrumentation

An Ortho System 50 H cytofluorograph (Ortho Instruments; Westwood, USA) fitted with an argon laser producing monochromatic radiation at 488 nm was used. A schematic outline of the major elements of the optical system of this cytofluorograph is presented in Fig. 2.3. The signal output was analysed and displayed by means of an Ortho Instruments Model 2150 computer and graphical workstation.

2.11.5 Cytofluorimetric analysis

The sample was aspirated into the flow cell of the cytofluorograph, the fluorochrome was excited at 488 nm and the red fluorescence recorded subsequent to transmission through a 630 nm long pass filter using linear amplification. Relative cellular DNA content was assessed after acquisition gating imposition which discriminated doublet nuclei (by peak height/coefficient of variation) to ensure the counting of single nuclei only. Gate settings

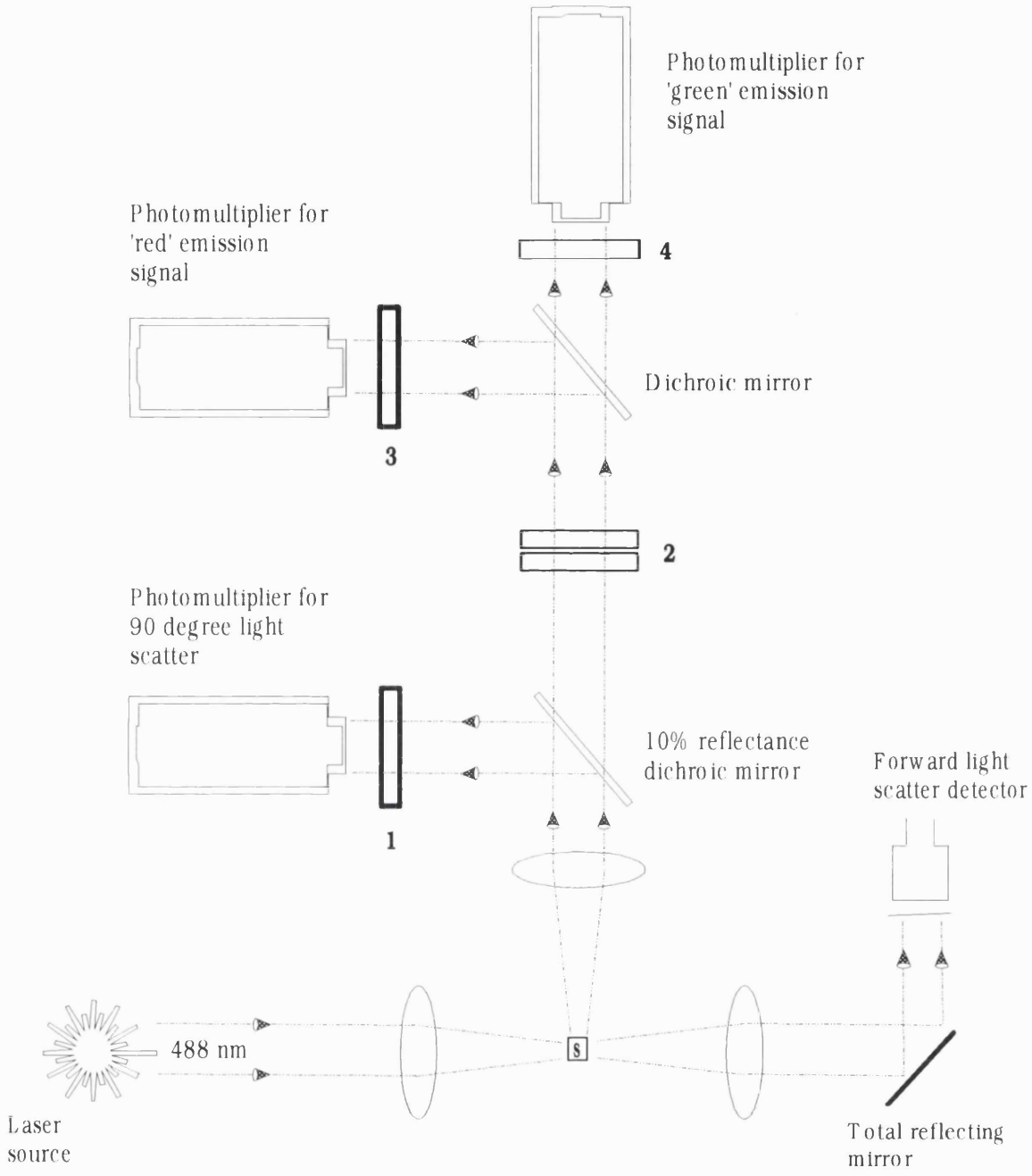

FIGURE 2.3 Stylised representation of optical system elements of the Ortho 50 H cytofluorograph used for thymocyte flow cytometric studies.

Not shown to scale. A four parameter layout is detailed although measurements were principally based on detection of red fluorescence arising from ethidium bromide-DNA interaction and also FSC. The sample carrier stream is above the plane of the diagram and intersects at S. Filter 1: Neutral density, 2: 520 nm long pass interference, 3: 630 nm long pass, 4: green barrier 510/550 nm.

were maintained throughout a series of experiments. A minimum of 10^4 counted singlet events was analysed for each sample. Forward light scatter (FSC) measurement was used to estimate particle size.

2.11.6 Data analysis

For cell cycle analysis, red fluorescence readings (> 630 nm) were assembled in real time as a 'X-Y' scatterplot of event number against fluorescence (linear scales). Based on fluorescence amplitude, gates were imposed to correspond to nuclei with increasing DNA content from 2N (G_0/G_1 phase), 2N-4N (S phase) and 4N (G_2/M phase). Data were analysed to give cumulative frequency values using a proprietary software package on an Ortho 2150 computer. FSC measurements were displayed concurrently on a linear scale.

2.12 MICROTUBULAR CYTOSKELETON ASSESSMENT

This method is described in chapter 5.

2.13 IN VIVO STUDIES

Experimental protocols and methods are detailed in chapter 6.

2.14 ORGANOTIN COMPOUND PURIFICATION AND HANDLING

Technical grade TBTO with a declared purity of 88.2% was obtained from Fluka Chemicals Ltd (Glossop, England). Since this was expected to contain impurities with potentially significant biological activities, e.g. bis(tri-n-butyltin) hydroxide, TBTC and di-n-butyltin oxide, it was repurified before use by fractional distillation. The original sample was gradually heated to 200-205° under a reduced ambient pressure of 2-3 mm Hg, and the evolved vapour collected by means of a vertical fractionating condenser. TBTO purified by this method was assayed by a combination of gravimetric microanalysis and nuclear magnetic resonance spectroscopy and was always found to be more than 99.5% pure. TBTC and DBTC were obtained from Fluka Chemicals Ltd (Glossop, England) or Aldrich Chemical Co. Ltd (Gillingham, England) respectively, and had declared purities in excess of 97%; these were used without further purification.

During storage, triorganotin compounds undergo redistribution reactions (Laughlin et al., 1986), viz.:

$$2R_3SnX \Leftrightarrow R_4Sn + R_2SnX_2$$

In addition, organotins are known to be light sensitive, and prone to gradual respeciation in the presence of moisture (Blunden and Chapman, 1982; Dr. A. Crowe, personal communication). Therefore all compounds were stored at 4° in the dark under desiccation and, as a precautionary measure, stock TBTO was repurified on a six monthly basis. Working solutions were freshly prepared immediately prior to each experiment by dissolving the required amounts of organotin compound in absolute ethanol.

CHAPTER 3

INVESTIGATION OF THE MODALITY AND CHARACTERISTICS OF CELL KILLING CAUSED BY THE IN VITRO EXPOSURE OF RAT THYMOCYTES TO TRI-n-BUTYLTIN.

ABSTRACT

Activation of apoptosis is an essential process in the regulation of the developing mammalian T lymphocyte repertoire and the deletion of autoreactive T cells. Exogenous stimuli, e.g. glucocorticoids, monoclonal antibodies to the CD3/TcR complex and γ irradiation, can also trigger thymocyte apoptosis.

The cytotoxicity of the immunotoxic tributyltin compound bis(tri-n-butyltin) oxide (TBTO) to isolated rat thymocytes was studied, and compared to cell killing resulting from exposure to methylprednisolone (MPS) or the divalent cation ionophore A23187. Cell killing after treatment with TBTO occurred in two disparate forms over the timeframe studied. At low TBTO concentrations (< 5 μM), viability loss was delayed and was preceded by extensive degradation of genomic DNA. When analysed by agarose gel electrophoresis, the DNA fragments produced appeared as a multimeric series with a repeat multiple of 180-200 base pairs, indicating that endonucleolytic internucleosomal cleavage had occurred. There was a corresponding marked increase in the incidence of cells that exhibited chromatin condensation, cytoplasmic contraction and the formation of apoptotic bodies. In quantitative terms, DNA fragmentation correlated highly with chromatin condensation. Ultrastructural studies demonstrated that this order of TBTO exposure caused nuclear changes principally involving chromatin compaction and nucleolar dissolution, whilst cytoplasmic organelles and membranes appeared to be structurally conserved until late in the process. Considered together, these morphological and biochemical findings were consistent with the activation of thymocyte apoptosis by TBTO and were essentially comparable to apoptotic cell killing stimulated by MPS or A23187.

Higher concentrations of TBTO were rapidly cytotoxic and caused cytopathological alterations typical of necrosis in the absence of extensive or specific DNA cleavage. A similar biphasic pattern of cell killing was associated with gradation in A23187 exposure concentration.

It is concluded that thymocyte apoptosis is stimulated in vitro by tributyltin at concentrations of relevance to those causing T cell immunodeficiency in vivo. These findings also add further support to the developing hypothesis that the amplitude of adverse stimuli, including toxic injury, is key in determining the mode of death in cells possessing an intrinsic capability for apoptosis.

3.1 INTRODUCTION

3.1.1 The thymocyte model of apoptosis

The rodent thymocyte model of apoptosis has a number of experimental advantages (Wyllie, 1985; Ellis et al., 1991): (i) the vast majority of cortical thymocytes die by this method during normal ontogeny and maintain a death program at a high state of readiness (Rothenberg, 1990; Kisielow et al., 1988; Smith et al., 1989); (ii) thymocytes are easily separated from non-lymphoid components to give a relatively homogenous population; (iii) thymocyte apoptosis is activated by short-term in vitro exposure to a number of stimuli of physiological (e.g. glucocorticoids) and pathological (e.g. ionising radiation) relevance. For these reasons, many publications of fundamental importance to the understanding of apoptosis stem from work in this system (for examples see Kaiser and Edelman, 1977; Wyllie, 1980; Yamada et al., 1981; Cohen and Duke, 1984; McConkey et al., 1989b). Recently, research has also focused on environmental agent thymotoxicity involving apoptosis (Wyllie, 1987b; Burchiel et al., 1992).

3.1.2 TBTO: An important environmental pollutant and immunotoxicant

As described in section 1.6, TBTO has high ecotoxicity and as a TBT compound exhibits selective in vivo toxicity toward mammalian lymphoid cells, and in particular thymocytes. The chemical structure of TBTO and some parameters of relevance to the conduct of in vitro studies are shown in Fig. 3.1 below:

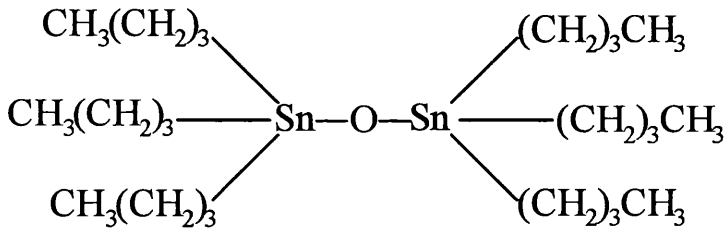

Synonyms: Bis(tri-n-butyltin) oxide; tributyltin oxide; TBTO; hexabutyldistannoxane; 6-oxa-5,7-distannaundecane, 5,5,7,7-tetra-butyl-	
CAS number: 56-35-9	Relative density: 1.17 - 1.18
Molecular mass: 596.16	log P_{ow}: 3.19-3.84 (distilled water); 3.54 (saline)
Solubility: distilled water 0.7-7 mg l^{-1}; saline 8-10 mg l^{-1}; phosphate buffer (pH 7.0-7.8) 1-4 mg l^{-1}; Tris-HCl buffer (pH 8.1) 31 mg l^{-1}. Freely soluble in ethanol, diethyl ether, halocarbons, other organic solvents and lipids.	
Vapour pressure: 1 x 10^{-3} Pa at 20°	
Stability: >2 months in the dark; t½ (decomposition) > 89 days in sunlight	

FIGURE 3.1 Structure and selected physico-chemical properties of TBTO.
Values taken from WHO, 1980; IPCS, 1990; Maguire et al., 1983.

Commercial grade TBTO is about 85% pure, the principal impurities are normally dibutyltin oxide, tetrabutyltin and other tributyltin compounds. The Sn-C bond of tributyltins is reported to be quite thermostable and light resistant to the visible spectrum,

but UV irradiation produces photolysis (Blunden and Chapman, 1982). It has been suggested that in aqueous solution TBTO dissociates to a hydrated TBT cation, which can then undergo reaction with any anions present (Maguire et al., 1983, Laughlin et al., 1986). Whilst the equilibrium constants are not available for these reactions, Laughlin and co-workers showed that TBTO reacts in aqueous saline mixtures to give the following:

$$(Bu_3Sn)_2O + H_2O \Rightarrow 2Bu_3SnOH$$
$$Bu_3SnOH + H_3O^+ \Rightarrow Bu_3SnOH_2^+ + H_2O$$
$$Bu_3SnOH_2^+ + HCO_3^- \Rightarrow Bu_3SnCO_3^- + H_3O^+$$
$$Bu_3SnOH_2^+ + Cl^- \Rightarrow Bu_3SnCl + H_2O$$

Thus in addition to TBTO, the predominant species are $Bu_3SnOH_2^+$, and Bu_3SnCl or its monoaquated $Bu_3SnCl(OH_2)$ variant at pH < 7; Bu_3SnCl, Bu_3SnOH and $Bu_3SnCO_3^-$ at pH 8; or the hydroxide and carbonate at pH > 10. The aqueous solubility of TBT compounds is strongly dependent on pH and other ionic constituents in solution (Maguire et al., 1983).

3.1.3 Cytotoxic effects of TBT in vitro

Many previous in vitro studies on TBT have demonstrated its cytopathic effects on a range of prokaryotic and eukaryotic cell types, e.g. bacteria (Bokranz and Plum, 1975), algae (IPCS, 1990), hamster kidney cells (Reinhardt et al., 1982), rat hepatocytes (Kanetoshi, 1983), and rodent lymphocytes or haemopoietic cells (Vos et al., 1984a). Effective concentrations usually range from the nanomolar level for inhibition of biochemical processes and production of cytostatic effects, to the low micromolar order for cytolethality. The spectrum of adverse biochemical and cellular changes elicited by TBT are both numerous and complex, and therefore due to this 'shotgun-like' action the relative importance of the various intracellular targets are not as yet fully defined.

The action of TBT as a cellular energetics poison has been much emphasised in the literature (Snoeij et al., 1986a; Boyer, 1989); resultant mitochondrial dysfunctions including direct inhibition of the proton translocase system, disruption of organelle volume homeostasis, and ionophore-like Cl^-/OH^- exchange, cause marked inhibition of oxidative phosphorylation. Such effects are reversible and occur at concentrations well below those affecting plasma membrane integrity (energetics effects are discussed further in Chapter 5).

Since the early observation that triorganotins could interact with phospholipids (Aldridge and Street, 1964), the membrane-directed toxicant actions of TBT have been intensively studied. Indeed some investigators consider that the primary cellular target for TBT is the cell membrane (Gray et al., 1987). TBT is lipophilic, partitions into lipid structures and has been shown to disturb the structure and function of a variety of biomembranes (Porvaznik et al., 1986; Selwyn, 1976; Zucker et al., 1989; Butterfield et al., 1991). Its molecular hydrophobicity and lack of charge are the physical properties which account for this

sequestration. Byington et al. (1974), in the first comprehensive study of organotin membrane toxicity, demonstrated that TBT was haemolytic to isolated rat or human erythrocytes, and that this occurred independently of the anionic substituent. At concentrations of 0.1-1 μM TBT produced a rapid, but reversible, transformation of red blood cell discocytes to echinocytes, and finally caused cytolysis in the range of 5-10 μM (Porvaznik et al., 1986; Gray et al., 1987). At haemolytic levels, molecular aggregates of TBT intercalated within the membrane bilayer were visible by TEM. It is probable that the amphipathic nature of TBT (its asymmetric arrangement of hydrophobic and hydrophilic groups) leads to self-aggregation when the local solubility limit is exceeded, in order to segregate its butyl moieties away from water molecules. Lipid soluble thiol reagents were able to reverse these membranal effects (Gray et al., 1986). In murine erythroleukemia cells (MELC), exposure to TBT at or above a critical product value (CPV) of concentration and treatment duration (e.g. 0.5-1 μM for 16 h) caused severe irreversible cytotoxicity including loss of plasma membrane integrity, membrane depolarisation, and plasmalemmal structural changes (Zucker et al., 1988; 1989; 1992). Based on the indirect measurements of increased resistance to surfactant-mediated cytolysis and inhibition of membranal protein mobility, these workers inferred that membrane fixation (cross-linking and protein denaturation) occurred after short-term exposure to 5-50 μM TBT (Zucker et al., 1988), in a manner reminiscent of ethanol or aldehyde action. As a possible alternate explanation to that of direct TBT involvement, it is notable that during apoptosis cells become resistant to detergent and chaotropic agent dissolution due to transglutaminase action (Fesus et al., 1991). Below the CPV, MELC exhibited increased retention of carboxyfluorescein, which was thought to represent diminished plasma membrane permeability (Zucker et al., 1988; 1989), and was reversible (Zucker et al., 1992). Cation uptake in macrophages incubated with various TBT concentrations followed a similar biphasic kinetic, and this has also been ascribed to thresholds in membrane injury (Rice and Weeks, 1989). Comparison of various organotins on MELC, using carboxyfluorescein fluorescence maxima as a marker of biomembrane perturbation, showed that TBT was 20, or 1000 fold more potent than TET or TMT, respectively (Zucker et al., 1989).

In keeping with the propensity of TBT compounds to affect ion translocating ATPases (Selwyn, 1976), the plasma membrane Na^+/K^+-ATPase system in several cell types is readily inhibited. The first report by Aldridge and Street (1964) indicated that in isolated preparations the IC_{50} was approximately 10 μM TBT, with 21% inhibition at 1 μM. Costa (1985) showed that the Na^+/K^+-ATPase of mouse brain synaptosomes is inhibited by TBT, with IC_{50} values of 3.3 and 8.7 μM, respectively for tributyltin bromide; or 4.7 and 7.7 μM for TBTO. For the range of triorganotins assessed, inhibitory activity correlated well with lipophilicity, i.e. TMT<TET<TBT<TPhT. A similar relationship to compound hydrophobicity has been reported in human erythrocytes and ox brain microsomes (Selwyn, 1976), and the effect development half-time is rapid (about 1 minute). For some excitable

cells, it seems that sodium pump activity can be affected at even lower TBT concentrations, since the IC_{50} for rat cardiac membrane Na^+/K^+-ATPase is about 0.6 μM with total cessation of activity apparent at 2 μM (Cameron et al., 1991). Based on ouabain binding studies and use of isolated membrane systems, organotin binding to the enzyme complex appears to be a critical event. Therefore energetics disturbance additional to this is liable to reduce the translocase activity still further. TBT at concentrations of 2.5-5 μM greatly impeded the membrane mobility of the Na^+/K^+-ATPase complex in porcine kidney membranes (Zucker et al., 1988). Extensive literature searches have revealed no specific data on the effects of TBT on the thymocyte or mature T lymphocyte enzyme.

The plasma membrane Ca^{2+}-ATPase of rat thymocytes is also significantly inhibited by TBT (Chow et al., 1992), though appreciable activity still remained after exposure to 10 μM TBTC, whereas DBT or TMT were ineffective. It is known that other mechanisms also contribute to the elevation in cytosolic Ca^{2+} seen in such circumstances (see 4.4). Sarcoplasmic reticulum preparations show a similar depression of Ca^{2+}-ATPase function, and the IC_{50} for TBT has been established as about 7 μM (Selwyn, 1976); disturbance of phospholipid molecules associated with this translocase may be causal.

The cytotoxicity of TBT to thymocytes has been systematically examined by Snoeij and co-workers (Snoeij et al., 1986a; 1986b, 1988b). Cells isolated from young Wistar rats were exposed to 0.01-10 μM TBTC for periods up to 30 h, and assessments made of cell count, trypan blue exclusion, ^{51}Cr-release, thymidine incorporation and cAMP formation. Treatment with 4 μM TBT produced early signs of plasma membrane dysfunction or damage within 5 h, as evidenced by vital dye inclusion and chromium marker loss, although cytolysis was not observed even at 10 μM. Lower concentrations (1-2 μM) did not affect membrane integrity until considerably later times. However, thymidine incorporation into DNA, the most sensitive parameter, was depressed at TBT levels as low as 10-50 nM; this was interpreted as evidence of antiproliferative activity. Further demonstration of the potent antiproliferative effects of TBT is shown by the depression of clonogenicity in a hamster kidney fibroblast cell line incubated with submicromolar levels of TBTC or TBTO (Reinhardt et al., 1982). More detailed studies of TBT effects on macromolecular synthesis (DNA, RNA and protein precursor incorporation) indicated that incubation at $\geqq 1$ μM was sufficient to severely curtail production after 15 minutes (Snoeij et al., 1986b), and that thymocyte subsets were differentially sensitive (Snoeij et al., 1988b). The influence of TBT on protein synthesis is further considered in Chapter 5. Certain triorganotins, in particular TBT, grossly perturb the cellular cytoskeleton, though this important target has received scant investigation to date (see also 5.1.2).

3.1.4 Modes of toxicant-induced cell death

The importance of apoptosis as an alternate death mode to necrosis following an injurious

stimulus such as toxicity is now acknowledged even amongst workers who have previously exclusively researched necrotic cytolethality (Trump and Berezesky, 1992). Recently it has become apparent that a widely divergent range of agents can activate apoptosis in susceptible cells (Cotter et al., 1990), and that the traditional concepts of cell injury staging need revision. The precept that gross injury, e.g. severe toxicity or ischaemia, causes rapid loss of intracellular homeostasis and subsequent necrosis remains valid. However, so called 'sublethal injury' (Trump and Berezesky, 1984) may result in either recovery or latent death by apoptosis. In terms of the delineation between necrogenic and apoptotic cell killing, several points are of relevance. Firstly, apoptosis requires maintenance of at least basal cellular integrity so that finely balanced signal transduction and active effector processes may occur (see section 1.3); implicit within this is the notion that severe injury will preclude completion of the apoptotic process. Therefore, apoptosis is induced in susceptible tissues by injurious stimuli of smaller amplitude (e.g. low toxicant concentrations) than those which produce necrosis in the same tissue (Wyllie, 1987b; Dyson, 1986; Lennon et al., 1991). Secondly, apoptosis will occur only in cell types that retain a physiological capability for this death mode, and will happen much more readily when pre-priming exists, for example in thymocytes (Arends and Wyllie, 1991) since then only a triggering event is required. In this context a moderate increase in $[Ca^{2+}]_i$ can constitute a triggering stimulus to a primed cell (Nicotera et al., 1992), though other signals may also be required. Passage through or blockade in a critical cell cycle phase and other enabling events may be a prerequisite in other cell types before an adequate signal exists to express an encrypted internal death program (Eastman, 1990; Dive and Hickman, 1991).

The causal biochemical events underlying necrosis remain poorly understood (Trump and Berezesky, 1992; Pounds and Rosen, 1988), and therefore the definition of effect thresholds separating this and non-necrotic death is just beginning. During necrosis, failure of the plasma membrane ATP-dependent Na^+/K^+ translocase with consequent loss of univalent cation homeostasis is clearly important. But there is good evidence to suggest that this in isolation is not the sole lethal stimulus, and that events including ATP depletion and elevated $[Ca^{2+}]_i$ are also required (Trump and Berezesky, 1984; Orrenius et al., 1989).

3.1.5 Aims of these studies

Ex vivo primary cultures of rodent thymocytes were employed as a test system in order to further investigate the known marked cytotoxicity of TBT to lymphoid cells. In view of the primed state of thymocytes to deletion by apoptosis, emphasis was placed on determining whether this physiological death mode could be accidentally activated by TBT toxicity. Findings described in this chapter have previously been partially communicated in the following publication:

Raffray M, Cohen GM (1991) Bis(tri-n-butyltin) oxide induces programmed cell death (apoptosis) in immature rat thymocytes. Arch Toxicol 65: 135-139.

3.2 METHODS

Monodisperse thymocyte suspensions were prepared from 4-6 week old male Wistar rats (School of Pharmacy breeding colony) by the disaggregation method described in section 2.1. After determination of initial viability (section 2.2), which was always in excess of 94%, the cells were diluted to 15, 20 or 25 x 10^6 ml^{-1} in either DMEM or RPMI-1640, each supplemented with 10% FCS. The primary buffer system of these media was sodium hydrogen carbonate 2 g l^{-1} (RPMI-1640) or 3.7 g l^{-1} (DMEM), and the pH was adjusted to 7.4 prior to use. The incubation medium and the initial cell density were standardised within experimental sets. Aliquots of the cell suspension were placed in polystyrene culture plates and incubated at 37° in a CO_2 incubator under an atmosphere of 5% CO_2 : 95% air.

As an alternative procedure, to allow comparison of basal culture technique variables, a rotating flask system was used in some early experiments. 10 ml aliquots of cell suspension diluted in DMEM/10% FCS to a density of 25 x 10^6 ml^{-1} were incubated at 37° in rotating 25 ml round bottomed flasks. These incubations were not conducted aseptically.

3.2.1 Materials

TBTO and TBTC (CAS no. 1461-22-9) were obtained from Fluka Chemicals Ltd (Glossop, England), MPS from Upjohn (Crawley, England), and A23187 (free acid) was from Sigma Chemical Co. Ltd (Poole, England). Detail of organotin purity is given in section 2.14, whilst MPS was declared to be greater than 95% pure.

3.2.2 Test compound handling

TBTO or TBTC were dissolved in absolute ethanol immediately prior to use (see 2.14). Solutions were prepared such that when added to cell suspensions, the incubations contained a final concentration of 0.2% ethanol. Methylprednisolone hemisuccinate as the sodium salt (MPS) was freshly prepared in incubation medium (without FCS) at 500 times the required final concentration, and this solution was added directly to cell suspensions. A stock preparation of cation ionophore A23187 was made in anhydrous DMSO at 5 mg ml^{-1}, and stored in the dark at 4°. This stock was serially diluted with DMSO before use; when the required amounts were added into incubations, the final concentration of DMSO was 0.17%. In all cases, control preparations were incubated with the respective solvent vehicle alone.

3.2.3 Experimental protocols

Schematics of the principle experimental protocols are given in Fig. 3.2a and b. Samples of cell suspension were removed for viability estimation after 0, 1, 2, 4, 6 and 24 h incubation. In some experiments, additional viability measurements were performed at 8 and 12 h. Cell counts were made concurrently with viability determinations as required. Acridine orange (AO) fluorescence assessments were conducted at the 0, 1, 2 , 4 and 6 h timepoints.

VIABILITY

(Initial D_V: 10/20/25 x 10^6 ml^{-1})

⇩

50 µl cell suspension

⇩

Add volume of 0.4% trypan blue solution to adjust to a cell count of 10^7 ml^{-1}

⇩

Introduce onto a haemocytometer for estimation **(section 2.2)**

Cell counts performed using a similar procedure; 1:1 dilution of suspension with trypan blue solution **(section 2.3)**

AO FLUORESCENT STAINING

(Initial D_V: 25 x 10^6 ml^{-1})

⇩

95 µl cell suspension

⇩

Add 5 µl of 100 µg ml^{-1} AO solution

⇩

Mix and place onto a glass slide; view by fluorescence microscopy **(section 2.4.2)**

MORPHOLOGICAL STUDIES

(Initial D_V: 20/25 x 10^6 ml^{-1})

⇩

Aliquot of approximately 10^7 cells

⇩

Add excess 2.5% glutaraldehyde in 0.1M sodium dimethylarsonate

⇩

Fix at 4° for 1 h

⇩

Centrifuge at 800 rpm for 15 min

⇩

Aspirate supernatant

⇩

Dehydrate in graded concentrations of methanol

⇩

Embed cell pellet in epoxy resin and prepare semi-thin sections

⇩

Stain with ethanolic 1% toluidine blue

⇩

View by light microscopy **(section 2.4.1)**

⇩

Post-fixation in OsO_4

⇩

Dehydrate in graded concentrations of methanol

⇩

Embed cell pellet in epoxy resin and prepare ultra-thin sections

⇩

Stain en bloc with uranyl acetate and lead citrate

⇩

View by TEM **(section 2.5)**

FIGURE 3.2a Flow chart showing the preparation of samples for microscopy.
Section numbers refer to the relevant parts of the Materials and Methods chapter.

DNA FRAGMENTATION

(Initial D_V: 10/20/25 x 10^6 ml^{-1})

⇩

Aliquot of 20-100 x 10^6 cells

⇩

Harvest cells (centrifuge at 1000 rpm for 10 min and discard medium)

⇩

Add hypotonic lysis buffer at a volume of 1 ml per 15 x 10^6 cells

⇩

Lyse at 4° for 30 min

⇩

Centrifuge at 27 000 x *g* for 20 min

⇩

Separate supernatant and pellet fractions

⇩ ⇘

Assay for relative DNA content by colorimetry using the modified diphenylamine reaction

(section 2.6)

DNA AGAROSE GEL ELECTROPHORESIS

Aliquot of supernatant corresponding to a minimum lysate of 20 x 10^6 cells

⇩

DNA concentrated by ethanol precipitation

⇩

Sequential extraction with phenol, phenol: chloroform, chloroform

⇩

DNA precipitated with ethanol

⇩

Treatment with 300 µg ml^{-1} RNase for 2 h at ambient temperature

⇩

DNA visualised after agarose gel electrophoresis

(section 2.8)

FIGURE 3.2b Flow chart showing the preparation of samples for analysis.
Section numbers refer to the relevant parts of the Materials and Methods chapter.

Timecourse studies of DNA fragmentation, and light microscope morphological studies utilised the same times as those indicated for viability estimation, otherwise these parameters were routinely assessed after 6 h of incubation. Electrophoresis of DNA was also normally performed at this timepoint. Samples for ultrastructural study were selected from representative resin embedded material prepared for light microscopy at the times designated above.

3.2.4 Statistical analysis

Except where otherwise stated, all results are presented as the mean (arithmetic) $\pm$ 1 SE. Comparisons were made using an unpaired two-tailed t-test, accepting a statistical significance for p of less than 0.05. This was preceded by analysis of data distribution and homogeneity of variance as appropriate. Where the correlation coefficient (r) was calculated, significance level testing was by means of interpolation of the derived t_r value against a t-distribution table.

3.3 RESULTS

3.3.1 Preliminary studies

The use of rotating 25 ml flasks containing 10 ml aliquots of cell suspension was found to be less satisfactory than stationary plate culture for a number of reasons. Although viability remained satisfactory, after several hours the cells had a tendency to form aggregates and also to adhere to the vessel walls, thereby reducing cell density. In addition, since aseptic technique could not be employed, culture periods in excess of 4-6 h were precluded. No differences in key parameters, including viability and DNA fragmentation, were noted between incubations conducted in DMEM and RPMI-1640. As the latter is most commonly cited in reports of lymphocyte experimentation, the decision was made to use this as the standard culture medium. Since RPMI-1640 has a lower HCO_3^- content, pH measurements were made at regular intervals during initial incubations. It was observed that under the gassing conditions employed (5% CO_2: 95% air), the pH of the medium was maintained within 2% bounds of the desired value of 7.4. There was no evidence of oxygenation problems or medium depletion for up to 30 h with cell densities in the range of 10-25 x 10^6 ml^{-1}, and parameters such as viability and DNA fragmentation were consistent within this range of cell densities. Unless otherwise stated, all subsequent experiments employed a standard initial density of 20 x 10^6 cells ml^{-1}. The viability of thymocytes freshly isolated at 4° by the disaggregation technique was routinely in excess of 95%.

Additions of various concentrations and combinations of the vehicles required for introduction of test compounds, or other agents (see also Chapter 4) were without apparent effect as indicated by the results given in Table 3.1.

TABLE 3.1 Effect of incubation with solvent vehicle alone on cell viability and DNA fragmentation.

Test addition	(%)	Viability (%)	DNA fragmentation (%)
None	-	97	16.7
Ethanol	0.12	97	15.4
	0.2	99	17.1
	0.3	96	16.7
DMSO	0.17	98	15.7
	0.3	99	15.0
Ethanol + DMSO	0.3/0.3	98	16.6
Acetone	0.125	96	18.6

Estimations were made after 6 h incubation in the presence of the respective vehicles as indicated, according to the methodologies described in sections 2.2 and 2.6. Results are from one experiment that was representative of two replicates.

3.3.2 Viability and cell count

In agreement with previously published studies on TBT compounds (Vos et al., 1984a; Snoeij et al., 1986a), incubation of thymocytes with TBTO caused a concentration-dependent decrease in viability (Fig. 3.3a). Treatment with TBTO at 5 or 10 μM produced signs of cell blebbing and a rapid loss of viability as evidenced by mean survival values of 45% and 23%, respectively, after 1 h. This contrasted with lower TBTO concentrations (0.1 or 1 μM) where the loss of membrane integrity was predominantly restricted to 6-24 h after the commencement of incubations. At early timepoints, up to 2 h, after addition of 0.1-2 μM TBTO it was noted that some viable (non-stained) cells had a spread or spindle-shaped appearance when visualised for the purposes of viability estimation.

A similar delayed viability loss was observed in cultures exposed to 1 or 10 μM MPS (Fig. 3.3b), and 0.25 or 0.5 μM A23187 (Fig. 3.3c). Slightly higher concentrations of A23187 (1 μM) produced an intermediate response whereby there was a rather gradual decline in the ability of cells to exclude trypan blue until 4 h. After this point a rapid fall in viability was noted which was commonly accompanied by the appearance of large pale staining lytic cells and evidence of cell aggregation and fragmentation. Preliminary experiments indicated that A23187 concentrations in the range of 3-15 μM were rapidly cytotoxic causing extensive blebbing, loss of membrane integrity and extensive cytolysis within 1 h of exposure.

In order to investigate whether cytolysis occurred after exposure to the test agents, cell counts were determined, by haemocytometer, as the incubation period progressed. Counts were unaffected by exposure for up to 6 h to less than 10 μM TBTO, A23187 at less than 1 μM, and after treatment with MPS at 10 μM. However, by the 24 h timepoint, limited decrements in cell density were apparent in these cultures relative to control values

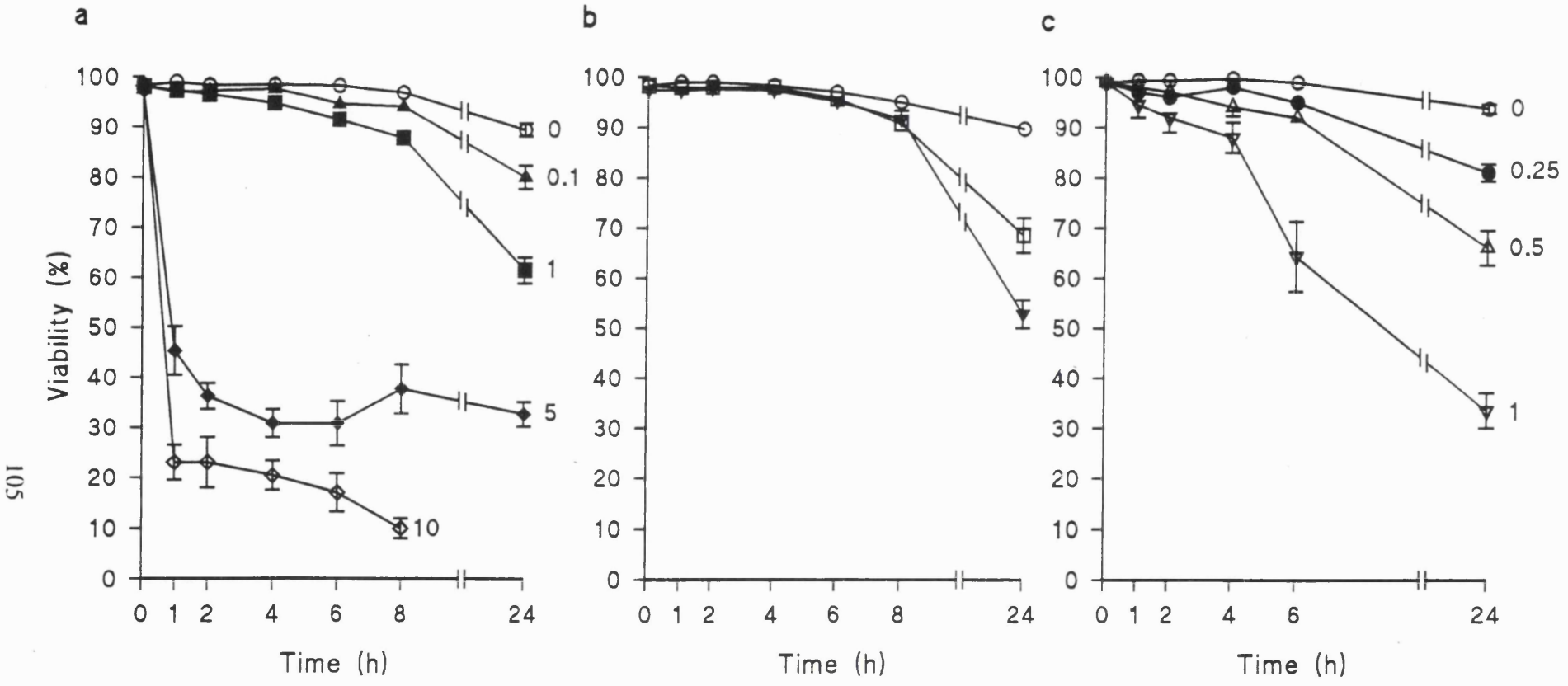

FIGURE 3.3a-c Effect of TBTO, MPS or A23187 on cell viability.

Cells were incubated in the absence (○), or presence of the following concentrations of TBTO: 0.1 μM (▲), 1 μM (■), 5 μM (◆), 10 μM (◇); or MPS: 1 μM (□), 10 μM (▼); or A23187: 0.25 μM (●), 0.5 μM (△) or 1 μM (▽). Results are the means ± SE from four separate experiments. Viability was determined by trypan blue dye exclusion (section 2.2). Due to extensive cytolysis, estimations could not be reliably performed beyond 8 h with 10 μM TBTO.

(Table 3.2). Higher TBTO or A23187 concentrations, caused marked cytolysis within 4-6 h, with commensurate reductions in total cell density.

TABLE 3.2 Effect of TBTO, A23187 or MPS on total cell counts.

Treatment		Cell count (x 10^6 ml^{-1})
Control		24 ± 0.4
TBTO	1 μM	18 ± 1.2
TBTO	5 μM	14 ± 1.5
A23187	0.5 μM	15 ± 1.8
MPS	10 μM	19 ± 0.6

Estimations were made after 24 h incubation in the presence of the indicated test agents according to the method detailed in section 2.3. Initial cell density was 25 x 10^6 ml^{-1}. Results are the mean ± SE from three preparations.

3.3.3 DNA fragmentation

It has previously been reported (Wyllie, 1980; Wyllie and Morris, 1982) that a DNA fragmentation (chromatin cleavage) assay based on non-ionic surfactant lysis of thymocytes under hypotonic conditions, followed by differential centrifugation, gave satisfactory recovery of cellular DNA for analysis. This was confirmed in this study in a series of initial experiments, where it was found that the total DNA recovered from the supernatant and pellet fractions, by the technique detailed in section 2.6, amounted to 84-108% of the DNA content found in uncentrifuged cell lysates.

In freshly isolated thymocytes preparations, initial DNA fragmentation values, i.e. the percentage of DNA resisting sedimentation at 27 000 x *g*, were typically less than 4%. Measurements made during the first 12 h of the incubation period indicated that gradual increases occurred in the controls (Fig. 3.4a), with mean DNA fragmentation reaching approximately 16% after 6 h. These results are consistent with previous studies using rodent thymocytes (Cohen and Duke, 1984; Kizaki et al., 1989).

TBTO treatment at 0.1 or 1 μM stimulated DNA fragmentation in a concentration-dependent manner (Fig. 3.4a). Statistical analysis revealed that mean values at 1 μM were significantly higher than the respective control at all the timepoints; achieving a differential of 258% over the control by 6 h of exposure. An increase was also evident for cells exposed to 0.1 μM TBTO, whereby DNA fragmentation was 142-145% of the control mean by 6-12 h after commencement of treatment. It was notable that at low TBTO concentrations, elevations in DNA fragmentation preceded measurable viability loss by approximately 2-4 h (refer to Fig. 3.3a). These observations were in marked contrast to

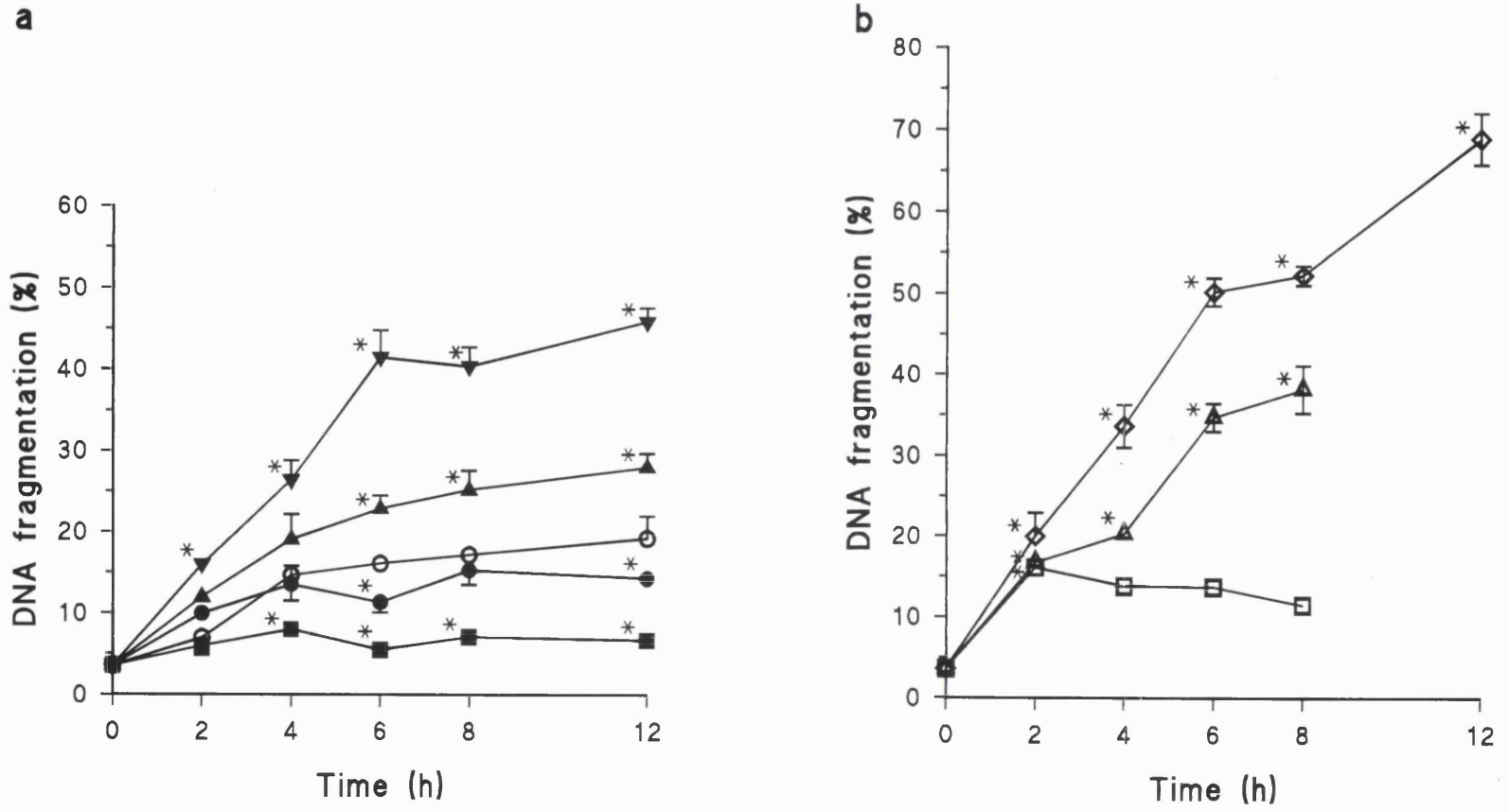

FIGURE 3.4 DNA fragmentation after exposure to TBTO, MPS or A23187.

Cells were incubated in the absence (○) or presence of **a)** TBTO 0.1 (▲), 1 (▼), 5 (●), 10 μM (■); or **b)** MPS 10 μM (◇); or A23187 0.5 (△), 1 μM (□). Results are the means ± SE from three separate experiments, and are expressed as the percentage of DNA that resisted sedimentation at 27 000 x *g*. The methodology employed was as described in section 2.6. Mean values in all vehicle control incubations differed by less than 10%; therefore a single representative series is shown. Determinations were not made after 8 h in A23187-treated cultures. *Result significantly different from control value, $p < 0.05$.

the findings obtained with either 5 or 10 μM TBTO (Fig. 3.4a). At the latter concentration, values essentially remained at basal levels at all timepoints and therefore were found to be significantly below the control from 4 h onwards. A less pronounced, but parallel effect was evident with 5 μM TBTO.

DNA fragmentation in MPS-treated cells was significantly elevated by 2 h of treatment and continued to increase in an almost linear fashion, until at the end of studied timeframe, approximately 70% of genomic DNA appeared as low molecular weight fragments in the supernatant (Fig. 3.4b). Progressive DNA fragmentation was also apparent in thymocyte cultures exposed to 0.5 μM A23187 (Fig. 3.4b), and after 6 h the mean value was 215% of the respective control. After treatment with 0.25 μM A23187, there was a less pronounced increase which occurred over a similar time-scale. Although the DNA fragmentation value was initially elevated at 1 μM A23187, no further increase was detected after 2 h, and levels were seen to diminish to below that recorded in untreated cultures during the latter part of the incubation period (Fig. 3.4b).

Further studies were undertaken to study the dose-response and temporal relationships of organotin-mediated DNA fragmentation using a more closely graduated series of TBTO concentrations (Fig. 3.5a) Fragmentation was significantly increased after 1 h exposure to 2 or 3.5 μM TBTO. At the former treatment level, values continued to increase in an approximately linear manner; indeed, this was found to be the most effective concentration tested in stimulating DNA fragmentation. However with exposure to 3.5 μM there was evidence of development of an effect plateau by the 2 h timepoint. As might be expected, the effects of 2 or 3.5 μM TBTO on thymocyte viability (Fig. 3.5b) were intermediate between those described for bounding concentrations in section 3.3.2. It was noted that disturbed cellular morphologies occurred after 1 h of treatment with TBTO at 3.5 μM, including the development of surface blebbing and cell swelling. These effects were comparable to those seen at higher TBTO concentrations, but were of lower incidence.

Supplementary experiments were also performed to compare the effect of TBTC exposure on DNA fragmentation in short term thymocyte culture. After 6 h of exposure to 1 μM TBTC, the mean fragmentation value obtained of 33.2% was rather lower than that observed following an equimolar addition of TBTO (38.6%).

3.3.4 DNA gel electrophoresis

In order to examine the nature of the DNA degradation described in section 3.3.3, DNA isolates from 27 000 x *g* supernatants obtained after lysis of TBTO-treated cells were subjected to agarose gel electrophoresis. Similarly prepared samples from thymocytes exposed to MPS were used as a comparator.

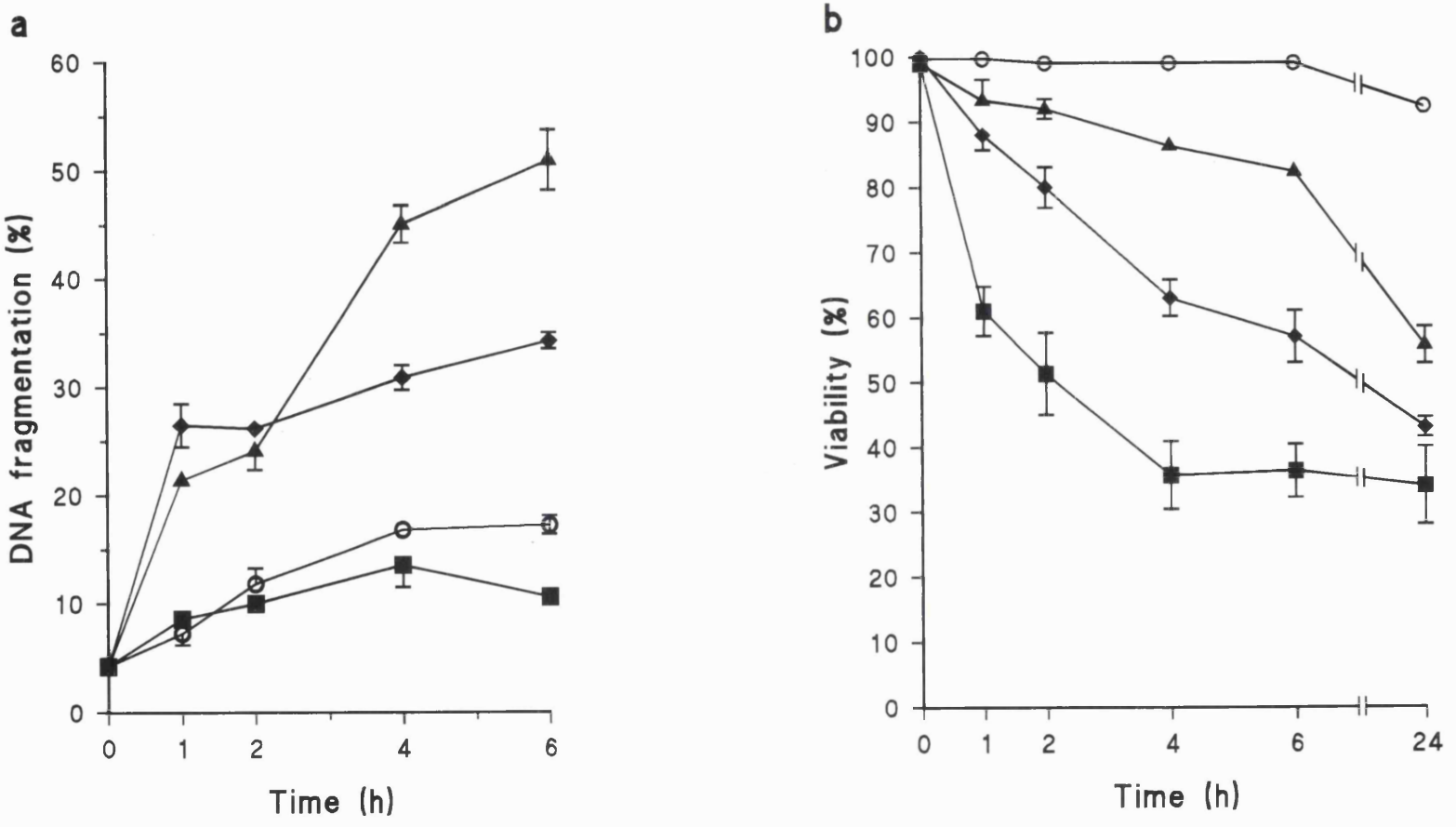

FIGURE 3.5 Effects of TBTO on a) timecourse of DNA fragmentation and b) cell viability.

Cells were incubated in the absence (○), or presence of 2 (▲), 3.5 (◆) or 5 (■) μM TBTO. DNA fragmentation was measured as described in section 2.6, and viability was determined by trypan blue dye exclusion (section 2.2). Results are the means ± SE from three separate experiments.

After incubation with 0.1 or 1 μM TBTO for 6 h, a regular series of DNA fragments were identifiable by gel electrophoresis (Fig. 3.6). A concentration-dependent increment in the observed intensity of band fluorescence obtained was normally evident within the range 0.1-2 μM TBTO. By visual appraisal, the character of the cleavage pattern closely resembled that which resulted from exposure of cells to 10 μM MPS for an equivalent period (Fig. 3.6). Under the electrophoresis conditions employed, at least 10 discrete bands were routinely visible, although DNA species of a higher order molecular weight were also present. Although similar DNA 'ladders' were also observed quite frequently in 27 000 x *g* supernatant fractions from untreated control cells, the intensity of these bands was typically much less than after treatment with MPS or TBTO.

Assessment of the size of DNA fragments was made by simple measurement of their respective migration distance from the gel track origin, and comparison of these values against a DNA calibration standard consisting of multiples of 123 bp. By this means it was estimated that the fragments obtained from both TBTO or MPS-treated cells corresponded to a multimeric series with an integer repeat of between 180 to 200 bp. This was confirmed using an image analysis technique, whereby gel photographs were scanned and a digital densitometric profile was assembled for each track, which allowed delineation of the position and maximal signal intensity for discrete bands. The results of a typical experiment are shown in Fig. 3.7; in the case of cells exposed to 1 μM TBTO, interpolation of the migration distance of bands in the DNA 'ladder' against the calibration standard indicated that the fragment size ranged from 176-197 bp. The modal average for the point of maximum signal amplitude corresponded to 186 bp. Comparable results were obtained with MPS, and the variation between the median size of the multimeric fragment series produced by this agent or TBTO was always less than 5%.

In contrast to these findings, DNA fragments were essentially absent from the supernatant fractions derived from cells exposed to 5 μM (Fig. 3.6) or higher concentrations of TBTO. In supernatant samples derived from such treatments, it was also noted that only small amounts of high molecular weight DNA were visible in the region proximate to the gel track origins.

3.3.5 Morphological studies (AO fluorescence)

The majority of control thymocytes stained with acridine orange (AO) exhibited a uniform and low level of fluorescence (Fig. 3.8a and b). A different staining profile was observed in cells incubated for up to 6 h with either 1 μM TBTO (Fig. 3.8c) or 10 μM MPS (Fig. 3.8d), which was qualitatively similar for both treatments. In these preparations, increased numbers of cells showed bright yellow-green fluorescence of the nuclear or perinuclear region, sometimes involving the presence of discrete hyperchromatic foci. It was noted that the latter pattern of focal intensities was commonly associated with smaller cell bodies.

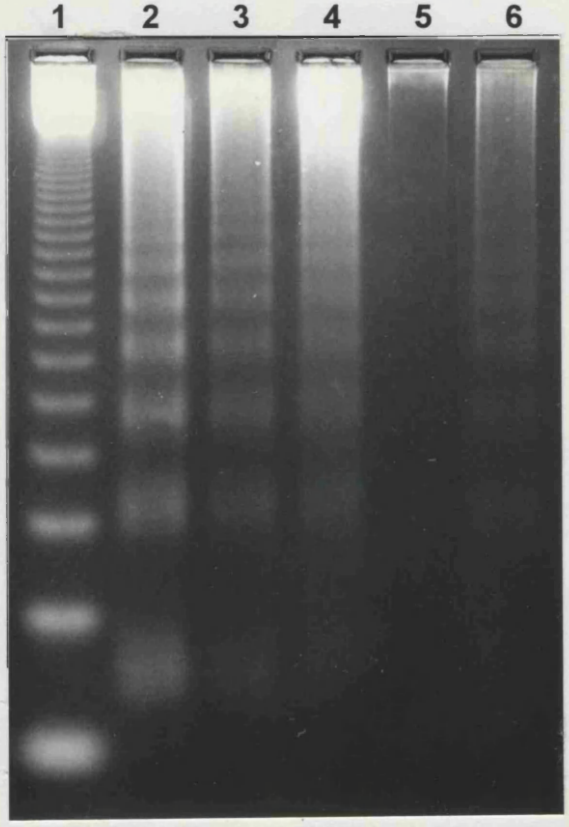

FIGURE 3.6 Agarose gel electrophoresis of DNA obtained from thymocytes exposed to TBTO or MPS.

DNA samples were prepared from supernatants obtained after centrifugation of cell lysates at 27 000 x *g*, (see sections 2.6 and 2.8). Thymocytes were incubated with the test agents for 6 h, and the gel tracks shown correspond to the following treatments: (1) DNA molecular weight calibration standard comprising of multiples of 123 bp; (2) 10 μM MPS; (3) 0.1 μM TBTO; (4) 1 μM TBTO; (5) 5 μM TBTO; (6) control.

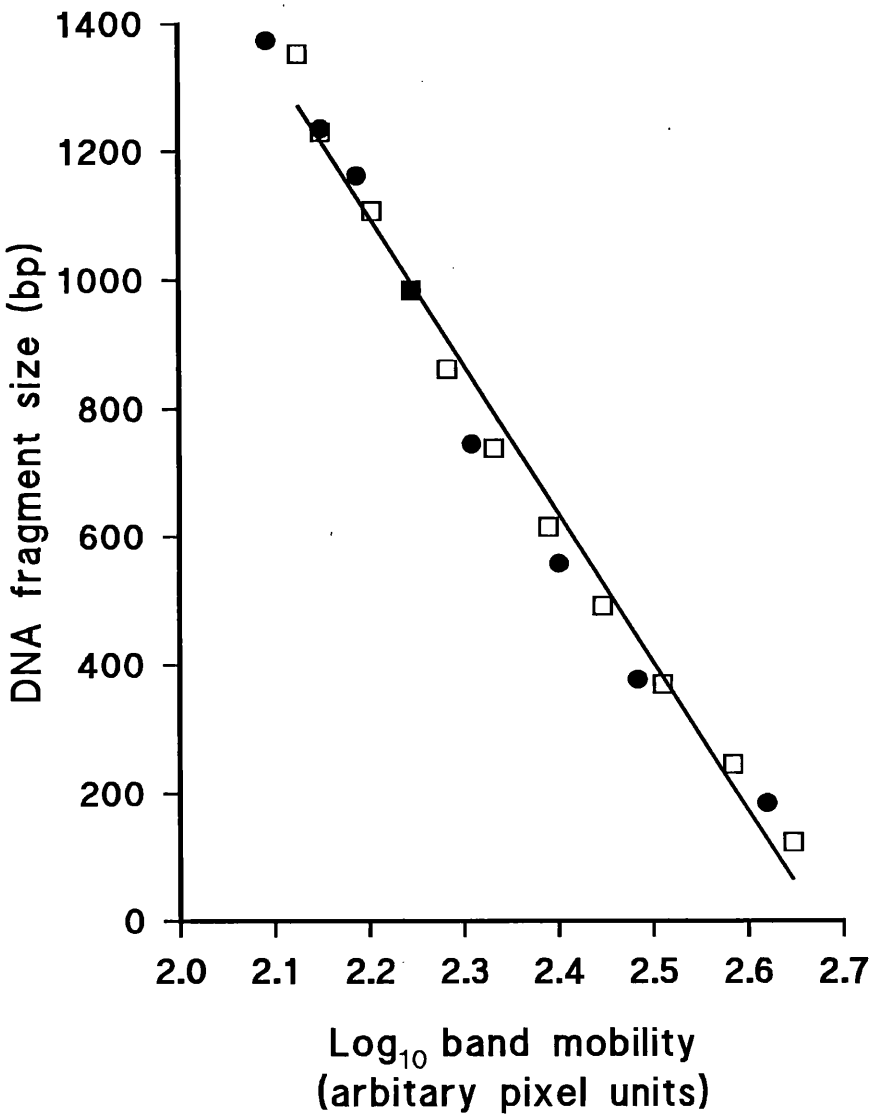

FIGURE 3.7 Size estimation of DNA fragments from apoptotic TBTO treatments. DNA was prepared from the supernatant fraction of lysed cells previously treated for 6 h with 1 μM TBTO, and subjected to electrophoresis as detailed in section 2.8, in a gel track adjacent to a DNA molecular weight calibration standard corresponding to multiples of 123 bp. Fragment positions and maximum fluorescence amplitudes were scanned and digitised as detailed in section 2.8.6. The relative migration position of the calibration standard fragments from the track origin was correlated with their respective sizes and plotted (□). The migration position and interpolated size (bp) of the DNA species obtained after TBTO treatment is shown as a superimposed series (●). Results of one experiment typical of three.

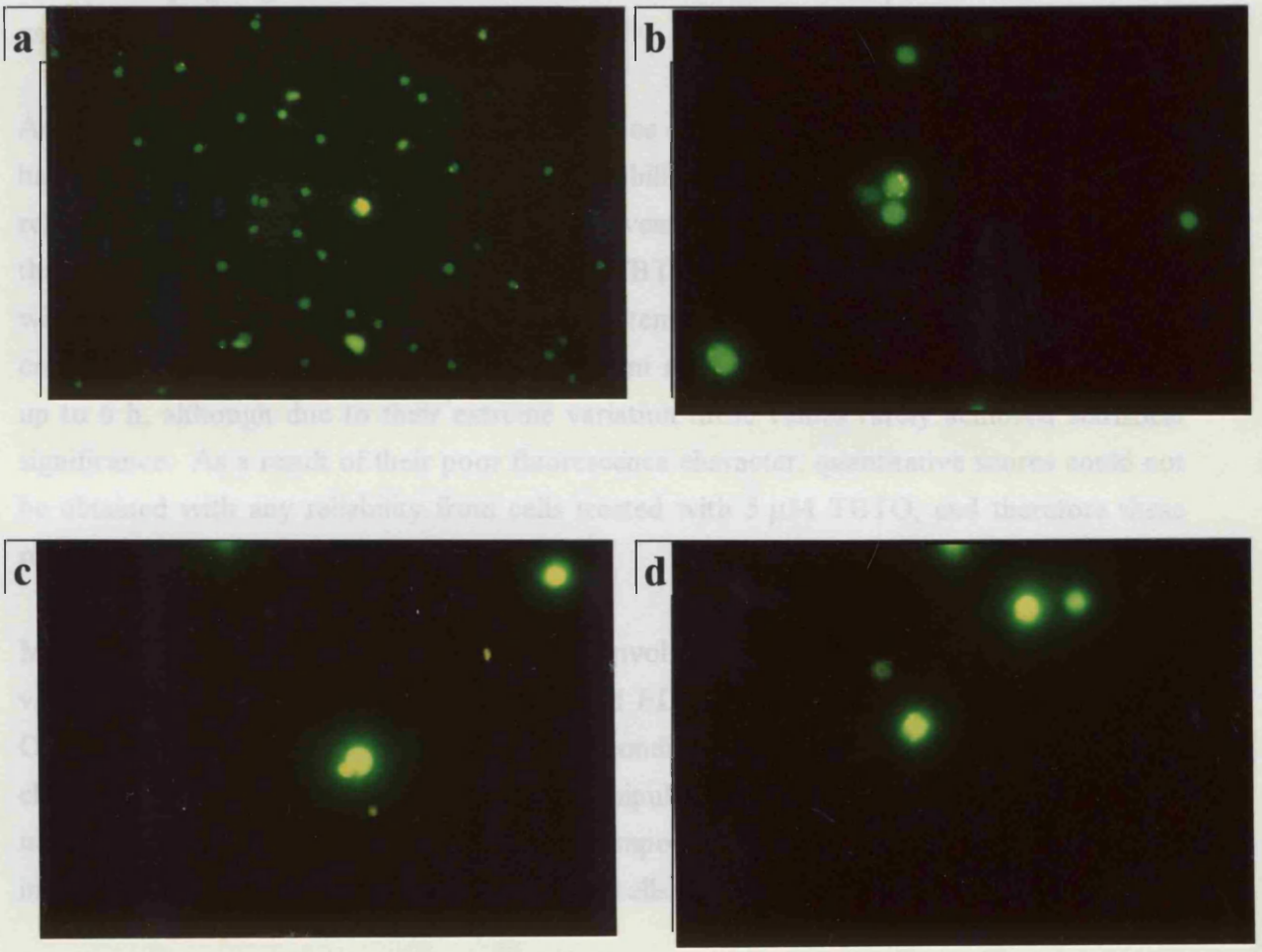

FIGURE 3.8 Acridine orange fluorescence staining of thymocytes.
Cells were incubated with the test agents for 4 h and then visualised by fluorescence microscopy after addition of AO, as described in section 2.4.2. Original magnifications are x 500, except for *a* which is x 250. **a** Control: predominantly cells with uniform minimal levels of fluorescence. **b** Control: several thymocytes with one cell exhibiting fluorescent inclusions. **c** TBTO 1 μM: Two cells with fluorescent nuclear structures; the most central of which is exhibiting apoptotic body formation. **d** MPS 10 μM: Two cells with increased nuclear fluorescence, and one hyperchromatic apoptotic body.

At 5 μM TBTO, highly variable and irregular staining characteristics were obtained with AO which were difficult to visualise properly. Occasional cells (< 1%) in all preparations showed varying degrees of red metachromatic fluorescence. This phenomenon was often associated with mitotic cell doublets.

Accurate quantitative estimations of the incidence of cells with high AO fluorescence were hampered by the high inter-experimental variability that was apparent (Fig. 3.9), which related primarily to fluorescence intensity and event discrimination. However, it was noted that following exposure to MPS (10 μM) or TBTO (1 μM) the mean proportion of cells with highly fluorescent inclusions was consistently increased above the corresponding control values (Fig. 3.9). This trend was evident after 1 h and was essentially progressive up to 6 h, although due to their extreme variation these values rarely achieved statistical significance. As a result of their poor fluorescence character, quantitative scores could not be obtained with any reliability from cells treated with 5 μM TBTO, and therefore these results are not shown.

Modifications of this procedure were devised involving the addition of Triton X-100 (0.1% v/v) as a cell permeabilising agent, or 0.1 mM EDTA to denature double stranded RNA. On a subjective assessment basis, neither condition change affected the fluorescence characteristics of the preparation. Limited manipulation of fluorochrome solution variables including concentration, pH and ionic composition did not result in appreciable improvements in the visualisation of apoptotic cells (results not shown).

3.3.6 Morphological studies (resin sections)

As an alternative to fluorescence microscopy using AO fluorochrome, morphological studies were performed on resin embedded sections of suspension fixed cells. At high magnification, nuclear chromatin could readily be differentiated due to basophilic staining by toluidine blue (Bancroft and Cook, 1984). Freshly prepared cell suspensions were visually evaluated on the basis of parameters such as cell size, aspect ratio, nuclear morphology and nucleocytoplasmic ratio. Within the limitations of this simple morphometric assessment, the cell population was considered to consist essentially of lymphoid cell types. Erythrocytes and stromal cells were also very occasionally present.

A representative preparation of control thymocytes obtained after 6 h incubation is shown in Fig. 3.10a. The majority of cells had nuclear heterochromatin patterns, whilst fewer than 4% had nuclear morphologies consistent with mitotic events. In addition, a small proportion of cells exhibited chromatin condensation. When thymocytes treated with 0.1 or 1 μM TBTO for an equivalent period were examined, substantial numbers of cells displayed varying degrees of chromatin condensation and reduction in nuclear size (Fig. 3.10b and c). Intensely stained nuclear material appeared as homogeneous spherical

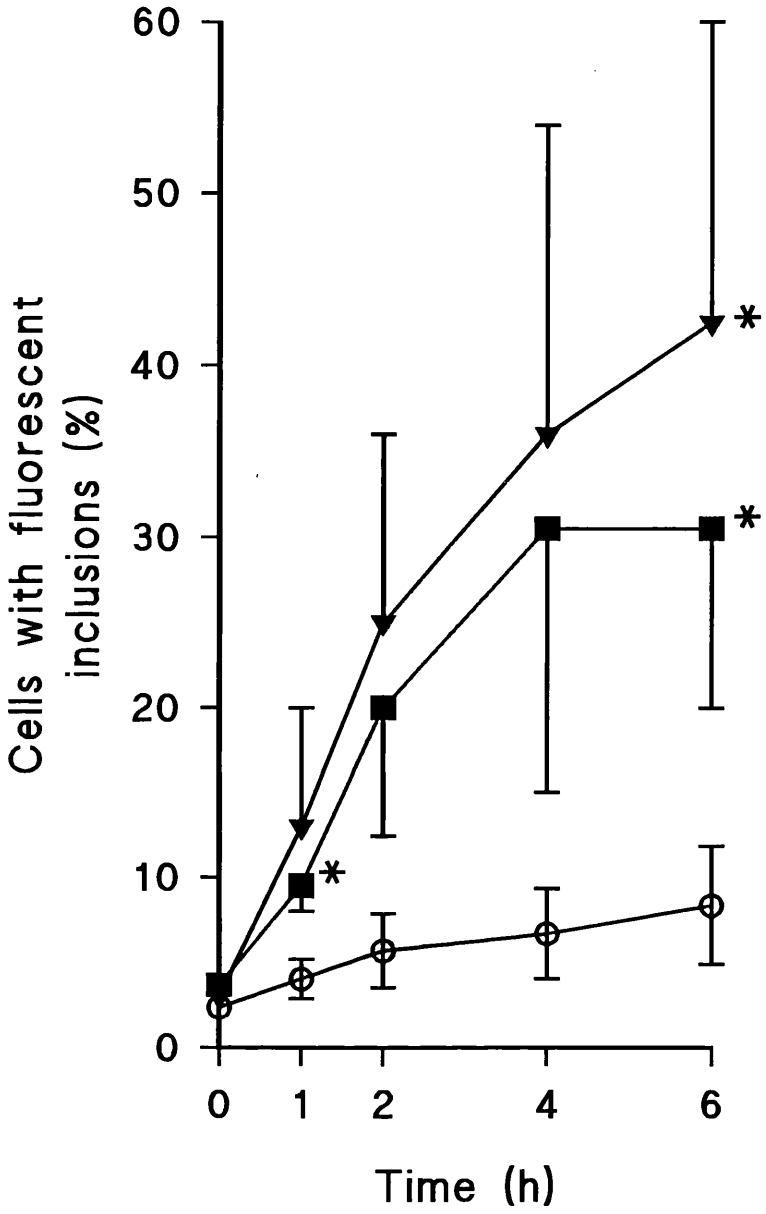

FIGURE 3.9 Effect of TBTO or MPS on the incidence cells with highly fluorescent inclusions after acridine orange staining.

Thymocytes were incubated in the absence (○) or presence of TBTO 1 μM (■) or MPS 10 μM (▼) at an initial cell density of 25 x 10^6 ml^{-1}. Results are the means ± SE from three separate experiments. AO fluorescence was scored using the technique described in section 2.4.2. *Result significantly different from control value, $p < 0.05$.

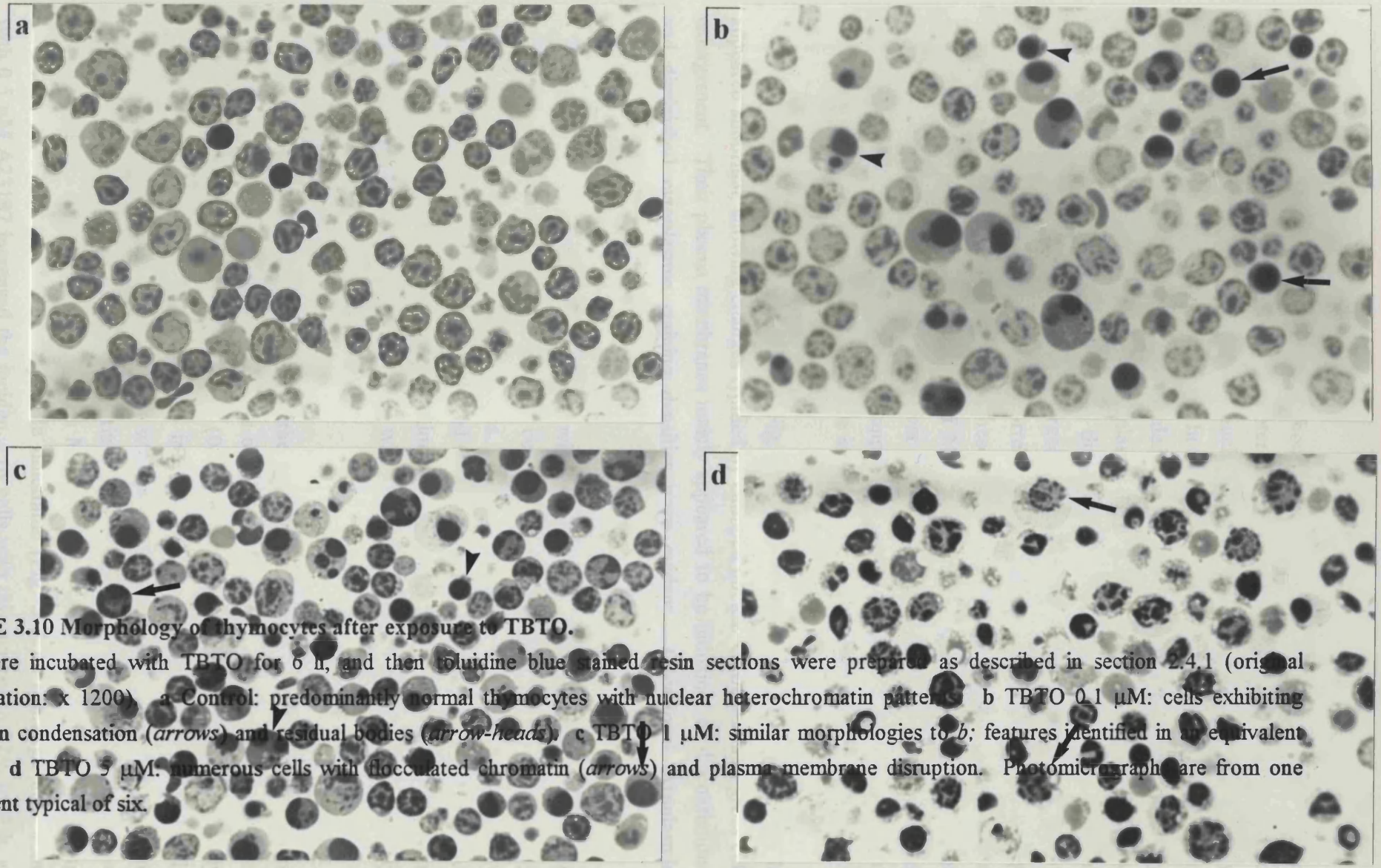

FIGURE 3.10 Morphology of thymocytes after exposure to TBTO.

Cells were incubated with TBTO for 6 h, and then toluidine blue stained resin sections were prepared as described in section 2.4.1 (original magnification: x 1200). **a** Control: predominantly normal thymocytes with nuclear heterochromatin patterns. **b** TBTO 0.1 µM: cells exhibiting chromatin condensation (*arrows*) and residual bodies (*arrow-heads*). **c** TBTO 1 µM: similar morphologies to *b;* features identified in an equivalent manner. **d** TBTO 5 µM: numerous cells with flocculated chromatin (*arrows*) and plasma membrane disruption. Photomicrographs are from one experiment typical of six.

or crescentic masses. Discrete membrane-bounded residual cell bodies spanning a diverse range of sizes from almost full cell diameter to considerably smaller particles were also evident. The majority of these contained nuclear remnants, whilst others were apparently limited only to a cytoplasmic component. In some instances these cell bodies appeared to be degenerate, showing changes that included karyorrhexis or karyolysis accompanied by loss of distinct plasma membranes. Cytoplasmic vacuolation was visible in cells bearing both aberrant nuclear features and also in those with apparently normal heterochromatin distributions. It was noted that a few enlarged, pale staining thymocytes were also present and that their incidence approximately correlated with the proportion of cells including trypan blue in assessments of viability. These changes were qualitatively similar to those observed in cells exposed to 1 or 10 μM MPS (Fig. 3.11a) or A23187 (Fig. 3.11b) at concentrations lower than 1 μM. However, it was considered that the nuclear changes produced by MPS were more uniform in appearance and staining character. In addition, less cytoplasmic vacuolation was discernible after glucocorticoid or ionophore exposure.

Following exposure to TBTO at 5 μM (Fig. 3.10d) or 10 μM for 6 h most of the cells appeared abnormal, showing changes typified by clumped nuclear chromatin and gross cell enlargement. Their plasma membranes mainly appeared to be indistinct or discontinuous and diminished cytoplasmic staining densities were evident. Occasional cytoplasmic vacuolation was noted.

The morphology of thymocytes incubated with 1 μM A23187 for 4 h or more showed a higher degree of diversity. Although many cells were apparently pale-staining, the majority did exhibit nuclear heterochromatin patterns. However, significant numbers of irregularly-shaped cells, lacking distinguishable internal features were also present (Fig. 3.11c). Few thymocytes exhibited chromatin condensation and small cell bodies containing chromatin remnants were rare. Grossly swollen cells with chromatin flocculation patterns apparently constituted less than 10% of the total.

Comparative quantitative assessments of the incidence of chromatin condensation were performed between various concentrations of TBTO and either MPS or A23187. After exposure to low concentrations of TBTO (0.1 or 1 μM) for 6 h there was a statistically significant and dose-dependent increase in the incidence of cells scored with this characteristic (Fig. 3.12). This contrasted with the findings at 5 or 10 μM TBTO, where the mean proportion of cells with chromatin condensation remained below the respective control value (Fig. 3.12). Treatment with MPS (10 μM) was very effective in inducing chromatin condensation over a comparable timeframe (Fig. 3.12). Although incubation with 0.5 μM A23187 increased the incidence to cells with this marker to 22% by 6 h, at 1 μM the mean value was limited to 5% (Fig. 3.12).

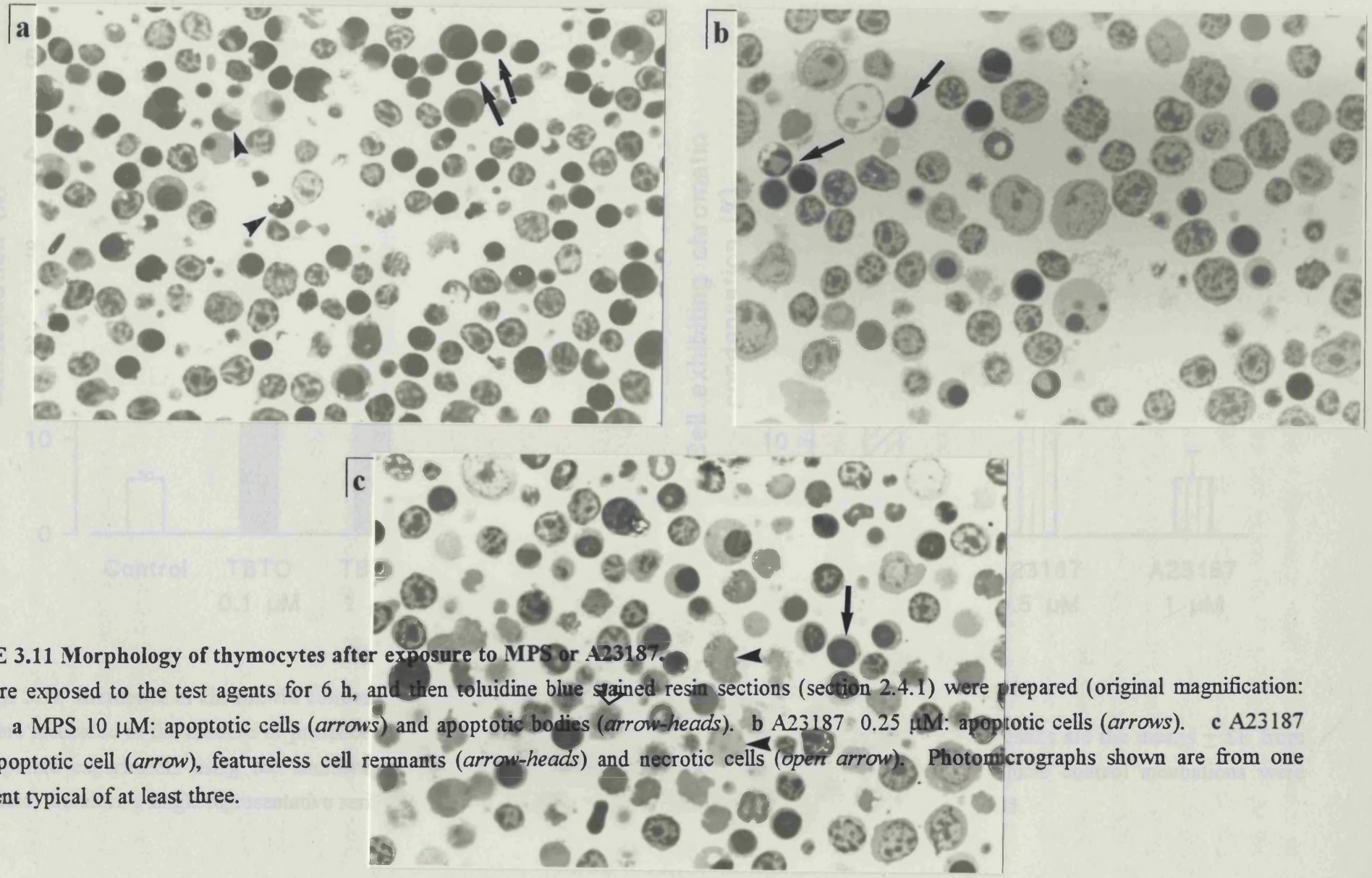

FIGURE 3.11 Morphology of thymocytes after exposure to MPS or A23187.
Cells were exposed to the test agents for 6 h, and then toluidine blue stained resin sections (section 2.4.1) were prepared (original magnification: x 1200). a MPS 10 μM: apoptotic cells (*arrows*) and apoptotic bodies (*arrow-heads*). b A23187 0.25 μM: apoptotic cells (*arrows*). c A23187 1 μM: apoptotic cell (*arrow*), featureless cell remnants (*arrow-heads*) and necrotic cells (*open arrow*). Photomicrographs shown are from one experiment typical of at least three.

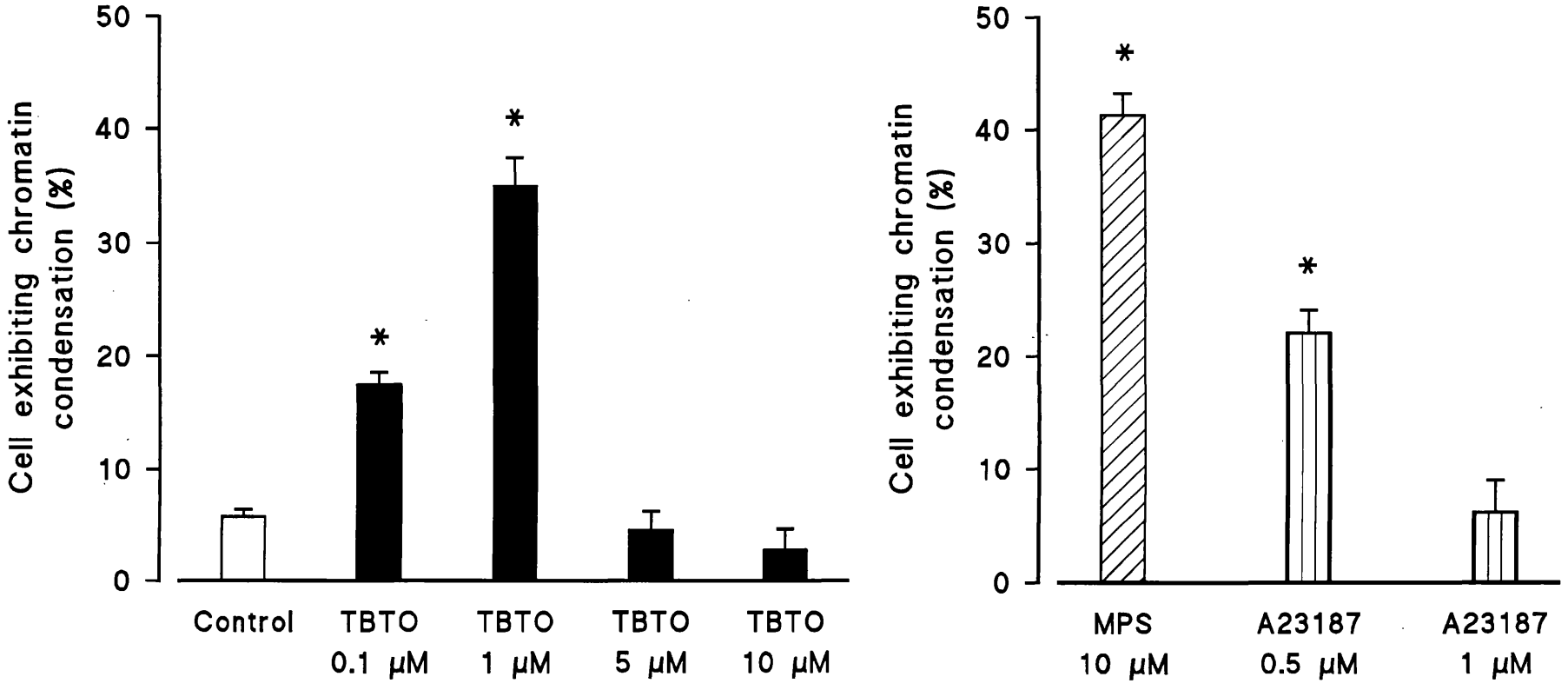

FIGURE 3.12 Incidence of chromatin condensation after exposure to TBTO, MPS or A23187.

Cells were incubated in the absence or presence of the stated concentrations of TBTO, MPS or A23187 for 6 h. Results are the means ± SE from three separate experiments using the enumeration technique described in section 2.4.1. Mean values in all vehicle control incubations were comparable; therefore a single representative series is shown. *Result significantly different from control value, $p < 0.05$.

These initial observations were extended into a timecourse study of the incidence of chromatin condensation using exposures to the test agents for 12 h (Fig. 3.13). At the lowest TBTO concentration tested (0.1 μM) the number of cells scored with this characteristic showed a gradual increment over the incubation period, until by 12 h the mean incidence approximated to 280% of the respective control value. A more pronounced increase in incidence was observed with 1 μM TBTO. Treatment with MPS (10 μM) increased the proportion of cells exhibiting chromatin condensation to 19% by 3 h, whilst by 12 h this value had risen to over 50%. Although the mean value recorded after 3 h treatment with 5 μM TBTO showed a slight but statistically significantly increase, the incidence of chromatin condensation recorded at later timepoints declined to parity with the control. At the highest TBTO concentration tested (10 μM), very few cells were scored as having condensed chromatin patterns.

To investigate the progression of the morphological alterations seen with low concentrations of TBTO, samples were obtained for examination after 24 h and compared to preparations from parallel incubations with 10 μM MPS. At either 0.1 or 1 μM TBTO, essentially all cells in the examined fields showed evidence of chromatin condensation (Fig. 3.14) although some were pale staining with signs of secondary degenerative changes such as loss of nuclear outline. The mean incidence of chromatin condensation at this timepoint in parallel control cultures was limited to 23%.

3.3.7 Ultrastructural studies

In order to further investigate the nature of the morphological changes associated with in vitro exposure to TBTO, cellular ultrastructural features were examined by TEM and compared with those of thymocytes treated with either MPS or A23187.

Control cultures predominantly consisted of cells with nuclear patterns typified by moderately electron-dense peripheral heterochromatin patches interspersed with euchromatic regions (Fig. 3.15a). A common finding was the presence of a central chromatin mass which obscured nucleolar structures. Large cytoplasmic organelles, e.g. mitochondria were observed to be relatively sparse and well separated. A few microvilli were normally present on the surface of thymocytes.

Exposure to low concentrations of TBTO (0.1 or 1 μM) caused a number of nuclear and cytoplasmic changes commencing within 4 h of treatment. A typical abnormal cell selected from a preparation made after 6 h incubation with 1 μM TBTO is shown in Figure 3.15b. The outlines of affected cells adopted more rounded contours and microvilli were lost. Extensive cytoplasmic vacuolation was noted in some cells involving the presence of vesicles with a range of sizes, that were most prevalent in the outer cytoplasmic region, and often appeared to fuse with the cell exterior leading to fenestration of the plasma membrane

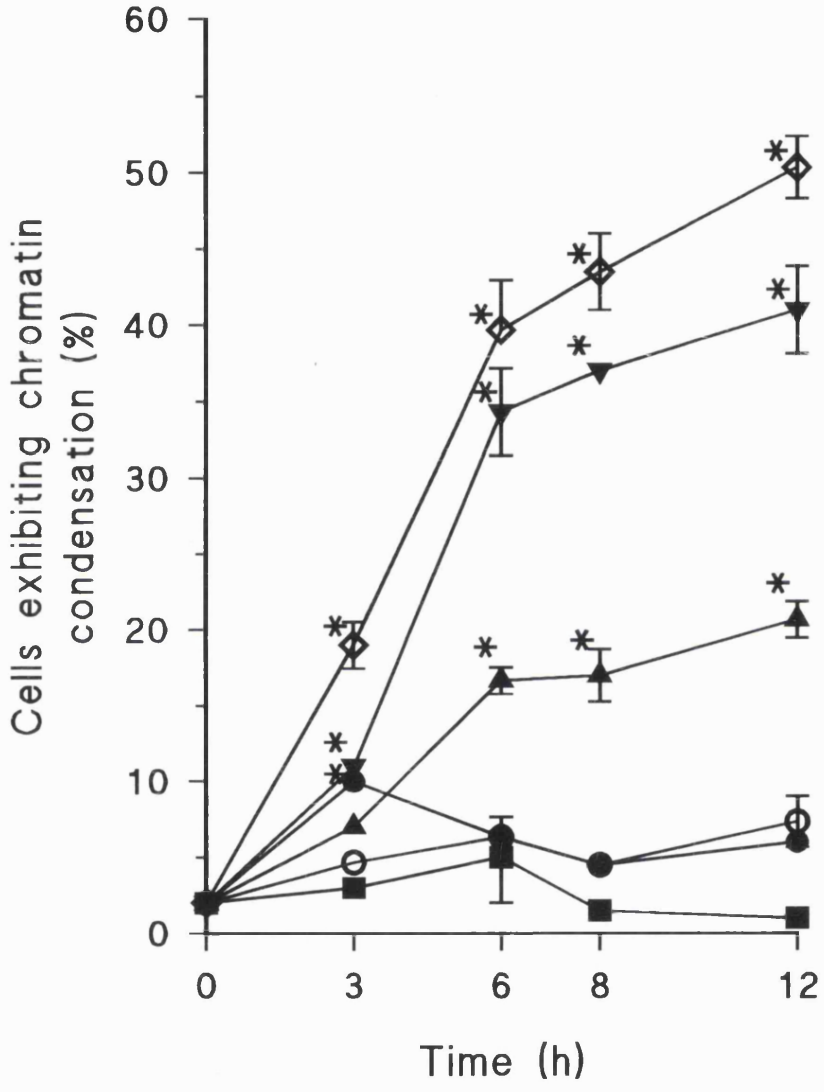

FIGURE 3.13 Timecourse of chromatin condensation after exposure to TBTO or MPS.

Cells were incubated in the absence (○) or presence of TBTO 0.1 (▲), 1 (▼), 5 (●) or 10 μM (■); or MPS 10 μM (◇). Results are the means ± SE from three separate experiments. The methodology employed was as described in section 2.4.1. *Result significantly different from control value, $p < 0.05$.

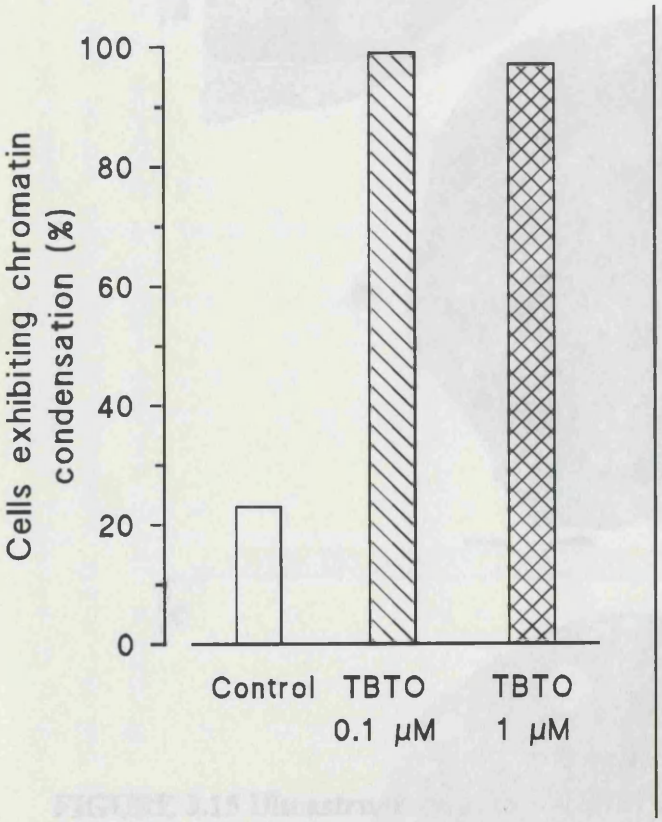

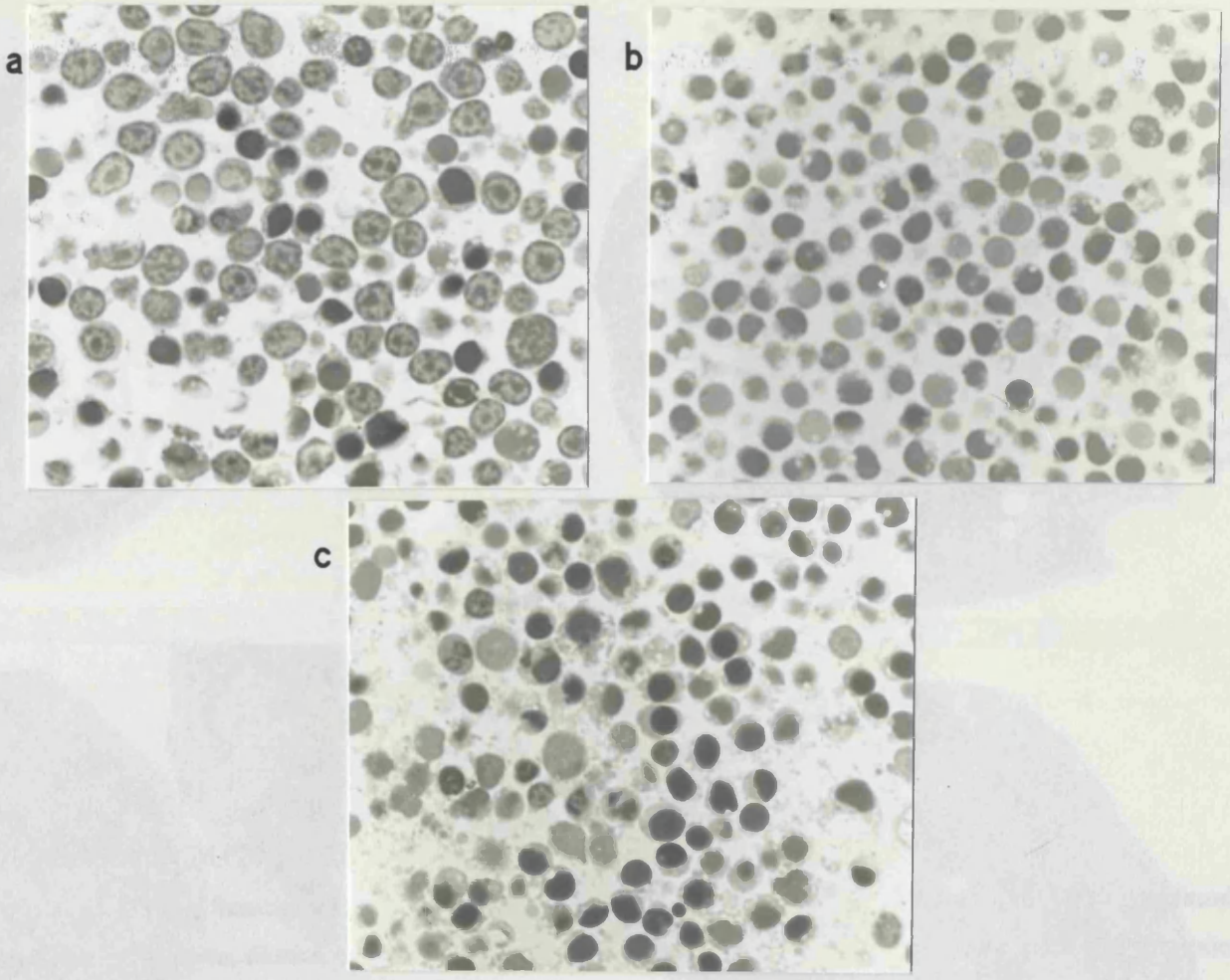

FIGURE 3.14 Effect of long term exposure to TBTO on the incidence of chromatin condensation.

Cells were incubated with the stated concentrations of TBTO for 24 h. Left panel: proportion of thymocytes exhibiting evidence of chromatin condensation (determined as described in section 2.4.1). Results are from one experiment that was typical of three. Right panel: representative appearance of cells incubated **a** without; or with **b** 0.1 μM, **c** 1 μM TBTO (toluidine blue stained resin sections; original magnification: x 900).

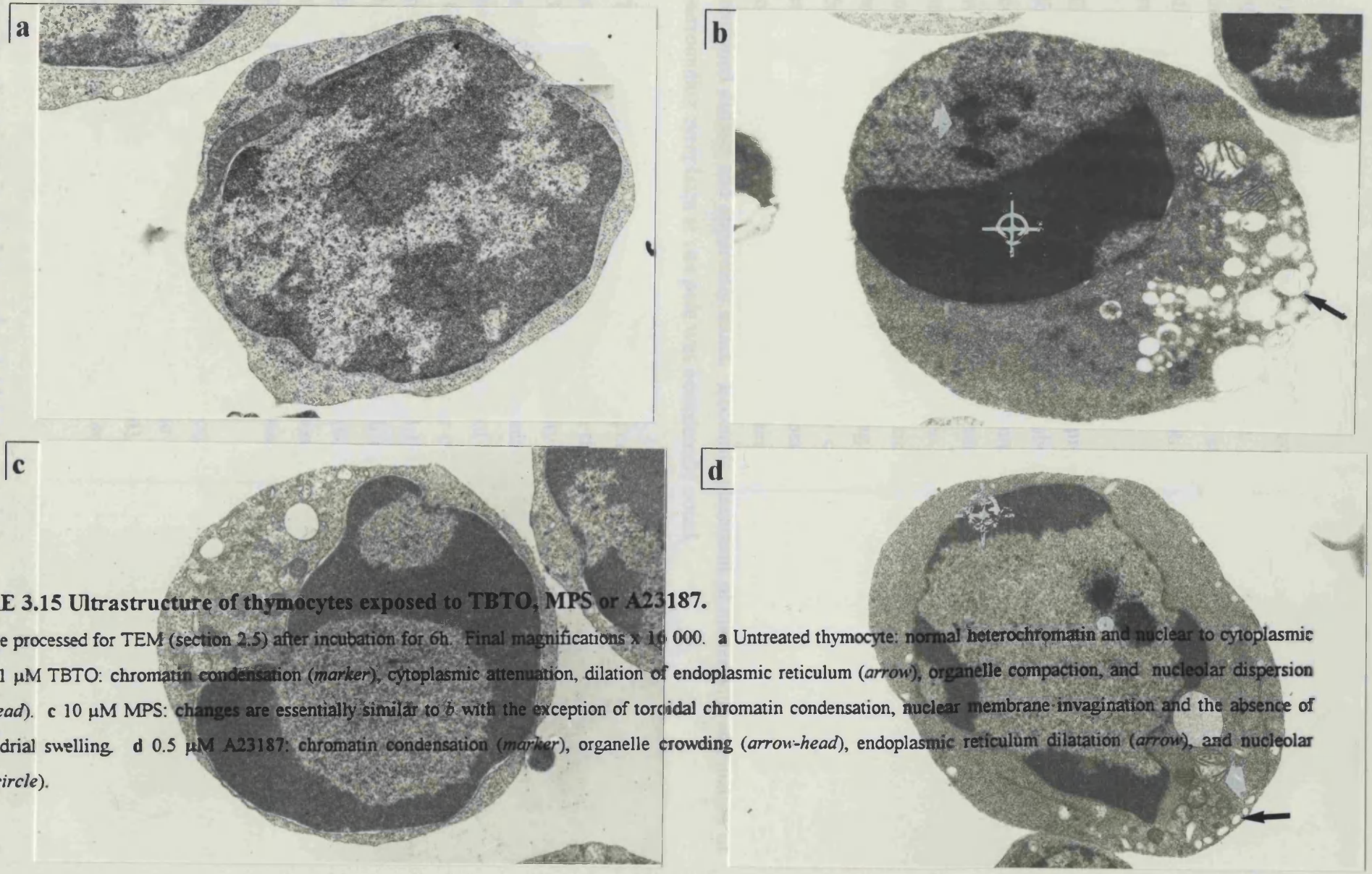

FIGURE 3.15 Ultrastructure of thymocytes exposed to TBTO, MPS or A23187.

Cells were processed for TEM (section 2.5) after incubation for 6h. Final magnifications x 10 000. **a** Untreated thymocyte: normal heterochromatin and nuclear to cytoplasmic ratio. **b** 1 μM TBTO: chromatin condensation (*marker*), cytoplasmic attenuation, dilation of endoplasmic reticulum (*arrow*), organelle compaction, and nucleolar dispersion (*arrow-head*). **c** 10 μM MPS: changes are essentially similar to *b* with the exception of toroidal chromatin condensation, nuclear membrane invagination and the absence of mitochondrial swelling. **d** 0.5 μM A23187: chromatin condensation (*marker*), organelle crowding (*arrow-head*), endoplasmic reticulum dilatation (*arrow*), and nucleolar change (*circle*).

(Fig. 3.15b). Cytoplasmic organelles were commonly compacted together giving the appearance of a crowded organisation (Fig. 3.15b and Fig. 3.16b), although gross disturbance of these structures was not seen as an early change. Low level TBTO exposure did produce moderate swelling of mitochondria, but the mitochondrial envelope and cristae remained readily discernible (Fig. 3.16c).

Changes in the nuclear compartment were a prominent feature in thymocytes exposed to low concentrations of TBTO. The most obvious alteration was extensive chromatin condensation which appeared in a restricted number of forms. In some cells the chromatin was condensed to give crescentic or hemilunar caps which abutted onto the nuclear membrane (Fig. 3.15b and Fig. 3.16b), whilst in others the chromatin masses were rounded or ovoid (Fig. 3.16a). The latter characteristic appeared to correlate with diminution of nuclear diameter. Nucleoplasm not containing very dense chromatin was more electron-lucent, and altered nucleolar structures were commonly visible in these regions. These nucleoli appeared as dispersed showers of osmiophilic granules (Fig. 3.15b), though in occasional cells only vestigial elements remained. Nuclear membranes of aberrant cells remained distinct and apparently intact. Eccentric placement of nuclei with attenuation of surrounding cytoplasm at one pole was occasionally noted.

TBTO exposure produced residual cell bodies comprising a wide range of sizes, from those approximating to the dimensions of complete thymocytes to much smaller structures (Fig. 3.16a and d; Fig. 3.17a and b). The majority contained compacted chromatin, although smaller anucleate membrane-bound cytoplasmic bodies were also observed. Convolution of the nuclear membrane and segmentation of condensed chromatin (Fig. 3.16d and Fig. 3.17b) were observed. In other bodies, the chromatin formed separate round or ovoid masses usually bounded by membranes (Fig. 3.16a and Fig. 3.17a). Figure 3.17a shows the latter type of nuclear alteration together with extensive organelle disorganisation and the presence of vacuoles containing included material. More degenerate forms of this change were also noted (Fig. 3.16a), whereby condensed chromatin masses became more coarsely granular in appearance and organelle and plasma membranes showed signs of dissolution.

Other abnormalities were noted less commonly in thymocytes treated with low TBTO concentrations. These included the presence of arrays formed of unidentified filaments which appeared in the cytoplasm (Fig. 3.16d), or as intranuclear inclusions (Fig. 3.16c). Cytoplasmic protrusions involving relatively small amounts of cellular material were seen infrequently after TBTO exposure.

Similar alterations in nuclear and cytoplasmic morphology, and also the formation of apoptotic bodies, were noted in occasional control cells and in many cells from cultures treated with MPS for several hours (Fig. 3.15c and Fig. 3.18a-c). Some minor differences

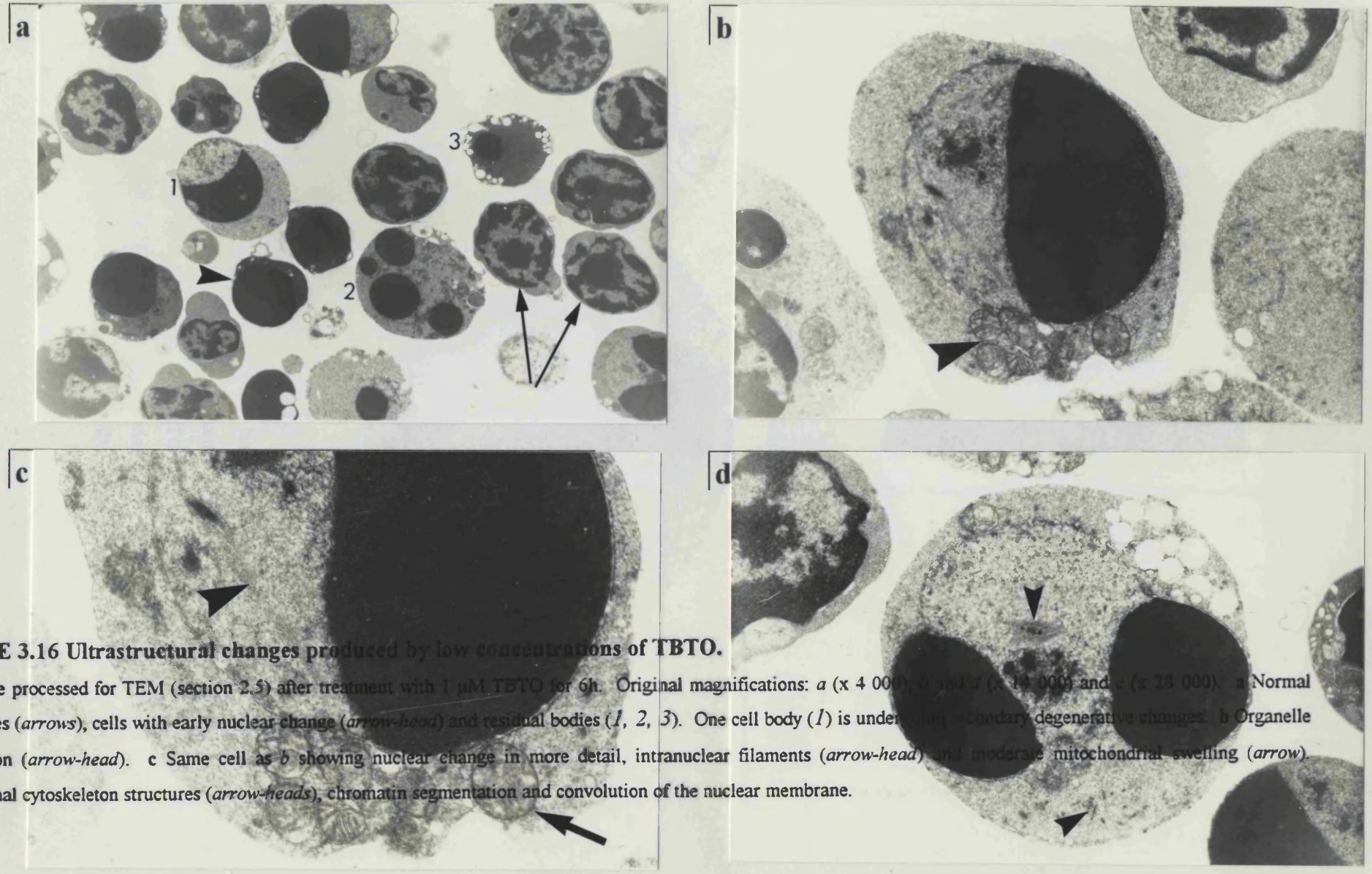

FIGURE 3.16 Ultrastructural changes produced by low concentrations of TBTO.

Cells were processed for TEM (section 2.5) after treatment with 1 μM TBTO for 6h. Original magnifications: *a* (x 4 000), *b* and *d* (x 14 000) and *c* (x 23 000). **a** Normal thymocytes (*arrows*), cells with early nuclear change (*arrow-head*) and residual bodies (*1, 2, 3*). One cell body (*1*) is undergoing secondary degenerative changes. **b** Organelle compaction (*arrow-head*). **c** Same cell as *b* showing nuclear change in more detail, intranuclear filaments (*arrow-head*) and moderate mitochondrial swelling (*arrow*). **d** Abnormal cytoskeleton structures (*arrow-heads*), chromatin segmentation and convolution of the nuclear membrane.

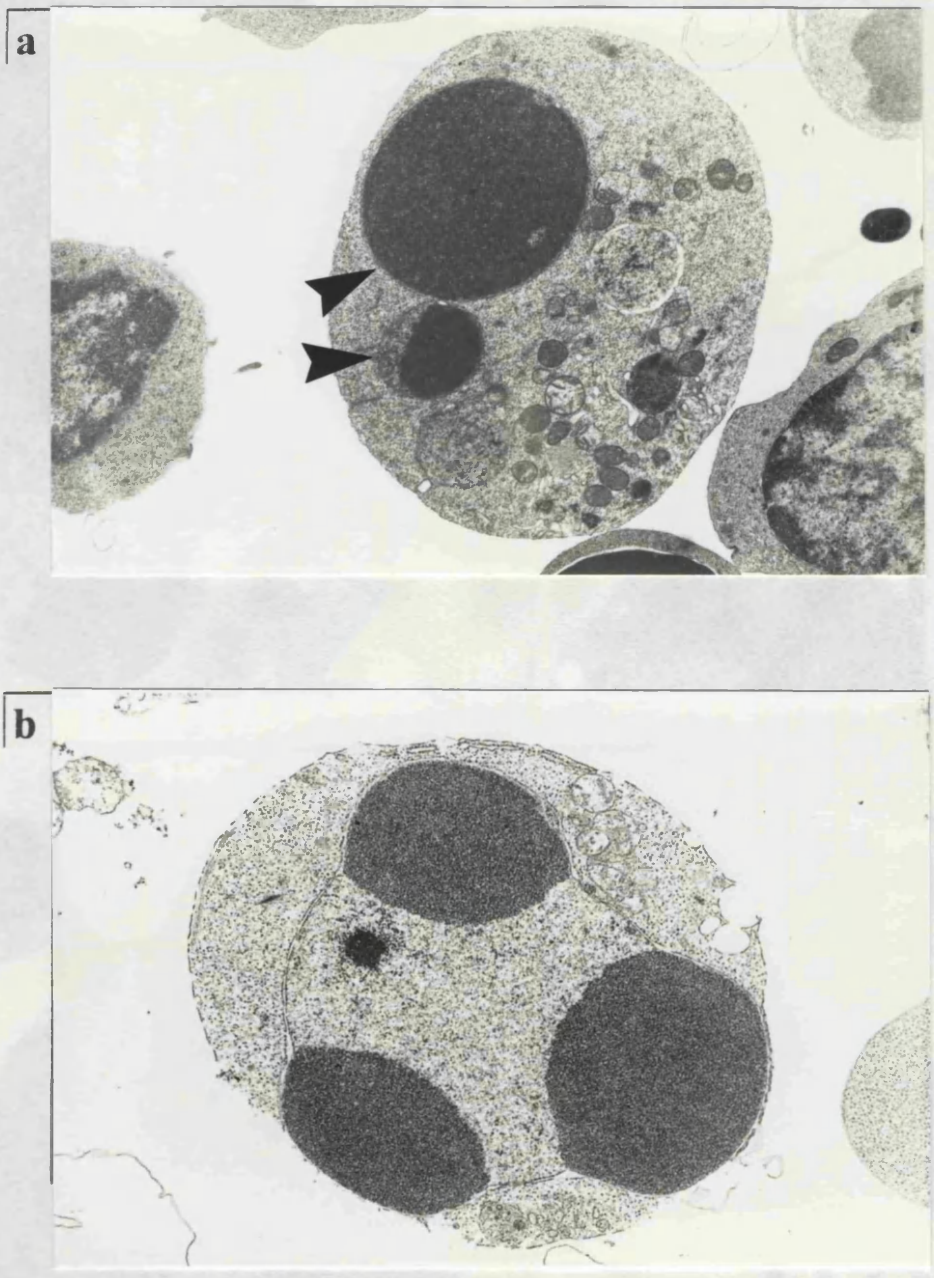

FIGURE 3.17 Representative residual cell bodies formed after TBTO treatment.

Cells were processed for TEM (section 2.5) after treatment with TBTO for the indicated periods; original magnifications are shown within parentheses. **a** TBTO 0.1 μM: 4h (x 10 000); several nuclear remnants (*arrow-heads*) and widespread positional disorganisation of cytoplasmic organelles—note the conservation of organellar structure. **b** TBTO 1μM, 6h (x 14 500): early segmentation of chromatin masses together with nuclear membrane convolution.

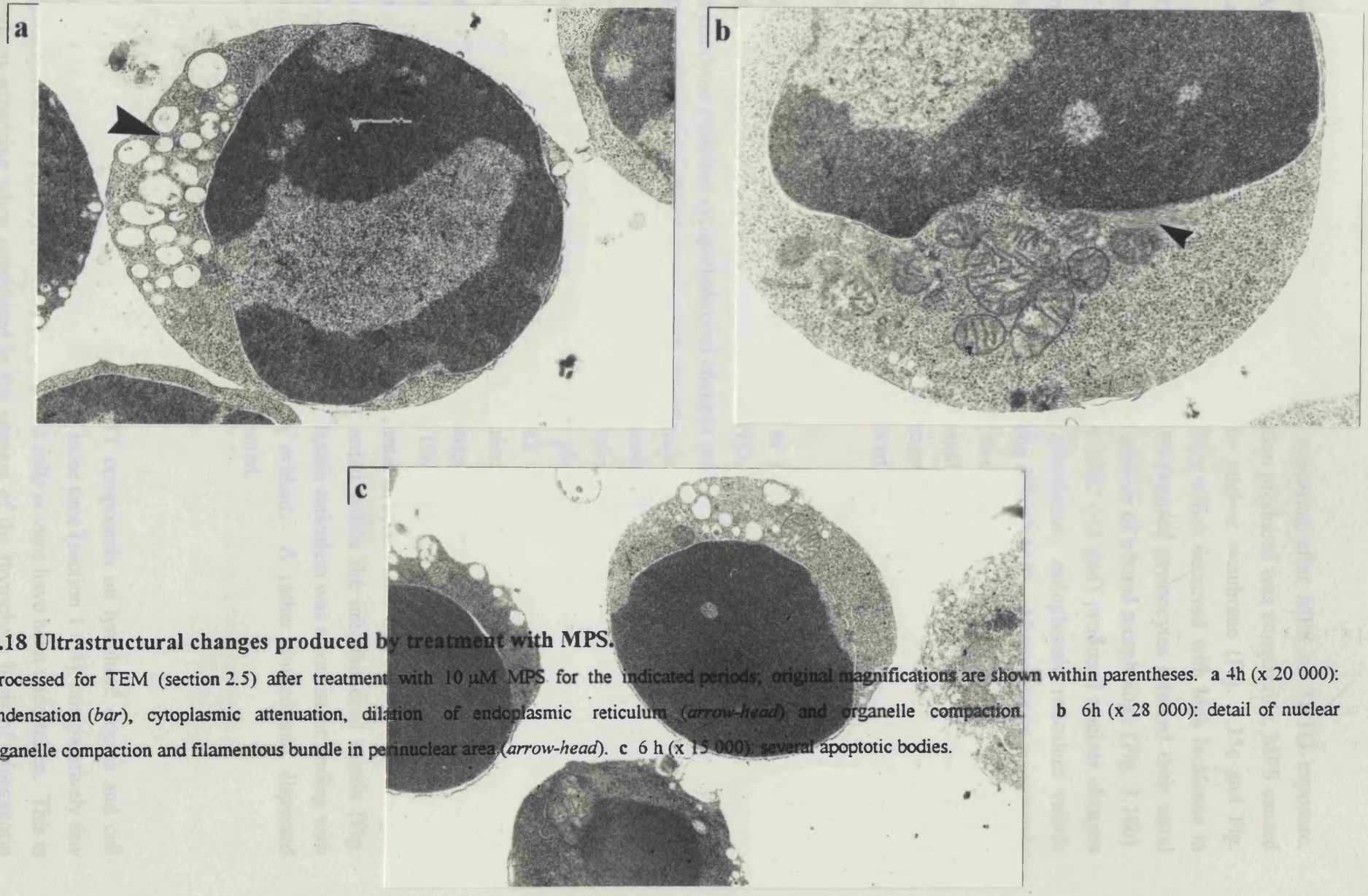

FIGURE 3.18 Ultrastructural changes produced by treatment with MPS.

Cells were processed for TEM (section 2.5) after treatment with 10 μM MPS for the indicated periods; original magnifications are shown within parentheses. **a** 4h (x 20 000): chromatin condensation (*bar*), cytoplasmic attenuation, dilation of endoplasmic reticulum (*arrow-head*) and organelle compaction. **b** 6h (x 28 000): detail of nuclear alterations, organelle compaction and filamentous bundle in perinuclear area (*arrow-head*). **c** 6 h (x 15 000): several apoptotic bodies.

were however noted between aberrant cells appearing after MPS or TBTO exposure. Although the character of chromatin condensation produced was comparable, MPS caused earlier and more extensive invagination of the nuclear membrane (Fig. 3.15c and Fig. 3.18a). In contrast to the mitochondrial swelling which occurred with high incidence in TBTO-treated cells, most mitochondria in MPS-exposed thymocytes retained their usual level of electron-density and showed little disturbance of normal morphology (Fig. 3.18b). Exposure of cells to low concentrations of A23187 (<1 μM) produced nuclear changes including chromatin condensation, nucleolar dissolution, endoplasmic reticulum vesicle formation and migration and organelle crowding (Fig. 3.15d). Alterations in cytoplasmic volume were noted, although the effect was bi-directional; a minority of cells exhibited cytoplasmic contraction, whilst in other abnormal cells there was evidence of swelling of this compartment. Ionophore-treated thymocytes were more prone to rupture and therefore artefactual changes were considered to be more commonplace in these preparations.

The appearance of thymocytes exposed to 5 or 10 μM TBTO was markedly different to that described for lower concentrations of TBTO. After 6 h of incubation, the majority of thymocytes exhibited cytopathological changes exemplified by those shown in Figure 3.19a. The cells were swollen (compare the magnification of Figure 3.19a to Figure 3.15a), with heterogeneous cytoplasmic densities mainly considered to represent ribosomal dissolution. Cell surface alterations included the loss of microvilli and the presence of multiple, and sometimes severe, focal discontinuities of the plasma membrane. The nuclear membrane was also disrupted and difficult to visualise, with disunion evident at the nucleocytoplasmic border. Nuclear heterochromatin was flocculated to give a coarsely granular 'clumped' appearance (Fig. 3.19b). There was gross enlargement of mitochondria consistent with the induction of high amplitude swelling (Fig. 3.19b), and this was accompanied by loss of matrix electron density and perturbation of internal structure such that cristae were vestigial or absent. Focal flux densities were often noted within the mitochondrial matrix (Fig. 3.19b). Severe disruption of the rough endoplasmic reticulum was a consistent finding with degranulation and ribosomal dispersal being evident. A rather limited and dispersed vacuolation of endoplasmic vesicles was also noted.

3.4 DISCUSSION

Although the selective in vivo effects of TBT compounds on lymphoid organs and cell mediated immunity have been appreciated for some time (section 1.6.4), comparatively few investigations of TBT cytotoxicity to lymphoid cells in vitro have been undertaken. This is perhaps surprising when considered in the context of the thymolytic basis of triorganotin immunotoxicity (Boyer, 1989), and their potent biochemical effects. In view of the predisposition of certain lymphoid cell types to apoptotic cell death (section 1.4), a series of

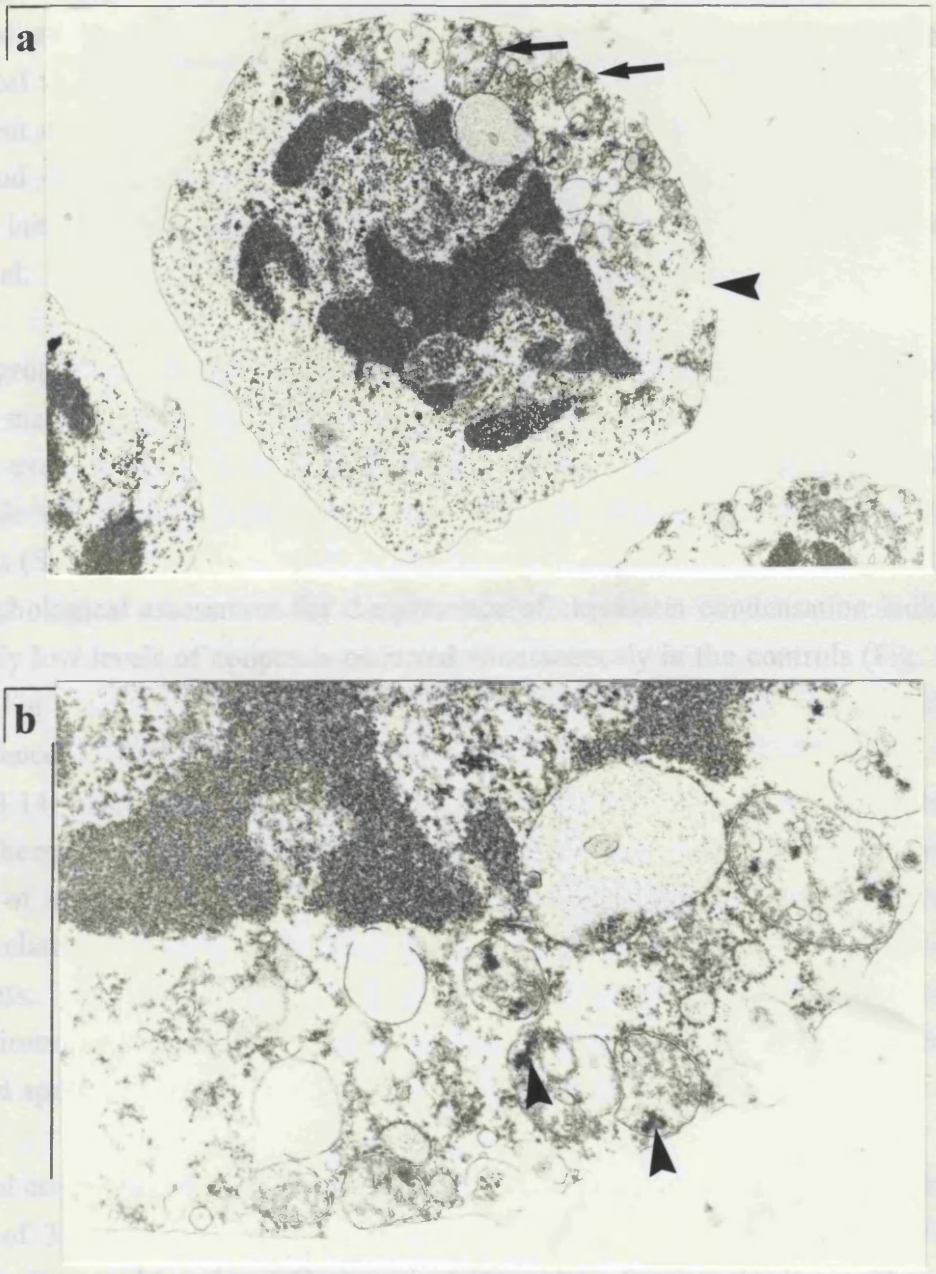

FIGURE 3.19 Cytopathology of thymocytes exposed to high concentrations of TBTO. Cells were processed for TEM (section 2.5) after treatment with 5 μM TBTO for 6h; original magnifications are shown within parentheses. **a** (x 10 000): cell enlargement, chromatin flocculation, disruption of the nuclear membrane, focal discontinuities of plasma membrane (*arrow-head*) and gross mitochondrial swelling (*arrows*). **b** (x 22 000): same cell as *a* indicating the presence of mitochondrial matrix flux densities (*arrow-heads*) and dispersal of ribosomes.

experiments was designed to investigate whether exposure to TBT could cause this form of cell killing in ex vivo thymocyte cultures. As no single parameter in isolation can be considered as an unequivocal marker for apoptosis, a battery of morphological and biochemical techniques was employed. The synthetic glucocorticoid hormone MPS, and the divalent cation ionophore A23187 were selected as positive controls since both these agents, and closely related compounds, have been extensively studied in terms of their ability to initiate thymocyte apoptosis (Wyllie and Morris, 1982; Umansky et al., 1981; Wyllie et al. 1984a; Compton and Cidlowski, 1986; Durant et al., 1980).

A high proportion of untreated cells maintained in serum-supplemented RPMI-1640 complete medium remained viable for in excess of 24 h (Fig. 3.3a), as evidenced by their ability to exclude trypan blue dye. Survival curves for these control preparations were comparable with those reported previously for rodent thymocytes cultured under similar conditions (Snoeij, 1987; McConkey et al., 1990a). Estimation of DNA fragmentation and also morphological assessment for the presence of chromatin condensation indicated that moderately low levels of apoptosis occurred spontaneously in the controls (Fig. 3.4a, Fig. 3.10 and Fig. 3.12). This was in accord with previously published findings (Wyllie, 1980). The incidence of apoptotic markers showed a time-dependent increase (Fig. 3.4a, Fig. 3.13 and Fig. 3.14) such that after 24 h in culture, more than 20% of cells were considered to be dying. These observations may simply reflect the outcome of the intrinsic precommitment to death of a substantial number of cortical thymocytes (section 1.4.3). However, the greatest relative increase in DNA degradation took place within 4 h of commencement of incubations; thus it is also plausible that factors such as the loss of thymic microenvironment or isolation-related stress, e.g. hypothermia (Nagle et al., 1990) stimulated apoptosis.

Snoeij and co-workers investigated the in vitro cytotoxicity of graded concentrations (0.01-10 μM) of TBTC to thymocytes derived from Wistar rats (Snoeij et al., 1986a). As previously discussed (section 1.6), the anionic grouping of organotins is considered to be of limited consequence to their cellular activity and therefore it should be possible to interrelate their observations to my work with TBTO (note that 1 mol of TBTO is equivalent to 2 mol TBT). In terms of the action of TBTO on intracellular inclusion of trypan blue dye, the concentration-effect profiles determined in this study (section 3.3.2) were broadly similar to those described by Snoeij et al. They reported that incubation with TBTC at up to 2 μM had little effect on membrane integrity within 10 h, whereas immediate cytotoxicity was apparent with higher concentrations. TBTO and TBTC have comparable n-octanol/water partition coefficients (section 1.6.1) which reinforces their finding that this parameter correlates strongly with the degree of cytotoxicity produced by triorganotin homologues. One rather limited investigation of the effect of TBTO on the viability of isolated rat thymocytes has previously been published (Vos et al., 1984a).

TBTO at up to 0.7 μM produced no increase in the inclusion of trypan blue after 1.5 h exposure, but did subsequently cause a delayed gradual viability loss. Higher concentrations (approximating to 3.4 or 16.8 μM) were rapidly cytotoxic.

Due to the specificity of the linkage between apoptotic cell death and endonucleolytic DNA cleavage, much previous work has relied on the extent of DNA fragmentation as a primary parameter for the quantification of apoptosis in cell populations. Thus the assay devised by Wyllie (1980) has, with some condition modifications, been commonly cited in the subject literature. Provided that the internucleosomal character of the DNA cleavage pattern is clearly established, the accumulated evidence from many studies shows that it is a precise and reproducible measure of apoptosis. Although some researchers have instead chosen sequential agarose gel electrophoresis for timecourse studies (Barry et al., 1990), in this work DNA fragmentation assays were prefered due to their intrinsically superior precision.

At TBTO concentrations below 2 μM, DNA degradation preceded appreciable viability loss by several hours (Fig. 3.4a; Fig. 3.3a), and this response was paralleled in MPS-treated cultures and by those exposed to low levels of A23187. Such findings appear to be typical of the course of the apoptotic process activated in various lymphoid cells by disparate agents such as glucocorticoids (Compton et al., 1987; Nieto and Lopez-Rivas, 1989), nucleosides (Kizaki et al., 1988), topoisomerase II inhibitors (Alnemri and Litwack, 1990) and γ-irradiation (Umansky, 1991). Exposure to TBTO at levels that were categorised as necrogenic by morphological criteria (5 or 10 μM), caused lethality in the absence of appreciable DNA degradation (Fig. 3.3a; Fig. 3.4a).

Analysis of the DNA isolated from the 27 000 x *g* supernatant from cells incubated with up to 2 μM TBTO showed that it electrophoresed in a ladder pattern comparable to that from MPS treated thymocytes (Fig. 3.6). It has previously been shown this fragmentation profile represents multiples of a subunit of approximately 180-200 bp and is a stereotypic characteristic in thymocytes undergoing apoptosis initiated under a variety of physiological and non-physiological conditions (Facchinetti et al., 1991; Skalka et al., 1976; Cohen and Duke, 1984; Smith et al., 1989). Whilst many of the original descriptions of equivalent DNA degradation have been for lymphoid cells, it is now considered to represent a cardinal biochemical feature in many instances of apoptosis (section 1.3.5), although its universal applicability is challenged (Bursch et al., 1992a). The size distribution of DNA fragments isolated from cells incubated with low concentrations of TBTO (Fig. 3.7), was essentially identical to that described by Arends et al. (1990) in their characterisation of the nucleosomal-length cleavage products generated by a specific Ca^{2+}/Mg^{2+} endonuclease activity after glucocorticoid treatment of thymocytes.

No comparable DNA cleavage pattern was observed with overtly cytotoxic concentrations (5 μM) of TBTO (Fig. 3.6). This correlated with the quantitatively low levels of DNA fragmentation detected after such treatments (Fig. 3.4a), and is compatible with a number of reports indicating that internucleosomal cleavage is either absent, or present at very low levels, in several cell types dying by necrosis (Afanas'ev et al., 1986; Lennon et al., 1991). However, it should be noted that currently there is a dearth of data comparing thymocyte genomic DNA integrity after necrogenic or apoptotic stimuli. It is probable that the unfragmented nature of the genomic DNA in necrotic TBTO-injured cells reflects an essential difference in the degradative processes between necrosis and apoptosis. Thus during necrosis, DNA degradation is a non-site specific event involving the combined action of proteases and nucleases such that chromatin histone components are degraded and the whole length of DNA is eventually exposed to attack (section 1.1.2). Evaluation of such small DNA fragments would therefore require quite different detection techniques and timecourse studies than those applied in this work.

Of the two methodologies applied to monitor for the occurrence of the morphological changes associated with apoptosis, AO fluorescence was the less satisfactory technique. After treatment with TBTO at less than 5 μM or MPS, a time-dependent increase in the proportion of cells exhibiting brightly fluorescent inclusions was apparent (Fig. 3.9), which had an apparently similar character to the condensed chromatin noted in apoptotic cells by other investigators using this technique (Wyllie, 1980; McConkey et al., 1988a). In addition, this phenomenon correlated with the extent of attendant DNA fragmentation (Fig. 3.4). However, for reasons that were unclear, a high degree of variability was evident in the scored incidence of inclusions for both MPS and TBTO-treated thymocytes. Since neither the presence of non-ionic surfactant, or the use of EDTA (Traganos et al., 1977), afforded appreciable improvements in standardisation of fluorescence character, it was considered unlikely that these technical problems related simply to cell permeability problems or to binding by double stranded RNA. It is however possible that the fluorochrome staining of live cells was inferior to that achievable with fixed preparations.

Due to the subjectivity problems encountered with the AO technique, subsequent morphological studies were performed by light microscopy of toluidine blue stained resin sections. This had the advantage of superior resolution of nuclear chromatin patterns; ease of discrimination of apoptotic bodies; the ability to allow simultaneous assessment of cell preparations for gross necrotic cytopathological changes; and permanency of record. Previous commentary on methods for the visualisation and classification of dying cells has alluded to the utility of plastic-embedded preparations (Hume, 1987). Since nuclear chromatin condensation is a well established idiotype in apoptosis that is also easily discerned, this marker was used to score the proportion of affected cells. Consequently any cells bearing only early cytoplasmic changes would be omitted from the calculated

incidences of apoptosis, and it should be noted that this limited underscoring of apoptosis is inherent to this and similar techniques.

At light microscopy level, the nuclear morphology of most abnormal cells exposed to low concentrations of TBTO (Fig. 3.10b and c) closely paralleled that described by many investigators in thymocytes undergoing apoptosis after in vitro or in vivo exposure to glucocorticoids (van Haelst, 1967; La Pushin and de Harven, 1971). The principle change was condensation of chromatin into sharply delineated and densely stained spheroids or crescents, concomitant with a reduction in nuclear size. Further corroboration that these aberrations were apoptotic in character was obtained when very similar alterations were noted after treatment of cells with the positive control compounds MPS and A23187 (Fig. 3.11a and b, Fig. 3.12). Equivalent basophilic, Feulgen-positive nuclear aggregates correspond to the distinctive condensed chromatin structures observed by electron microscopy in apoptotic cells (Robertson et al., 1978; Wyllie et al., 1980). At agent concentrations which were not overtly cytotoxic, a high proportion of cells exhibited chromatin condensation several hours prior to the appearance of appreciable numbers of nonviable cells (Fig. 3.3a-c, Fig. 3.12). The residual cell bodies discernible (Fig. 3.10b and c) after exposure to low levels of TBTO (0.1-2 μM) were considered to be a further idiomorphic indication that apoptosis had been initiated in these cells. Their appearance matched those detected after MPS exposure (Fig. 3.11a) and it is well documented that such *apoptotic bodies* are a cardinal marker in cytopathology studies of the apoptotic process (Kerr et al., 1972; Allan et al., 1987; Bursch et al., 1990a; Cotter et al., 1992).

TBTO or A23187 concentrations which caused rapid and overt cytotoxicity as indicated by widespread loss of membrane integrity, early signs of cell blebbing and cytolysis (Fig. 3.3a and c, Table 3.2) produced dissimilar morphological changes. The scored incidence of apoptotic nuclear alteration in these cultures remained comparable to that in untreated cells, or with the more extreme treatments, e.g. 10 μM TBTO, were depressed below the respective control means (Fig. 3.12, Fig. 3.13). Light microscopy evaluation of the abnormal cells appearing after exposure to 5-10 μM TBTO indicated that a number of stereotypic changes were present including severe cell swelling and cell fragmentation, nuclear chromatin flocculation, gross disruption of nuclear and plasma membranes, and decreased cytoplasmic basophilia (Fig. 3.10d). In overview these cytopathological findings corresponded well with the numerous descriptions of necrotic morphological change, and are further discussed in the subsequent discourse on ultrastructural level findings. It is considered implausible that the morphological changes observed in thymocytes exposed to high TBTO concentrations (5 or 10 μM) could be the result of secondary necrosis following a preceding rapid wave of apoptosis. This conclusion is based on the small degree of DNA fragmentation evident at the first timepoint examined (Fig. 3.5a), and the known asynchronous nature of thymocyte apoptosis initiated by a variety of agents. In the

context of the operationally convenient timeframe of the first 6 h after TBTO addition, it is considered that the concentration range of 2-3.5 μM delineated the commencement of the transition from predominantly apoptotic to necrotic cell killing (Fig. 3.5).

The synthetic glucocorticoid MPS, and related compounds such as dexamethasone, provide a consistent response in terms of the induction of apoptosis in the immature rodent thymocyte model (Wyllie, 1980; Cohen and Duke, 1984; McConkey et al., 1989b). When cells were exposed to 10 μM MPS they underwent apoptosis in a manner that was entirely consistent, in qualitative appearance, incidence and temporal aspects, to previous reports. Similarly, the activation of apoptosis after short-term in vitro exposure to ionophore A23187 was in accord with observations made previously by a number of groups using rat, mouse and human thymocytes (Wyllie et al., 1984a; Kizaki et al., 1989; McConkey et al., 1989c). These investigators have demonstrated that moderate concentrations of A23187, typically within the range 50-500 nM, produce chromatin cleavage and delayed viability loss, which was confirmed in this study, together with the appearance of apoptotic morphologies (Fig. 3.3c, Fig. 3.4b, Fig. 3.12 and Fig. 3.11b). A rather complex spectrum of morphological change was evident in thymocytes exposed to 1 μM A23187 for 4 h or more (Fig. 3.11c), which paralleled a downturn in the extent of DNA fragmentation (Fig. 3.4b). Only a small proportion of the aberrant cells were judged to exhibit either typical apoptotic or necrotic change, but this level of ionophore-injury did produce irregularly-shaped cells that appeared to have undergone lytic change with loss of internal structure. These findings were accompanied by evidence of increased cytolysis and may reflect direct membrane damage. Thymocytes are known to undergo lysis at comparable A23187 concentrations when incubated in Ca^{2+}-containing medium (Durant et al., 1980) and other workers have commonly cited this order of exposure as progressively producing necrosis (McConkey et al., 1989a). It is probable that a particularly steep dose-response curve exists in terms of the transition from apoptotic to necrotic killing of lymphoid cells by A23187. Some support for this conclusion is drawn from findings with this agent in mouse thymocytes, whereby inhibition of DNA fragmentation by cycloheximide was unaccompanied by a protective effect on membrane integrity after only a limited increment in A23187 concentration (Kizaki et al., 1989).

For all three agents studied including TBTO, the interrelationship of apoptotic nuclear changes to DNA fragmentation was evidenced by the close quantitative identity linking both parameters at any given timepoint. Thus for example, when the linear correlation coefficient was calculated between the scored incidence of cells with chromatin condensation and the extent of DNA cleavage (characterised electrophorectically as internucleosomal in nature) after 6 h exposure (Fig. 3.20), a highly significant association was apparent (t_r = 12.25 with 5 degrees of freedom; $p < 0.01$). The relationship was also maintained when experimental series were analysed from TBTO and A23187 exposures

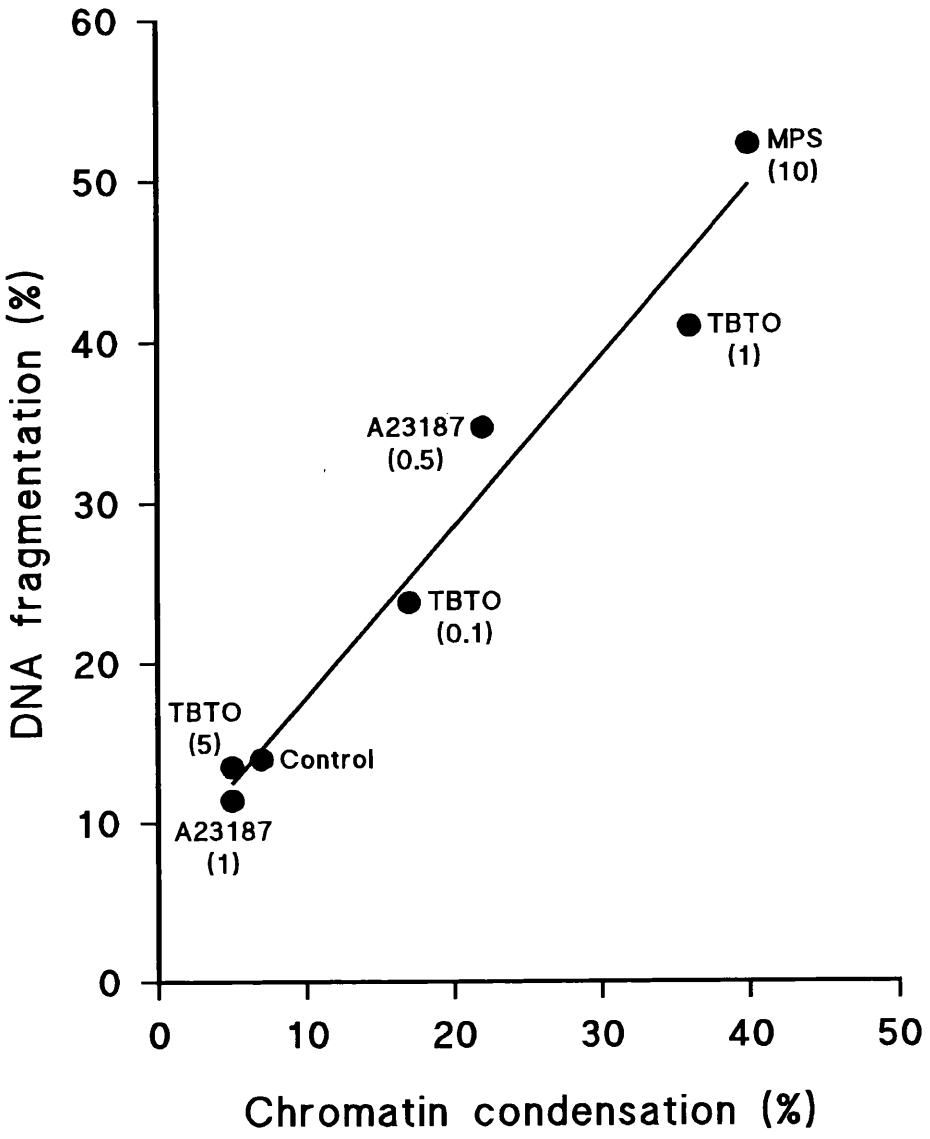

FIGURE 3.20 Correlation of DNA fragmentation with the incidence of chromatin condensation.

Thymocytes were incubated with the test agents at the concentrations (μM) indicated in parentheses beside each datapoint. DNA fragmentation and the incidence of cells exhibiting chromatin condensation were both determined after 6 h exposure by the methods detailed in section 2.6 and 2.4.1 respectively. The mean values obtained for each parameter from three separate experiments were then plotted to determine the degree of linear correlation between the data pairs.

putatively considered to cause cell killing by necrosis, i.e. both indicators were uniformly low. As these findings involve agents with disparate modes of action, it reinforces the generality of the causal linkage previously established between endonucleolytic internucleosomal cleavage and several of the endstage chromatin changes occurring during apoptosis (Arends and Wyllie, 1991). In addition, it suggests that classification of cytopathological change in thymocytes as either *apoptotic* or *necrotic* is probably secure when based on either nuclear morphology or the extent of internucleosomal DNA cleavage.

No experiments were designed to test the reversibility of TBT toxicity to thymocytes. However, in terms of initiation of cell killing it is clear that whilst continuous exposure to low levels of TBTO (0.1 μM) almost exclusively activated apoptotic rather than necrotic cell killing, all cells still became committed to death within 24 h (Fig. 3.14). It is probable that provided activation of intranuclear endonucleolytic activity is sufficient to produce appreciable DNA damage, apoptosis is irreversibly initiated.

The nature of the ultrastructural alterations occurring in thymocytes treated for up to 6 h with low concentrations of TBTO (0.1-2 μM) provided confirmatory evidence that the mode of cell killing invoked was apoptosis. This conclusion was based on their close similarity to features described as stereotypic of apoptosis in major reviews of the subject area (Wyllie et al., 1980; Searle et al., 1982; Kerr and Harmon, 1991). Among the most salient observations were chromatin compaction and redistribution that occurred in the presence of nucleolar dispersal (Fig. 3.15b). Comparable findings have been described in apoptotic thymocytes exposed to glucocorticoids or calcium ionophores (Wyllie et al., 1984a), and this was confirmed with the positive control compounds MPS and A23187 used here (Fig. 3.15c and d). The membrane-bounded residual cell bodies seen after TBTO exposure were considered to be structurally homologous with the diagnostically significant apoptotic bodies formed during apoptosis of lymphoid and other cells (Robertson et al., 1978; Zheng et al., 1991; and compare Fig. 3.16b and Fig. 3.17 with Fig. 3.18c). Furthermore, TBTO-exposed cells exhibited a pattern of extranuclear alterations that when taken together are characteristic of apoptosis; these included cytoplasmic vacuolation, loss of cell surface features, and repositioning of organelles with maintenance of their structural integrity (Fig. 3.15b, Fig. 3.16b and d; and compare with the MPS-mediated changes depicted in Fig. 3.18a-c). The first finding was indistinguishable from the focal dilation of the Golgi apparatus and adjacent endoplasmic reticulum previously recorded for glucocorticoid-injured thymocytes (Morris et al., 1984). It was notable that after 4-6 h exposure to TBTO, or the positive control agents, the development of various morphological alterations in affected cells were relatively asynchronous, which seems to be a function of the rapidly evolving nature of apoptotic changes (Matter, 1979). Cytoplasmic protuberances, a commonly described precursor to the formation of apoptotic bodies, were only rarely seen in TBTO-injured thymocytes at the timepoints examined. However, this

was also the case after MPS treatment and has been ascribed to the high nucleocytoplasmic ratio of thymocytes (Kerr and Harmon, 1991).

Mitochondrial swelling is a well known cellular effect of triorganotins (Aldridge, 1976), and TEM studies showed that a moderate degree of enlargement was common in thymocytes exposed to sub-necrotic levels of TBTO Fig. 3.16c). However, gross structural abnormalities were absent after such exposures. Although mitochondrial swelling is not usually associated with the spectrum of apoptotic morphological change, it has on occasion been described even for glucocorticoids (Galili et al., 1982). Here it is considered more likely that direct action of TBT on the organelle was involved. Enlargement of mitochondria, in the presence of apoptotic nuclear change, is induced by some K^+-ionophores, a class of compounds causing mitochondrial dysfunction (Ojcius et al., 1991).

Compared to the apoptotic changes caused by low organotin concentrations, very dissimilar cytopathological changes were manifest after exposure to higher levels of TBTO. Marked (high-amplitude) swelling of mitochondria, the appearance of mitochondrial flux densities, and dissolution of internal and plasma membranes (Fig. 3.19) were widespread. Equivalent ultrastructural criteria to these have been ascribed to irreversible stages of the degenerative failure of homeostasis during necrosis (Trump et al., 1981). Notably, chromatin in abnormal cells showed minimal redistribution and had a flocculated (clumped) appearance with poorly defined margins; a further established difference between the nuclear compartment changes in necrosis and apoptosis (Searle et al., 1982).

Secondary necrosis, a phenomenon known to occur in apoptotic bodies in suspension cultures (Kerr et al., 1987), was observed after low level TBTO-injury (Fig. 3.16a) and also with MPS. This was typified by cell swelling, degradation of previously condensed chromatin masses, and membranal disruption, and it presumably relates to the eventual activation of lysosomal hydrolases. Initially a small percentage of cells were involved but light microscopy findings detailed previously (section 3.3.6; Fig. 3.14b and c) indicated that the change progressively affected the population of dying cells. It was notable that treatment with concentrations of TBTO or MPS that caused apoptosis in a high proportion of thymocytes had only a limited effect on cell count even after incubation for 24 h (Table 3.2). This finding indicates that cytolysis as a result of terminal apoptotic changes is a rather slow process in the thymocyte suspension culture model. This contrasts with the short persistence of similar apoptotic bodies in vivo due to phagocytosis (Wyllie, 1987a). Extensive cytolysis was however evident after a few hours exposure to levels of TBTO or A23187 that caused cell killing by necrosis (Table 3.2).

On the basis of the techniques employed here, only limited conclusions can be drawn regarding agent effects on thymocyte sub-populations. Without CD marker assessment of

freshly isolated thymocytes it is not possible to be definitive as to whether the isolation methodology was in any way selective for certain cell phenotypes. However, more than 80% of rodent thymocytes are located in the cortex, and it is within this population that cells with greatest sensitivity to both physiological and induced apoptosis reside (section 1.4). Therefore it can be surmised that a high proportion of cells killed by TBTO-stimulated apoptosis are cortical in origin, but their phenotypic subset and relative sensitivity is unknown. Preliminary results from other laboratories suggest that cells of $CD4^+CD8^+$, and to a lesser extent, $CD4^-CD8^-$ phenotype are preferentially killed by TBT (Prof. S. Orrenius, personal communication). Selective cytotoxicity following TBTO exposure may not solely be limited to apoptotic cell killing. The viability result obtained with 5 μM TBTO, whereby an effect plateau was observed after 4 h (Fig. 3.3a), was reproducible and may suggest the existence of differential population sensitivity.

During the course of this work, Orrenius and co-workers reported that TBT could activate apoptosis in thymocytes obtained from immature Sprague-Dawley rats (Aw et al., 1990). They found that 5 μM TBTC (the only concentration specified) caused a Ca^{2+}-mediated increase in DNA degradation that was closely followed by loss of membrane integrity. Whilst my findings are in agreement with the stimulation of apoptosis by TBT, a number of methodological differences between our studies, particularly their use of short-term incubations in a simple serum-free salt solution, complicate direct comparison. In terms of concentration-effect, the profile of DNA fragmentation and decline in viability reported by Aw et al. most closely resembles that described here for 2 μM TBTO. Assuming that the TBT cation is the toxic species, this is as would be predicted on an equimolal concentration basis. Since they performed no morphological assessments, and in view of the rapid appearance of nonviable cells, it cannot be excluded that 5 μM TBTC was a borderline necrotic exposure in their experiments. It should also be noted that the extent of oligonucleosomal cleavage detected by electrophoresis in their study at 15 minutes and 2 h did not correlate with the marked differential in the respective quantitative DNA fragmentation values. Although it has been suggested that DNA fragmentation in TBT-mediated apoptosis occurs with much greater rapidity than that achieved with glucocorticoids (McConkey et al., 1992), the difference noted between TBTO and MPS was unremarkable (Fig. 3.4a and b; Fig. 3.5a). Further corroboration that low concentrations of TBT can activate apoptosis comes from a recent report of its action in a vertebrate model; human T-lymphoblastoid CEM cells, and also in an invertebrate system; the marine sponge Geodia cydonium (Batel et al., 1993).

An early conclusion reached by Kerr and co-workers was that several lethal stimuli e.g. radiation or genotoxic chemicals were capable of initiating either apoptosis or necrosis (Kerr et al., 1972). This has been extended into the pivotal hypothesis that, whilst it is a distinct process, apoptosis can be induced in susceptible tissues by injurious stimuli of a

smaller amplitude than those causing necrosis in the same tissue (Wyllie, 1987b). However it is conceivable that there are subtle variations in the form of non-necrotic cell death produced by various lethal stimuli. Dependent on the agent concerned, this may approximate in character to apoptosis caused by prototypical inducers, e.g. glucocorticoid hormones, to a greater or lesser degree. Thus for example, characteristic nuclear changes may occur in the absence of cytoplasmic contraction and increased cell density (Dyson et al., 1986). Such considerations are likely to be of particular relevance where membrane-active agents such as ionophores and TBT may cause focal membrane disruption or marked changes in membrane fluidity. It has been proposed that a third type of cell death can be elicited by certain K^+-ionophores and TNFα, involving internucleosomal DNA fragmentation and apoptotic nuclear changes in conjunction with cytoplasmic alterations reminiscent of necrosis (Ojcius et al., 1991; Goldstein et al., 1991). Whether this finding has general applicability remains to be established, and it should be noted that caution is required when interrelating population-based parameters, e.g. DNA fragmentation, to morphological findings in single cells. Although a few atypical morphological features were noted in cells undergoing apoptosis after low level TBTO or A23187 exposure, key stigmata of necrosis were absent. It is concluded that, within the constraints of the timescales and concentrations examined, thymocytes with hybrid morphologies were not formed under such circumstances.

The question arises as to what in mechanistic terms differentiates the apoptotic and necrogenic cellular responses to TBT exposure. It has been suggested that, for some agents at least, a critical $[Ca^{2+}]_i$ threshold may be involved (McConkey et al., 1988b; McConkey et al., 1989a), which if exceeded causes ablation of apoptosis, e.g. by activation of Ca^{2+}-dependent phospholipases or proteases. In thymocytes exposed to 1-15 μM TBT (Chow et al., 1992), $[Ca^{2+}]_i$ increases rapidly but at the maximally effective TBTC level (5 μM) it plateaus at about 1400 nM and shows little change with further TBT addition. Therefore, unlike the very marked differences in $[Ca^{2+}]_i$ reported to exist between apoptotic and necrogenic exposures to agents such as menadione and A23187 (McConkey et al., 1988b; Prof. S. Orrenius, personal communication), it does not appear that TBT elicits a change of similar amplitude. Consequently it is less likely that excursions above a $[Ca^{2+}]_i$ threshold can alone provide the basis for the transition from apoptotic to necrotic cell killing. High concentrations of TBT can actually antagonise extracellular Ca^{2+} ingress (Rice and Weeks, 1989). In terms of cellular ion homeostasis, it is postulated that the plasma membrane Na^+, K^+-ATPase is perhaps a more critical biochemical target at high level TBT exposures. This is due to the very sharp dose-response curve for direct inhibition of this translocase by triorganotins (Selwyn, 1976), which would be expected to act synergistically with indirect effects via the diminished intracellular ATP pool already established at lower triorganotin concentrations. High TBT concentrations could thereby sufficiently disrupt the intracellular ionic environment to prevent activation of apoptosis and

consequently lead to cell death by necrosis. It is of interest that the degree of hydrophobic interaction of various triorganotins with the translocase in isolated membrane preparations correlates very well with their lipophilicity and relative cytotoxicity. Further aspects of the biochemical toxicity of TBTO are considered in chapter 5.

In summary, a number of broad conclusions can be drawn from these investigations:

1. In vitro exposure to TBTO can activate apoptosis in thymocytes derived from immature rats. This suggests a possible effector mechanism for the extensive thymolytic action of TBT in vivo.
2. In terms of morphological and biochemical character the process has similarities with apoptosis induced by glucocorticoid hormones or Ca^{2+}/Mg^{2+}-ionophores; in particular, chromatin is extensively degraded in a manner which is compatible with endonucleolytic cleavage at internucleosomal regions of DNA.
3. DNA fragmentation precedes viability loss mediated by low TBT concentrations, in a manner which appears causal.
4. Exposure of cells to slightly higher levels of TBTO causes overt cytotoxicity corresponding to necrotic cell death.

CHAPTER 4

THE EFFECTS OF MODULATORS OF THE APOPTOTIC PROCESS ON THYMOCYTE CYTOTOXICITY CAUSED BY TRI-n-BUTYLTIN.

ABSTRACT

The biochemically active nature of apoptosis provides a number of loci which can be manipulated so as to modulate the initiator or effector arms of the process. In order to further characterise the nature of non-necrotic cell killing by TBT, these experiments examined the effect of several agents, with reported potential as inhibitors of apoptotic cell death, on rat thymocyte apoptosis instigated by TBTO. The synthetic glucocorticoid hormone MPS was employed as a positive control.

Pretreatment with the membrane-permeant intracellular chelators BAPTA-AM or Quin-2 AM protected cells from internucleosomal DNA cleavage, chromatin condensation and delayed cell death resulting from exposure to apoptotic concentrations of TBTO. Similar inhibitory effects were apparent in the case of MPS treatment. These findings confirm that, in common with thymocyte apoptosis induced by glucocorticoids, and a variety of other stimuli, a rise in $[Ca^{2+}]_i$ is central to the process activated by TBT.

The presence of Zn^{2+} markedly inhibited DNA fragmentation and viability loss arising from exposure to either TBTO or MPS. However, ultrastructural examination of such cells indicated that some early cytopathological changes were present. Aurintricarboxylic acid (ATA), an inhibitor of protein-nucleic acid interactions, provided a moderate degree of protection from TBT-stimulated DNA degradation and the appearance of apoptotic morphological markers. H33258, a bisbenzimidazole with DNA minor groove binding affinity which also interferes with the action of some DNA-binding proteins, e.g. topoisomerase II, partially prevented DNA cleavage following TBTO exposure. Paradoxically, this was accompanied by a disproportionately high degree of protection from viability loss. H33258 was rather less effective in preventing MPS-induced apoptosis. In the case of apoptosis inhibition by Zn^{2+}, ATA or H33258 it is considered probable that their intervention in the apoptotic process was at the DNA level, e.g. inhibition of one or more effector endonucleases; alteration of DNA conformation; or possibly interference with an accessory enzyme such as topoisomerase II.

In apparent contradiction to some recent reports concerning blockade of apoptosis in rat thymocytes by phorbol esters, TPA and PDBu were found to be ineffective in preventing DNA fragmentation induced during short-term exposure to glucocorticoid or TBT.

4.1 INTRODUCTION

This chapter focuses primarily on events in thymocyte apoptotic processes (also refer to sections 1.3 and 1.4). A truly comprehensive review of the nature and interrelationships of these signalling pathways is beyond the scope of this thesis, and is in any case limited by the fragmentary state of current knowledge. The following sections seek to provide an overview of important aspects but must be viewed as inevitably eclectic in their coverage.

4.1.1 Intracellular signal transduction in thymocyte apoptosis

Considerable study has been devoted to Ca^{2+} homeostasis in the cytopathology of cell death (Trump and Berezesky, 1984; Boobis et al., 1989; Nicotera et al., 1990). With the realisation of the importance of non-necrotic death, reviewers in this area have broadened their treatment of the subject to include the role of Ca^{2+} signal transduction processes in apoptosis (Orrenius et al., 1989; Nicotera et al., 1992; Trump and Berezesky, 1992; Corcoran and Ray, 1992). In particular, emphasis has been placed on the importance of Ca^{2+}-mediated endonuclease activation (Fawthrop et al., 1991; McConkey et al., 1992).

As is typical of mammalian cells (Carafoli, 1987), the $[Ca^{2+}]_i$ of resting T lymphocytes is maintained at around 80-120 nM (Tsien, 1981; McConkey et al., 1988a), against a much higher extracellular ionic gradient by a series of processes involving translocases and specific Ca^{2+} sequestering molecules (Fig. 4.1). Subtle modulations of $[Ca^{2+}]_i$ play a key role in T cell intracellular signalling, in the case of both thymocytes and mature cells (Finkel et al., 1991; section 1.4.3). Based on a number of independent observations, these physiologically relevant signal transduction pathways also appear to be involved in the activation of thymocyte apoptosis. As early as 1977, Bachvaroff et al. showed that internucleosomal DNA cleavage in murine lymphocyte nuclei by a constitutive endonuclease activity required Ca^{2+} as a cofactor. Simultaneously, it was demonstrated that the cytolytic effects of glucocorticoids or ionophore A23187 on rat thymocytes were Ca^{2+}-dependent, and involved Ca^{2+} influx (Kaiser and Edelman, 1977). Subsequent findings suggested that this mechanism was more easily activated in thymocytes as opposed to mature lymphocytes (Kaiser and Edelman, 1978). Cohen and Duke (1984), linked glucocorticoid-mediated thymocyte apoptosis to Ca^{2+} and Mg^{2+}-dependent internucleosomal DNA degradation, and postulated that such cell killing might be due to intracellular calcium fluxes. Sustained early increases (up to 800 nM) in cytosolic (*sic*) Ca^{2+} levels, preceding DNA fragmentation, were found in MPS-treated thymocytes (McConkey et al., 1989b); both effects could be prevented by intracellular Ca^{2+} buffering or extracellular chelation by EGTA. Since the Ca^{2+} elevation could also be blocked by transcriptional or translational inhibitors, and apparently depended on a labile cytosolic factor, these investigators concluded that synthesis of a Ca^{2+} transport protein permitted extracellular Ca^{2+} ingress which then activated apoptosis. Analogous observations were later made in the case of X-irradiated thymocytes (Zhivotovsky et al., 1993). As chromatin

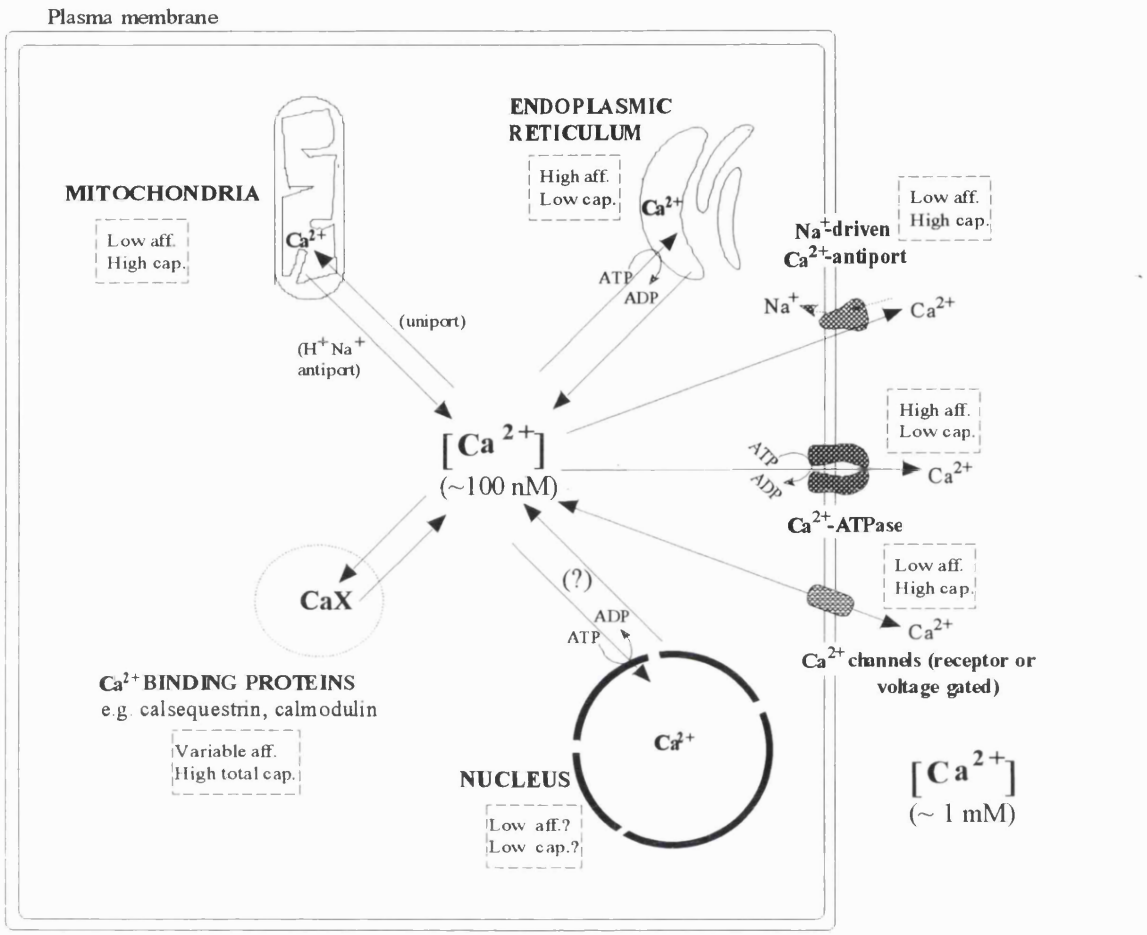

FIGURE 4.1 Stylised schematic of Ca^{2+} homeostasis processes in mammalian cells. Differential intracellular and extracellular Ca^{2+} concentrations are shown in indicative terms only. Where known, the relative affinities (*aff.*) and capacities (*cap.*) for Ca^{2+} transport are given in boxed inserts. The plasmalemmal sodium-calcium ion antiport system and voltage-gated calcium ion channels are primarily associated with excitable cell types. The intranuclear system is currently poorly defined and demonstration of its general applicability is lacking. References Alberts et al., (1989); Carafoli (1987); Nicotera et al. (1989; 1990; 1992).

cleavage shows a close temporal and concentration-dependent relationship with increased $[Ca^{2+}]_i$, it has been suggested that this indicates a causal effect between elevations in Ca^{2+} level, subsequent activation of DNA fragmentation and eventual apoptotic killing (McConkey et al., 1989a).

There is a physiological role for the TcR complex in activating apoptosis during clonal deletion (Smith et al., 1989), and a phosphoinositide/Ca^{2+} pathway is linked to the TcR sensor (Finkel et al., 1991; Fig. 4.2). In keeping with this, a sustained Ca^{2+} increase, mostly extracellular in origin, leading to endonuclease activation and cell death can also be actuated in thymocytes by anti-CD3 antibodies (McConkey et al., 1989c). These investigators reported that engagement of the CD3/TcR complex, or exposure to A23187, caused apoptosis in human thymocytes but not in mature peripheral T cells, although elevations in $[Ca^{2+}]_i$ were claimed in both cell types. This suggests that susceptibility to apoptosis is regulated at a point distal to the production of calcium fluxes. At least in the case of apoptosis due to X-irradiation, there seems to be a qualitative difference in the response of thymocytes and splenocytes (Zhivotovsky et al., 1993)—DNA fragmentation is Ca^{2+}-dependent in both cases, but only thymocytes exhibit a Ca^{2+} flux transient after injury. Furthermore, internucleosomal DNA cleavage activated by cAMP analogues is not Ca^{2+}-stimulated but is Ca^{2+}-dependent (McConkey et al., 1990a). In summary, these findings indicate that in developing T cells there is a Ca^{2+}-linked signal transduction pathway which can participate in proliferation or apoptosis. As discussed later in this section, a Ca^{2+} flux is only mitogenic when accompanied by other signals (normally via cytokines). In contrast, Ca^{2+}-modulated signalling leading to apoptosis variously results from inappropriate TcR binding, e.g. in clonal deletion; artificial CD3/TcR engagement or other triggers of phosphoinositide hydrolysis; or Ca^{2+} fluxes from receptor-linked processes, e.g. glucocorticoids, synthesis of calcium-porter proteins, e.g. X-irradiation or glucocorticoids, or stimuli directly raising $[Ca^{2+}]_i$, e.g. ionophores. In addition, Ca^{2+}-dependent apoptotic effector processes participate downstream of signal transduction.

Beyond receptor/phosphoinositide/Ca^{2+} elements, elucidation of the specific calcium-dependent signalling events leading to endonuclease activation is awaited. In thymocytes or thymoma cells, the calmodulin antagonist, calmidazolium, prevents MPS or ATP-mediated DNA fragmentation without affecting the rise in $[Ca^{2+}]_i$ (McConkey et al., 1989b; Zheng et al., 1991); this suggests that calmodulin is involved at an intermediate point in the activation of endonucleolytic activity. Ca^{2+}/calmodulin complexes regulate many enzymes and receptors (Alberts, 1989) including important kinases such as Ca-kinase II, and it is tempting to speculate that the signal cascade at this point involves one or more kinases. In addition, an important recent study (Fruman et al., 1992) has drawn attention to the role of calcineurin A, a Ca^{2+}/calmodulin-dependent serine/threonine phosphatase which is normally linked to the action of transcription factor NF-AT

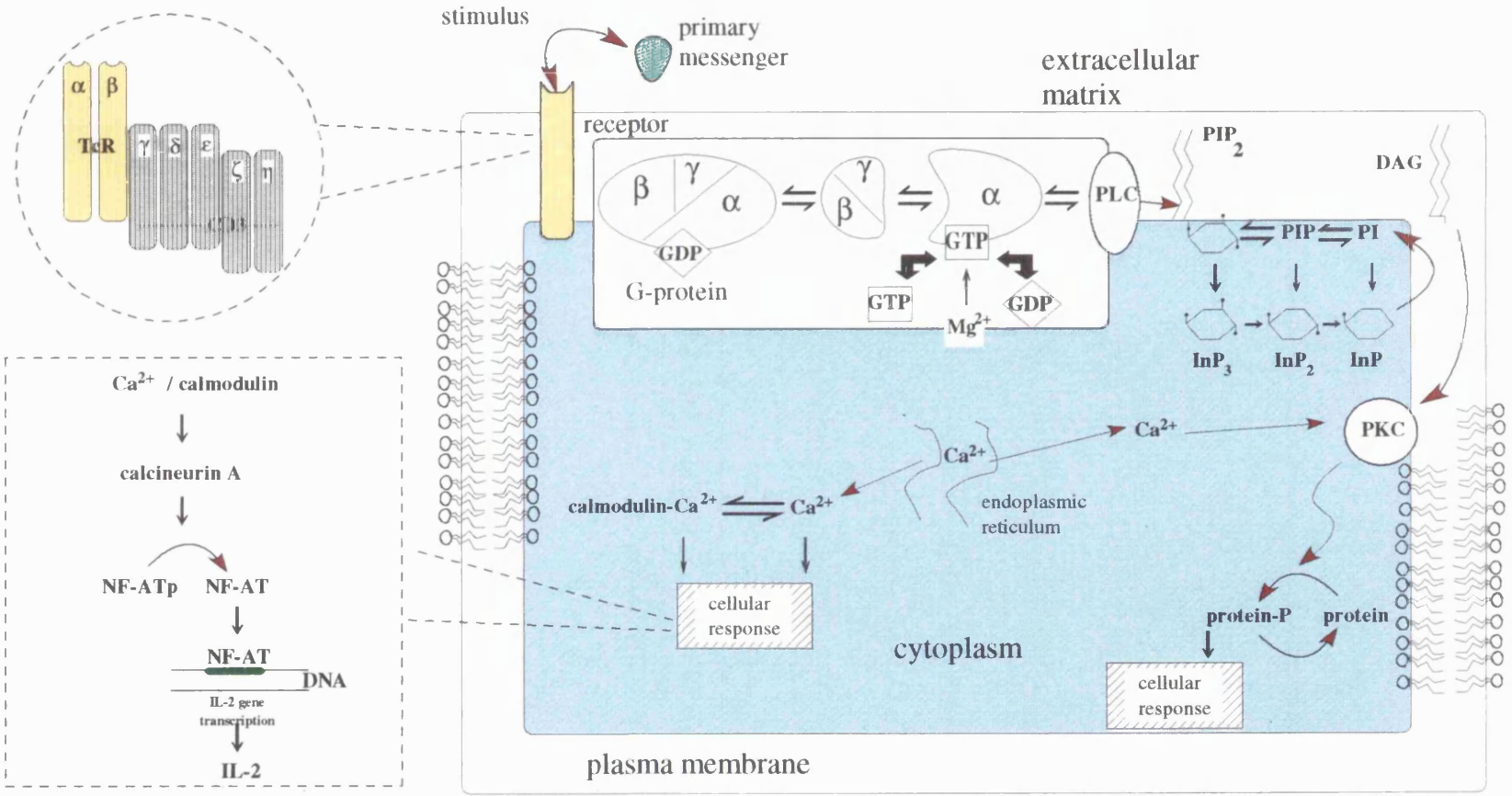

FIGURE 4.2 Simplified schematic of the cellular Ca^{2+} /phosphoinositide signal transduction pathway.
Signal input occurs by binding of a primary messenger molecule, or equivalent trigger, to a receptor at the cell surface. The G-protein assembly translocates the signal to phospholipase C (PLC) which cleaves phosphoinositidyl[4, 5]biphosphate (PIP_2). The secondary messengers formed, including inositol triphosphate (InP_3) and diacylglycerol (DAG) then modulate transduction processes including release of intracellular Ca^{2+} stores and PKC activation, respectively. These lead to amplified cellular responses. Off-phase control is mediated via GTP hydrolysis allowing reassembly of G-protein subunits. PIP_2 is resynthesised according to the pathway shown. To exemplify a specific process, the insets show the coupling of this pathway to the sensor and one transduction arm of the T-cell activation process involving the calcium/calmodulin-dependent phosphatase calcineurin, and an IL-2 gene targeted nuclear transcription factor (NF-AT). Inappropriate activation of calcineurin-linked processes can lead to apoptosis. In the case of TcR activation, the tyrosine kinase $pp59^{fyn}$ is thought to activate PLC.

(see Fig. 4.2); it appears that the ability of murine T cell hybridomas to undergo apoptosis following ligation of the CD3/TcR correlates directly with calcineurin activity.

As an increase in $[Ca^{2+}]_i$ has been linked with both T cell proliferation and apoptosis, there has been much interest in control via multiple signal transduction mechanisms. Based mainly on work with modulators such as phorbol esters and protein kinase inhibitors, it has been postulated that PKC pathway activation status might be responsible for 'switching', such that thymocyte apoptosis would occur only in the event of 'unbalanced signalling', i.e. when the PKC arm was inactive (McConkey et al., 1990c; McConkey and Orrenius, 1991). TPA or PDBu were reported to prevent DNA fragmentation in rat thymocytes exposed to cAMP agonists (McConkey et al., 1990a), anti-CD3 antibodies (McConkey et al., 1989c), A23187 or MPS (McConkey et al., 1989d; Perotti et al., 1991), and phorbol esters also reduced endonuclease activity in isolated thymocyte nuclei (McConkey et al., 1989d). In the latter study, supplementary evidence for antagonism of apoptosis by PKC stimulation was derived from the DNA fragmentation arising in cells exposed to a mitogen and H-7, a protein kinase inhibitor. Contrary findings have been described; equivalent concentrations of phorbol esters were paradoxically ineffective against, or stimulated apoptosis in murine thymocytes (Smith et al., 1989; Kizaki et al., 1989). Furthermore, inhibition of protein phosphorylation by H-7 antagonised nucleoside or ionophore-activated thymocyte apoptosis (Kizaki et al., 1988; Kizaki et al., 1989). Accessory cell production of cytokines, and in particular IL-1, is thought to have a pivotal role in the instigating T cell proliferation as a co-signal with antigen-stimulated Ca^{2+} fluxes (see section 1.4) IL-1 prevented human and rat thymocyte apoptosis due to glucocorticoids, CD3/TcR engagement, ionophore A23187, or cAMP analogues (McConkey et al., 1989e; McConkey et al., 1990a) IL-1 is known to induce DAG production, thereby activating PKC, and whilst there is no direct evidence to suggest that this locus is the mode of inhibition of apoptosis, McConkey et al. (1989e) claimed that the protein kinase inhibitors H-7 and sphingosine could reverse the protective effect of IL-1. IL-2 abrogated glucocorticoid-induced apoptosis in IL-2-dependent T lymphocytes (Nieto and Lopez-Rivas, 1989), but was ineffective on thymocytes (McConkey and Orrenius, 1991); this may be due to the transient unresponsiveness of immature T cells to this cytokine (Rothenberg, 1990).

Upregulation of PKA activity via the second messenger cAMP depresses T cell responses and inhibits T cell proliferation (Kammer, 1988), and cAMP has been implicated in some forms of programmed cell death and in lymphocytolysis (McConkey and Orrenius, 1991). Exposure of rat thymocytes to either the PKA pathway receptor binding agent prostaglandin E_2, the adenylate cyclase agonist forskolin, or cAMP analogues, caused apoptosis without promoting intracellular Ca^{2+} elevation (McConkey et al., 1990a). These workers concluded that the PKA pathway could be a general mechanism for endonuclease activation and consequent apoptosis. More recently, potentiation of murine thymocyte

apoptosis caused by glucocorticoids, but not A23187, via agents which elevated cAMP was described; possibly involving a glucocorticoid receptor modification event (McConkey et al., 1993).

It has been suggested that poly(ADP-ribose) polymerase may function as a regulator toward the distal end of apoptotic signal transduction pathways. Its postulated action may involve facilitation of the repair of both DNA strand breaks and fragmentation arising from stimuli such as γ-irradiation or glucocorticoid treatment (Wielckens et al., 1987), and also direct inhibition of Ca^{2+}/Mg^{2+}-dependent nuclease activity (Umansky, 1991). Some support for this notion is derived from the potentiation of apoptosis in certain lymphoid cells, including thymocytes, by poly(ADP-ribose) polymerase inhibitors (Wielckens and Delfs, 1986; Nelipovich et al., 1988). Direct involvement of poly(ADP-ribose) polymerase in thymocyte apoptosis activated by A23187 or glucocorticoid has been discounted (McConkey et al., 1989a) since no fall in NAD^+ levels occurred, and cell killing was insensitive to 3-aminobenzamide (later confirmed by Barbieri et al., 1992). The conformational state of genomic DNA can obviously have a marked effect on its susceptibility to nuclease attack, but at the time of writing, a sound molecular basis for a modulatory role of this enzyme on apoptotic effectors remains to be established.

In conclusion, the signal transduction mechanisms activating apoptosis in immature thymocytes are now partially understood. A striking feature is their overlap with physiologically relevant pathways regulating cell division and activation state. Attempts have been made to unify this information into schemes for apoptosis initiation (e.g. McConkey et al., 1990c), but these proposals still require more complete validation.

4.1.2 Other modulators of T cell apoptosis

Apoptotic cell death can often be prevented or diminished by inhibitors of transcription or translation; this subject is covered in section 1.3.3 and in Chapter 5. Other than the modulators described in the previous section, a number of other compounds have been found to inhibit apoptosis in a variety of model systems, including rodent thymocytes. In most cases, the mechanism of their inhibitory effect is poorly understood, or has only been localised to either the initiator or effector arms of the process.

Since it was established that Zn^{2+} was highly effective in inhibiting DNA fragmentation arising from glucocorticoid-mediated apoptosis in rodent thymocytes (Cohen and Duke, 1984), a large number of studies have reported similar blockade of apoptotic parameters by zinc in a variety of test systems exposed to disparate stimuli. Therefore zinc has come to be regarded as almost a universal inhibitor of apoptosis. Table 4.1 summarises some of the data available for T lymphocytes and related lymphoid cells, and includes for comparative purposes references to other cell types. Nearly all investigations show that Zn^{2+}, at or

Reference	System [1]/ agent	Parameter: DNA degradation/ internucleosomal cleavage	Apoptotic morphology	Cytolethality /cytolysis	Other
Duke et al., 1983	CTL target killing	⇩		⇩	
Cohen and Duke, 1984	Thymocytes (m)/ glucocorticoid	⇩			
	Thymocyte nuclei/ Ca^{2+}	⇩			
Sellins and Cohen, 1987	Thymocytes (m)/ γ-irradiation	⇩		⇩	
Cohen et al., 1992	Thymocytes (r)/ glucocorticoid	⇩	⇳		▫ [2]
Barbieri et al., 1992	Thymocytes (r)/ glucocorticoid	⇩		▫ [3]	
Migliorati et al., 1992	Thymocytes (m)/ heat shock	⇩	⇩		
McCabe et al., 1993	Thymocytes (r)/ zinc chelation[4]-replacement	⇩		⇩	
Nieto and Lopez-Rivas, 1989	CTLL-2 T cell nuclei (h)/ Ca^{2+}	⇩			
Gaido and Cidlowski, 1991	Endonuclease NUC18 (r)/ Ca^{2+}	⇩			
Compton, 1992	Thymocyte (c) nuclear protein extract[5]	⇩			
Zheng et al., 1991	EL4 thymoma cells (h)/ ATP	⇩		▫	
Martin et al., 1991	HL-60 (h), Raji cells (h)/ zinc deprivation-replacement		⇩		
Giannakis et al., 1992	Splenocytes(r), CLL, cells (h), hepatocytes (r)/ colchicine	⇩			
Waring et al., 1990	T blasts, macrophages (m)/ gliotoxin	⇩	⇩		

TABLE 4.1 Inhibition of apoptosis, or in vitro endonucleolytic DNA cleavage, by zinc. The effect of Zn^{2+} on apoptotic markers, or internucleosomal DNA cleavage occuring in vitro systems, is indicated as causing either substantial inhibition or elimination (⇩); partial or otherwise qualified inhibition (⇳); or no effect (▫). Nota: [1] Source of cells: m - mouse; r - rat; c - chicken; h - human; [2] Modal density; fluorochrome staining character; [3] Insecure result due to high Zn^{2+} concentration and prolonged incubation time; [4] Using N, N, N', N',-tetrakis (2-pyridylmethyl)ethylenediamine (TPEN). [5] Obtained after glucocorticoid treatment, erythrocyte DNA used as a substrate with appropriate cofactors.

above high micromolar concentrations, effectively eliminates internucleosomal cleavage produced in either intact cells, isolated nuclei containing constitutive Ca^{2+}/Mg^{2+}-dependent endonuclease activity, or mediated by candidate apoptotic endonucleases (see Table 4.1). Under these circumstances, and consistent with the hypothesis that DNA fragmentation in apoptosis leads to cell death, subsequent protection by Zn^{2+} from viability loss or cytolysis has also been demonstrated (Table 4.1). Although isolated nuclei studies and in vitro endonuclease assays point toward Zn^{2+} interfering with apoptotic effector enzymes, it is unclear to what extent this entails direct nuclease inhibition or chromatin substrate effects. A role for Zn^{2+} in intranuclear signal transduction mechanisms has also been suggested (Cohen and Duke, 1984; McCabe et al., 1993). There have been occasional reports that endonucleases thought to be implicated in apoptosis are not zinc-sensitive, e.g. DNase II (Barry and Eastman, 1993), but this is unlikely to be of relevance to T cell apoptosis.

The non-specific DNA-protein interaction inhibitor aurintricarboxylic acid (ATA) inhibited glucocorticoid or calcium ionophore-mediated DNA fragmentation and latent cytolethality in rodent thymocytes (McConkey et al., 1989a), and it was subsequently demonstrated that ATA prevented the appearance of apoptotic cells after glucocorticoid treatment (Cohen et al., 1992). ATA also antagonised DNA fragmentation and cytolysis in leukemic Jurkat T-cells caused by NK cell cytotoxicity (McConkey et al., 1990), and activation-induced cell death in T cell hybridomas (Shi et al., 1990). In common with Zn^{2+}, ATA appears able to directly inhibit putative Ca^{2+}/Mg^{2+}-dependent endonucleases which may be involved in apoptosis (Gaido and Cidlowski, 1991).

Following from the discovery that polyamines, such as spermine and spermidine, could interfere with DNA autodigestion in isolated nuclei (Vanderbilt et al., 1982), Orrenius and co-workers showed that, probably by altering DNA conformation, exogenously added polyamines could decrease thymocyte DNA fragmentation arising from apoptotic treatments with glucocorticoid, A23187 or TBT (Brune et al., 1991). Since a polyamine synthesis inhibitor promoted chromatin cleavage, they concluded that polyamine protection of DNA from nuclease attack is a physiologically relevant process.

Cyclosporin A (CsA) blocked activation-induced apoptosis in T cell hybridomas and murine thymocytes in vivo (Shi et al., 1989), and it was suggested that this effect may underlie its ability to interfere with the deletion of autoreactive T cells. Similarly, CsA was able to prevent apoptosis in $CD4^+$ T cells infected with human immunodeficiency virus (Groux et al., 1992). Cyclophilin has recently been identified as the intracellular receptor for CsA, and the drug-complex is thought to interfere with signal transduction by inhibiting the phosphatase calcineurin (Clipstone and Crabtree, 1992); therefore this pathway may be the locus for antagonism of apoptosis by CsA.

4.1.3 Characteristics of modulator compounds used in these studies

Calcium chelators

A new generation of Ca^{2+}-chelators was introduced in the early 1980's (Tsien, 1980) that have a structural homology with EGTA, and retain the selectivity of the latter in binding Ca^{2+} in preference to Mg^{2+} and H^+ (approximately a 10^5 fold higher stability constant). BAPTA was prototypal in this series, has a higher affinity for Ca^{2+} than EGTA and also a higher buffering speed, whilst the related compound Quin-2 has slightly lower selectivity over Mg^{2+} than BAPTA but has the advantage of a still higher Ca^{2+} affinity. Hydrophobic acetoxymethyl derivatives of these chelators have been synthesised (e.g. BAPTA-AM and Quin-2 AM) with increased biomembrane permeability. Once in the cell, cytoplasmic esterases cleave the acetoxymethyl ester bonds to yield the free parent compound which due to its polar form can only re-cross the plasma membrane very slowly, thereby facilitating intracellular loading (Tsien, 1981). These compounds are then able to buffer changes in $[Ca^{2+}]_i$. Concentrations of EGTA in the millimolar range have been widely used to deplete media of Ca^{2+} and thereby reduce the potential for influx of this ion from the extracellular milieu (e.g. see McConkey et al., 1988a).

Zinc

Zinc, an essential trace element required by mammalian cells, has been shown to be critical to maintenance of cell mediated immunity (Fernandes et al., 1979). As discussed in the previous section, Zn^{2+} has also been shown to inhibit the endonucleolytic internucleosomal DNA cleavage associated with apoptosis, and also has a variety of cellular effects including stabilisation of DNA structures (Koizumi and Waalkes, 1990). Prior studies of the modulation of apoptosis by zinc, have principally utilised the sulphate or chloride salts, whereas zinc acetate was the compound of choice here due to its better compatibility with complex incubation media and lesser perturbation of extracellular pH.

Aurintricarboxylic acid

The triphenylmethane compound aurintricarboxylic acid (ATA), and its salts, have been used, in the high micromolar concentration range, as general inhibitors of nucleases, e.g. DNase I, exonuclease II and RNase A (Hallick et al., 1977). Reports on the mechanism of action and spectrum of biochemical processes affected by ATA have been confusing and contradictory, but there is consensus that it interferes with many protein-nucleic acid interactions and may also inhibit RNA and protein synthesis.

DNA minor groove binding agents

Distamycin A, the bisbenzimidazole compound H33258, and its homologue H33342, possess crescent-shaped molecular structures enabling them to bind reversibly to AT base-pair rich sequences in the minor groove of the DNA double helix (Zimmer and Wahnert, 1986). The interaction is complex, but hydrogen bonding is involved (Stokke and Steen, 1985), and it can be monitored by virtue of the fluorescence enhancement which occurs on binding (see also section 2.7). These compounds interfere with nuclear enzymes including topoisomerases and DNases, and affect DNA superstructure-determined parameters such

as nucleoid sedimentation (Woynarowski et al., 1989; Tempel and Ignatius, 1993).

Phorbol esters

12-O-tetradecanoylphorbol-13-acetate (TPA; phorbol 12-myristate 13-acetate), and 12,13 phorbol dibutyrate (PDBu) are examples of complex diester cyclic alcohols derived from the oil of *Croton* species, *Euphorbiaceae*, known collectively as phorbol esters. They have pleiotropic effects on cellular systems, are highly active (nanomolar levels elicit some effects), and can function as co-mitogenic stimuli (Taylor et al., 1984) and tumour promoters. An important property is their ability to mimic the effects of DAG by binding to PKC and thereby causing its activation and transposition (Kraft and Anderson, 1983).

Cyclosporin A

Cyclosporin A (CsA) is derived from the fungus *Tolypocladium inflatum Gams* and is a member of a family of non-polar cyclic polypeptides which are designated as cyclosporin A-I. It possesses powerful and clinically useful immunosuppressive properties, mainly relating to cell mediated immune responses, but can also cause T cell graft-versus-host disease and various autoimmune syndromes. CsA has been shown experimentally to cause abnormal differentiation of thymocytes, and to prevent deletion of T cell clones with high avidity to self-antigens during thymic ontogeny (Gao et al., 1988).

Calmidazolium

Calmidazolium is a competitive calmodulin antagonist that is more potent and possesses more selectivity than trifluoperazine. It inhibits a wide variety of Ca^{2+}/calmodulin-dependent enzymes (Gietzen et al., 1982), e.g. plasma membrane Ca^{2+} translocase; phosphodiesterase (IC_{50} 30 nM); and myosin light chain kinase (IC_{50} 0.5 μM). It should be noted that it is not entirely specific, and may also affect calmodulin independent enzymes such as PKC, IC_{50} 5 μM (Mazzei et al., 1984).

4.1.4 Aims of these studies

The characteristics of TBT-stimulated non-necrotic thymocyte killing were studied by means of a number of agents previously established as being capable of manipulating the initiation and effector arms of apoptosis. Though these agents were selected on the basis that they had previously been classified as inhibitors of apoptosis, or were predicted to have such potential, in some cases their effects or mechanisms of action remain contentious. Therefore they have been referred to primarily as apoptotic *modulators* rather than *inhibitors*. MPS was used as a positive control since there was extensive existing literature relating to manipulation of glucocorticoid-induced apoptosis by equivalent modulators.

Elements of the work in this chapter have previously been published in:

Raffray M, McCarthy D, Snowden RT, Cohen GM (1993) Apoptosis as a mechanism of tributyltin cytotoxicity to thymocytes: Relationship of apoptotic markers to biochemical and cellular effects. Toxicol Appl Pharmacol 119: 122-130

Raffray M, Cohen GM (1991) Activation of programmed cell death in immature rat thymocytes by bis(tri-n-butyltin) oxide (TBTO): 2. Biochemical mechanisms. Human Exp Toxicol 10: 482-483A

4.2 METHODS

4.2.1 Materials

TBTO obtained from Fluka Chemicals Ltd (Glossop, England) was purified as described in section 2.14. MPS (> 95%) was from Upjohn (Crawley, England). Table 4.2 details the identity, source and stated purity of the various modulators used. All other materials and reagents were obtained from the sources indicated in the appropriate sections of chapter 2.

4.2.2 Cell incubation, and test compound and modulator handling

Monodisperse thymocyte suspensions were prepared from 4-6 week old male Wistar rats (School of Pharmacy breeding colony) by the disaggregation method described in section 2.1. After determination of initial viability (section 2.2), the cells were diluted to a final density of 20 x 10^6 ml^{-1} in RPMI-1640 medium supplemented with 10% FCS. The viability of freshly isolated thymocytes was always in excess of 95%. Incubations were conducted according to the protocol reported in section 2.1.9.

TBTO and MPS additions were made as described in section 3.2.2; the latter was used at a standard plate concentration of 10 μM. Details relating to the preparation of modulator stocks are shown in Table 4.2. Aqueous solutions were prepared with sterile medium or buffer and filtered through 0.22 μm filters prior to use. Modulators, or the appropriate vehicle controls, were added to cultures at the timepoints indicated in Table 4.2.

4.2.3 Experimental protocols

Samples of cell suspension were removed after 0, 1, 2, 4 and 6 h incubation (and at 24 h in some experiments) for determination of viability by trypan blue dye exclusion (section 2.2). Aliquots of approximately 10^7 cells were routinely taken after 6 h incubation in order to process these for morphological study (section 2.4.1 or 2.5). Samples were also obtained at the same timepoint for the quantitation of DNA fragmentation (section 2.6) and for neutral agarose gel DNA electrophoresis (section 2.8).

4.2.4 Statistical analysis

All results are presented as the mean (arithmetic) $\pm$ 1 SE unless otherwise stated. The effect of modulator treatment on parameters was compared using a two-tailed t-test, accepting a statistical significance for p of less than 0.05. This was preceded by analysis of data distribution and homogeneity of variance as appropriate.

TABLE 4.2 Identification of modulators, handling procedures and addition regimens.

Modulator	Source[1]	Purity (%)	Stock preparation[2]	Vehicle control	Addition timepoint[3]
BAPTA-AM	Novabiochem	>90	DMSO ❶	DMSO 0.15-0.3%	- 20 min
Quin-2 AM	Novabiochem	>98	DMSO ❶	DMSO 0.3%	- 15 min
EGTA	Sigma	97	Solubilised in 0.1M NaOH prior to dilution to 10 times required concentration in medium ❷	Medium	- 30 min
Zinc acetate dihydrate (Zn^{2+})	Aldrich	>99	Medium ❷	Medium	- 20 min
Aurintricarboxylic acid, trisodium salt (ATA)	Sigma	>90	Medium ❷	Medium	- 60 or + 90 min
H33258	Novabiochem	>98	Solubilised in 5mM Tris HCl/0.9% saline ❸	Tris/saline	- 20 min
Distamycin A hydrochloride	Sigma	95	Medium ❷	Medium	- 45 min
12-O-tetradecanoylphorbol-13-acetate (TPA)	Fluka	>98	Dissolved in acetone at 200 μg ml^{-1} ❹; diluted to 4 μg ml^{-1} in medium	Medium	0 min
12,13 phorbol dibutyrate (PDBu)	Fluka	>98	Dissolved in acetone at 5 mg ml^{-1} ❹; diluted to 800 times required concentration in acetone	Acetone 0.125%	0 min
Cyclosporin A (CsA)	Sandoz	>90	Solubilised at 2 mg ml^{-1} in ethanol prior to dilution to 100 times required concentration in medium ❷	Medium	0 min
Calmidazolium	Novobiochem	>99	DMSO at 300 times the required concentration ❶	DMSO 0.3%	- 10 or - 30 min

Footnotes:

[1] Novabiochem (Nottingham, England); Sigma (Poole, England); Aldrich (Gillingham, England); Sandoz (Basle, Switzerland); Fluka (Glossop, England)

[2] ❶ Prepared in anhydrous DMSO and stored frozen at -20° until required.
❷ Freshly prepared for each experiment.
❸ Stored frozen at -20° until required.
❹ Stored desiccated at -20° until required.

[3] Time of introduction to cultures before (-) or after (+) test agent addition.

4.3 RESULTS

When considering the effects of various modulators on TBT-activated apoptosis, for convenience they have been grouped on their supposed mode of action established to date in the literature, or on a generic basis. This organisational grouping has been introduced primarily for ease of presentation, and does not necessarily infer mechanistic identity. During all experiments, the concentrations of the solvent vehicles used for the introduction of modulators to cultures had no overt effect on system parameters either alone or in the presence of the test agent vehicles. Some representative data in respect of cell viability and DNA fragmentation levels have previously been given in Table 3.1.

4.3.1 Action of intracellular Ca^{2+}-selective chelators on thymocyte apoptosis

Buffering of $[Ca^{2+}]_i$ was achieved by loading cells with either BAPTA-AM or Quin-2 AM prior to test agent addition. Thymocytes exposed to 1 μM TBTO or 10 μM MPS alone, exhibited a marked increase in the extent of DNA fragmentation detected after 6 h. In contrast, pretreatment with 40 μM BAPTA-AM reduced fragmentation in parallel TBTO-exposed cultures to control values (Fig. 4.3a). In the case of MPS, a similar statistically significant, but slightly less pronounced inhibitory effect, was produced by BAPTA-AM (Fig. 4.3a). BAPTA-AM pretreatment abolished the appearance of the multimeric 180-200 bp DNA cleavage pattern that normally resulted from incubation with 1 μM TBTO (Fig. 4.4). Cell preparations obtained after 6 h incubation with 1 μM TBTO or 10 μM MPS had statistically significant reductions in the proportion of cells exhibiting chromatin condensation when BAPTA-AM was present (Fig. 4.3b). This chelator also protected against latent thymocyte viability loss stimulated by TBTO (1 μM) or MPS (Fig. 4.3c), since mean viability values after 24 h exposure to 1 μM TBTO or 10 μM MPS were 65% or 50% respectively, whilst in the presence of the BAPTA-AM, 81% and 80% of cells excluded trypan blue dye.

Though slightly higher levels of DNA fragmentation occurred with 5 μM TBTO in this series of experiments than previously observed (see chapter 3), the extent of DNA degradation was essentially unaffected by BAPTA-AM pretreatment (Fig. 4.3a). Similarly, the very low proportion of apoptotic cells apparent was not influenced by BAPTA-AM (Fig. 4.3b), and furthermore, the severe viability loss evident at this TBTO concentration (Fig. 4.3c) was not prevented.

Minimal to moderate cell blebbing was observed in some experiments after the addition of BAPTA-AM, although this effect was transient and gradually receded within 1-2 h. At the standardised BAPTA-AM concentration of 40 μM, a marginal effect on control thymocyte viability was apparent from 6 to 24 h after the commencement of incubations. In quantitative terms, the maximum decrement in trypan blue exclusion observed for BAPTA-AM treated controls relative to cells treated with DMSO alone was only in the order of 5%

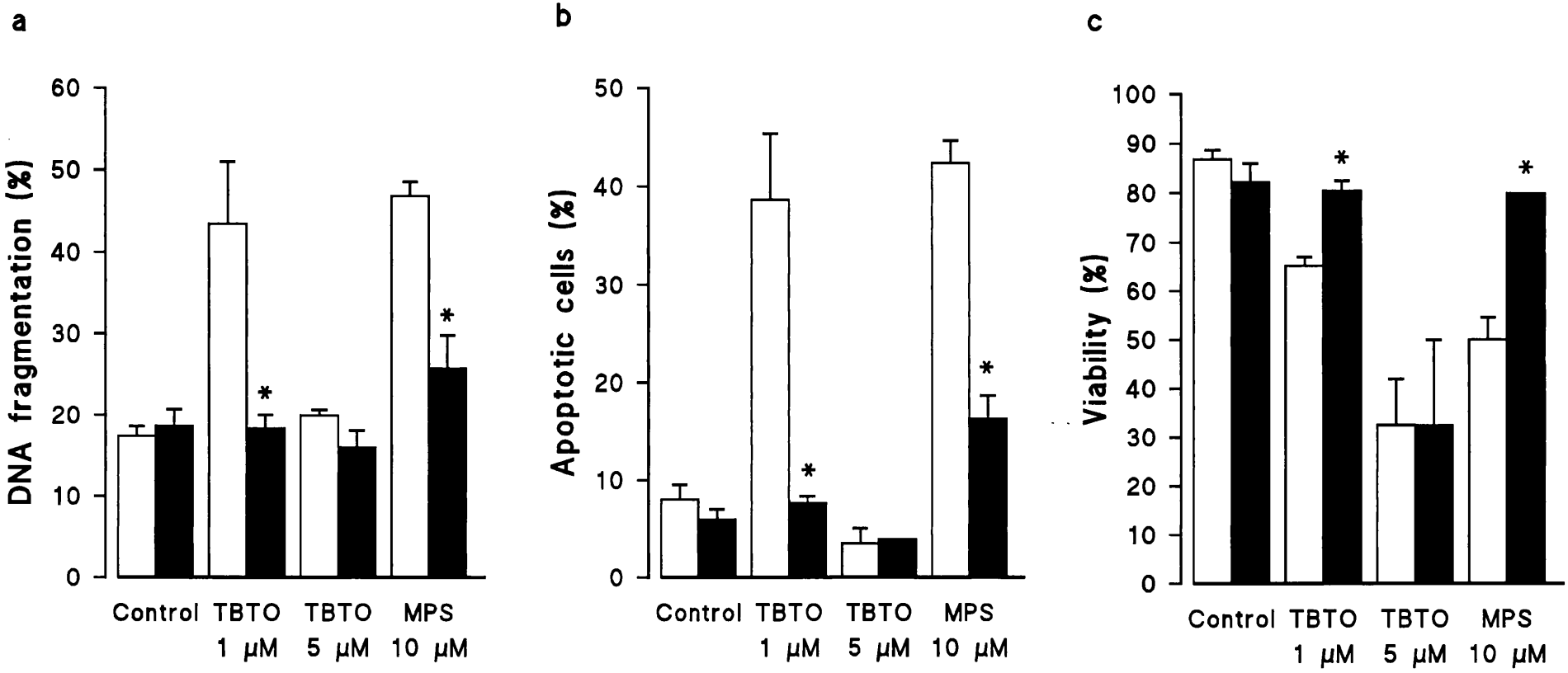

FIGURE 4.3 Effect of BAPTA-AM on a) DNA fragmentation, b) chromatin condensation and c) viability after exposure to TBTO or MPS. Cells were exposed to the stated concentrations of TBTO or MPS following preincubation without (*open bars*) or with 40 μM BAPTA-AM (*solid bars*). Results are the means ± SE of at least three separate experiments. *Significantly different from result in the absence of BAPTA-AM, $p < 0.05$. **a** DNA fragmentation determined after 6 h (section 2.6). **b** Proportion of thymocytes exhibiting evidence of chromatin condensation (section 2.4.1) after 6 h. **c** cell viability estimated (section 2.2) after 24 h except in the case of 5 μM TBTO when this was performed after 6 h.

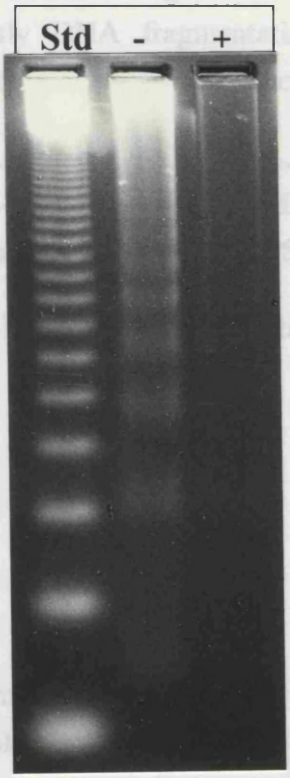

FIGURE 4.4 Effect of BAPTA-AM on TBTO-mediated internucleosomal DNA cleavage.

Thymocytes were preincubated in the absence (-) or presence (+) of 40 μM BAPTA-AM before exposure to 1 μM TBTO for 6 h. Cellular DNA was subsequently isolated from matched aliquots of cells and subjected to agarose gel electrophoresis as detailed in section 2.8. Std; DNA 123 bp multimer molecular weight calibration standard. Results are from one experiment typical of two replicates.

(Fig. 4.3c). Reduction of the BAPTA-AM concentration to 20 μM resulted in a disproportionate loss of protection from apoptotic cell killing by TBTO and MPS.

Preincubation with Quin-2 AM at concentrations up to 80 μM was less effective than 40 μM BAPTA-AM in inhibiting either TBTO or MPS-stimulated apoptosis. The maximal protective effect noted after this pretreatment regimen was apparent 5 h after the test agent additions (Table 4.3); subsequently DNA fragmentation values in modulator-treated preparations began to increase. Higher Quin-2 AM concentrations adversely affected control cell viability.

TABLE 4.3 Effect of Quin-2 AM on DNA fragmentation and chromatin condensation following incubation with TBTO or MPS.

Addition	Quin-2 AM (μM)	DNA fragmentation (%)[1]	Chromatin condensation (%)[2]
Control	0	16.7	5
	80	20.4	8
TBTO 1 μM	0	29.8	23
	80	21.6	8
MPS 10 μM	0	40.3	37
	80	24.3	14

Following Quin-2 AM pretreatment, determinations were performed 5 h after test agent addition according to the methodologies described in sections 2.6(1) or 2.4.1(2). Results shown are from one experiment that was typical of two replicates.

4.3.2 Effect of depletion of extracellular Ca^{2+} using EGTA

In order to assess the effect of chelation of Ca^{2+} present in the incubation medium on apoptosis stimulated by TBTO or MPS, studies were performed using EGTA. Initial studies employed an EGTA concentration previously reported to be effective in inhibiting thymocyte apoptosis (McConkey et al., 1989c; Aw et al., 1990) in media with Ca^{2+} concentrations calculated to be similar or rather higher than the incubation medium used here. Pretreatment of cells for 30 minutes with 8 mM EGTA partially inhibited DNA fragmentation resulting from a subsequent 6 h exposure to 10 μM MPS, but was without effect in TBTO-treated cultures (Table 4.4). However, it should be noted that 8 mM EGTA caused an early reduction in control viability values which continued to decline up to the 6 h timepoint, and also appeared to have a stimulatory effect on DNA fragmentation in these cultures (Table 4.4). With due allowance for dose-response, broadly similar results were obtained when the EGTA concentration was reduced to 4 mM (Table 4.4).

4.3.3 Effect of Zn^{2+} on thymocyte apoptosis caused by TBTO or MPS

Since exogenous Zn^{2+} had been shown to very effective in abrogating internucleosomal DNA cleavage and subsequent apoptotic cell death in systems including the rodent

TABLE 4.4 Effect of EGTA on DNA fragmentation and viability following incubation with TBTO or MPS.

Addition	EGTA (mM)	DNA fragmentation (%)[1]	Viability (%)[2]
Control	0	15.8	98
	4	26.0	94
	8	26.9	86
TBTO 1 μM	0	37.8	92
	4	39.6	90
	8	40.4	84
MPS 10 μM	0	50.3	97
	4	40.1	92
	8	31.2	94

Following EGTA pretreatment, estimations were performed 6 h after test agent addition according to the methodologies described in sections 2.6(1) or 2.2(2). Results shown are mean values from two separate replicates.

thymocyte model (Cohen and Duke, 1984; Sellins and Cohen, 1987), its effect on TBTO-mediated apoptosis was investigated. DNA fragmentation resulting from exposure to MPS, or to 1 μM TBTO was markedly inhibited by the presence of 0.5 or 1 mM Zn^{2+} (Fig. 4.5a), with the highest zinc concentration even causing a statistically significant reduction in spontaneous control culture DNA fragmentation (Fig. 4.5a). It was found that internucleosomal DNA cleavage was virtually abolished by 1 mM Zn^{2+} (Fig. 4.5b). Zn^{2+} addition also caused concurrent reductions in the number of cells exhibiting overt chromatin condensation (and the proportion of apoptotic bodies) arising after apoptotic MPS or TBTO treatments (Fig. 4.6). Delayed viability loss (assessed after 24 h) due to TBTO or MPS was antagonised by Zn^{2+} (Fig. 4.6) to a statistically significant degree. In short-term experiments of up to 8 h duration, the presence of up to 1 mM zinc did not affect the viability of control cells, but longer incubations did produce minor cytotoxicity (Fig. 4.6). It was notable that up to 1 mM Zn^{2+} had no protective effect against necrotic cell killing arising from exposure to 5 μM TBTO (results not shown).

Though the incidence of chromatin condensation in cells protected by zinc from undergoing apoptosis was low, their nuclear morphologies at the light microscope level did not appear comparable to control thymocytes (Fig. 4.6). Therefore ultrastructural studies were performed to further examine cytopathological changes. The majority of TBTO-injured cells showed classical apoptotic nuclear and cytoplasmic compartment alterations (Fig. 4.7a). Zn^{2+}-treated cells did not undergo volume reduction, marked chromatin condensation, nuclear fragmentation, or the formation of significant numbers of apoptotic bodies (Fig. 4.7b and c), but most did not exhibit ultrastructural features typical of normal thymocytes. Abnormalities included the development of electron dense cytoplasm

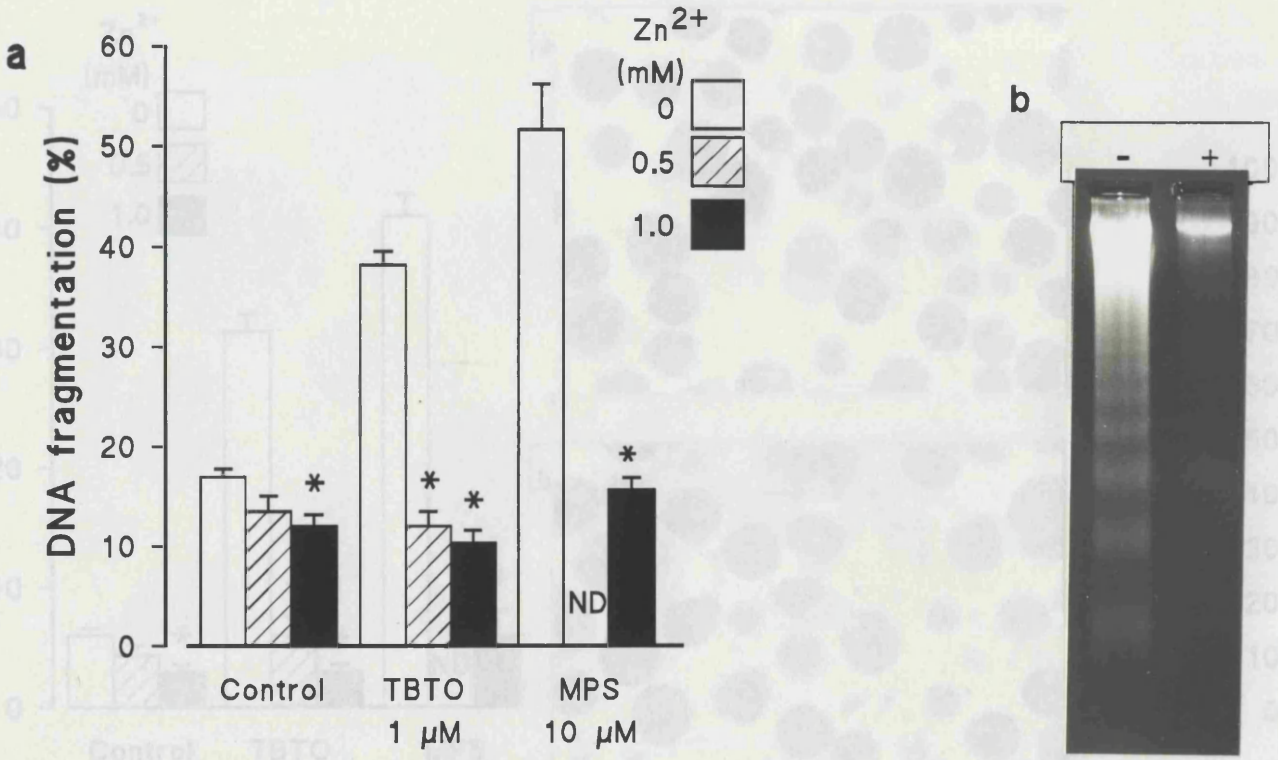

FIGURE 4.5 Effect of Zn^{2+} on TBTO-mediated DNA degradation.

a Cells were pretreated with the stated concentrations of Zn^{2+} prior to incubation with TBTO or MPS for 6 h. DNA fragmentation was determined according to the methodology described in section 2.6. Results are the means ± SE of at least three separate experiments. *Significantly different from result in the absence of Zn^{2+}, $p < 0.05$. ND; not determined. b Cells were preincubated in the absence (-) or presence (+) of 1 mM Zn^{2+} before exposure to 1 μM TBTO for 6 h. Cellular DNA was subsequently isolated and subjected to agarose gel electrophoresis as detailed in section 2.8. Results are from one experiment typical of two replicates.

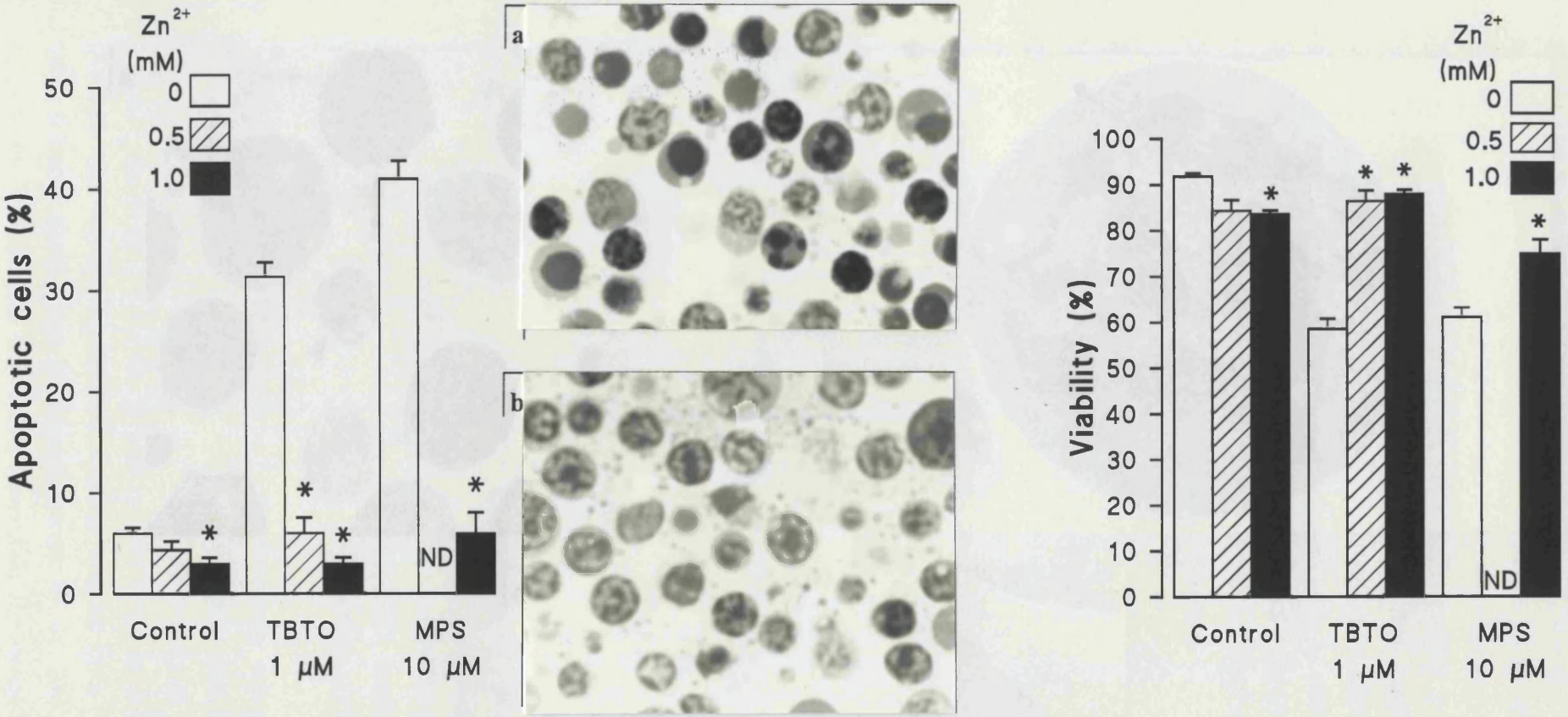

FIGURE 4.6 Effect of Zn^{2+} on TBTO-mediated apoptosis

Cells were pretreated with the stated concentrations of Zn^{2+} prior to incubation in the absence or presence of TBTO or MPS. Left panel: proportion of thymocytes exhibiting chromatin condensation at 6 h (method described in section 2.4.1). Results are the means ± SE of three separate experiments. Mid-panel: representative appearance of cells incubated **a** without, or **b** with 0.5 mM Zn^{2+}, prior to treatment with 1 μM TBTO for 6 h. Toluidine blue stained resin sections were prepared as described in section 2.4.1 (original magnification: x 1200). Right panel: Proportion of viable cells estimated by trypan blue exclusion at 24 h (section 2.2). Results are the means ± SE from at least three separate experiments. *Significantly different from result in the absence of Zn^{2+}, $p < 0.05$. ND; not determined.

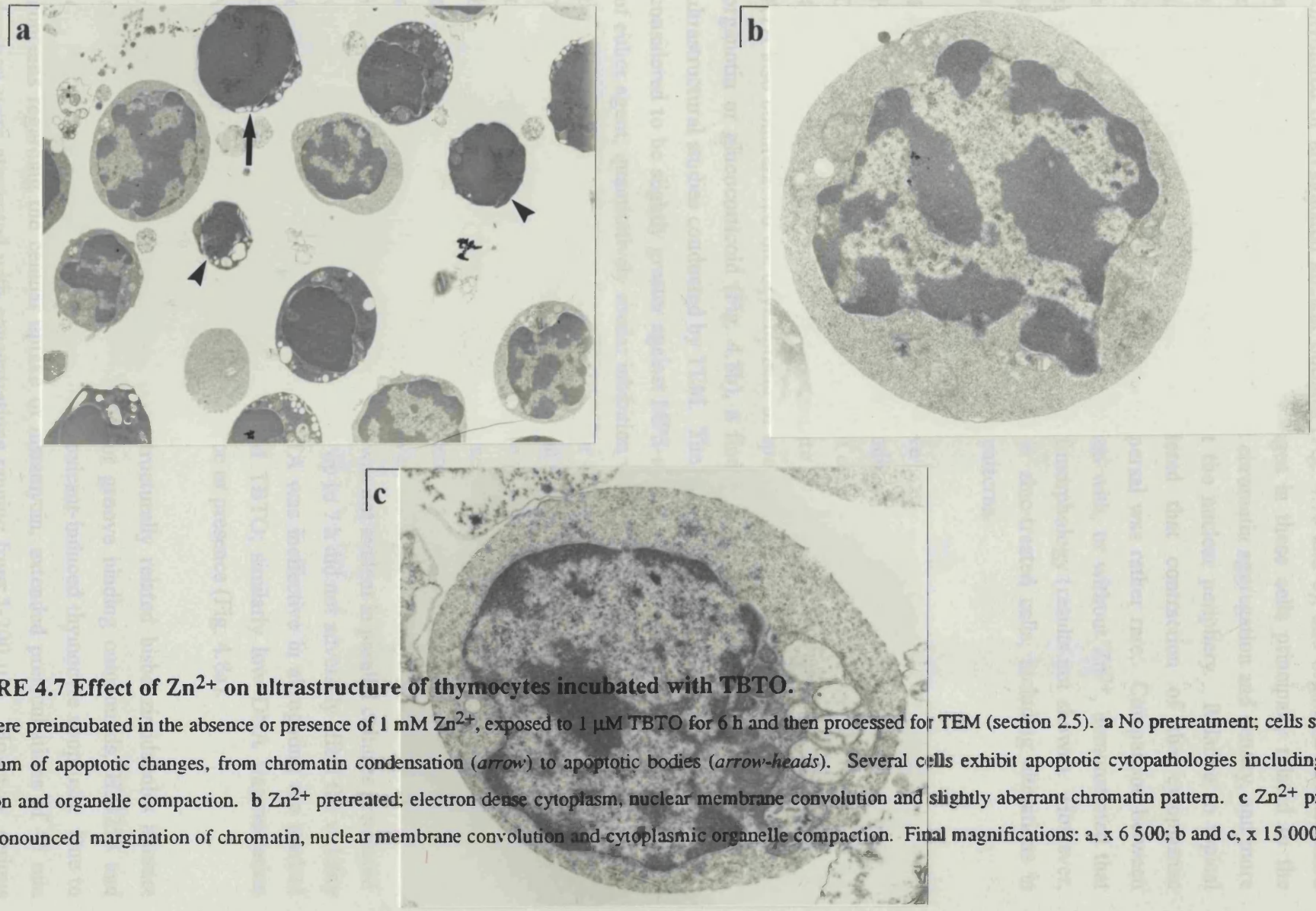

FIGURE 4.7 Effect of Zn^{2+} on ultrastructure of thymocytes incubated with TBTO.

Cells were preincubated in the absence or presence of 1 mM Zn^{2+}, exposed to 1 µM TBTO for 6 h and then processed for TEM (section 2.5). **a** No pretreatment; cells showing a continuum of apoptotic changes, from chromatin condensation (*arrow*) to apoptotic bodies (*arrow-heads*). Several cells exhibit apoptotic cytopathologies including volume reduction and organelle compaction. **b** Zn^{2+} pretreated; electron dense cytoplasm, nuclear membrane convolution and slightly aberrant chromatin pattern. **c** Zn^{2+} pretreated; more pronounced margination of chromatin, nuclear membrane convolution and cytoplasmic organelle compaction. Final magnifications: a, x 6 500; b and c, x 15 000.

(Fig. 4.7b); varying degrees of endoplasmic reticulum dilatation (Fig. 4.7b and c); convoluted or invaginated nuclear outlines (Fig. 4.7b and c); and organelle redistribution and compaction (Fig. 4.7c). Nuclear changes in these cells principally related to the expansion of euchromatin domains, increased chromatin aggregation and density, and more pronounced abutment of heterochromatin at the nuclear periphery. Relative to typical apoptotic thymocytes, it was not considered that contraction of the cytoplasmic compartment was evident, and nucleolar dispersal was rather rare. Comparison between control preparations made after 6 h incubation with, or without Zn^{2+}, demonstrated that zinc itself did not cause gross perturbation of morphology (results not shown). However, some subtle nuclear changes were evident in zinc-treated cells, including alterations in normal euchromatin/heterochromatin density patterns.

4.3.4 Action of ATA and DNA minor groove binding agents

Pretreatment of thymocytes with 0.5 mM sodium aurintricarboxylate (ATA) antagonised DNA fragmentation stimulated by exposure of cells to 1 μM TBTO or to 10 μM MPS (Fig. 4.8a), but this inhibitory effect was incomplete and did not achieve statistical significance. ATA also counteracted the development of apoptotic morphologies following exposure to organotin or glucocorticoid (Fig. 4.8b), a finding that was confirmed by supplementary ultrastructural studies conducted by TEM. The degree of protection afforded by ATA was considered to be slightly greater against MPS-stimulated apoptosis. However, in the case of either agent, quantitatively similar inhibition was achieved whether ATA was included in the culture medium 1 h before, or 1.5 h after the addition of the test agents (Table 4.5). There was a clear dose-response relationship in the protective effect of ATA, e.g. a reduced concentration of 100 μM resulted in negligible protection from DNA fragmentation caused by exposure to either TBTO or MPS. Since these experiments were designed around short-term incubations, no definitive statement can be made on ATA protection from delayed cell killing by TBTO or MPS. However, the slight viability reduction seen after 6 h incubation with 1 μM TBTO or 10 μM MPS was not evident in parallel cultures pretreated with ATA. Incubation with 0.5 mM ATA for up to 7 h did not adversely affect the viability of control cultures (results not shown). ATA was ineffective in abrogating the marked cytotoxicity produced by exposure to 5 μM TBTO; similarly low DNA fragmentation values were apparent irrespective of its absence or presence (Fig. 4.8a).

As discussed in the introduction, several structurally related bisbenzimidazoles interact strongly with DNA; the effect of two minor groove binding compounds, H33258 and distamycin, was examined in the context of toxicant-induced thymocyte apoptosis. Due to concerns regarding the cellular uptake of distamycin, extended preincubations of 45 min duration were attempted with concentrations ranging from 5-200 μM. However, serious cell clumping arose from distamycin levels of 20 μM upwards, and fluorescence microscopy revealed that only barely detectable distamycin-DNA originated fluorescence

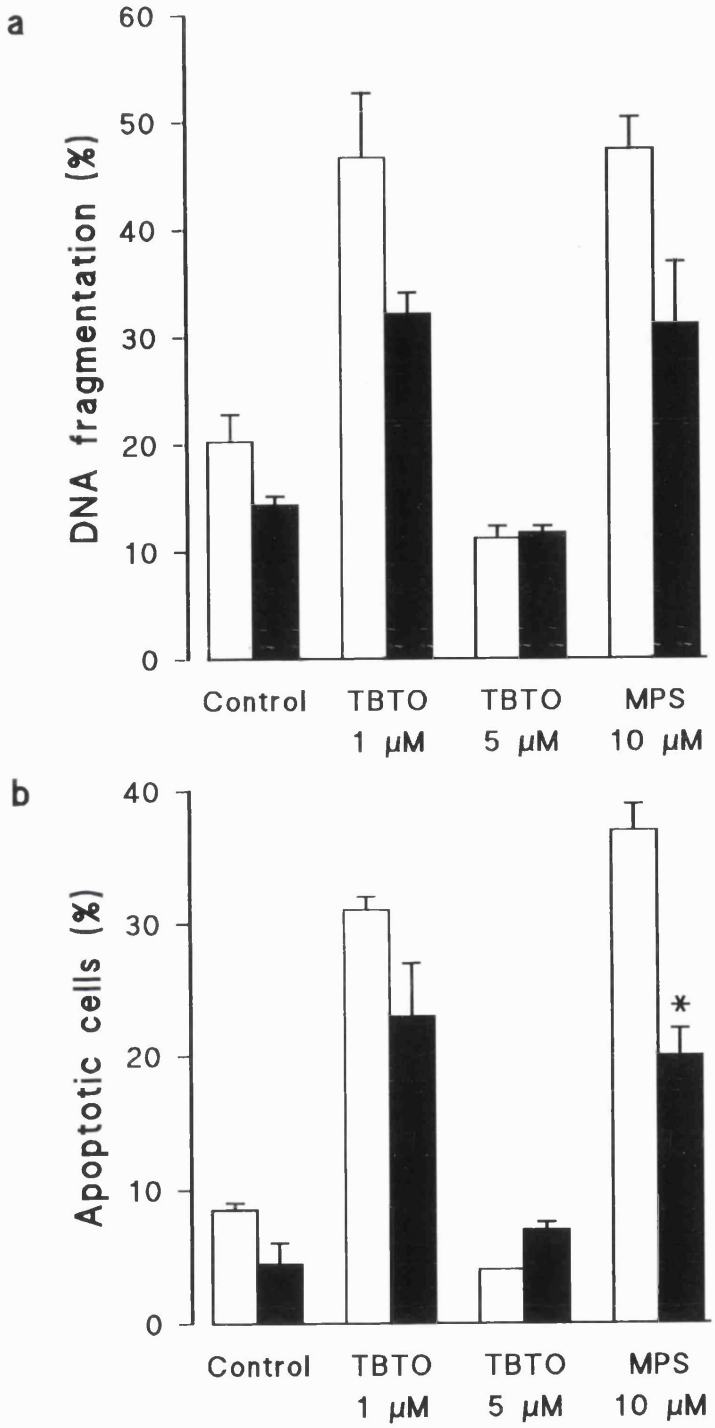

FIGURE 4.8 Effect of ATA on a) DNA fragmentation or b) chromatin condensation after exposure to TBTO or MPS.

Cells were exposed to the stated concentrations of TBTO or MPS following preincubation without (*open bars*) or with 0.5 mM ATA (*solid bars*) for 1 h. Determinations were performed after 6 h incubation according to the methodologies described in section 2.6 or 2.4.1 respectively. Results are the means ± SE from three separate experiments. *Significantly different from result in the absence of ATA, $p < 0.05$.

TABLE 4.5 Effect of the timepoint of ATA addition on the inhibition of DNA fragmentation stimulated by TBTO or MPS.

	Degree of inhibition		
ATA addition timepoint	Control	TBTO 1 μM	MPS 10 μM
- 1 h	0.71 ± 0.08	0.69 ± 0.09	0.67 ± 0.14
+ 1.5 h	0.95 ± 0.02	0.76 ± 0.06	0.63 ± 0.10

ATA was added at the stated times before (-) or after (+) exposure of cells to TBTO or MPS. DNA fragmentation was determined after 6 h incubation with the test agents (section 2.6). Results (means ± SE; n=3) are expressed in terms of the fractional DNA fragmentation value relative to that obtained for the test agent in the absence of ATA.

had resulted even from loading concentrations of 100-200 μM. Therefore, further experiments with this modulator were not attempted. In contrast, DNA-fluorophore studies established that satisfactory cellular uptake was achieved with H33258 at extracellular concentrations of 5 to 200 μM (higher levels caused cell agglutination). Preliminary cytotoxicity evaluations indicated that 50 μM H33258 was well tolerated for up to 24 h, though some viability loss occurred at 100 μM.

H33258 (50 μM) reduced the DNA fragmentation detectable at the 6 h timepoint in cells exposed to apoptotic concentrations of TBTO or MPS to 67% or 80%, respectively, of the mean values found in the absence of this modulator (Table 4.6). This was accompanied by

TABLE 4.6 Effect of H33258 on DNA fragmentation and viability following incubation with TBTO or MPS.

Addition	H33258 (μM)	DNA fragmentation (%)[1]	Viability (%)[2]
Control	0	17.5 ± 0.9	90 ± 1
	50	16.2 ± 2.1	92 ± 1
TBTO 1 μM	0	44.9 ± 5.7	62 ± 2
	50	30.1 ± 2.5*	86 ± 1*
MPS 10 μM	0	46.3 ± 0.8	50 ± 3
	50	37.1 ± 1.7*	73 ± 6*

Cells were pretreated with H33258 and incubated in the presence of the indicated concentrations of the test agents. Determinations were performed 6 h[(1)] or 24 h[(2)] respectively, after test agent addition according to the methodologies described in sections 2.6[(1)] or 2.2[(2)]. Results are the means ± SE from three separate experiments. *Significantly different from result in the absence of H33258, $p < 0.05$.

a consistent statistically significant degree of protection against delayed viability loss (Table 4.6). The H33258 concentration-response relationship for these two parameters was further explored in the case of TBTO-mediated apoptosis (Fig. 4.9). Maximal, though incomplete, inhibition of DNA fragmentation was achieved in the region of 10-20 μM H33258 (Fig. 4.9a), and the degree of internucleosomal DNA cleavage present in these cells was correspondingly lowered (Fig. 4.9b). This was paralleled by almost total abrogation of TBT-stimulated viability loss (Fig. 4.9a). Mean DNA fragmentation levels in the controls were unaffected by the presence of H33258. Statistically significant reductions were also caused by H33258 to the proportion of cells scored as apoptotic in morphological assessments of thymocytes exposed to 1 μM TBTO. At 20 or 50 μM H33258, the mean incidence of chromatin condensation was reduced to 25% and 17%, respectively, compared to a value of 41% for cells exposed for 6 h to TBTO alone.

4.3.5 Effects of phorbol esters on toxicant-induced apoptosis

The effect of the potent phorbol ester, TPA, and also a more hydrophilic compound, PDBu, were assessed on rat thymocyte apoptosis activated by TBT or MPS. The concentrations chosen were of the order previously reported to be effective in preventing apoptosis (McConkey et al., 1989d; Perotti et al., 1991). By the 6 h timepoint, TPA at or above 1 ng/10^6 cells ($\geqq$ 34 nM) approximately halved the spontaneous DNA degradation observed in control cells, whilst PDBu produced about a 25% reduction in this parameter (Fig. 4.10). However, both TPA (8-136 nM) or PDBu (100 nM) had little or no antagonistic effect on the incremental apoptosis resulting from MPS or TBTO (1 μM) exposure (Fig. 4.10).

4.3.6 Effects of other modulators on toxicant-induced apoptosis

The inclusion of CsA at 200 ng ml^{-1} caused only a very modest diminution effect on DNA fragmentation arising from TBTO or MPS treatment. The mean percentage alterations in this parameter produced by CsA in relation to parallel plates without the modulator were: control, 107%; 1 μM TBTO, 79%; 10 μM MPS, 90%.

Concurrent treatment with 10 μM calmidazolium and 1 μM TBTO caused an extremely marked loss of viability, such that after 6 h incubation typically only 5% of cells continued to exclude trypan blue dye (Fig. 4.11). Since the viability reduction directly attributable to TBTO was in the order of 10% relative to the control, and that calmidazolium alone reduced viability to 60-70% after 6 h, this suggests that the presence of both agents led to synergistic cytotoxicity. It was noted that in parallel cultures incubated with MPS in the presence of calmidazolium, the former apparently made no contribution to viability loss. An altered regimen, involving preincubation (for 30 minutes) with 1 μM calmidazolium was apparently non-toxic to thymocytes over a similar timescale. However, this treatment

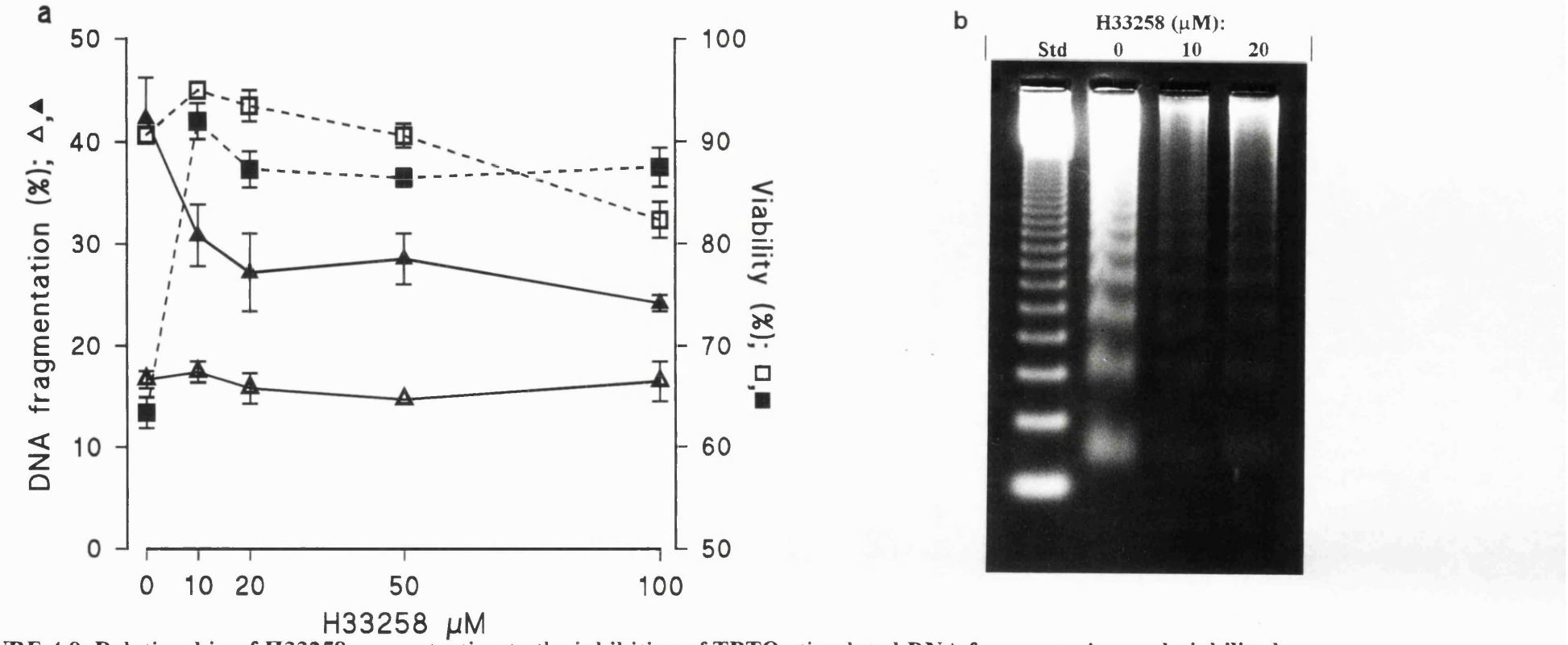

FIGURE 4.9 Relationship of H33258 concentration to the inhibition of TBTO-stimulated DNA fragmentation and viability loss.

a Cells were incubated in the absence (*open symbols*) or presence (*solid symbols*) of 1 μM TBTO following pretreatment with the indicated concentrations of H33258. DNA fragmentation (△,▲) and cell viability (□,■) were determined after 6 h and 24 h respectively as detailed in sections 2.2 and 2.6. Results are the means ± SE of at least three separate experiments. b Agarose gel electrophoresis (section 2.5) of DNA extracted from standardised aliquots of cells incubated with 1 μM TBTO for 6 h after pretreatment with the indicated concentrations of H33258. Std; DNA 123 bp molecular weight calibration standard. Results shown are from one experiment typical of two replicates.

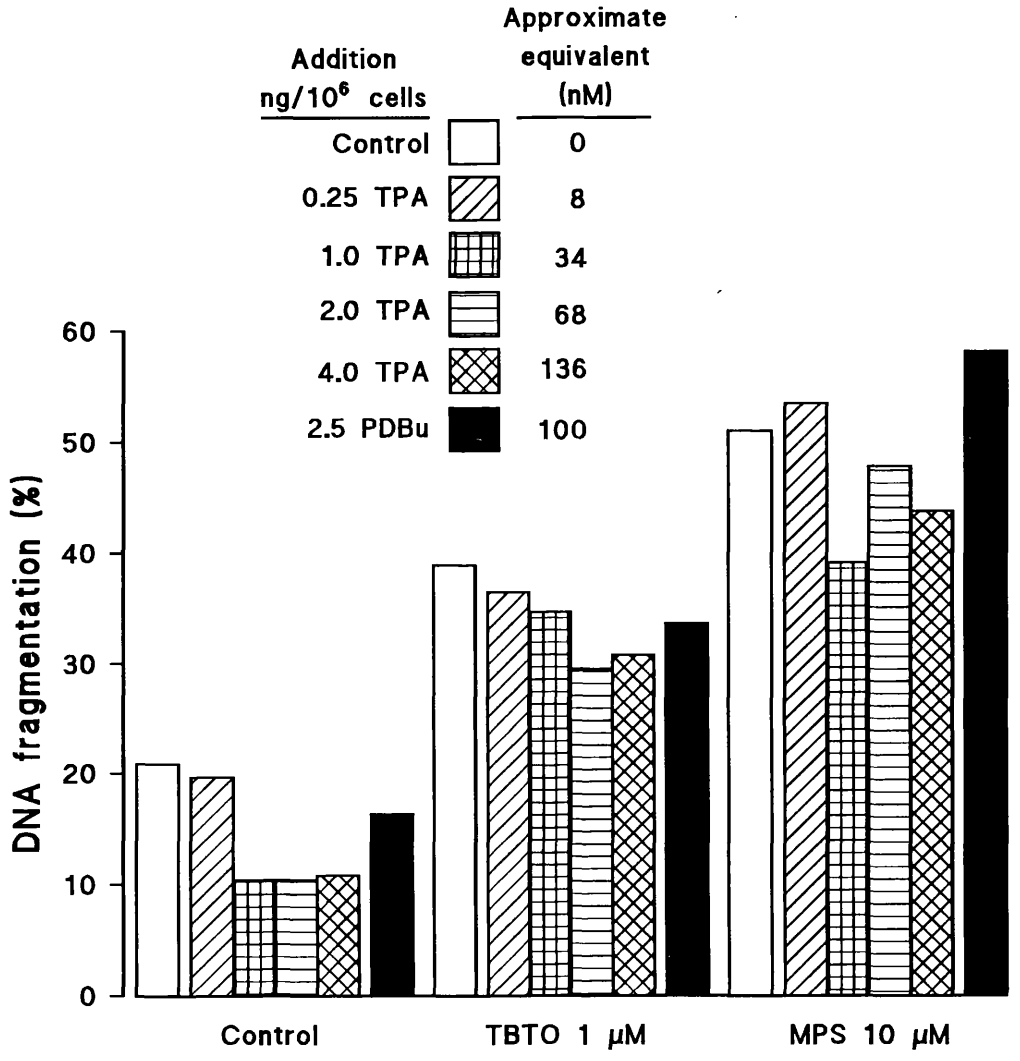

FIGURE 4.10 Effect of phorbol esters on DNA fragmentation caused by treatment with TBTO or MPS.

The stated additions of either TPA or PDBu were introduced into cultures immediately prior to incubation with TBTO or MPS for 6 h. DNA fragmentation was determined according to the methodology described in section 2.6. Results are the mean values from at least two experiments.

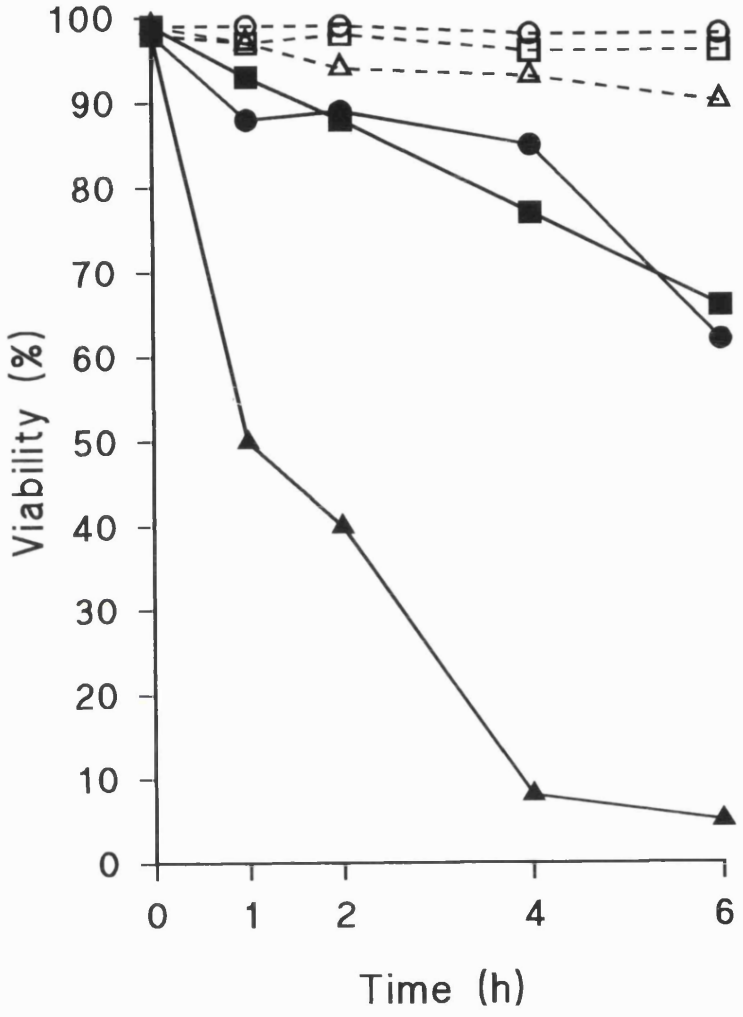

FIGURE 4.11 Effect of calmidazolium on cell viability after treatment with TBTO or MPS.

Cells were preincubated in the absence (*open symbols; dashed line*) or presence (*solid symbols; solid line*) of 10 μM calmidazolium prior to treatment with TBTO 1 μM (△,▲), MPS 10 μM (□,■) or vehicle control (○,●). Viability was assessed at intervals up to 6 h by trypan blue dye exclusion as described in section 2.2. Results are from one experiment that was typical of two replicates.

approximately doubled the extent of DNA fragmentation observed in the control, and had no inhibitory effect on this parameter in either MPS or TBTO-treated cells.

4.4 DISCUSSION

When considering the effect of various modulators in inhibiting apoptotic markers, and in particular the parameters of DNA fragmentation and internucleosomal cleavage, due account must be given to possible confounding effects of modulator cytotoxicity. For example, production of inadvertent necrotic cell killing can result in a false positive finding due simply to ablation of apoptosis rather than a specific inhibitory effect. Therefore adequate control viability and morphology assessments must always be conducted; this has been neglected in some previously published studies. In the following discussion, unless specific reference is made to modulator cytotoxicity, no overt effects were apparent.

As discussed in the introduction, a sustained increase in $[Ca^{2+}]_i$ is a trigger for thymocyte apoptosis caused by a number of stimuli including glucocorticoid hormones, cation ionophores, anti-CD3 antibodies, and ionising radiation. Since buffering of intracellular Ca^{2+} by membrane-permeant chelators, or extracellular depletion of Ca^{2+} by EGTA have been reported to abrogate this response (McConkey et al., 1988a; 1989b; 1989c), the effect of these modulators on TBT-mediated apoptosis was investigated. BAPTA-AM (40 μM) reduced both DNA fragmentation and the incidence of morphological markers of apoptosis in TBTO-exposed cells to control levels (Fig. 4.3a, b), and subsequently inhibited delayed viability loss (Fig. 4.3c). BAPTA-AM also abolished the internucleosomal DNA cleavage normally observed after treatment with apoptotic concentrations of TBTO (Fig. 4.4). BAPTA-AM had similar effects on MPS-activated apoptosis, which was in agreement with previous findings by other investigators (McConkey et al., 1989b; 1989c). BAPTA has previously been shown to antagonise apoptotic cell killing, but its effectiveness in preventing long-term viability loss assessed at the 24 h timepoint was unexpected. The related chelator, Quin-2 AM, had a qualitatively similar inhibitory profile in relation to DNA fragmentation and the incidence of apoptotic cells (Table 4.3), but was less effective; other publications indicate that there is gradual loss of Quin-2 from cells after 2-3 h (McConkey et al., 1988a; 1989b).

These findings suggest that TBT-activated apoptosis occurs as a result of a rise in $[Ca^{2+}]_i$. Though parallel measurements of intracellular Ca^{2+} were not conducted, the inhibitory action of BAPTA-AM and Quin-2 AM was considered to be due to Ca^{2+} buffering, for the following reasons. The $[Ca^{2+}]_i$ in unstimulated thymocytes reportedly ranges from 50 to 100 nM (Zhivotovsky et al., 1993; McConkey et al., 1988a; Aw et al., 1990), and equivalent additions of BAPTA or Quin-2 to those used here reduce this to about half the control level even in media containing more than double the calcium concentration of RPMI-1640. Under such circumstances both chelators have proven ability to prevent Ca^{2+}

stimulation of apoptosis (see above; Zhivotovsky et al., 1993; Ojcius et al., 1991; Perotti et al., 1990). Preliminary experiments, subsequently confirmed elsewhere (Aw et al., 1990), demonstrated that BAPTA or Quin-2 caused no alteration in the diphenylthiocarbazone binding characteristics of TBT, indicating that neither directly sequestered TBT. In addition, these chelators do not directly influence endonucleolytic DNA cleavage (McConkey et al., 1989b). While Ca^{2+} chelation is considered to their principal effect, this does not preclude the possibility of other actions, such as membrane stabilisation.

During the course of this work, Aw and colleagues (1990) published evidence that an increase in $[Ca^{2+}]_i$ is a primary event in TBTC-mediated apoptosis in vitro of thymocytes from Sprague Dawley rats. This conclusion was based on four key findings: (i) 5 μM TBT caused an early and sustained elevation in $[Ca^{2+}]_i$ to about 700 nM; (ii) this effect paralleled DNA fragmentation and preceded appreciable cell death; (iii) BAPTA-AM and Quin-2 AM protected against DNA degradation and were cytoprotective, whilst EGTA apparently prevented viability loss; (iv) extracellular ingress of Ca^{2+} was inhibited by the presence of Ni^{2+}, presumptively by blocking uptake through plasma membrane channels. This group later determined that the TBT-stimulated rise in Ca^{2+} was a composite of its mobilisation of intracellular Ca^{2+}, activation of a pathway for entry of extracellular Ca^{2+}, and inhibition of the plasma membrane Ca^{2+}-ATPase (Chow et al., 1992). It was inferred that TBT-induced ingress of Ca^{2+} was effected by a capacitative Ca^{2+}-mediated mechanism. Since TBTC is structurally homologous with TBTO, their findings are applicable to my work. The concentration of 1 μM TBTO used here equates to that found by Chow et al. to produce half-maximal $[Ca^{2+}]_i$ elevation, and approximates to their established IC_{50} for the plasmalemmal Ca^{2+} translocase. For reasons that are unclear, but could involve methodological differences between our studies, equimolar concentrations of TBTO are more effective than TBTC in depressing thymocyte ATP levels (section 5.3.2; Chow et al., 1992). As maintenance of cellular Ca^{2+} homeostasis is tightly coupled to ATP levels, TBTO may therefore be more potent than TBTC in causing $[Ca^{2+}]_i$ elevation.

In my hands, EGTA partially inhibited DNA fragmentation caused by MPS, though it had no effect on TBTO apoptosis (Table 4.4). Even in respect of glucocorticoid, the magnitude of the effect was considerably less than has been cited (McConkey et al., 1989b; 1989c; Perotti et al., 1991). In addition, EGTA at concentrations reported to be effective produced viability loss and increased DNA degradation in the controls (Table 4.4), further complicating interpretation of the results. I was unable to confirm the findings of Aw et al. (1990) on EGTA protection from TBT-induced viability loss. Intuitively, EGTA would not be expected to be very effective against TBT apoptosis, since Chow et al. (1992) showed that in medium calcium-depleted by EGTA, the $[Ca^{2+}]_i$ still rose 4-fold after TBT treatment due to intracellular mobilisation. Such increases can still be significant in initiating gradual DNA fragmentation, e.g. in the case of low level glucocorticoid exposure.

Some studies have found that EGTA had no protective effect on T lymphocyte apoptosis (e.g. Kizaki et al., 1988; Deeg and Bazar, 1991). In conclusion, EGTA depletion of extracellular Ca^{2+} did not give unequivocal protection from glucocorticoid or TBT-initiated apoptosis, which was in apparent contradiction to results published by other workers. Furthermore, its use as a modulator needs re-examination, e.g. the divalent cation selectivity of EGTA may be problematic: an apparent stability constant series at pH 7.5 is calculated to be; Ca^{2+} 7.7, Mg^{2+} 1.7, Zn^{2+} 11.2; thus it may deplete exogenous Zn^{2+}.

When considering Ca^{2+}-dependency in apoptosis, a clear distinction must be made between its involvement in signal transduction processes, and the obligate requirement of the endonuclease involved in endstage internucleosomal cleavage for this cation (the latter is addressed later in this section). It is not clear to what extent the $[Ca^{2+}]_i$ elevation caused by TBT actuates signalling processes, as opposed to increasing intranuclear Ca^{2+} and thus directly stimulating endonuclease activity. The relative contribution of the components of the TBT-stimulated Ca^{2+} rise is also unclear; TBT has similar inhibitory effects as tert-butylbenzohydroquinone and thapsigargin (Chow et al., 1992), so inhibition of the endoplasmic reticular Ca^{2+}-ATPase may be pivotal. The biphasic nature of its effects on extracellular Ca^{2+} ingress in other cells (Rice and Weeks, 1989) also requires more study.

These observations on TBT can be extended into consideration of the signal transduction mechanisms of toxicant-activated thymocyte apoptosis. The maximal increase in thymocyte $[Ca^{2+}]_i$ caused by 5 μM TBT is about 1200 nM (Chow et al., 1992), which is of the same order as that occurring after exposure to 10 μM MPS or 1 μM A23187 (McConkey et al., 1989a), i.e. approximately 800 or 1500 nM, respectively. Such treatments produce comparable levels of DNA fragmentation to CD3/TcR complex ligation, but the latter activation-induced cell death is caused by smaller $[Ca^{2+}]_i$ rises (McConkey et al., 1989c). This may indicate that multiple Ca^{2+}-linked signalling pathways to apoptosis exist in thymocytes. Elevation of intracellular Ca^{2+} levels by TBT is unaffected by macromolecular synthesis inhibitors (Aw et al., 1990), therefore it differs from the case of glucocorticoid hormones where a porter protein is thought to be expressed. This postulate has been integrated into a general schema for the involvement of Ca^{2+} fluxes in thymocyte apoptosis, whereby TBT circumvents the need for synthesis of cation transport systems (McConkey et al., 1992). However, a resolution to the paradox of the protein synthesis dependency of apoptosis caused by the cation ionophore A23187 (Wyllie et al., 1984a) remains outstanding. A capacitative receptor-gated calcium channel exists in T cells (Ng et al., 1988), and the observations relating to TBT, suggest that it may have a role in apoptosis.

Calmodulin antagonists, e.g. calmidazolium and flunarizine, apparently block DNA fragmentation caused by various apoptotic stimuli in several cell types including thymocytes (Perotti et al., 1990; 1991; Zheng et al., 1991). Calmidazolium at 10 μM in rat thymocyte

cultures was stated to be as effective as calcium chelators in preventing glucocorticoid-induced DNA degradation (McConkey et al., 1989b). Calmodulin does not directly activate the constitutive Ca^{2+}/Mg^{2+}-dependent endonuclease of thymocyte nuclei (Compton, 1991), but it has been suggested that a nuclear calmodulin-dependent Ca^{2+} transport system may be involved in apoptosis (Jones et al., 1989; Nicotera et al., 1989). Incubation of cells with 10 μM calmidazolium alone caused appreciable viability loss within a short period (Fig. 4.11). Severe cell blebbing, and the rapidity of this killing suggested that necrosis had occurred. It was necessary to reduce the calmidazolium concentration to 1-2 μM to prevent cytotoxicity in controls; under these conditions, no protection was afforded against MPS or TBT-stimulated apoptosis. In the absence of adequately reported control data, the possibility exists that in the previous studies referred to above, supervening calmidazolium cytotoxicity precluded the development of DNA fragmentation and apoptosis. The marked potentiation of cytolethality observed on addition of TBT to calmidazolium pretreated cells (Fig. 4.11) is of note. Triorganotins are potent inhibitors of calmodulin-linked biochemical processes both in vitro and in vivo (Yallapragada et al., 1990; 1991). The IC_{50} for TBT to calmodulin-stimulated synaptic membrane Ca^{2+}-ATPase, at 50 nM, was more than tenfold lower than the value for the basal translocase, and calmodulin-dependent phosphodiesterase was similarly inhibited by TBT (Yallapragada et al., 1990). As TBT inhibits Ca^{2+} translocases at such low concentrations, its synergistic toxicity with calmidazolium could be due to gross disturbance of calcium ion homeostasis.

CsA can prevent DNA fragmentation and delayed cell killing in thymocytes, mature T cells, or T cell hybridomas (Shi et al., 1989; 1990; Groux et al., 1992; Fruman et al., 1992). These studies shared the common feature that apoptosis was initiated by TcR or CD3 complex ligation, i.e. was activation-induced cell death, presumably with signalling via coupled and specific signal transduction pathways. Equivalent CsA regimens had little inhibitory effect on DNA fragmentation caused by TBT or MPS treatment (section 4.3.6). This finding is in accord with the lack of protection afforded by CsA (even in the higher concentration range of 0.1-10 μg ml^{-1}), against γ-irradiation apoptosis in thymocytes (Sellins and Cohen, 1987). Unlike many apoptosis modulators, CsA is a relatively specific agent which interferes with the Ca^{2+}-calcineurin-linked pathway regulating transcription factors such as NF-AT and NF-IL2A (Crabtree, 1989; Clipstone and Crabtree, 1992), thereby blocking T cell programmed cell death. My findings are preliminary, e.g. only one treatment level was used, but it is concluded that thymocyte apoptosis provoked by pathological stimuli such as glucocorticoids, TBT or irradiation may differ from activation induced apoptosis in respect of the initiating signal transduction events involved.

Phorbol esters can abrogate apoptosis in some systems (reviewed by Waring, 1991; Tomei, 1991), but as discussed in the introduction, their modulation of T lymphocyte apoptosis represents an area in which confusion and contradiction abounds. Prototypical phorbol

esters like TPA or PDBu have been claimed to inhibit thymocyte apoptosis triggered by glucocorticoids, cation ionophores, CD3/TcR ligation or cAMP analogues in cells of rat (McConkey et al., 1989d; McConkey et al., 1990a; Perotti et al., 1991), or human origin (McConkey et al., 1989c; McConkey et al., 1990e). In experiments reported here with glucocorticoid-treated rat thymocytes, it was not possible to replicate a substantive inhibition of DNA fragmentation. TPA or PDBu at concentrations previously reported to be effective had either no, or a marginal effect in cells exposed to either 10 μM MPS or 1 μM TBTO (Fig. 4.10). The reduction of spontaneous apoptosis in control cultures by 50-70% percent was considered to confirm that the phorbol ester treatments were biologically active. Also the results obtained with a series of TPA concentrations in the controls indicates progression from an ineffective level of 0.25 ng TPA/10^6 cells to saturation of the protective response at 1-4 ng/10^6 cells; hence dose-response bracketing was considered to be acceptable. The use of higher phorbol ester levels was not considered to be prudent due to the potential for non-specific effects. It could be argued that in the case of pathological agent-stimulated thymocyte apoptosis, longer incubations (e.g. 18 h) are required for efficacy. However, this would entail reversion of the high levels of DNA fragmentation, and therefore apoptosis, observed after 6 h, which is biologically implausible. Recent data from thymocytes (Migliorati et al., 1992) or T cell hybridomas (Iseki et al., 1991) shows in murine T cells, phorbol ester treatments can actually stimulate apoptosis, and that PKC activation enables signalling pathways for apoptotic killing. At best, phorbol esters may inhibit activation-induced death in human thymocytes, and based on my results, be very weakly protective toward rat cell apoptosis. Although compounds like H-7 have been described as PKC antagonists, and employed as such, they are quite non-specific and affect many protein kinases. Therefore over-reliance should not be placed on conclusions stemming from their use. On balance, there is reason to doubt the general applicability of hypotheses advancing an anti-apoptosis role for PKC-coupled processes in immature T cells (McConkey et al., 1990c; McConkey and Orrenius, 1991).

Investigation of the modulation of the effector mechanisms of TBT apoptosis was conducted using Zn^{2+} and ATA, two agents widely acknowledged as being capable of inhibiting apoptotic DNA degradation. It was also postulated that DNA minor groove ligands might also be inhibitory. Since this had not been investigated when the experimental phase of this work was conducted, the effect of two minor groove binders, H33258 and distamycin A, on thymocyte apoptosis caused by TBT or MPS was assessed.

As detailed in the introduction, non-necrotic cell death is inhibited in diverse systems by the addition of exogenous Zn^{2+} (Table 4.1; Waring et al., 1991), and therefore zinc sensitivity has often been viewed as a biochemical characteristic of apoptosis. Zn^{2+} inhibits terminal apoptotic processes even in circumstances where protective agents, such as cytokines or macromolecular synthesis inhibitors, are ineffective, e.g. in heat shock exposed thymocytes

(Migliorati et al., 1992). Based on experiments here, this cation is also effective against TBT-mediated thymocyte apoptosis. Zn^{2+} abolished internucleosomal DNA cleavage stimulated by 1μM TBTO (Fig. 4.5b), or MPS, and also prevented the concurrent elevation in DNA fragmentation (Fig. 4.5a) detectable by the differential centrifugation method used (see 2.6.1). Correlated with this, the increase in apoptotic cells (i.e. at the light microscopy level those exhibiting overt chromatin condensation or apoptotic body formation) normally observed after exposure to either TBT or glucocorticoid was also blocked by Zn^{2+} (Fig. 4.6). Zn^{2+} treatment also apparently conferred partial protection from delayed cell killing (Fig. 4.6). Although protracted incubation with Zn^{2+} alone adversely affected cell survival in the controls (Fig. 4.6), the cytotoxicity was delayed in onset (occurring after 6 h of incubation), gradual, and relatively minor in degree. Therefore it is considered highly unlikely that this influenced inhibition of early apoptotic markers (Fig. 4.5; Fig. 4.6), though it does complicate the interpretation of the viability results. It is notable that the presence of Zn^{2+} also abrogated apoptosis caused by exposure of thymocytes to the microtubular-disruptor nocodazole (see section 5.3.3).

Zn^{2+} abolished gross chromatin changes but some subtle nuclear abnormalities were evident by light microscopy which were further studied by TEM. Overt stigmata of apoptosis were absent in cells exposed to TBTO in the presence of Zn^{2+}, but a high proportion exhibited some cytoplasmic changes reminiscent of the early stages of apoptosis, including organelle redistribution and compaction, and endoplasmic reticulum dilatation (Fig. 4.7b, c). Slight margination of chromatin to the nuclear periphery was also considered to be a significant finding (Fig. 4.7c). Equivalent ultrastructural findings in thymocytes treated with glucocorticoid and Zn^{2+} have been described by Cohen and co-workers (1992), and a degree of chromatin margination was also evident in Zn^{2+}-exposed T blasts following gliotoxin exposure (Waring, 1990). It was noted by Cohen et al. that Zn^{2+} did not affect H33342 fluorochrome staining, cell volume reduction, and modal density increases linked with the induction of apoptosis. They concluded that Zn^{2+} prevented internucleosomal DNA cleavage, but did not halt some early apoptotic changes including initial DNA degradation, and suggested that the chromatin changes occurring in thymocyte apoptosis are caused by more than one effector enzyme. This group subsequently published confirmatory evidence for the existence of high order DNA degradation ($\geqq$700 kbp, 200-245 kbp and 30-50 kbp), preceding internucleosomal scission, during apoptosis which is unaffected by Zn^{2+}, is Mg^{2+}-dependent, but has no obligate requirement for Ca^{2+} (Brown et al., 1993; Sun and Cohen, 1994). Similar conclusions have been drawn from thymocyte apoptosis studies with other agents (Filipski et al., 1990; Walker et al., 1991), with the inference that this degradation sequence is governed by chromatin periodicity (see section 1.3.4). Zn^{2+} probably blocks final nuclear collapse in apoptotic cells; at least in thymocytes, an event directly linked to the activation status of a constitutive Ca^{2+}, Mg^{2+}-dependent endonuclease (Arends et al., 1990). In

other cell types, high order chromatin cleavage may itself be sufficient to elicit the nuclear morphological changes of apoptosis (Oberhammer et al., 1993b). In respect of my DNA fragmentation assay results (Fig. 4.5a), if Zn^{2+} does not prevent high order chromatin degradation, then this technique is incapable of detecting the production of such high molecular weight DNA cleavage products, i.e. supra-internucleosomal cleavage.

The notion of cytoprotection by Zn^{2+} has been challenged. Barbieri et al. (1992), confirmed that Zn^{2+} inhibited glucocorticoid-induced DNA fragmentation, but disputed its prevention of cell killing. This assertion was based on the absence of an effect by 5mM zinc sulphate on the percentage of cells excluding trypan blue after 24 h incubation, and the lack of cell proliferation after incubation for up to 7 days. However, their report omits suitable control data, and very significant cytotoxicity would be expected due to such a high concentration of Zn^{2+}. Cytolysis occurring after apoptosis can be unaffected by Zn^{2+} at levels which abrogate DNA fragmentation (Zheng et al., 1991; Zychlinsky et al., 1991), suggesting that it is possible that these two phenomena can be dissociated.

A full concentration-effect profile of the inhibitory action of Zn^{2+} on TBT-mediated thymocyte apoptosis was not conducted. However, it is noted that the concentrations of Zn^{2+} required to prevent internucleosomal DNA degradation occurring during apoptosis have routinely been shown to be high (Duke et al., 1983; Telford et al., 1991; Waring et al., 1991), i.e. not less than 250 μM (McCabe et al, 1993). Lower levels are effective in isolated nuclei, or in intact cells if zinc ionophores are used (Giannakis et al., 1991). Therefore cellular uptake of Zn^{2+} seems to be limited, though the effective inhibitory intranuclear concentrations may be quite low. Zn^{2+} inhibits the Ca^{2+}-mediated autodigestion of DNA in isolated nuclei (Cohen and Duke, 1984; Nieto and Lopez-Rivas, 1989), and thymocyte apoptosis caused by zinc chelation is independent of macromolecular synthesis (McCabe et al., 1993). The most obvious explanation for these phenomena is that the mode of action for the inhibition of endstage apoptotic processes by Zn^{2+} is direct inhibition of a constitutive endonuclease. Additional indirect evidence for this hypothesis comes from the observation that partially purified, Ca^{2+}/Mg^{2+}-dependent endonucleases derived from thymocytes are readily inhibited by Zn^{2+} (Dykes et al., 1987; Gaido and Cidlowski, 1991; Compton, 1992). As already mentioned, whilst internucleosomal DNA cleavage is prevented by Zn^{2+} this cation does permit early endonucleolytic DNA degradative processes to occur. Definitive identification of the critical zinc-dependent intracellular site awaits full characterisation of the apoptotic effector enzymes; therefore currently it is not possible to preclude the plausible alternate hypothesis that raised intranuclear Zn^{2+} concentrations affect the chromatin substrate. For instance, phosphoprotein phosphatases regulate histone hyperphosphorylation, e.g. of histone H1, and indirectly reduce chromatin condensation. These enzymes are known to be inhibited by zinc (Tanphaichitr and Chalkley, 1976), and in theory, reduced dephosphorylation would

favour masking of DNA by histone H1, and consequently more condensed nuclease-resistant chromatin structures. Due to physical constraints on the degree of DNA-phosphate charge stabilisation possible via divalent cation interactions, it is unlikely that Zn^{2+} directly causes appreciable chromatin condensation (Widom and Baldwin, 1980). The balance of evidence does not suggest a role for Zn^{2+} in signal transduction pathways, unless this is at an intranuclear level, but this possibility cannot be entirely excluded.

In spite of its extensive use as an inhibitor, the relationship of cellular Zn^{2+} homeostasis to the mechanisms of physiological and pathological apoptosis is far from clear. It obviously has an important physiological role in suppression of apoptosis. Zinc deficiency in vivo causes reversible involution of the thymic cortex (Fraker et al., 1978; Fernandes, 1979). In vitro, Zn^{2+} deprivation activates apoptosis in newly mature thymocytes and peripheral lymphocytes (McCabe et al., 1993) which has lead to the theory that it may be involved in negative selection processes in lymphopoiesis. Myeloid, as well as lymphoid, cell lines also engage apoptotic death programs if denied this cation (Martin et al., 1991). As a final cautionary note in terms of the design of experimental systems involving thymocyte incubations, the zinc content of culture medium may be a significant experimental parameter, e.g. simple or minimally supplemented salt mixtures would appear to be unsuitable. The greatest contribution to the zinc content of complex media comes from sera such as FCS (Dr S. Martin, personal communication); this may be relevant in terms of the anti-apoptotic properties of serum supplementation.

High micromolar concentrations of ATA provided a quantitatively similar, moderate degree of protection against DNA fragmentation stimulated by either TBT or MPS (Fig. 4.8a). This was accompanied by a corresponding diminution in the incidence of apoptotic cells (Fig. 4.8b). In the case of glucocorticoids, the quoted degree of protection conferred by ATA against DNA fragmentation in other publications has varied from high (McConkey et al., 1989b), to moderate (Cohen et al., 1992). The former reported that 0.5 mM ATA did not interfere with [^{3}H]leucine incorporation in thymocytes, and in common with their observations, the extent of DNA degradation inhibition by ATA was similar irrespective of whether it was included before or 1.5 h after addition of the test agents (Table 4.5). This confirms that protein synthesis inhibition was not involved, and further secondary effects such as modulation of $[Ca^{2+}]_i$ have also been excluded (McConkey et al., 1989b). It is concluded that, in common with its effect on MPS-treated cells, ATA partially inhibited DNA fragmentation and apoptotic death after TBT exposure. Due to its potential effects on multiple polynucleotide enzymes and other biochemical processes, e.g. macromolecular synthesis (Hallick et al., 1977), and the dearth of knowledge on its ligand binding character, ATA must be viewed as a rather unsatisfactory modulator for apoptosis studies. Although it can apparently directly inhibit thymocyte endonucleases producing internucleosomal cleavage (Gaido and Cidlowski, 1991), or generating larger 300 and 50 kbp fragments

(Filipski et al., 1990), its effect in suppressing DNA cleavage is equally compatible with interference with other regulatory proteins or interaction with the chromatin substrate.

Distamycin and H33258 were perceived to have more promise since their binding site (AT-rich DNA regions), and the nature of their interaction with DNA is better understood. Although distamycin had been successfully applied as a probe in isolated DNA systems, it proved to be problematic when added to cell cultures, since it caused thymocyte agglutination and had poor intracellular uptake characteristics. In contrast, H33258 was rapidly included in cells and bound to DNA. It partially antagonised DNA fragmentation arising after TBTO or MPS treatment (Table 4.6; Fig. 4.9a), though for reasons that are unclear, it was less effective on glucocorticoid stimulated apoptosis. H33258 clearly diminished TBT-stimulated internucleosomal cleavage (Fig. 4.9b), and concurrently reduced the incidence of apoptotic cells. Whilst DNA fragmentation inhibition by H33258 paralleled its reversal of latent thymocyte viability loss (Fig. 4.9a), the degree of protection conferred against cell death was higher than expected from the partial effect on the former parameter. It is possible that H33258 merely affected plasma membrane permeability consequently confounding the trypan blue exclusion results (no other viability estimation methodologies were applied). However, more speculatively, there is another possible mechanism of action for this modulator. Apoptotic DNA degradation in thymocytes has high order and internucleosomal cleavage components, and H33258 may have acted differentially to reduce internucleosomal DNA cleavage more than larger fragment generation. This would be consistent with detection of some DNA fragmentation by the assay used, and since internucleosomal degradation is thought to be more directly linked to cell killing, might account for the protection against viability loss. Non-pulsed gel electrophoresis cannot discern high order DNA damage, and therefore further experiments would be necessary to test this hypothesis. Shortly after completion of this work, Tempel and Ignatius (1993) reported that H33258, at similar concentration orders to those used here, inhibited spontaneous DNA fragmentation in a chick embryo cell lysate system proposed as a model for apoptotic DNA degradation. Since they showed that H33258 markedly increased DNA supercoiling it is postulated that this modulator may function, at least partially, by blocking apoptotic effector enzyme access by inducing unfavourable DNA conformations.

These investigators also focused on the DNase I inhibition by H33258 (an IC_{50} of 28 μM was cited), but it must be stressed that DNA minor groove binders have the potential to interfere with the activity of many DNA-binding proteins. Therefore the possibility cannot be excluded that H33258 directly inhibited one or more apoptotic effector enzymes, in a manner similar perhaps to the unspecific, non-competitive, action of ATA. As discussed in section 1.3.4 and 1.3.5, topoisomerase II an enzyme critical to regulation of chromatin superstructure and capable of relaxing high order DNA conformations, is preferentially

bound to AT-rich DNA scaffold-associated regions. H33258 or related minor groove ligands can (i) abolish the interaction of topoisomerase II with scaffold-associated regions (Adachi et al., 1989); (ii) alter the catalytic activity of this enzyme, and block the trapping of cleavable complexes by topoisomerase II-directed agents (Woynarowski et al., 1989; Smith et al., 1990). Arends and Wyllie (1991) have described a Ca^{2+}- and Mg^{2+}-dependent nuclease activity in thymocytes active at neutral pH which is apparently homologous, with the subunit of topoisomerase II. As they point out, topoisomerase II would be capable of producing stabilised DNA ds-breaks under conditions of cellular stress, e.g. ATP depletion. Tributyltin exposures causing apoptosis jointly depress intracellular ATP levels (see chapter 5) and moderately elevate Ca^{2+}. Osheroff et al. (1987) noted that high calcium concentrations trapped topoisomerase II in a form which cleaved but did not religate DNA. From what is known about the archetypal constitutive thymocyte endonuclease, it seems unlikely that topoisomerase II could directly produce the internucleosomal chromatin cleavage which is a hallmark of apoptosis. But this does not preclude it mediating changes in DNA conformation thereby facilitating nuclease activity; there is limited data to implicate its activation in non-necrotic killing by CTL (Duke and Sellins, 1989). Though thymocytes apparently have a high content of topoisomerase II (Holden et al., 1990), and readily undergo apoptosis after topoisomerase II-directed agent exposure (Walker et al., 1991), mature resting T cells are deficient in this enzyme and are refractory to apoptosis induced by etoposide, and other stimuli (Kaufman, 1989).

As detailed in section 1.3.4, high order DNA topology alterations (i.e. changes in tertiary and quarternary supercoiling) are central to the control of substrate accessibility of non-histone DNA binding proteins like endonucleases. This suggests a bridging hypothesis relating the action of certain apoptotic effector stage inhibitors, to models proposing apoptosis regulation at the level of chromatin superstructure (e.g. see Tomei, 1991). Distinct from direct inhibition of effector enzymes, DNA stabilisation by promotion of supercoiling could be a unifying locus of action for seemingly disparate agents such as Zn^{2+}, H33258 and polyamines. Coincident with their inhibition of endonucleolytic cleavage, Zn^{2+}, H33258, spermine and to a lesser extent spermidine, increase nucleoid DNA supercoiling (Tempel and Ignatius, 1993). Brune et al. (1991) found that, in a parallel effect order, exogenous spermine and spermidine prevented thymocyte apoptosis. Promotion of DNA supercoiling by polyamines has been noted (Lipetz et al., 1982), and whilst this has been disputed for occasional cell types (Snyder, 1989), there is no doubt that polyamines play an important role in charge stabilisation of high-order DNA conformation, and that polyamine depleted DNA is hypersusceptible to nuclease scission (Snyder, 1989). Ligands like H33258 and polyamines (Schmid and Behr, 1991) share the same strong minor groove and weak AT binding preferences though it is not clear whether this is mechanistically important. Novobiocin reduces DNA superhelicity, and Litwack and Alnemri (1990) deduced that this compound activated apoptosis in CEM lymphocytes by

causing decondensation of stabilised high-order DNA structures. Some evidence from a reconstituted chromatin system was presented to implicate novobiocin disturbance of histone-DNA interaction and then double stranded cleavage by a constitutive endonuclease. It is notable that the intercalator ethidium bromide, which at low concentrations forces DNA into a more extended conformation, was ineffective in preventing spontaneous DNA fragmentation (Tempel and Ignatius, 1993). A hypothesis of apoptosis modulation by superstructural alterations allows for the integration of eukaryotic topoisomerase action, since both type I and II enzymes can relax high-order DNA conformations (Liu, 1989). In addition, phorbol esters via PKC also appear to promote DNA supercoiling under certain circumstances (Lipetz et al., 1982; McCabe et al., 1992), e.g. TPA affects this parameter in mixed lymphocyte cultures. However, they noted that phorbol esters may also cause opposite effects in leukemic lymphocytes, which already have supercondensed DNA, and suggest that whether phorbol esters increase or decrease supercoiling is dependent on the cell type and pre-existing DNA conformation. This could explain the often contradictory findings regarding the inhibition of apoptosis by phorbol esters. TPA does appear to reduce the susceptibility of chromatin to drug-induced, topoisomerase II-mediated DNA cleavage, by a mechanism thought to involve altered DNA topology (Zwelling et al., 1988).

The data established here on the action of various modulators provides additional security for the conclusion that TBT-mediated non-necrotic thymocyte killing is apoptosis. This is based on: (i) a requirement for an elevation in $[Ca^{2+}]_i$; (ii) the sensitivity of the internucleosomal DNA cleavage component to inhibition by zinc; (iii) that compounds with proven ability, or the potential, to antagonise the DNA degradation typical of apoptosis are protective. In the case of both MPS and TBT-stimulated apoptosis, the results obtained with phorbol esters, EGTA and calmidazolium apparently contradict some established observations; further confirmatory work to resolve these discrepancies would seem prudent. Intracellular signalling and effector coupling in thymocyte apoptosis is a rapidly evolving subject of vast proportions; the findings discussed here on TBT make a small contribution which can now be integrated.

CHAPTER 5

FURTHER STUDIES ON THE MECHANISMS AND CELLULAR PROCESSES INVOLVED IN THYMOCYTE APOPTOSIS ACTIVATED BY THE TOXIC AGENTS TRI-n-BUTYLTIN, METHYLPREDNISOLONE AND NOCODAZOLE.

ABSTRACT

Recent in vitro studies have suggested that activation of apoptosis could account for the profound depletion of cortical thymocytes, which characterises tributyltin immunotoxicity. However, it is also known that TBT disrupts macromolecular synthesis and cellular energetics to an extent that might be expected to interfere with the initiation of apoptosis. The objective of these studies was to further evaluate TBT-mediated thymocyte killing in the context of key cellular processes. The synthetic glucocorticoid MPS was used as a positive control. In addition, to examine the possible involvement of cellular microtubules (MT) in toxicant-induced apoptosis, comparisons were made to nocodazole, a compound which has a relatively specific MT disrupting action.

In cells exposed to TBTO concentrations causing a rapid and apparently maximal inhibition of protein synthesis, it remained possible to demonstrate the stereotypic internucleosomal DNA cleavage and morphological changes indicative of apoptosis. Further confirmation that apoptosis following TBT injury occurred independently from protein synthesis was provided by the absence of a protective effect following cycloheximide (CyH) pretreatment; which contrasted with the results obtained in cells exposed to MPS after inclusion of CyH. Apoptosis still proceeded in TBTO-treated thymocytes although intracellular ATP levels were depressed to 20% or less of control values. Nocodazole also activated thymocyte apoptosis, and immunocytochemistry using an anti-α tubulin-directed monoclonal antibody showed that this was preceded by major disruption of the microtubular cytoskeleton. Under these circumstances, the MT stabilising agent taxol protected against nocodazole-actuated DNA fragmentation and latent cytolethality. Although TBTO also deranged MT, in this case taxol was ineffective in preventing cell killing, suggesting that this locus is not pivotal in initiation of TBT-mediated apoptosis. During TBTO-mediated apoptosis a thymocyte population was detected by flow cytometry with a relative DNA content below normal diploidy, but there was no overt disturbance of the cell cycle.

These results indicate that, unlike many other previously studied agents, thymocyte apoptosis as a result of TBT exposure occurs independently of a requirement for protein synthesis, and can also take place under conditions where cellular energetics function is severely compromised.

5.1 INTRODUCTION

5.1.1 Macromolecular synthesis and energetics as prerequisites in apoptosis

This section concentrates on this subject in the context of thymocyte apoptosis; see also 1.3.3 for additional coverage. A principal biochemical feature widely referenced as a discriminator between necrosis and activation-induced cell death modes (PCD and apoptosis) is the macromolecular synthesis dependency of the latter (Lockshin and Zakeri, 1991; Bowen and Bowen, 1990). Much of the dogma originates from indirect evidence in the much studied rodent thymocyte model which demonstrated that transcriptional and translational inhibitors protected cells from apoptotic stimuli. The emergent tenet was that, in thymocytes at least, apoptosis is invariably dependent on active protein synthesis (Wyllie, 1987a; McConkey et al., 1992; Lockshin and Zakeri-Milovanovic, 1984); though this concept appears not to be universally applicable to all cells (section 1.3.3).

Thymocyte apoptosis stimulated by prototypical agents such as glucocorticoids or ionising radiation is abrogated by RNA or protein synthesis inhibitors (Table 5.1). This finding does not necessarily mean that new gene expression within dying cells is required, since it is also compatible with the existence of short-lived intracellular survival or apoptotic suppressor factors, or with effector proteins (or mRNA) in rapid turnover. Direct evidence for *de novo* synthesis of 'death program proteins' remains limited, and stems from early work which showed the appearance of a small number of new proteins occurring in synchrony with thymocyte killing by glucocorticoids (Voris and Young, 1981). Gamma-irradiation of immature rat thymocytes resulted in the transcription of two mRNA species, RP-2 and RP-8, that have been classified as death-associated (Owens et al., 1991). However, in spite of many investigations seeking to identify an induced death protein, such as a newly transcribed endonuclease capable of internucleosomal cleavage, no crucial candidate has been found. Reports of putative nucleases induced in thymocytes by glucocorticoids (Compton et al., 1987) have been subject to refutation (Alnemri and Litwack, 1989), and counter-claim (Gaido and Cidlowski, 1991; Caron-Leslie et al., 1991). It should be noted that thymocytes are known to possess constitutive Ca^{2+}/Mg^{2+}-endonuclease activity (Cohen and Duke, 1984; Alnemri and Litwack, 1989; Wyllie, 1987b), although its biochemical characteristics and control are ill-defined. The fact that it is possible to upregulate nuclease activity under circumstances where no macromolecular synthesis could be implicated, e.g. in isolated nuclei (Umansky, 1991), suggests that protein synthesis need not be a prerequisite for *directly* activating the apoptotic effector in intact cells. Control mechanisms could involve: (i) proteolysis of a proenzyme (Gaido and Cidlowski, 1991; Caron-Leslie et al., 1991); (ii) changes in DNA conformation making it more susceptible to cleavage; (iii) loss of one or more suppressor proteins; (iv) low level expression and differential mRNA half-lives associated with effector and suppressor elements (Sellins and Cohen, 1987); (v) a physiological apoptotic signal transduction pathway (e.g. Ca^{2+} flux) that normally requires porter protein synthesis, but which can be

Apoptotic agent	Inhibitor[1]	Effect	Reference/cell type[2]
a) Thymocyte apoptosis			
MPS	CyH, Act D	–, –	Wyllie et al., 1984a (R)
Dexamethasone	CyH, Act D, Emet	–, –, –	Cohen and Duke, 1984 (M)
A23187	Act D, CyH	–, –	McConkey et al., 1989a (R)
	Act D, CyH	–, –	Kizaki et al., 1989 (M)
Purine nucleosides	CyH	–	Kizaki et al., 1988 (M)
Colchicine	CyH	–	Afanas'ev et al., 1988 (R)
TCDD	Act D, CyH	–, –	McConkey et al., 1988a (R)
Gliotoxin	CyH	NE	Waring, 1990 (M)
γ-irradiation	CyH, Emet, Act D, DRFB	–, –, –, –	Sellins and Cohen, 1987 (M)
Hyperthermia	CyH, Emet, Act D,	NE, NE, NE,	
	DRFB	NE	Sellins and Cohen, 1991a (M)
Zinc chelation	CyH, Emet	NE, NE	McCabe et al., 1993 (R)
b) Other lymphoid cell apoptosis			
Cortisol	Act D, CyH, Pur	–, –, –	Galili et al., 1982 (CLL)
Novobiocin	CyH	NE	Alnemri and Litwack, 1990 (CEM-C7)
ATP	Act D, DRFB	–, –	Zheng et al., 1991 (EL4)
UVB or γ-irradiation	Act D, CyH	+, +	Deeg and Bazar, 1991 (T cells/ Jurkat)
TcR stimulation	Act D, CyH	–, –	Shi et al., 1990 (T cell hybridoma)
CTL target cytolysis	Act D, CyH	NE, NE	Duke et al., 1983
CTL target cytolysis	Pur, Emet, Act D, DRFB	–, –, –, –	Zychlinsky et al., 1991
Pur, CyH		+, +	Vedeckis and Bradshaw, 1983 (S49)
CyH		+	Collins et al., 1991 (CLL/PBL)
Act D, CyH		+, +	Bansal et al., 1991 (CEM-C7/CEM-C1)

TABLE 5.1 The macromolecular synthesis dependency of apoptosis in: a) thymocytes or b) other lymphoid cells. The effect of translational or transcriptional inhibitors is shown as inhibiting (–), having no effect on (NE), or stimulating (+) the incidence of apoptotic markers following exposure to the indicated agents. [1] CyH - cycloheximide; Act D - actinomycin D; Emet - emetine; Pur - puromycin; DRFB - 5,6-dichloro-1-β-D-ribofuranosylbenzimidazole. [2] R - rat thymocytes; M - mouse thymocytes; CEM - CEM T cell leukemia cells; CLL - chronic lymphocytic leukemia cells; EL4 - thymoma cell line; PBL - peripheral blood lymphocytes; Jurkat - Jurkat leukemia cells; S49 - S49 lymphoma cells.

engaged by alternate stimuli in injured cells; (vi) altered macromolecular modification, e.g. loss of protein poly ADP-ribosylation (Wielckens and Delfs, 1986; Umansky, 1991).

Whilst it is true that in thymocytes the majority of apoptotic stimuli appear to be antagonised by RNA and protein synthesis inhibitors, occasional exceptions exist, e.g. hyperthermia (Table 5.1). But to date, no translational or transcriptional inhibitor has unequivocally been shown to stimulate apoptosis in this system, a finding of direct relevance to TBT. Other lymphoid cells do die by apoptosis when exposed to macromolecular synthesis inhibitors like cycloheximide and actinomycin D (Table 5.1). However, the rather non-specific nature of these agents must always be recognised, for instance, apart from blocking peptidyl transferase activity of the 60S ribosomal subunit, CyH has multiple effects including DNA synthesis inhibition and the ability to deplete DNA repressor proteins (Collins et al., 1991).

Apoptosis has been characterised as an active process, though its exact energetics requirements are unknown. Energy precursors, presumptively ATP, may be required for endonucleolytic cleavage, macromolecular synthesis, fluid transport during cellular contraction, intracellular signal transduction, and possibly cytoskeleton movements involved in apoptotic body formation. Examples of energetics dependency include the observation that rat thymocyte nuclei require ATP to generate internucleosomal DNA cleavage products (Jones et al., 1989), and that topoisomerase II-directed agent damage does not result in apoptosis if oxidative phosphorylation is inhibited (Kaufmann, 1989; Kupfer et al., 1987). Though no gross changes in mitochondrial structure initially occur during apoptosis, recent findings have cast some doubt on the tenet that the functional capability of this organelle is necessarily preserved. For instance, loss of mitochondrial function was observed in fibroblasts or oligodendrocytes after apoptotic treatments with staurosporine or, in the latter case, after growth factor deprivation (Jacobson et al., 1994).

5.1.2 The cytoskeleton in apoptosis

The role of the cytoskeleton in apoptosis has received little study. However, cell shape, motility, and internal organisation are completely dependent on cytoskeletal elements including microtubules (MT), actin microfilaments, and intermediate filaments (Alberts et al., 1989). Since MT maintain cellular asymmetry and organelle localisation, it is highly probable that they must undergo some reorganisation during apoptotic phenomena like cell rounding, rapid contraction, and the compaction of organelles. It has also been suggested that due to the interrelationship between the cell membrane, nuclear matrix and nucleic acids via cytoskeletal scaffolds, collapse of the intracellular skeleton could result in increased susceptibility of DNA to endonucleolytic attack (Lockshin and Zakeri-Milovanovic, 1984). Increases in $[Ca^{2+}]_i$ inhibit MT assembly and promote disassembly

(Nishida, 1978), and it is tempting to speculate that the Ca^{2+} fluxes common to apoptosis could, at least in part, act at such a locus.

Agents that depolymerise MT commonly activate apoptosis, though it is important to causally distinguish between this effect and non-necrotic cell death arising from the consequent arrest of mitosis in dividing cell populations. Non-lymphoid cells exposed to colchicine, colcemid, vinca alkaloids, or cold-shock MT destabilisation undergo DNA fragmentation and delayed cell death (Martin et al., 1990; Kaufmann, 1989; Nagle et al., 1990), whilst colchicine similarly causes apoptosis in lymphoma cells (Vedeckis and Bradshaw, 1983), lymphocytic leukemia cells (Giannakis et al., 1991) and lymphoid tissues in vivo (Afanas'ev et al., 1988). After observing that apoptotic terminally differentiated HL-60 cells lost their MT network, Martin and Cotter (1990) showed that the MT-disrupting agents colchicine, vinblastine, or the more specific drug, nocodazole, caused apoptosis in HL-60 cells which was paralleled by loss of normal MT architecture. They also suggested that A23187 might also cause apoptosis due to Ca^{2+}-mediated derangement of MT, though no direct evidence was presented to support this hypothesis.

Conflicting reports exist for microfilament-disrupting compounds in relation to the mode of their cytotoxicity. Cytochalasin B and E, or villin, apparently cause internucleosomal DNA cleavage in several cell lines (Kolber et al., 1990), although similar concentrations of cytochalasin B were reported to activate necrosis rather than apoptosis in HL-60 cells (Martin and Cotter, 1990). The latter investigators later claimed that cytochalasin B prevented cellular fragmentation in HL-60, Molt-4 or U937 cells exposed to various apoptotic stimuli without inhibiting endonucleolytic DNA degradation (Cotter et al., 1992), suggesting a pivotal role for microfilaments in the formation of apoptotic bodies. In contrast, MT disruption using nocodazole did not inhibit apoptotic body budding.

5.1.3 TBT biochemical and cellular effects of relevance to the apoptotic process

Since the original work by Aldridge and Cremer (1955), triorganotins have been recognised as potent inhibitors of cellular energy metabolism. The principal target of their action is the mitochondrion (reviewed by Aldridge, 1976; Selwyn, 1976; Boyer, 1989), and they are effective antagonists of mitochondrial ATP production, e.g. the IC_{50} for TBT is about 0.6 μM (Aldridge, 1958). Reduced ADP phosphorylation appears to result from direct interference, uncoupling of oxidative phosphorylation, inhibition of electron transfer, and disturbed substrate transport. Triorganotins of intermediate lipophilicity, amongst them TBT, have three major mitochondrial effects. (i) They act as artificial ionophores and mediate an electrically silent exchange of chloride for hydroxyl ions across membranes (Selwyn et al., 1970). The process involves the formation of electroneutral ion pairs between the R_3Sn^+ moiety and an anion X^- at aqueous interfaces of membranes allowing translocation across the permeability barrier. Neutralisation of both membranal pH

difference (by Cl^-/OH^- exchange) and the differential electrical potential (by anion uniport) results in uncoupling (Selwyn, 1976). (ii) Triorganotins bind in a specific manner to a component of the ATP synthetase complex (F_1F_0 ATPase) leading to a direct inhibition of phosphorylation reactions (Selwyn, 1976). The IC_{50} for this Cl^--independent effect for TBT is reported to be around 1.2 μM (Aldridge, 1976). (iii) At comparable concentrations to those affecting other mitochondrial functions, triorganotins cause mitochondrial swelling (Aldridge and Street, 1964). This loss of volume homeostasis has recently been tentatively linked to binding to the inner membrane anion channel (IMAC); in the case of TBT this results in 95% inhibition of IMAC transport at 0.9 μM (Powers and Beavis, 1991). Together with the binding to ATP synthetase, this interaction represents one of the few specific protein targets identified for TBT.

Exposure of rat thymocytes to TBTC concentrations exceeding 0.1 μM interfered with cellular energetics, as demonstrated by increased glucose consumption and accumulation of lactate (Snoeij et al., 1986b; Snoeij et al., 1986c). Intracellular ATP levels declined rapidly, and were approximately halved after 1 h at 1 μM, though more drastic reductions occurred when glucose was omitted from the medium. These results suggest that inhibition of oxidative phosphorylation causes stimulation of glycolysis and conversion of pyruvate, which is no longer transported into mitochondria, into lactate (Snoeij et al., 1987). FCCP, a potent uncoupler of oxidative phosphorylation, which is about 100-fold more effective than 2,4-dinitrophenol, caused a similar profile of effects to triorganotins in rat thymocytes, i.e. ATP depletion, glycolysis stimulation, and lactate build-up (Snoeij et al., 1986c).

In thymocytes and other cells, triorganotins of intermediate lipophilicity inhibit macromolecular synthesis (Snoeij et al., 1986b; 1986c; 1988b; Marinovich et al., 1990a). With TBT, incorporation of DNA, RNA and protein precursors are all affected, though DNA and protein synthesis are inhibited the most. Protein synthesis is very rapidly inhibited by micromolar quantities of TBT, such that maximal depression is evident within 10-15 minutes (Snoeij et al., 1986b; Marinovich et al., 1990a). Incubation of unseparated thymocyte populations in simple media with 1 μM TBTC causes synthetic activity to decline to about 10% of the controls (Snoeij et al., 1986b), and IC_{50} values of just over 0.3 μM have been reported for TBTC. Some studies indicate a direct correlation between diminished biosynthetic production and suppression of cellular energetics (Snoeij et al., 1986b; 1986c), and there is no evidence for involvement of indirect mechanisms such as inhibition of nucleotide kinase phosphorylation or diminished amino acid uptake. This has led these investigators to conclude that loss of energetics function is the key precursor to the inhibition of macromolecular synthesis. At least in the case of protein synthesis this may not be the exclusive mechanism. Later studies in fractionated thymocytes showed that although ATP levels were equally affected in all populations, differential inhibition of protein synthesis occurred (Snoeij et al., 1988b). In addition, restitution of protein

synthesis after TBT removal is much slower than recovery of the ATP pool, and the manner of dithiol reagent reversal of inhibition indicates that TBT may bind to a critical target (Marinovich et al., 1990a). Whilst depletion of ATP by TBT must affect the rate of protein synthesis, there is also evidence to support a hypothesis of direct interaction with a critical protein site.

Triorganotins, especially hydrophobic members such as TBT, inhibit MT tubulin polymerisation in isolated preparations and in cells in vitro (Tan et al., 1978; Bondy and Hall, 1986), and TBT exposure depletes the polymeric F-actin form of microfilaments (Marinovich et al., 1990b). The relationship of such phenomena to modes of cytotoxicity has not been investigated, but they may be the basis for some cellular effects caused by TBT indicative of gross disruption of the cytoskeleton, including cell detachment (Reinhardt et al., 1982) and aneuploidy induction (Jensen et al., 1991).

At concentrations not causing rapid loss of viability, e.g. 1 μM for 4 h, TBT blocks the cell cycle in murine erythroleukemic cells (Zucker et al., 1989). Affected cells accumulate in G_2/M phase.

5.1.4 Aims of these studies

As outlined in this introduction, previously it has been widely accepted that thymocyte apoptosis is dependent on maintenance of *de novo* protein synthesis after the triggering stimulus, and is also an active process demanding conserved cellular energetics. This needs to be considered in the context of the rapid and very marked inhibition of protein synthesis which occurs following incubation with TBT compounds (Snoeij et al., 1986b; Marinovich et al., 1990a), and the finding that TBT exposure causes gross disruption of mitochondrial function (Aldridge and Street, 1964). In the light of these apparent anomalies, additional studies were conducted to further elucidate the biochemical characteristics of non-necrotic killing of rat thymocytes by TBTO. FCCP, an uncoupler of mitochondrial oxidative phosphorylation, with similar energy metabolism effects to TBT was also investigated.

Since TBT may possess significant potential to disrupt elements of the cellular cytoskeleton, an established apoptotic trigger in some cells, this locus of action was studied to determine if it had any mechanistic relevance. The antimicrotubular compound nocodazole was employed as positive control. Use was also made of Taxol A, a novel potential antagonist of MT-directed agent cytotoxicity. Taxol is a naturally occurring compound isolated from the bark of the Pacific yew tree (*Taxus brevifolia*) that has been used clinically as an antitumour and antileukemic agent. It promotes assembly of MT, inhibits tubulin disassembly, and stabilises against the depolymerising effects of cold, Ca^{2+}, and MT-disruptors such as colchicine (Manfredi and Horwitz, 1986; Horwitz et al., 1986).

Flow cytometric techniques were employed to examine whether nuclear changes related to TBTO-mediated apoptosis could be followed, and to determine whether cell cycle disturbances were involved.

A number of the experiments detailed hereafter were reported in the following publication:

Raffray M, McCarthy D, Snowden RT, Cohen GM (1993) Apoptosis as a mechanism of tributyltin cytotoxicity to thymocytes: Relationship of apoptotic markers to biochemical and cellular effects. Toxicol Appl Pharmacol 119: 122-130.

5.2 METHODS

5.2.1 Materials

TBTO was obtained from Fluka Chemicals Ltd (Glossop, England) and purified as described in section 2.14; MPS (> 95% pure) was from Upjohn (Crawley, England); nocodazole (methyl [5-(2-thienylcarbonyl)-1*H*-benzimidazol-2-yl] carbamate) and carbonyl cyanide p-(trifluoromethoxy)-phenylhydrazone (FCCP) both of which were declared to be > 99% pure, were from Sigma Chemical Co. Ltd (Poole, England). Information on the source and purity of zinc acetate dihydrate is given in section 4.2.2. Cycloheximide was from Sigma Chemical Co. Ltd (Poole, England) with a certified purity of 98%. Taxol A was from Novabiochem UK Ltd (Nottingham, England) with a stated purity of > 98%.

The following pertain to the method described below for microtubule visualisation: neutral buffered formalin (3.7% formaldehyde), saponin, trypan blue, DM-1A antibody and FITC conjugated anti-IgG were from Sigma Chemical Co. Ltd (Poole, England); PBS was prepared according to the formulation given in section 2.1.6.

U937 cells were a kind gift from Dr. Winston Morgan. All other materials not mentioned above were from BDH Ltd (Poole, England).

5.2.2 Test compound handling and cell incubation

In experiments requiring in vitro culture of rat thymocytes, the methodology used was as outlined in section 4.2.2. Human U937 leukemia cells were grown in culture at 37° under 5% CO_2 : 95% air in DMEM medium containing 10% (v/v) FCS, penicillin (20 units ml^{-1}), streptomycin (20 $\mu g\ ml^{-1}$) and neomycin (8 $\mu g\ ml^{-1}$). Exponentially growing U937 cells were utilised in MT observation experiments. The details of TBTO and MPS handling and addition regimens were as given previously in section 4.2.2. Nocodazole was dissolved in anhydrous DMSO, by gentle shaking for 20 minutes to encourage dissolution, to give a stock solution of 5 or 10 mg ml^{-1}, and then stored frozen at -20° until required. This stock was further diluted prior to use such that when additions of nocodazole were made, these

incubations contained a maximum concentration of 0.3% DMSO. Equivalent amounts of DMSO were introduced into control cultures.

In the studies where Zn^{2+} was used, it was freshly prepared for each experiment as a sterile-filtered stock solution of zinc acetate dihydrate at 10 mg ml^{-1} in RMPI-1640 medium. Cells were preincubated with the required concentrations of Zn^{2+} for 20 minutes prior to the introduction of test compounds. Cycloheximide was freshly prepared for each experiment as a solution of 2 mg ml^{-1} in distilled water before sterilisation by passage through a 0.22 μm filter. This stock was added to cultures 15 minutes before addition of the test agents to achieve a final concentration of either 10, 30 or 100 μM. FCCP was dissolved in ethanol to give a 5 mM stock solution. Before use, this stock was serially diluted so as to maintain a consistent final concentration of 0.2% ethanol in the cultures. Taxol was prepared as a stock solution in anhydrous DMSO at 350 times the highest final concentration required, and stored at -20° until required. Serial dilutions in DMSO were made as necessary to produce lower concentration stocks. Parallel control cultures received equivalent DMSO additions.

5.2.3 Standard methodologies

Determinations of viability, DNA fragmentation (colorimetric method), morphological studies by light microscopy and TEM, and neutral agarose gel DNA electrophoresis were performed according to the methods and at the timepoints referred to in section 4.2.3. The procedures and sample times relating to protein synthesis, intracellular ATP levels and flow cytometry were as described in sections 2.9, 2.10 and 2.11 respectively.

5.2.4 Microtubule (MT) visualisation

This technique is based on visualisation of cellular microtubules by indirect immunofluorescence using an anti-α-tubulin directed monoclonal antibody (MAb). Since cold can cause MT depolymerisation (Watson and Morris, 1987), all centrifugation and handling stages prior to cell fixation were performed at ambient temperature. Thymocyte permeabilisation was achieved using saponin, a sapogenin glycoside. As a crude indicator of permeability, preliminary experiments included reserve samples of cells which were all shown to be fully stained when admixed with 0.4% trypan blue following saponin treatment. A schematic of the experimental protocol is given in Fig. 5.1; the following details are intended to supplement that information. Sampling times were at 0, 1, 2 and 3 h after test compound addition. Aliquots of 0.2 ml of cell suspension (4 x 10^6 thymocytes) were placed into 75 x 12 mm plastic tubes. After cell harvesting and fixation, all subsequent manipulations were performed in 1.5 ml Eppendorf tubes (Atom Medical, Lewes, England). Mouse anti-chicken MAb (clone DM-1A) to brain α-tubulin, with known immunospecificity to rodent MT preparations was used as the primary antibody. A working dilution of 1:500 was determined to be optimal. Goat anti-mouse IgG conjugated

MICROTUBULE VISUALISATION

Aliquots of 4 x 10^6 cells taken in triplicate

⇩

Harvest cells (centrifuge at 1500 rpm for 5 min at ambient temperature; discard medium)

⇩

Add excess neutral buffered formalin (3.7% formaldehyde), pH 7.2.
Fix for 30 min at ambient temperature

⇩

Centrifuge at 1000 rpm for 5 min and discard supernatant

⇩

Wash three times with 1 ml PBS (these and all subsequent centrifugation steps performed at 1000 rpm for 5 min)

⇩

Resuspend in PBS/0.1% saponin (0.75 ml per tube)

⇩

Add anti-α tubulin (DM-1A) at 1:500 dilution; mix gently

⇩

Incubate for 30 min at ambient temperature

⇩

Wash twice with PBS/0.1% saponin (0.75 ml per tube)

⇩

Place final cell suspension into Eppendorf plastic tubes

⇩

(continued above right)

⇩

Add FITC-conjugated anti-IgG at 1:50 dilution; mix gently

⇩

Incubate for 30 min in the dark at ambient temperature

⇩

Wash twice with PBS/0.1% saponin (0.2 ml per tube)

⇩

Wash twice with PBS alone (0.15 ml per tube)

⇩

Resuspend cells into a final volume of 0.1 ml PBS

⇩

Mix gently and place on glass slide, mount under coverslip; view by UV fluorescence microscopy (FITC filter setting)

FIGURE 5.1 Flow chart showing the preparation of samples for visualisation of cellular microtubules.

See section 5.2.4 for additional methodological detail.

to FITC, with known reactivity to major IgG subclasses was used as a fluorescent marker. Working dilutions of 1:25, 1:50 and 1:100 were examined and a dilution of 1:50 was found to be optimal.

Fluorescence microscopy under epifluorescent UV illumination, FITC filter set, was performed using a Nikon Microphot FXA (Nikon Corporation, Tokyo, Japan). Cell preparations were kept at 30° prior to examination in order to maximise the fluorescence yield. Cellular MT structures were distinguished by their differential high yellow-green fluorescence, and the incidence of cells classified as having a complete MT network, including a microtubule organising centre (MTOC), was quantified by examination of contiguous fields of a minimum of 100 cells. Photomicrography was with Ektachrom 35 mm ASA 400 colour film (Kodak; Hemel Hempstead, England).

Negative control experiments were conducted during preliminary studies by including preparations in which the MAb or IgG binding stage was omitted, and also by examining unprocessed fixed cells for autofluorescence. In addition, cultured human U937 cells, a promonocytic line, which are larger than thymocytes and possess a prominent MT network were examined using the immunofluorescence technique to serve as a positive control.

5.2.5 Statistical analysis

Unless otherwise stated, all results are presented as the mean (arithmetic) $\pm$ 1 SE. Comparisons were made using a two-tailed t-test, accepting a statistical significance for p of less than 0.05. This was preceded by analysis of data distribution and homogeneity of variance as appropriate.

5.3 RESULTS

5.3.1 Relationship of protein synthesis to TBTO-mediated thymocyte apoptosis

A number of investigators have reported that triorganotins, of intermediate lipophilicity, are potent inhibitors of protein synthesis in a variety of cell types (see section 5.1.3). This series of experiments were designed to evaluate the interrelationship of markers of apoptotic cell death in TBTO-injured thymocytes (see Chapter 3) to protein synthesis, and to compare these observations to the situation of glucocorticoid-mediated apoptosis.

Preliminary studies of cellular [^{3}H]-leucine incorporation, when radiolabel addition was coincident with the test compounds, demonstrated that TBTO had a marked inhibitory effect. However, in order to clearly discriminate early effects on the rate of protein synthesis it was decided to modify the protocol such that cells were prelabelled with [^{3}H]-leucine for 60 minutes prior to the commencement of the various treatments. These experiments showed that protein synthesis was virtually arrested after 10 minutes exposure

to TBTO (Fig. 5.2). No further precursor incorporation was apparent at this treatment level over the period spanning the 30 minute to the 6 h timepoint; at the latter a 32% diminution of radioactive label counted had occurred relative to the 0-hour baseline. Parallel determinations of DNA fragmentation and the incidence of apoptotic cells (morphological observations) in cultures treated with 1 μM TBTO gave mean values of 41 and 36%, respectively, at the 6 h timepoint. Treatment with 0.1 μM TBTO also initially caused a rapid decline in L-leucine incorporation rate, although after 1 h this effect began to reverse.

Inhibition of protein synthesis did occur after exposure to 10 μM MPS (Fig. 5.2). However, the effect profile was very different in this case, whereby precursor incorporation only gradually diverged from the control rate during the last segment of the treatment period. In controls it was noted that the rate of precursor incorporation increased in an essentially linear fashion throughout experimental timecourse.

In order to extend this work, a separate series of experiments was performed in which thymocytes were preincubated with the translational inhibitor CyH prior to addition of TBTO or MPS, and subsequently assessed for markers of apoptosis. A TBTO concentration of 1 μM was selected as an appropriate non-necrotic treatment, and the assessments were made after 6 h. CyH levels previously shown to be effective in abrogating thymocyte apoptosis were selected (Wyllie et al., 1984a; McConkey et al., 1989a). CyH (10 μM) had no significant protective effect on either the TBTO-stimulated increase in DNA fragmentation (Fig. 5.3a) or incidence of apoptotic cells (Fig. 5.3b). As might be expected, 30 or 100 μM CyH was similarly ineffective. In marked contrast, CyH greatly inhibited the extent of DNA fragmentation arising from treatment with 10 μM MPS; causing a reduction in the 6 h mean value of 48.5% to 21.1% (Fig. 5.3a), and a concomitant reduction in the degree of internucleosomal cleavage observable by gel electrophoresis (results not shown). CyH also effected a parallel antagonism on the proportion of MPS-treated cells exhibiting apoptotic morphologies (Fig. 5.3b). During these short-term studies (6 h duration) CyH treatments did not alter the viability or the degree of spontaneous apoptosis in control cultures.

5.3.2 Reduction in cellular ATP levels after TBTO exposure

Since energetics effects, predominantly affecting oxidative phosphorylation, are a principle feature of TBT cytotoxicity (see section 5.1.3), measurements of thymocyte ATP levels were examined in the context of apoptotic and necrotic cell killing by TBTO. Nocodazole, a MT-disrupting agent, was also included in this experimental series (see also 5.3.3).

Rat thymocyte ATP content, as determined by a luciferin-luciferase linked bioluminescence method, at approximately 0.4 fmol/cell was in reasonable accord with the calculated unitary

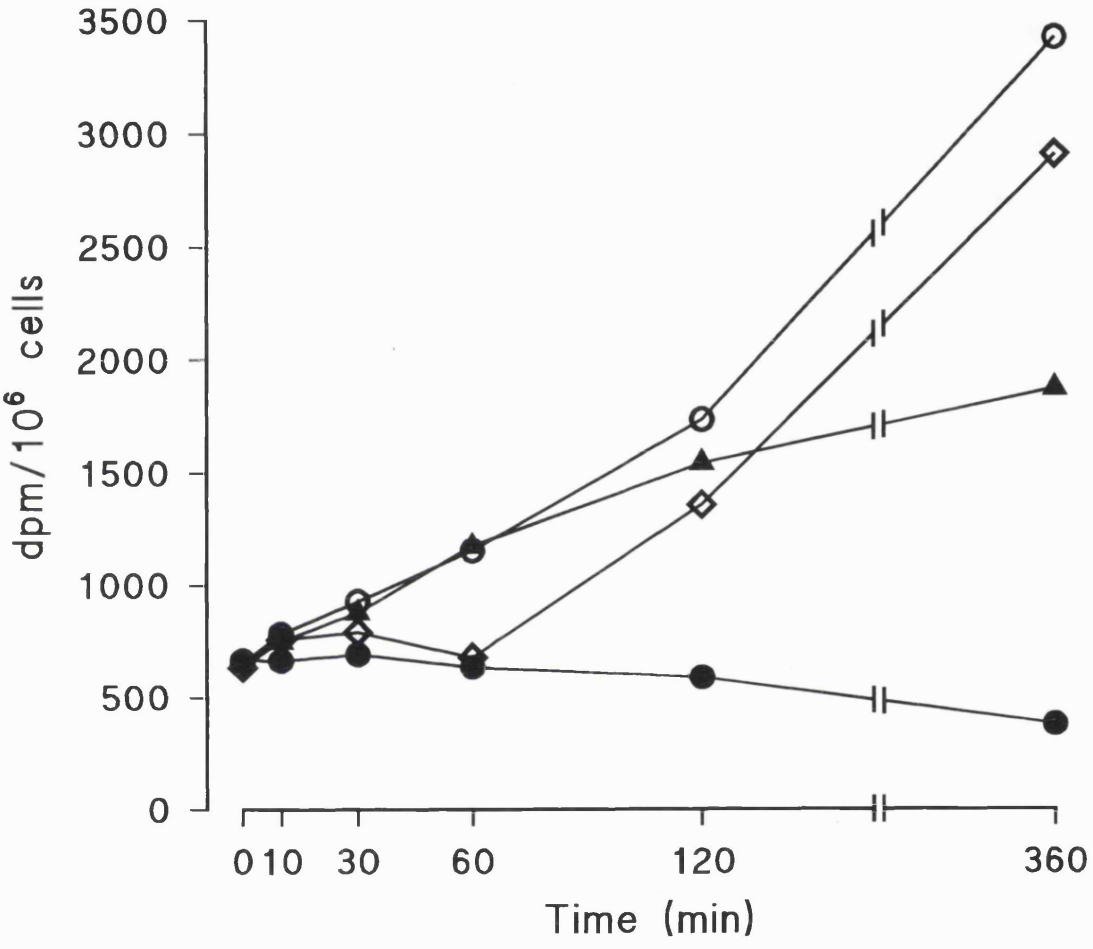

FIGURE 5.2 Effect of TBTO or MPS on protein synthesis.

Thymocytes were prelabelled with [^{3}H]-leucine before incubation in the absence (○) or presence of 0.1 μM (◇) or 1 μM TBTO (●), or MPS 10 μM (▲). At the indicated timepoints after test agent addition, [^{3}H]-leucine incorporation into acid-precipitable material from cells was determined by scintillation counting according to the method described in section 2.9. Results are the means from two experiments.

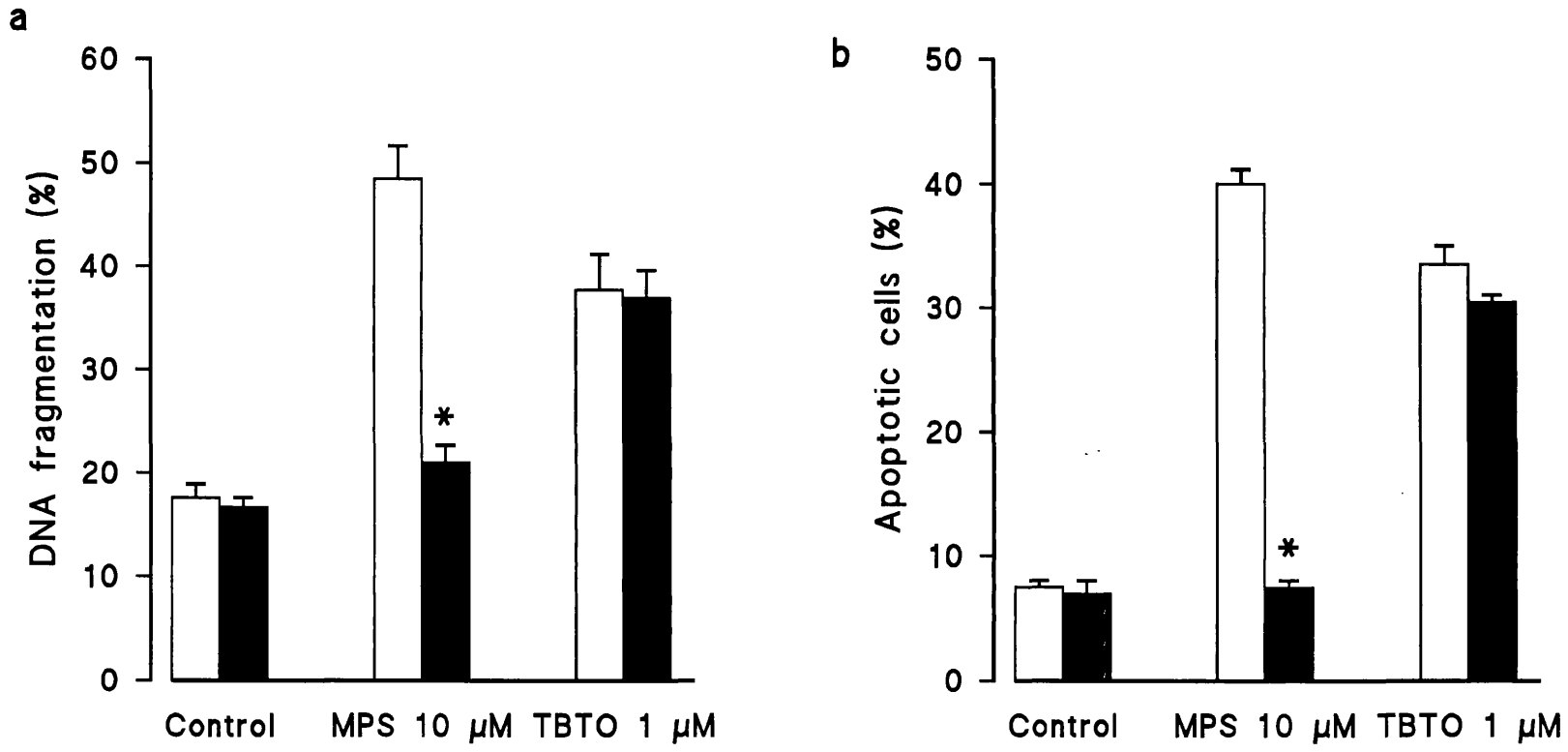

FIGURE 5.3 Comparison of the effect of cycloheximide pretreatment on thymocyte apoptosis activated by TBTO or MPS.
Cells were exposed to the stated concentrations of TBTO or MPS following preincubation without (*open bars*) or with 10 μM cycloheximide (*closed bars).* Results are the means ± SE from three separate experiments. *Significantly different from result in the absence of cycloheximide, $p < 0.05$. Determinations were performed after incubation with the test agents for 6 h. **a** DNA fragmentation (section 2.6). **b** Proportion of thymocytes exhibiting evidence of chromatin condensation (section 2.4.1).

concentration reported by Snoeij, using an alternative enzyme-linked spectrofluorimetric assay (Snoeij, 1987). During the progression of the experimental timecourse, ATP levels in control cultures maintained a consistent steady state (Fig. 5.4). A concentration-dependent decrease in intracellular ATP levels was observed when thymocytes were incubated with graded concentrations of TBTO (Fig. 5.4) in RPMI-1640 medium containing approximately 10 mM D-glucose. ATP depletion was very rapid, with levels showing the greatest relative reduction within 15 minutes from the commencement of treatment. At concentrations of TBTO (5 μM) which produced necrosis (as evidenced by low DNA fragmentation values and the presence of diagnostic morphological markers), ATP levels declined to basal levels and showed no evidence of recovery by 6 h. Exposure to 1 μM TBTO depleted ATP to 18% of the respective control value by 4 h, at which point DNA fragmentation was determined to be 220% of the mean control value. After 6 h at 1 μM TBTO, although the order of ATP depletion approached that in cells exposed to 5 μM, there was a clear disparity between these treatments such that increases in apoptotic markers (DNA fragmentation and chromatin condensation) were confined to the lower concentration only. Exposure to nocodazole caused only limited effects on cellular ATP levels (Fig. 5.4); initially a slight rise was observed, with a slow reduction occurring only after protracted incubation. The latter phase of this biphasic response was recognised to be coincident with the initiation of cell killing by this level of nocodazole.

When thymocytes were incubated with graded concentrations of FCCP (1-10 μM) there was little or no indication that apoptosis was stimulated, since DNA fragmentation values approximated to control levels (Fig. 5.5). Cell viability also remained unaffected for up to 24 h by even the highest concentration of FCCP used (Fig. 5.5). An incidental observation was that from 1-6 h after the commencement of incubations, a moderately high number of these viable cells had a spread appearance when visualised by microscopy.

5.3.3 Characterisation of the mode of nocodazole cytotoxicity to thymocytes in vitro

A number of agents able to disrupt the cellular MT cytoskeleton stimulate apoptosis in a variety of cell types (see 1.5.3 and 5.1.2). One such compound, the antitumour agent nocodazole, has been investigated on a limited basis but not in the context of lymphoid cell apoptosis. The opportunity was taken to investigate its mode of action in the rat thymocyte model.

A graded series of nocodazole concentrations spanning 0.5-100 μM was initially investigated; solubilisation problems arose at or above 100 μM. Introduction of 10-50 μM nocodazole into cultures caused a concentration-dependent loss of viability (Fig. 5.6) that was delayed in onset. The temporal aspects of cell killing were reminiscent of the action of MPS or low TBTO levels, whereby appreciable viability loss took place only 6-24 h after commencement of treatment. During these assessments, it was observed that nocodazole

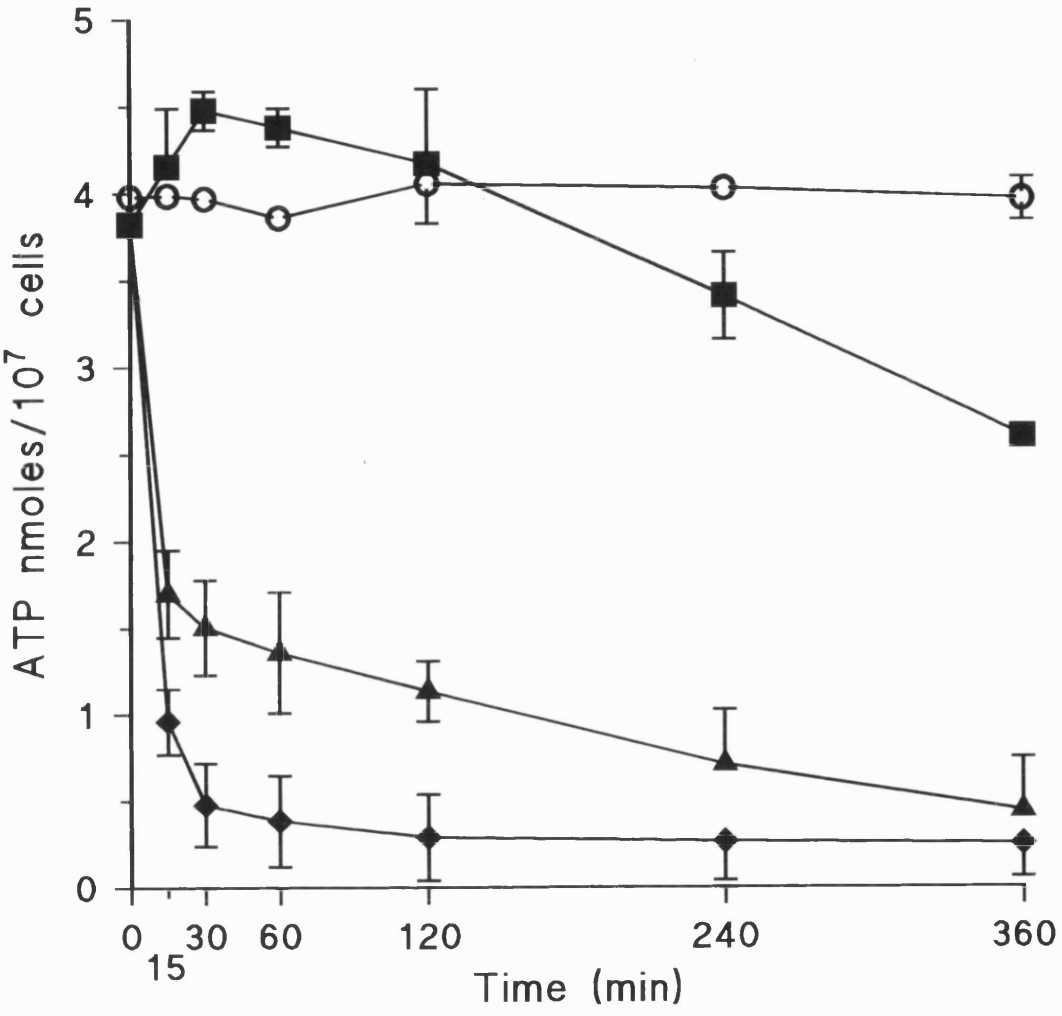

FIGURE 5.4 Intracellular ATP concentrations in thymocytes exposed to TBTO or nocodazole.

Cells were incubated in the absence (○); or presence of 1 μM (▲) or 5 μM TBTO (◆); or nocodazole 50 μM (■). At the indicated timepoints after test agent addition, aliquots of cells were removed and their ATP content determined according to the method described in section 2.10. Results are the means ± SE from three separate experiments.

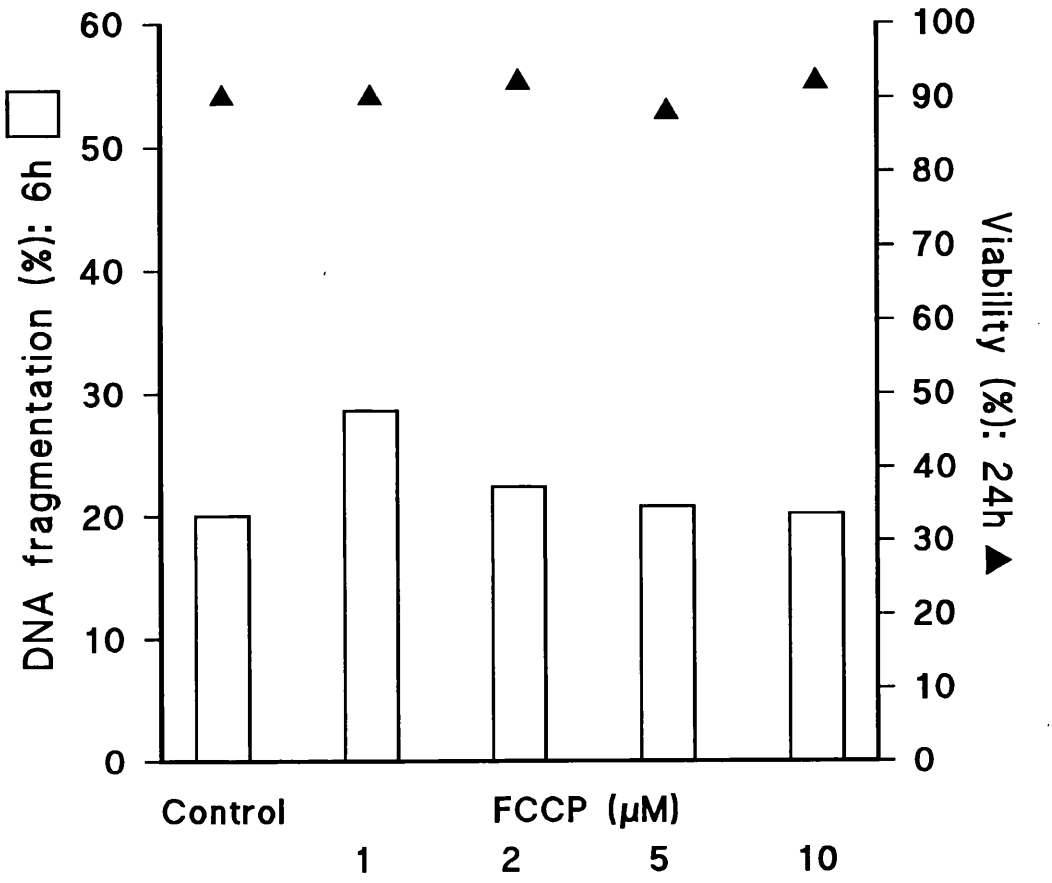

FIGURE 5.5 Effect of FCCP on DNA fragmentation and cell viability.
Cells were exposed to the stated concentrations of FCCP, and determinations made of DNA fragmentation (*open bars*) and cell viability (▲). These assessments were performed after 6 or 24 h respectively, according to the methods described in sections 2.6 and 2.2. Results are from one experiment using means of values from internal sample duplicates.

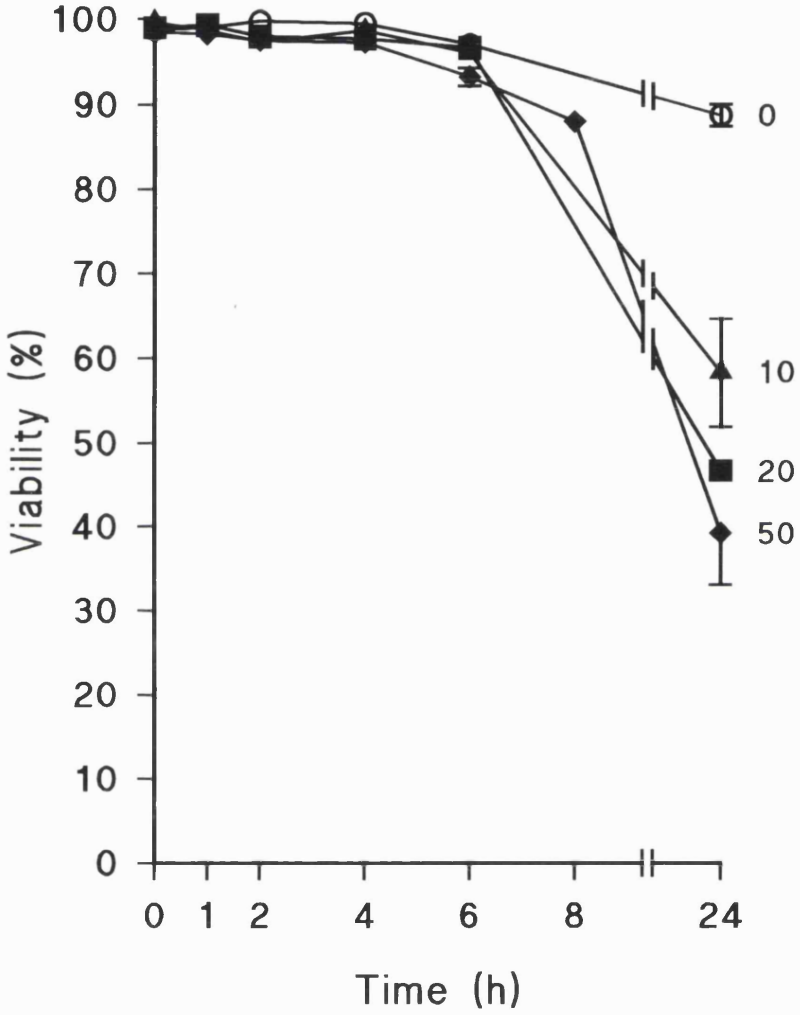

FIGURE 5.6 Effect of nocodazole on thymocyte viability.

Cells were incubated in the absence (○), or presence of the following concentrations of nocodazole: 10 μM (▲), 20 μM (■) or 50 μM (◆). Results are the means ± SE from four separate experiments. Viability was assessed by trypan blue dye exclusion (section 2.2). Determinations were made at 0, 1, 2, 4, 6, and 24 h for all treatment levels and additionally after 8 h in the case of 50 μM nocodazole.

(>1 μM) produced a number of bizarre thymocyte shape changes. Their occurrence was principally restricted to 1-4 h after the start of incubation, and was typified by the presence of a significant proportion of spindle-shaped or smear cells, together with limited cell blebbing at early timepoints. Such cells apparently remained viable and their morphologies normalised with the progression of the exposure periods.

Loss of viability was preceded by extensive DNA fragmentation which showed a clear concentration-dependency (Fig. 5.7a). When corresponding DNA extracts from 27 000 x *g* supernatants, obtained by lysing nocodazole-treated cells, were subjected to agarose gel electrophoresis, the DNA fragments could be discerned as a multimeric series corresponding to 180-200 bp, i.e. an internucleosomal cleavage pattern (Fig. 5.7b).

Examination of toluidine blue stained resin sections of thymocytes exposed to 10-50 μM nocodazole showed increased numbers of cells displaying chromatin condensation and apoptotic body formation (Fig. 5.8a). In concordance with the trypan blue uptake viability estimates, necrotic cell morphologies were essentially absent in the sections prepared after 6 h of incubation.

Figure 5.8b compares the extent of DNA fragmentation and incidence of apoptotic cells 6 h after exposure to 50 μM nocodazole to the corresponding values obtained with benchmark concentrations of MPS and TBTO. Although micromolar quantities of nocodazole caused a substantial stimulation of apoptosis, in equimolar terms it was less active than either of the other two agents.

Studies involving modulation of nocodazole-activated apoptosis were limited to the use of Zn^{2+} as an inhibitor. Pretreatment with 1 mM Zn^{2+} before incubation with 50 μM nocodazole reduced resulting DNA fragmentation to a level comparable to that in controls, and conferred considerable protection against subsequent cell killing (Table 5.2). Electrophoresis of corresponding DNA extracts demonstrated that internucleosomal DNA cleavage had been abolished by Zn^{2+} (not shown). It was noted that inclusion of Zn^{2+} also greatly reduced the appearance of the aberrant cell morphologies at the early stages of nocodazole treatment.

5.3.4 Studies of the effects of TBTO and nocodazole on the microtubule cytoskeleton

As briefly discussed in section 3.3.7, during ultrastructural examination of thymocytes exposed to non-necrotic concentrations of TBTO (0.1-2 μM) unusual filamentous features were evident in some cells. These were most prevalent in the case of TBTO-injured apoptotic cells, but similar structures were also less commonly observed after MPS exposure, though they were very rare in non-apoptotic treated or control cells. The filaments were often, but not exclusively, localised in regions adjacent to cytoplasmic

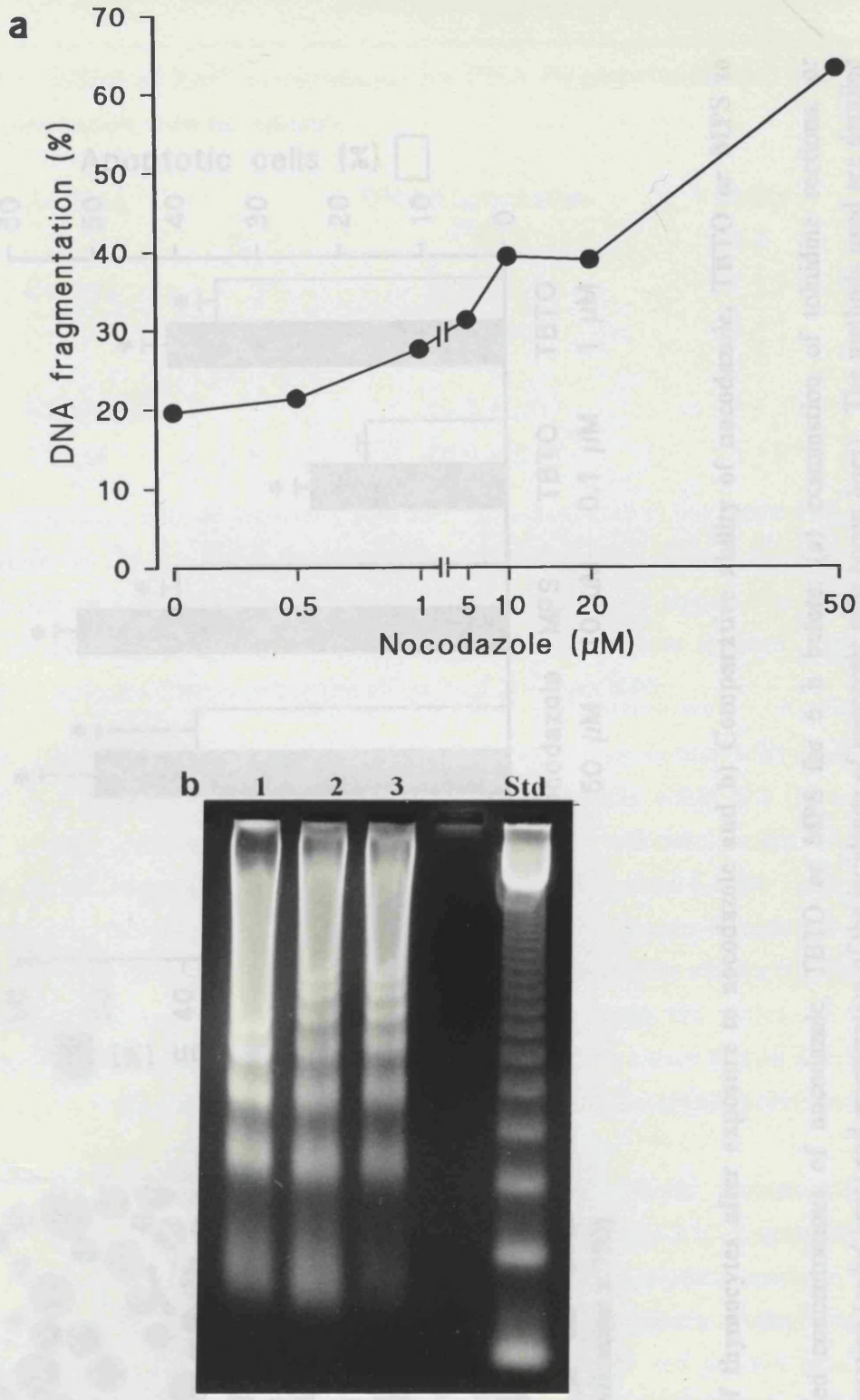

FIGURE 5.7 a) Concentration-response curve of nocodazole-stimulated DNA fragmentation and b) electrophoretic appearance of DNA after nocodazole exposure. a) Thymocytes were exposed to the indicated concentrations of nocodazole for 6 h prior to quantitation of DNA fragmentation (section 2.6). Results are from a single representative experimental series. b) Cellular DNA was isolated from matched aliquots of cells and subjected to gel electrophoresis (section 2.8). The gel tracks shown correspond to the following treatments: (Std) DNA molecular weight calibration standard comprising of 123 bp multimers; (1) 50 μM nocodazole, (2) 100 μM nocodazole, (3) 10 μM MPS. Results are from one experiment that was typical of two replicates.

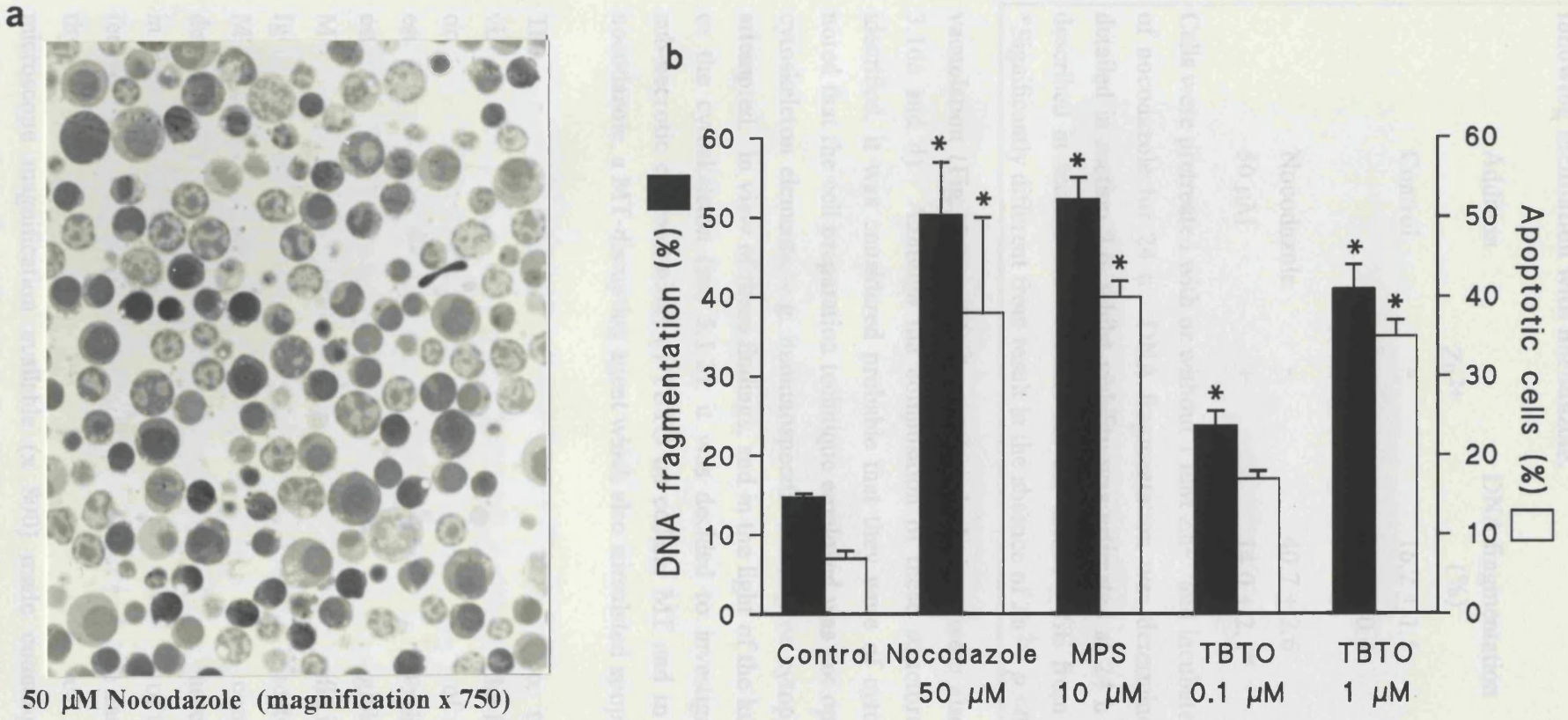

FIGURE 5.8 a) Morphology of thymocytes after exposure to nocodazole and b) Comparative ability of nocodazole, TBTO or MPS to activate thymocyte apoptosis.

Cells were exposed to the stated concentrations of nocodazole, TBTO or MPS for 6 h before: (a) examination of toluidine sections, or (b) determination of DNA fragmentation (*solid bars*) and enumeration of the incidence of apoptotic cells (*open bars*). The methods used are detailed in section 2.4.1 and 2.6. Results are the means ± SE of at least three separate experiments. *Mean value significantly different from control, $p < 0.05$.

TABLE 5.2 Effect of Zn^{2+} pretreatment on DNA fragmentation and cell viability following incubation with nocodazole.

Addition	Zn^{2+}	DNA fragmentation (%)	Viability (%)
Control	-	16.2 ± 1.5	92 ± 1
	+	14.1 ± 0.4	85 ± 2
Nocodazole 50 μM	-	40.7 ± 2.6	49 ± 2
	+	14.0 ± 2.1*	86 ± 6*

Cells were pretreated with or without 1 mM Zn^{2+} and incubated in the absence or presence of nocodazole for 24 h. DNA fragmentation was determined after 6 h by the method detailed in section 2.6, whilst viability was estimated at 24 h by trypan blue exclusion as described in section 2.2. Results are the means ± SE from three separate experiments. *Significantly different from result in the absence of Zn^{2+}, $p < 0.05$

vacuolation (Fig. 5.9). Fibrillar nuclear inclusions were also occasionally evident (Fig. 3.16c and d). Although the composition of these structures could not be definitively identified, it was considered probable that they were of cytoskeletal origin. It must be noted that the cell preparation technique employed was not optimal for the visualisation of cytoskeleton elements, e.g. immunospecific staining or cytoplasmic denudation were not attempted. In view of these findings, and in the light of the known effects of triorganotins or the cytoskeleton (see 5.1.2), it was decided to investigate the action of toxic but sub-necrotic concentrations of TBTO on cellular MT and to relate this to the effects of nocodazole, a MT-disrupting agent which also stimulated apoptosis (see previous section).

The technique selected was based on indirect anti-α tubulin immunofluorescence visualisation of MT. The experimental design focused on the first 3 h of agent exposure in order to interrelate the findings with the first appearance of apoptotic markers, and thus establish whether possible causal relationships existed. Preliminary control experiments established that (i) thymocyte autofluorescence was negligible and did not interfere with MT observation; (ii) fluorescence was absent or non-specific if the anti-α tubulin MAb or IgG-FITC label were omitted; (iii) the method could delineate the MTOC and associated MT network of the U937 cells used as a positive control. Initial investigations demonstrated that it was possible to selectively stain and thereby visualise MTOC and MT in typical rat thymocyte preparations, and that quantitation of the number of such cells was feasible. However, several methodological difficulties were encountered. The small size of thymocytes (approximately 8-10 μm), their non-flattened profile, and the maximum microscope magnification available (x 800) made counting cells rather difficult and time-consuming. In addition, the FITC fluorophore exhibited a rapid fluorescence decay

FIGURE 5.9 Abnormal putative cytoskeletal features in an apoptotic thymocyte treated with TBTO.

Cells were processed for TEM (section 2.5) after incubation for 6h with 1 μM TBTO. Final magnification is indicated within parentheses. Several filamentous structures (*arrow-heads*) are visible within the cytoplasm of the affected cell (x 63 000).

(around 1 minute of satisfactory output after positioning the UV-illumination onto a field) which complicated photomicrography. The latter was partially circumvented by increasing cell dilutions and optimising the working concentration of IgG-FITC antibody. The classification of whether cells possessed a *complete* MT network was inherently subjective, but in practice the marked effect of the both test agents limited this concern.

At up to 3 h after commencement of incubation the majority of control cells had a single MTOC and a linked and extensive array of MT (Fig. 5.10a). In contrast, 1 μM TBTO rapidly disrupted the normal MT cytoskeleton (Fig. 5.10b) which led to a scattered and diffuse cellular staining pattern, in which the perinuclear MTOC was often absent or shortened to a small aster-like structure. The typical appearance of thymocytes after short-term exposure to 50 μM nocodazole is shown in Figure 5.10c; in place of individual MT there were aggregate areas of highly fluorescent but non-filamentous staining localised in the cell periphery. Very few nocodazole-treated cells retained a recognisable MTOC. Quantitation of the incidence of cells with a normal MT network (Table 5.3) revealed that after only 1 h of exposure to TBTO or nocodazole it was possible to classify only a very small proportion of cells into this category—usually less than 5% for both agents. This effect persisted until the 3 h timepoint, though there was normally a slight recovery in the case of TBTO-exposed cells. When thymocytes were preincubated with 1 mM Zn^{2+} for 20 minutes before addition of 1 μM TBTO or 50 μM nocodazole, this disruption was inhibited by a factor of about 2 or 5 fold, respectively (Fig. 5.11). However, for nocodazole this protection only accounted for 33% of cells in absolute terms. An even higher proportion of control cells exhibited well formed MT cytoskeletons in the presence of Zn^{2+}.

TABLE 5.3 Effect of TBTO or nocodazole on the cellular microtubule network.

	Proportion of cells possessing a MTOC and associated microtubule network (%)		
	Control	TBTO 1 μM	Nocodazole 50 μM
Timepoint (h)			
0	62		
1	58	4	4
3	66	10	2

Thymocytes were incubated in the absence or presence of 1 μM TBTO or 50 μM nocodazole for the stated periods. The incidence of cells exhibiting a MTOC and an associated microtubule array (judged to be complete) was then scored using the fluorescence technique described in section 5.2.4. Results are the means of triplicate determinations from a single representative experiment.

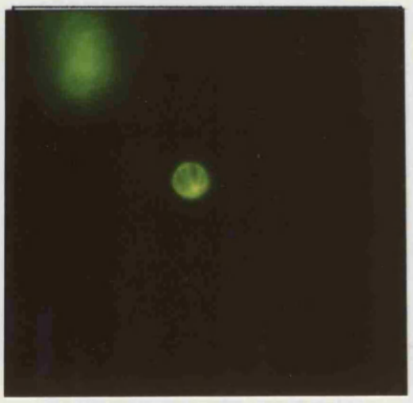

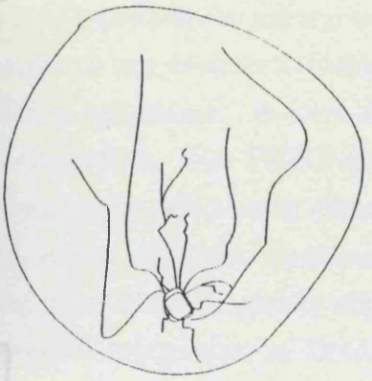

a) Control: extensive array of microtubules extending from perinuclear MTOC. Minimal staining present in extreme cytoplasmic periphery.

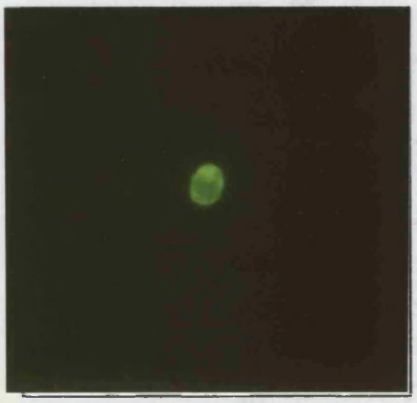

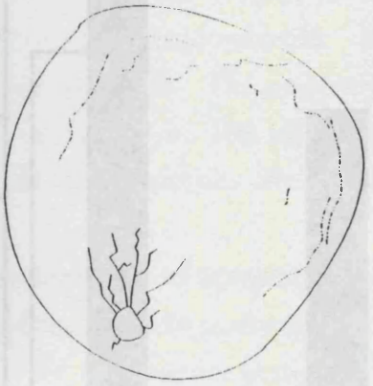

b) TBTO 1 μM: Microtubule array either absent or shortened to aster-like structure. Diffuse fluorescent staining in poorly ordered forms in the outer cytoplasm.

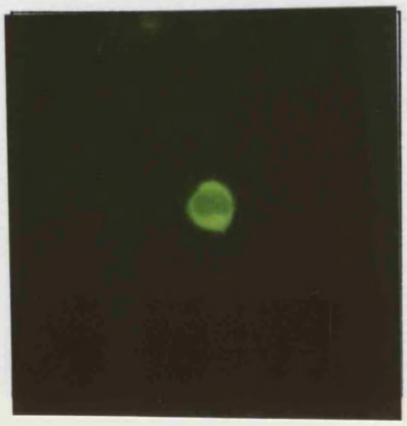

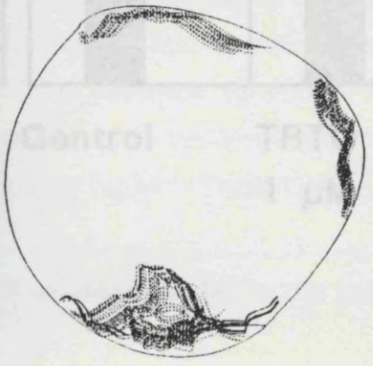

c) Nocodazole 50 μM: Little or no evidence of organised microtubular cytoskeleton. Disorganised areas of staining, some highly fluorescent, adjacent to cell periphery and particularly evident in polar regions.

FIGURE 5.10 Appearance of thymocyte microtubule cytoskeleton after treatment with TBTO or nocodazole.

Cells were treated for 2 h with the test agents and photomicrographs (original magnifications x 800) were obtained following anti-α tubulin directed fluorescence staining (see section 5.2.4). Diagrammatic representations of typical cellular microtubule cytoskeletons observed after the respective treatments are also shown to assist interpretation.

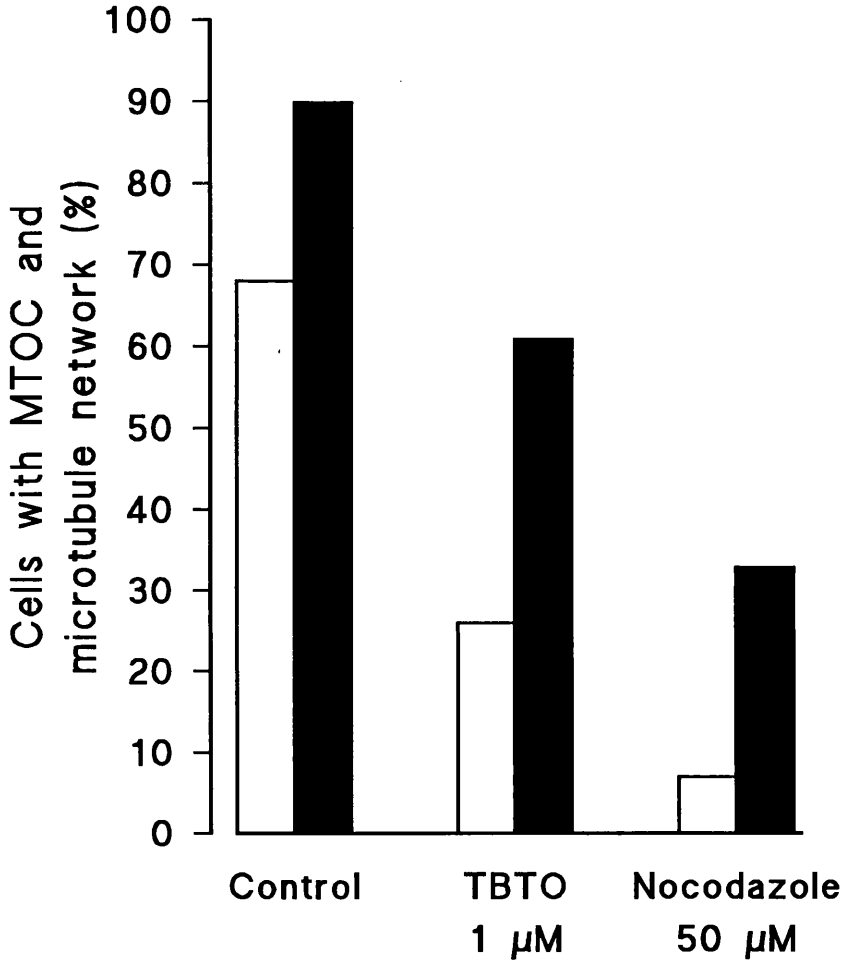

FIGURE 5.11 Effect of Zn^{2+} on microtubule disruption produced by TBTO or nocodazole.

Cells were preincubated without (*open bars*) or with 1 mM Zn^{2+} (*solid bars*) prior to treatment with TBTO or nocodazole for 3 h. The proportion of cells exhibiting a MTOC and a complete associated microtubule network was then scored using the fluorescence technique described in section 5.2.4. Results are the means of triplicate determinations from a single experiment that was typical of two replicates.

Supplementary inhibitor studies, of a preliminary nature, were conducted using taxol A, an agent able to stabilise MT, in order to test whether cytoskeleton disruption is central to the activation of apoptosis by TBTO or nocodazole. A level of 100 μM taxol approximated to the solubility limit in RPMI-1640 medium. The TBTO concentration selected (2 μM) had previously been shown to be maximally effective in stimulating apoptosis. Pretreatment with taxol did not affect the extent of DNA fragmentation in TBTO-exposed cells, although long term viability may have been marginally improved at the higher taxol levels (Fig. 5.12). However, a substantial antagonism of DNA fragmentation was detected in taxol-pretreated cultures subsequently exposed to 50 μM nocodazole (Fig. 5.12). Protection against delayed viability loss due to nocodazole cytotoxicity was also evident. During the microscopy assessments of trypan blue exclusion, it was noted that taxol greatly diminished the usual increase in aberrant cellular morphologies, e.g. spindle-shapes normally associated with the presence of nocodazole. No similar reversal of abnormal profiles was noted in TBTO-exposed cells. The presence of 30 μM taxol had no major effect on control parameters, though 60 or 100 μM caused minimal increases in DNA fragmentation and also a slight decline in viability after 24 h in culture.

5.3.5 Flow cytofluorimetric assessments of apoptotic thymocyte populations

Flow cytometry is increasingly being used to probe modes of cell death, and it can also be applied to analysis of the cell cycle; a parameter perturbed by some apoptotic stimuli. Cell cycle analysis of unfractionated freshly isolated thymocytes indicated that mean cycle distributions were G_0/G_1 phase, 91%; S phase, 5% and G_2/M phase, 4% (n=3). Although data on Wistar rat thymocyte cell cycle fractional duration is lacking, Baron and Penit (1990) previously established timings for murine cells as: total cycle, 10 h; S phase, 6.5 h; and both G_1 and G_2/M, 1.5 h. In thymocytes exposed to TBTO for up to 24 h, there was no evidence that concentrations known to produce apoptosis (1-2 μM) caused blockade at any cell cycle phase, including G_2/M (Table 5.4).

TABLE 5.4 Effect of TBTO or nocodazole on the proportion of cells in the G_2/M phase of the cell cycle.

	Cells in G_2/M (%)		
	Control	TBTO 1 μM	Nocodazole 50 μM
Timepoint (h)			
6	4	5	11
24	3	5	3

Thymocytes were incubated in the absence or presence of 1 μM TBTO or 50 μM nocodazole prior to examination of relative cellular DNA content by flow cytofluorography (section 2.11). Results are the means of three separate experiments.

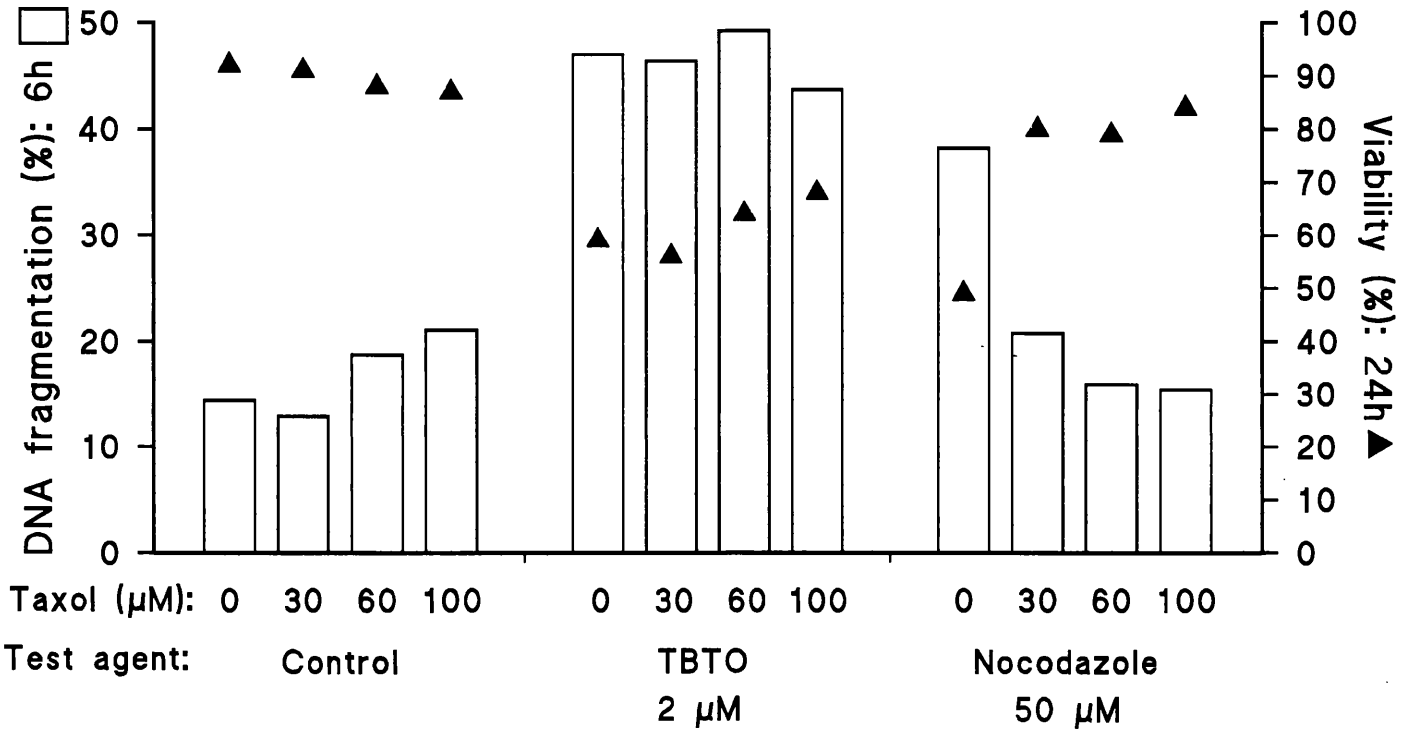

FIGURE 5.12 Effect of taxol on DNA fragmentation and viability loss after TBTO or nocodazole treatment.

Cells were exposed to TBTO or nocodazole following preincubation with taxol at the concentrations indicated. DNA fragmentation (*open bars*) was determined after 6 h according to the method given in section 2.6, whilst cell viability (▲) was estimated after 24 h by the method detailed in section 2.2. Results are the means from two separate experiments.

An increase in the proportion of cells in G_2/M phase was noted, at intermediate timepoints only, with 50 μM nocodazole.

Examination of DNA histograms from untreated cells revealed that after protracted incubation (8-24 h) a nuclear population appeared in the sub-G_0/G_1 region, i.e. was hypodiploid in character (Fig. 5.13), which had a quantitative correspondence with the proportion of apoptotic cells present (see 3.3.6). This change was accompanied by a left shift in FSC profile. TBTO (1-2 μM) provoked similar cumulative but more pronounced alterations that occurred at earlier timepoints (Fig. 5.14). There was however, rather a high degree of variation in the yield and timecourse of appearance of hypodiploid events after standardised TBTO exposures, such that values correlated rather poorly with other assessments of apoptotic cell prevalence e.g. DNA fragmentation and morphological estimates. Since similar anomalous results arose after MPS treatment, this may have related to methodological artefacts. These parameters were unaffected at all timepoints when cells were treated with higher concentrations of TBTO (5 μM). Hypodiploidy and mean FSC intensity reduction was most evident and reproducible with 50 μM nocodazole (Fig. 5.15). Irrespective of the test compound employed, preincubation of thymocytes with Zn^{2+} (1mM) for 20 minutes prior to commencement of treatment greatly reduced or eliminated both hypodiploidy and FSC shift (results not shown).

5.4 DISCUSSION

In agreement with previously published findings (Snoeij et al., 1986b; 1986c), TBT virtually abolished amino acid precursor incorporation into thymocyte proteins within 10 minutes of exposure, and caused a persistent and total inhibition for the remainder of the incubation period (Fig. 5.2). From the rapidity of onset it was concluded that the effect locus was *de novo* protein synthesis, though it is acknowledged that the experimental protocol did not investigate secondary factors that could also have been influenced by TBT, e.g. rate of precursor uptake or leakage, precursor pool size, or differences in protein turnover. The eventual loss of radioactive label from TBTO-treated cells (Fig. 5.2) may represent catabolism of proteins synthesised during the pretreatment period. MPS inhibition of protein synthesis was dissimilar in nature, as it occurred later and coincided with the onset of apoptosis. With allowance for averaging effects over an unseparated population, it was considered to be consistent with the arrest of biosynthesis in individual apoptotic cells reported following glucocorticoid exposure (Wyllie and Morris, 1982).

The finding that apoptotic cell death could still be activated by TBTO at a concentration (1 μM) which apparently completely inhibited protein synthesis, contrasted with the vast majority of previous reports on other agents in the rodent thymocyte model, and therefore ran contrary to established dogma (see section 5.1.1). However, the possibility that the precursor incorporation technique was insufficiently sensitive to detect brief expression of a

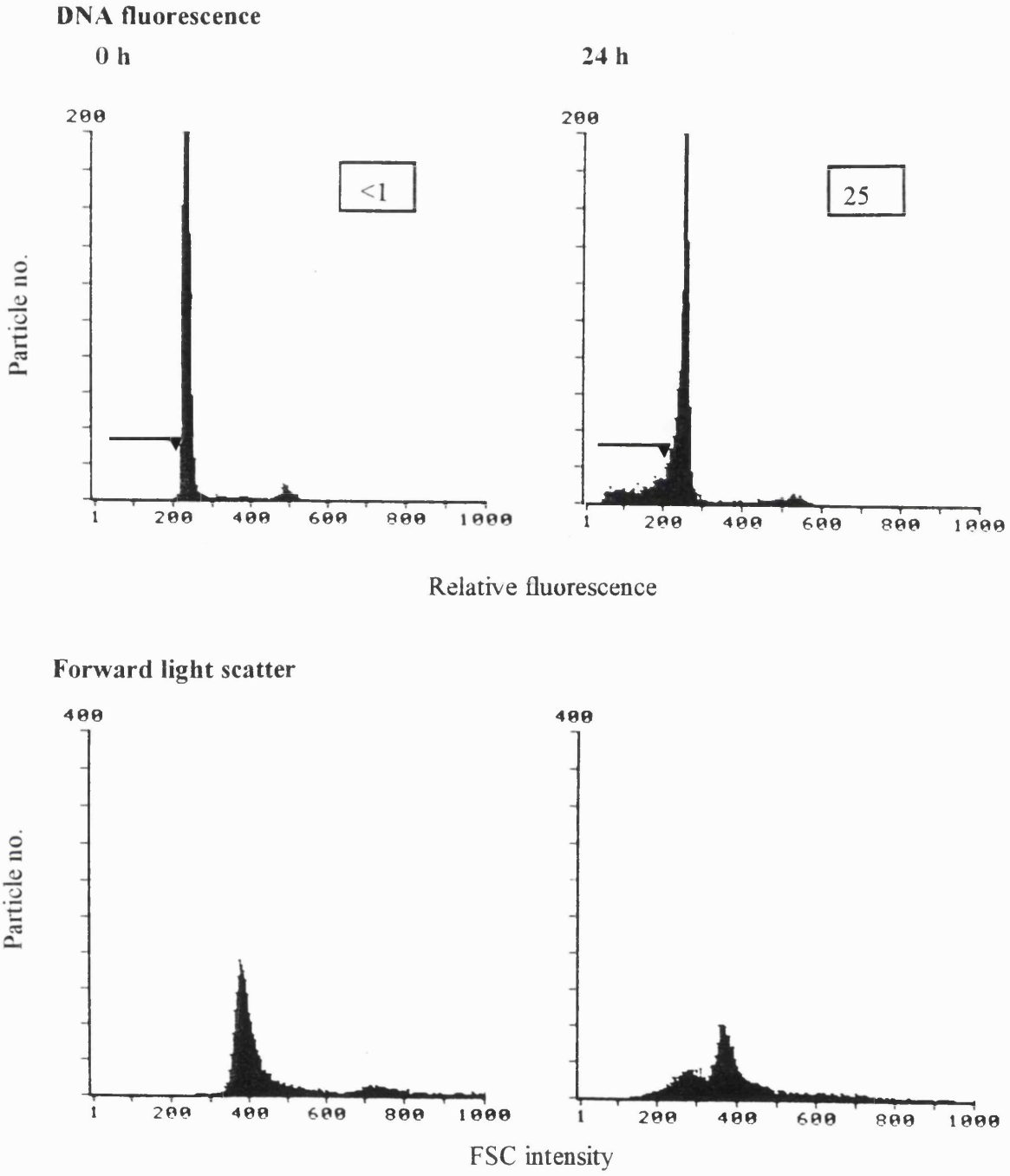

FIGURE 5.13 Spontaneous alteration in DNA fluorescence and forward light scatter profile of thymocytes after long term culture.

Aliquots of cells were obtained at commencement of incubations or after 24 h untreated in culture, stained with ethidium bromide, and subjected to flow cytometric analysis as detailed in section 2.11. Results are expressed as the number of counted events versus either relative fluorescence or forward light scatter and are from one experiment typical of three replicates. The boxed insets indicate hypodiploid events (region delineated by bar) as a percentage of total counted particles.

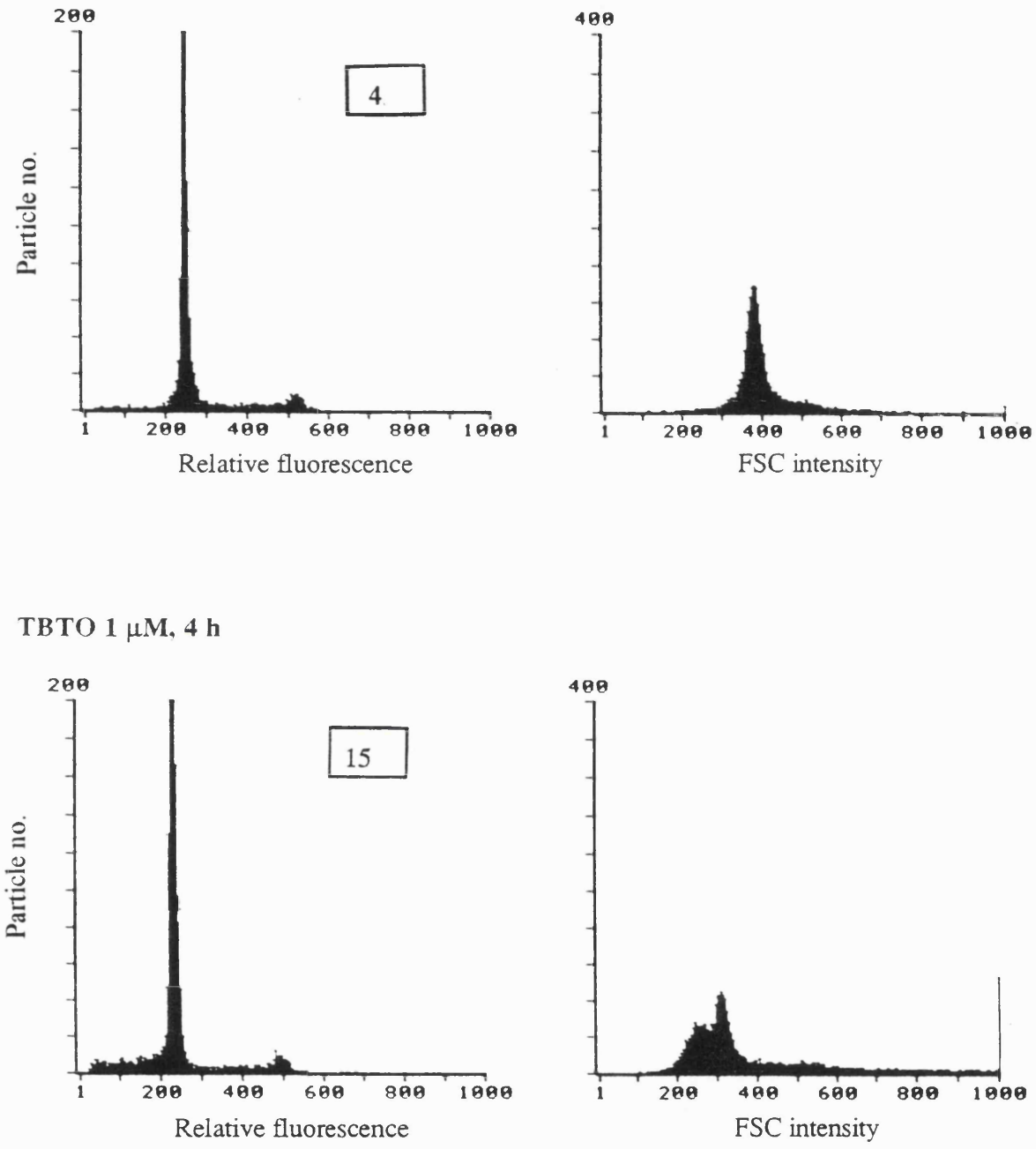

FIGURE 5.14 Effect of TBTO on DNA fluorescence and forward light scatter.
After their respective treatments as indicated, thymocytes were subjected to flow cytofluorographic analysis as detailed in section 2.11. Results are expressed as the number of counted events versus either relative fluorescence or forward light scatter and are from a single representative experiment. The boxed insets indicate hypodiploid events as a percentage of total counted particles.

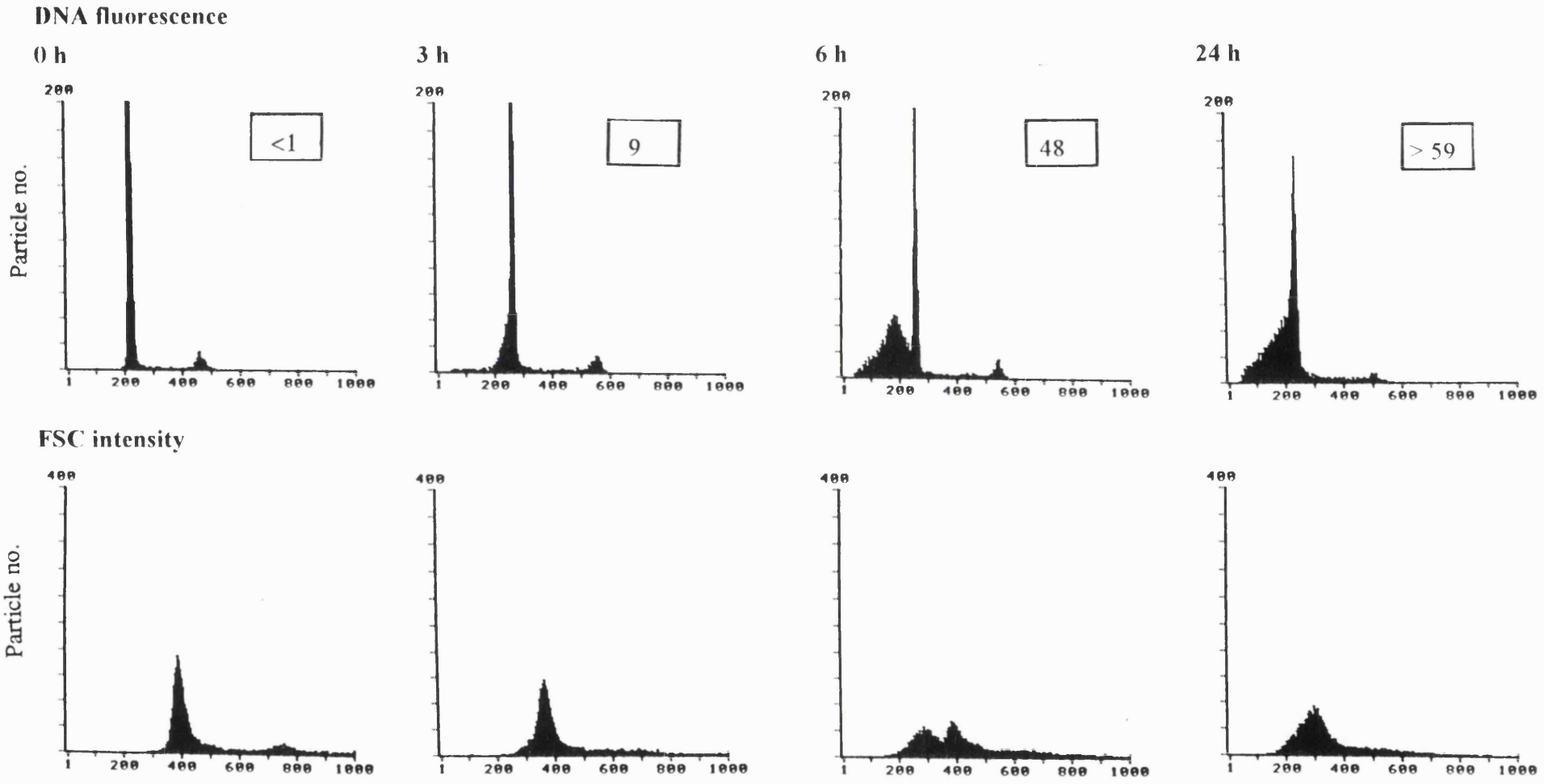

FIGURE 5.15 Timecourse of alteration in DNA fluorescence and forward light scatter profiles of thymocytes treated with nocodazole.
After incubation with 50 μM nocodazole for the designated periods, thymocytes were subjected to flow cytometric analysis as detailed in section 2.11. Results are expressed as the number of counted events versus either relative fluorescence or forward light scatter and are from one experiment typical of three replicates. Boxed insets indicate the calculated percentage of hypodiploid events.

key protein, for example an endonuclease, could not be excluded. As a technique like high specific activity [^{35}S]-methionine protein labelling and electrophoretic separation was unavailable, it was decided to further assess the protein synthesis independency of TBT-mediated apoptosis using the potent translational inhibitor cycloheximide (CyH). In contrast to its effect on MPS cytolethality, CyH conferred no protection against the stimulation of DNA fragmentation by 1 μM TBTO or the appearance of apoptotic cells (Fig. 5.3a and b). On the basis of this confirmatory evidence, it was concluded that TBT-activated thymocyte apoptosis was protein synthesis independent and biochemically disparate to that induced by glucocorticoids. The CyH concentrations used were equivalent to those shown by other investigators to be effective in abrogating thymocyte apoptosis following glucocorticoid or cation ionophore exposure (Wyllie et al., 1984a; McConkey et al., 1989a), though it should be noted that under such conditions amino acid incorporation was not completely inhibited. This illustrates the need to use adjunctive measurements of protein synthesis before definitive statements are made regarding the macromolecular synthesis dependency of apoptosis.

At the time the experimental phase of this work was completed, the failure of transcriptional and translational inhibitors to protect cells following hyperthermia (Sellins and Cohen, 1991a) appeared to be the only other definitively established instance where macromolecular synthesis was not a prerequisite for rodent thymocyte apoptosis, though DNA fragmentation still developed in thymocytes after exposure to levels of gliotoxin that strongly inhibited, but did not eliminate, translational activity in T blasts (Waring, 1990). It has been postulated that thymocyte apoptosis may require production of Ca^{2+} transport proteins (McConkey et al., 1989b) or resynthesis of an endogenous endonuclease in rapid turnover (McConkey et al., 1990b). In other cell types, macromolecular synthesis may be a prerequisite to priming cells previously lacking the constitutive effector components required for apoptosis (Arends and Wyllie, 1991), or in allowing progression to a critical cell cycle phase before death occurs (Sorenson et al., 1990). It could be argued that protein synthesis is not required in the case of TBT, since it is known to directly open plasma membrane Ca^{2+} channels (Aw et al., 1990) thus circumventing the requirement for the involvement of new proteins in signal transduction of Ca^{2+} fluxes. However this rationale is inconsistent with the protein synthesis dependency of thymocyte apoptosis triggered by calcium ionophores (Wyllie et al., 1984a; McConkey et al., 1989a), and sheds no light on the cases of hyperthermia or gliotoxin. Likewise it is difficult to envisage how the demonstrable protracted and incremental TBT stimulation of chromatin cleavage could be reconciled with the involvement of an endonuclease undergoing rapid turnover, particularly as triorganotins have not been reported to directly inhibit proteases. Therefore, the profound and sustained inhibition of protein synthesis caused by TBTO, and the observation that DNA fragmentation was gradual in onset, make it more likely that the effector enzyme concerned is normally expressed in thymocytes and is not subject to rapid

turnover. TBT might simply inhibit the synthesis of a labile suppressor protein acting to check a constitutive apoptotic effector. However, such a model must accommodate the observations that TBT-stimulated DNA fragmentation occurs rapidly, and that short-term CyH treatment alone is ineffective in activating thymocyte apoptosis. Flow cytometric results discussed later, preclude the involvement of a critical cell cycle phase or cell cycle blockade in the activation-induced cell death of thymocytes caused by TBT.

In common with some other mitochondria-directed agents (Morimoto et al., 1990), submicromolar concentrations of TBT can induce heat shock proteins such as hsp70 and hsp89 (Zhang and Lui, 1992; Cochrane et al., 1991). Upregulation of certain hsp genes has been observed during initiation of apoptosis (Lockshin and Zakeri, 1991), though heat shock, involving hsp70 and hsp100 expression, can protect thymocytes from apoptosis caused by glucocorticoids or cation ionophores whilst paradoxically stimulating apoptosis itself (Migliorati et al., 1992). The significance of these findings to TBT-mediated thymocyte killing is unclear, but the ablation of protein synthesis by 1 μM TBTO would seem to preclude an important role.

The emphasis placed on the 'energetics poison' effects of TBT has previously been stated (section 5.1.3), and the observations of mitochondrial abnormality in thymocytes exposed to TBTO in vitro, viz. organelle swelling, has been described in section 3.3.7. Treatment with either 1 or 5 μM TBTO caused a rapid and marked depletion of cellular ATP (Fig. 5.4) which presumably related to the inhibition of oxidative phosphorylation. However, it is notable that the appearance of apoptotic markers after exposure to 1 μM TBTO (refer to 5.3.2) was not dependent on conserved ATP levels . This conflicts with the generally referenced belief that conservation of cellular energetics function is required in apoptosis due its active nature (see section 5.1.1; Bowen and Bowen, 1990; Cotter et al., 1990; Fesus et al., 1991). It is highly probable that basal energetics function is necessary to allow apoptotic cell killing, since otherwise complete loss of internal cation homeostasis would result in the interruption of critical active processes. In the case of TBT-mediated apoptosis in thymocytes, a relatively metabolically inactive cell type, it is apparent that although oxidative phosphorylation is severely inhibited, the energy supplied by glycolysis must be adequate for activation of this death mode. Nonenergy consuming (*sic*) apoptosis has occasionally been cited, e.g. human CEM lymphocytes were not protected from novobiocin-mediated apoptosis by azide (Alnemri and Litwack, 1990).

As Snoeij et al. (1986c) demonstrated, severe depression of thymocyte intracellular ATP levels by short-term incubation with various energetics poisons (e.g. FCCP or 2,4-dinitrophenol) or anoxia, did not affect cell survival. Hence it is unlikely that an equivalent inhibition of oxidative metabolism by TBT is in itself a cytolethal event. This is further borne out by the lack of correlation between thymocyte ATP levels at 1 or 5 μM TBTO

(Fig. 5.4) and data on cell viability (mean values of 90 or 31%, respectively, at 6 h). In various cell types severe depletion of the intracellular ATP pool does not correlate with necrosis until univalent ion/Ca^{2+} homeostasis becomes disturbed (Trump and Berezesky, 1984), and the absence of extracellular Ca^{2+}, or use of Ca^{2+} channel blockers can be cytoprotective in such circumstances. In a previous report, incubation of thymocytes with 1 μM FCCP, a relatively specific uncoupler, for 1 h in PBS/glucose depleted ATP to 15% of normal (Snoeij et al., 1986c). Therefore the preliminary findings described here on the absence of stimulation of apoptosis by equivalent or higher FCCP concentrations (Fig. 5.5), suggest that ATP depletion *per se* is not an apoptotic triggering stimulus. FCCP appeared to have little or no effect on viability up to 24 h, essentially precluding the possibility that substantially delayed cell death was invoked by this agent. The kinetics of the early and marked reduction in intracellular ATP concentration observed with either 1 or 5 μM TBTO were quite similar, and it is evident that other events dictate whether the cell dies by apoptosis or necrosis. As discussed previously, these may centre on $[Ca^{2+}]_i$ flux signalling at apoptotic concentrations of TBT, or translocase inhibition and ion homeostasis breakdown in the case of TBT-mediated necrosis.

TBT facilitates Cl^- uptake into mitochondria (see 5.1.3) thereby producing pH clamping across the mitochondrial membrane and inhibiting proton pumping. This lowers internal mitochondrial pH (Aldridge, 1976) and has the potential to shift cytosolic pH upward. The impact of similar pH changes on the activation of apoptosis has been little studied, but since the potent uncoupler of oxidative phosphorylation FCCP produces equivalent alterations (Maro et al., 1982), yet has been shown here not to provoke apoptosis, these phenomena are unlikely to be significant. Contrary reasoning, presently untested, is that TBT could cause cellular acidification due to the accumulation both of lactate converted from pyruvate, and inorganic phosphate arising from ATP depletion (Snoeij et al., 1987; Dr Andre Penninks, personal communication). In HL-60 cells, diminution of intracellular pH, rather than $[Ca^{2+}]_i$ flux, stimulates endonucleolytic DNA cleavage (Barry and Eastman, 1992). If this is a general apoptotic trigger, then this effect may be of relevance to the thymocyte model. However, these notions are speculative, and the whole area of triorganotin-modulated intracellular pH changes clearly requires more investigation.

Apoptosis resulting from nocodazole-mediated MT disruption has been observed in the promyelocytic HL-60 cell line (Martin and Cotter, 1990). In the work described here, there was indirect evidence that nocodazole ($\geqq$ 1 μM) caused cytoskeleton disruption in thymocytes, since an early finding was the loss of normal cell morphology and appearance of aberrant forms. This effect was followed by DNA fragmentation (Fig. 5.7a), and electrophoresis demonstrated that extensive internucleosomal cleavage had occurred (Fig. 5.7b). Conclusive evidence that nocodazole-actuated thymocyte apoptosis was derived from morphological assessments which showed increased numbers of cells that exhibited

chromatin condensation and apoptotic body formation (Fig. 5.8a and b), whilst necrotic cells were essentially absent at up to 100 μM nocodazole. As typical of the inhibition of apoptosis by other agents (see chapter 4), pretreatment with Zn^{2+} prior to addition of nocodazole abrogated DNA fragmentation and protected against latent cytolethality (Table 5.2). Together these findings indicate that rat thymocytes are sensitive to nocodazole-activated apoptosis, and that this agent gives a usefully consistent response.

Although poorly studied to date, a number of investigations have shown that alteration or disruption of the intracellular microtubular network can activate apoptosis in a variety of cell types, including those of lymphoid lineage. As described above, the MT-disruptor nocodazole is readily able to trigger apoptotic killing of rat thymocytes. The question arose as to whether such an effect locus could also be relevant in the case of TBT-stimulated thymocyte apoptosis. MT preparations in vitro are depolymerised by increased Ca^{2+} concentrations (Nishida, 1978), and Ca^{2+}/calmodulin complexes produce similar disruption in vivo (Keith et al., 1985). Since a major effect of TBT is to raise $[Ca^{2+}]_i$, this in tandem with the known direct effects of TBT on the cytoskeleton (see 5.1.2) provided a possible rationale for such a hypothesis. Cytoskeletal changes were considered to be the likely basis for the aberrant cell shapes observed at apoptotic TBT concentrations (see section 3.3.2). The abnormal putative cytoskeletal elements seen in TBTO-injured thymocytes were very similar to those previously reported in cells dying by apoptosis (Wyllie et al., 1984a; 1984b), but could not be definitively identified as microtubular. However, they were commonly co-located with cell organelles (Fig. 5.9), and it should be noted that MT are associated with such structures (Alberts et al., 1989). Other investigators have suggested that the arrays observed in apposition to mitochondria in apoptotic lymphocytes after exposure to toxicants such as colchicine are 'alternative' adaptive cytoskeletons composed of vimentin intermediate filaments (Allen, 1987).

An immunocytochemical method of probing the cellular MT cytoskeleton was chosen in preference to assays of in vitro [^{3}H]-colchicine binding, viscometric or turbidimetric tubulin assessment, or TEM studies, since it allowed direct observations on living cells and easy interrelation with other parameters, i.e. viability and apoptotic markers. The somewhat subjective nature of the technique should be recognised, and improved methods are now available based on immunofluorescence flow cytometry. Both TBTO (1 μM) and nocodazole (50 μM) markedly and persistently disrupted the normal thymocyte MT network, such that approximately comparable numbers of cells were affected (Table 5.3). However, there were clear qualitative differences between the nature of the changes produced by TBT and nocodazole (Fig. 5.10b and c). Nocodazole caused massive depolymerisation and redistribution of tubulin to the cell periphery, whereas in TBTO-treated cells tubulin staining was more diffuse, and a few thymocytes retained a vestigial MTOC. It was surmised that this indicated a probable difference in the respective

mechanisms of action. In the case of both agents, MT disruption was rapid since it occurred within 1 hour, and it therefore preceded the appearance of apoptotic cells (Fig. 3.12; Fig. 5.8b). Zinc has been shown to stabilise MT preparations (Hesketh, 1984), and inhibit subsequent DNA degradation in cold-shocked fibroblasts which may have suffered depolymerisation of the microtubular cytoskeleton (Nagle et al., 1990). Zinc pretreatment conferred some protection against TBT or nocodazole-mediated thymocyte MT disruption (Fig. 5.11). Whilst this phenomenon is of interest, and illustrates the pleomorphic effects of Zn^{2+} at high concentrations, it does not necessarily mean that there is a basis for linkage of this inhibition to the antagonism by Zn^{2+} of apoptosis caused by TBT or nocodazole. At least in the case of nocodazole, the absolute number of cells protected against loss of the MT network was inconsistent with the high degree of protection afforded by Zn^{2+} against subsequent delayed cell killing. It is much more likely that the anti-apoptotic effect of zinc relates to its nuclear action in preventing extensive endonucleolytic DNA cleavage. However, this area probably merits further study, particularly in the light of the report that another MT stabilising agent, deuterium oxide, prevented apoptosis in thymocytes exposed to γ-irradiation or glucocorticoids, but was ineffective in inhibiting Ca^{2+}/Mg^{2+}-nuclease activity (Matylevich et al., 1991).

In an attempt to establish whether MT disruption by either TBT or nocodazole was causal to subsequent apoptotic cell killing, preliminary inhibitor experiments were performed using the MT-stabilising agent taxol. It has been reported that there appears to be a receptor site for taxol on tubulin, and after binding, taxol reduces the critical concentration of tubulin required to enable assembly and can prevent depolymerisation of formed MT by Ca^{2+}, cold-shock, or agents such as colchicine or nocodazole (Schiff et al., 1979; Manfredi and Horwitz, 1986). The taxol concentrations selected for this work were in excess of those required for stoichiometric receptor saturation, but in the region of those found to be effective against the more potent MT-disrupting agents. Taxol had no effect on TBTO-potentiated DNA fragmentation and delayed viability loss, but it inhibited both these parameters in the case of thymocytes treated with 50 μM nocodazole (Fig. 5.12). Whilst this appears to be an important finding, these results require further replication, and the evaluation of a full spectrum of apoptotic markers in tandem with an objective assessment of taxol on cellular MT status. Based on the above results, and given the known specificity in the action of nocodazole, it seems likely that the MT effects of this compound are responsible for the resultant apoptosis observed in thymocytes, and make it likely that a similar causal relationship exists for analogous non-necrotic cell killing in other systems (Martin and Cotter, 1990). Since taxol does not inhibit TBT-mediated DNA fragmentation and latent viability loss, it is improbable that this locus is important in the actuation of apoptosis by this agent.

Consideration of the possible biochemical mechanisms of TBT-induced MT disruption is

appropriate at this point. Cellular energetics inhibition by TBT is unlikely to be its mode of action, since ATP depletion by azide treatment does not affect the organisation of cellular MT (De Brabander et al., 1980). FCCP, a compound with quite similar effects to TBT on mitochondrial function , is thought to depolymerise MT by increasing intracellular pH and impairing the binding of microtubule-associated proteins (Maro et al., 1982). However, the action of TBT is probably more complex. At micromolar concentrations, triorganotins bind to tubulin and may interfere with the polymerisation of new MT structures (Tan et al., 1978). In addition, TBT can depolymerise lymphocyte F-actin, by a mechanism postulated to involve direct binding, since it can be reversed by use of membrane-permeable dithiol protectants, or thiol group blockade (Dr Sec Chow, personal communication). It is notable that many agents with protein sulphydryl group reactivity possess antimicrotubular activity (Pfeifer and Irons, 1983). The physiological dynamic equilibrium of MT is thought to be partially regulated by Ca^{2+} concentration fluctuations, and micromolar concentrations can inhibit MT formation (Keith et al., 1985) in vivo. These investigators demonstrated that microinjection of 1 mM Ca^{2+} into cells is ineffective in disrupting the existing MT skeleton (Keith et al., 1985), although Ca^{2+}-saturated calmodulin is more effective, suggesting a possible role for localised calmodulin-bound calcium in effect transduction. Apoptotic TBT concentrations increase $[Ca^{2+}]_i$ to the region of 1-2 μM (Chow et al., 1992), and therefore could potentially cause some inhibition of tubulin polymerisation. However, this is a relatively modest increase in $[Ca^{2+}]_i$, and in vitro, similar levels of Ca^{2+} provoked only slight inhibition of MT assembly even when potentiated by non-physiological levels of Mg^{2+} (Nishida, 1978). Such observations bring into doubt whether TBT-modulated Ca^{2+} flux is of pivotal importance, though agents which markedly raise $[Ca^{2+}]_i$ and also depolymerise MT, e.g. A23187, could have a primary action via this locus. In summary, it is probable that multiple mechanisms underlie the MT-disruption and inhibition of tubulin reassembly caused by TBT. It is postulated that direct binding to tubulin, interference with microtubule-associated proteins, and increased intracellular pH are important. More speculatively, raised $[Ca^{2+}]_i$, particularly if potentiated by localised Ca^{2+}/calmodulin complexes, might play a more minor role, as could eventual depletion of the GTP pool which is an obligate requirement for control of MT elongation (Alberts et al., 1989). These conclusions may have cautionary implications for the use of taxol as a cytoprotective agent, since it is unknown whether such a multifocal non-specific destabilisation of microtubules by TBT would be amenable to influence by taxol in the same manner as the tubulin-directed effect of more specific agents such as nocodazole or colchicine.

It has been adjudged that the cytoskeleton must be implicated in the apoptotic process (Allen, 1987). Nocodazole and TBT disrupt MT, and the latter also affects actin microfilaments, but nuclear and cellular fragmentation, and the formation of apoptotic bodies were observed during thymocyte apoptosis caused by both agents. Cotter et al. (1992) reasoned from differential studies with nocodazole and cytochalasins, that MT

were not necessary for apoptotic body formation. However, the role of the various cytoskeleton components, particularly intermediate filaments, in apoptosis is a much neglected subject. A further point of uncertainty is the potential for cold-shock destabilisation of MT during the routinely used thymocyte isolation methodology involving 4° handling stages (see section 2.1). It has always been assumed that the high spontaneous rate of apoptosis in isolated thymocytes is due to pre-priming and the loss of the trophic thymic microenvironment; the contribution of mild initial injury has not been evaluated.

Multiparameter flow cytometry is a relatively new and powerful tool being used to study cell death, and the opportunity was taken to apply this technique to examination of apoptosis activated by TBT, MPS or nocodazole in the rodent thymocyte model. DNA histograms obtained from untreated thymocytes incubated for protracted periods showed increased peak red fluorescence below the signal from the G_0/G_1 subpopulation, i.e. were hypodiploid in character (Fig. 5.13). This finding was temporally cumulative and associated with a reduction in nuclear remnant size (Fig. 5.13). Similar changes have been ascribed to the formation of apoptotic nuclei in thymocyte populations (Nicoletti et al., 1991) due to spontaneous cell death; a conclusion borne out in this work by the close quantitative identity with other apoptotic markers. A number of investigators have described equivalent, but earlier and more pronounced changes preceding viability loss in thymocytes exposed to various apoptotic stimuli, e.g. glucocorticoids or γ-irradiation (Afanas'ev et al., 1986; Telford et al., 1991). Hypodiploidy and left shifts in FSC were noted within 2-6 h after exposure to TBT (Fig. 5.14), MPS, or nocodazole (Fig. 5.15) indicating decrements in the DNA content of affected cells and the formation of apoptotic bodies. In the case of TBT, the observed variation in sub-G_0/G_1 DNA fluorescence, and rather poor correlation with other apoptotic markers, was initially thought to be due to fixation of the nuclear membrane by TBT. However, since similar anomalies were experienced with standardised MPS treatments, a methodological inadequacy was probably involved. In keeping with other reports (Nicoletti et al., 1991), cell killing by necrosis, viz. at 5 μM TBTO, did not cause hypodiploidy, presumably because internucleosomal DNA degradation was absent under such circumstances.

Exposure to TBT can rapidly block cells in the G_2/M phase of the cell cycle (Zucker et al., 1989), and this type of arrest can in certain circumstances be an apoptotic trigger (Eastman 1990; Dive and Hickman,1991). Since the majority of cells in a heterogeneous thymocyte isolate are not proliferating (Baron and Penit, 1990), i.e. are in G_0 or G_1 phase, such an effect could only ever make a partial contribution to the large scale apoptosis caused by TBT. But the thymocyte differentiation phenotypes most sensitive to apoptosis, i.e. increasingly vulnerable from $CD3^{-/low}$ $CD4^-CD8^-$ through to $CD4^+CD8^+$ cortical cells, are also those with the highest proliferative rate, e.g. 30% of $CD4^-CD8^-$ cells are actively cycling (Patterson et al., 1987; Baron and Penit, 1990). Therefore, it was necessary to

exclude the slim possibility that TBT arrested the cell cycle of, and subsequently killed, a key proliferating developmental subset. The results of cell cycle analysis (Table 5.4), showed that treatment with demonstrably apoptotic concentrations of TBTO caused no build up of thymocytes in G_2/M phase, or other overt disturbance to fractional cell cycle distributions when hypodiploidy was corrected for. It is notable that Pechatnikov and co-workers (1986) established that most thymocytes dying under the action of hydrocortisone or γ-irradiation were G_0 or G_1 phase cells. In thymocytes exposed to 50 μM nocodazole, a gradual increase in G_2/M phase cells was evident; with the effect maxima apparent at 6-8 h (Table 5.4)—this was attributed to the recognised antimitotic properties of nocodazole (De Brabander et al., 1976). Although the blockade apparently reversed by 24 h, the confounding influence of marked apoptotic death in these cultures must be taken into account.

From early work (Aldridge and Street, 1964) triorganotins have not been deemed to possess DNA reactivity, though recent findings indicate that they may have mutagenic potential (see section 1.6.3). Since there was a slight, theoretical possibility that TBT caused DNA damage or conformation changes of relevance to initiation of apoptosis, a series of experiments was designed to assess these parameters. Due to space limitations these have not been detailed in the results section of this chapter and are mentioned here only very briefly. TBTO was not found to be intrinsically reactive to DNA in the highly sensitive PM2 DNA cleavage assay, and ethidium bromide fluorochrome probe studies indicated that interaction at the level of primary DNA structure apparently did not occur.

At concentrations relevant to its lymphocytotoxicity, TBT disturbs numerous biochemical processes and as a consequence has multiple cytopathic effects. Whilst increased $[Ca^{2+}]_i$ plays an key role in T cell apoptosis activated by TBT (see Chapter 4), many other mechanistic details remain undefined, e.g. modes of signal transduction, the significance of the apparent independence from macromolecular synthesis, and which effector enzyme(s) are involved. It is perfectly possible that given the plethora of effects elicited by triorganotins, initiation of a death program under these circumstances involves more than one critical cellular target. However, TBT actuation of thymocyte apoptosis challenges the tenets that, in this system at least, this event is invariably highly regulated, i.e. obligately requires transcriptional and translational control, and conserved cellular energetics. This is affirmed by two more recent studies in thymocytes where apoptosis caused by either intracellular zinc chelation (McCabe et al., 1993) or heat shock (Migliorati et al., 1992) was not prevented by inhibitors of protein synthesis. In conclusion, my work demonstrates that TBT, a potent but relatively non-specific agent, activates thymocyte apoptosis independently of protein synthesis, in cells with severely compromised energetics status.

CHAPTER 6

THYMOCYTE DEPLETION AND THYMIC ATROPHY CAUSED BY IN VIVO ADMINISTRATION OF TBTO, AND ITS RELATIONSHIP TO APOPTOSIS AS A POSSIBLE MECHANISM IN TRIORGANOTIN-MEDIATED IMMUNOTOXICITY.

ABSTRACT

TBT immunotoxicity in rodent species is primarily characterised by a T cell deficiency resulting from a depletion of cortical thymocytes. In this study, the model trialkyltin compound TBTO was administered to male rats as a single p.o. dose of 30 or 60 mg/kg (100 or 200 μmol/kg TBT), and assessments were made of thymic cytopathology and the integrity of cellular DNA.

TBTO treatment did not cause severe toxicity or overt clinical signs, however by 48 h post-dosing the relative thymus weights at 30 and 60 mg/kg were reduced to 66% and 43% respectively of control values. Increased DNA fragmentation was evident in thymic cell isolates (principally thymocytes) obtained from treated animals during the period of thymic involution. When DNA purified from these cells was visualised by agarose gel electrophoresis a multimeric internucleosomal fragmentation pattern, indicative of supra-physiological levels of apoptosis, was detected.

Although unassociated apoptotic or necrotic thymocytes were essentially absent in cell preparations from TBTO-treated rats, significantly increased numbers of mononuclear phagocytic cells were detected by light microscopy. Ultrastructural observations suggested that these cells were probably macrophages. Many contained one or more large apoptotic bodies, with nuclear morphologies exhibiting chromatin condensation, or smaller engulfed cell remnants. The removal of discrete dying cells by phagocytes without accompanying inflammatory change has previously been characterised as a stereotypic marker for the occurrence of apoptosis in a number of physiological and pathological conditions.

Dibutyltin (DBT), a major metabolic dealkylation product of TBT, was appreciably less effective in stimulating apoptosis when added to isolated thymocytes in vitro.

Collectively, these findings indicate that activation of apoptosis is a process pivotal to thymocyte deletion after administration of TBT, and suggest that multiple mechanisms also involving DBT may underlie the thymic involution seen in vivo.

6.1 INTRODUCTION

Administration of tributyltin (TBT) compounds such as TBTO and tri-n-butyltin chloride (TBTC) to experimental animals has been shown to affect a number of immune parameters (IPCS 1990). Immature rodents are most sensitive and immunotoxicity is apparent at low doses which have limited effects on other systems. As mentioned in section 1.6.4, a central finding is the development of pronounced atrophy of the thymus due to a reduction in the number of cortical thymocytes present. This in turn leads to lymphocyte depletion in the thymus-dependent areas of secondary lymphoid organs including the spleen and lymph nodes, and the suppression of cell mediated immune responses.

6.1.1 Toxicokinetics (absorption/distribution/metabolism/excretion) of tributyltin compounds

Data on the toxicokinetics of TBT almost exclusively relate to rat and mice studies (Casida et al., 1971; Kimmel et al., 1977; Evans et al., 1979; Humpel et al., 1986; Snoeij, 1987). TBT compounds are moderately well absorbed from the intestinal tract of animals following oral administration, but the solvent vehicle used is of importance. After male Wistar rats received a single p.o. dose of about 20 mg/kg ^{14}C-TBTA in 5% ethanol/corn oil, approximately a quarter of the total radioactivity appeared in the body tissues or excreta suggesting an uptake of 25% (Snoeij, 1987). This was judged to be in keeping with similar results obtained with dialkyltins. ^{14}C-TBTO in drinking water was absorbed by mice exposed continuously for 30 days (Evans et al., 1979). Several relevant experiments have been performed by Humpel et al. (1986). An intragastric dose of ^{113}Sn-TBTO in peanut oil given to female rats resulted in a slow and prolonged absorption process. Compared to corresponding i.v. studies, the dose calculated to become systemically available was between 55-77%. A value of only 30% was obtained for pregnant rats using an equivalent vehicle, whilst intraduodenal instillation of TBTO as an aqueous suspension resulted in only 20% absorption in non-gravid females.

These investigators also provided information on further key kinetics parameters for TBTO in the rat. After a single p.o. dose, a biphasic plasma TBTO concentration was obtained with maxima at 8 and 24 h. This contrasted with the very rapid disappearance of radiolabel after i.v. administration (t½ 0.1 h). The Snoeij study referred to above demonstrated an equivalent profile, and in common with Humpel et al., he observed that TBT rapidly and preferentially partitioned into the cellular sub-compartment of blood. The volume of distribution obtained for TBTO of 15 l/kg suggests that it has a moderate to high affinity for tissues and passes readily into cell membranes. Both investigators reported comprehensive tissue distribution findings. Highest radiolabel levels were found in the liver and kidneys 1-4 days after dosing. Unchanged TBTO occurred predominantly in the these organs plus fatty tissues. Notably, no selective concentration of TBT was apparent in the thymus. Dietary administration of 5-320 ppm TBTO for 4 weeks resulted in high tin

concentrations in the liver, kidney and brain of male and female rats (Krajnc et al., 1984), which paralleled the findings of Bressa et al. (1991) on TBTC and TBTO. The latter found that total tin levels in the thymus and spleen were about a fifth of the hepatic values. Humpel and co-workers determined accumulation factors of 1.3 to 7.4 in radiolabel balance experiments (TBTO 5 mg/kg/day), and predicted that steady state concentrations would occur after 3-4 weeks, with maximum tissue accumulation factors of about 10.

Observations on the metabolism of TBT compounds in microsomal preparations, whole cells, or in vivo have demonstrated that dealkylation (sometimes referred to by its reciprocal, destannylation) is the overall consequence, leading to the generation of di- and monobutyltin. Fish et al. (1976) showed this is mediated by cellular microsomal cytochrome P_{450} dependent monooxygenase systems; first yielding α-, β-, γ-, and δ-hydroxybutyldibutyltin derivatives, with the major α- and β-hydroxyl metabolites then undergoing dealkylation, according to the following schema:

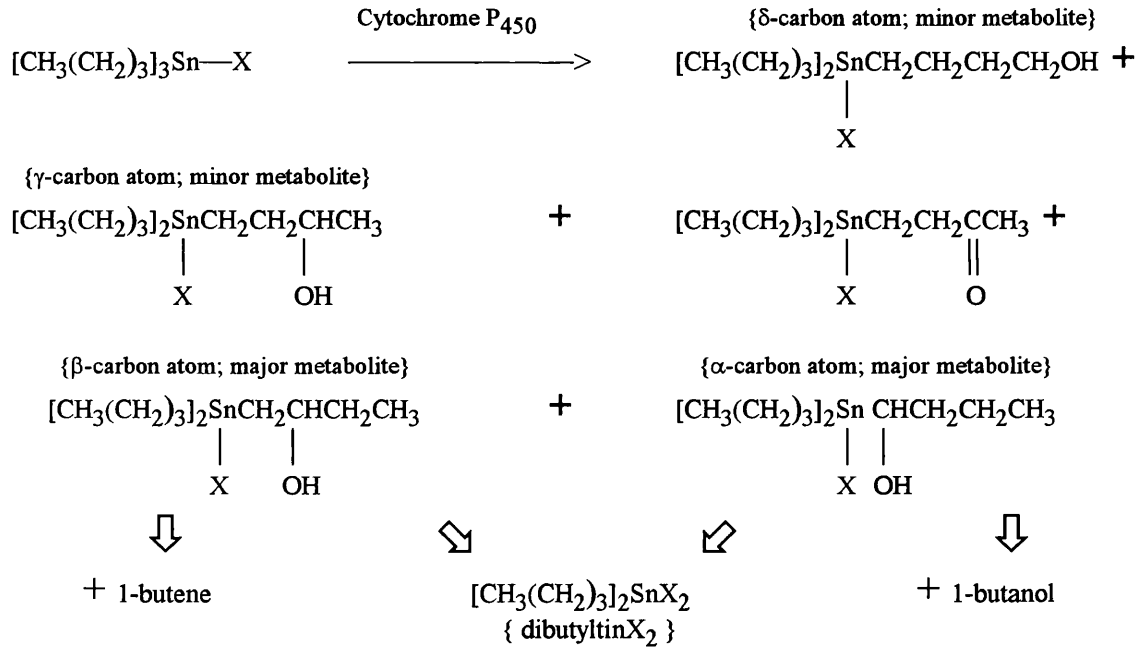

They suggest that a free radical mechanism may be important in the carbon atom hydroxylation reactions. Dibutyltin metabolites then undergo further monooxygenase or nonenzymatic cleavage to monobutyltin and inorganic tin. Their inhibitor studies, together with increased induction of the process by phenobarbital pretreatment (Kanetoshi, 1983) confirm the pivotal importance of cytochrome P_{450}. Comparable results were obtained in relation to other trialkyltin homologues, e.g. triethyltin, tripropyltin, tripentyltin and trihexyltin (Casida et al., 1971), and there is good evidence that analogous metabolic processes apply for both rats and mice. Though the exact degree of dealkylation and site of transformation in rodents are not unequivocally established, it is believed that the major sites are the liver and intestinal mucosa. Two or three compounds of increased polarity detected at 24 h in the plasma of female rats given bis(tri-n-butyl-^{113}tin) oxide, were

postulated to be dealkylation products (Humpel et al., 1986). Five major HPLC separation peaks and also a small amount of TBTO were identified in corresponding urine samples. Snoeij (1987) demonstrated that 3 or 27 h after a single oral dose of ^{14}C-TBTA (~13-16 mg/kg), inferred DBT and monobutyltin levels in the blood of rats were about 2-3 times higher than those of unmetabolised TBT. It should be noted that this experiment involved only a single animal at each timepoint. In conclusion, significant metabolism of TBT occurs within a few hours of administration, although appreciable amounts of unchanged parent compound are also present.

It is of interest that most of the hydroxylated butyldibutyltins exhibit some stability and marked biological activity at physiological pH (Fish et al., 1984); T lymphocytes (including thymocytes), unlike B cells, do possess several cytochrome P_{450} monooxygenase isoenzymes (Golovenko et al., 1986; Khromenkov et al., 1984).

No absolute measurement of thymic concentrations of the various organotin species arising in rodents after administration of TBT compounds has ever been conducted, but consideration of the preceding kinetics data allows some important conclusions regarding blood compartment levels and allows limited extrapolation in relation to the thymus. ^{14}C-TBTA, given as a single thymus atrophy-inducing dose of about 15 mg/kg, gave estimated blood levels of 0.3 μM TBT, 0.7 μM DBT and 0.8 μM monobutyltin after 1 day (Snoeij, 1987). At that time, the concentration of total radiolabel (dpm/mg tissue) in the thymus was three times higher than in the blood. In the study conducted by Humpel et al., the maximum plasma concentration of unchanged TBTO present 8-24 h after an intragastric administration of 25 mg/kg TBTO to female rats was calculated to be 0.27 μM. Total blood levels would have been 2-3 times greater. Findings exactly analogous to the above were apparent in respect of differential blood/thymus ^{113}Sn radiolabel distribution.

Excretion experiments show that following a single oral dose of ^{14}C-TBTA to rats or mice, about 53-75% of radiolabel is eliminated in the faeces, and 13-16% in the urine at 4-6 days (Snoeij, 1987; Kimmel et al., 1977); minor amounts are either retained or lost as $^{14}CO_2$. This is in broad agreement with other findings in mice (Evans et al., 1979) regarding TBTO metabolism and excretion. Unmetabolised TBTO clearance values in the rat have been determined as 40 ml/min/kg by Humpel and co-workers. Based on total radiolabel, by i.v. administration (1 mg/kg) they report 2 major process half-times ($t_{½\alpha}$, 0.15 h and $t_{½\beta}$, 4.9 h) with a minor one ($t_{½\gamma}$) of 19.7 h, whereas by the oral route (25 mg/kg) the elimination half-time is 14.2 h. During further studies with TBTO in male animals, a biphasic pattern of biliary and renal elimination was apparent with excretion half-lives of 12 h and 3 days, though the latter process represented less than 10% of the administered dose.

6.1.2 Mechanistic aspects of trialkyltin thymotoxicity

Of the triorganotins, TBTC and TBTO have been studied most extensively in terms of the mechanistic aspects of their thymolytic action. Considerable research has also been done on DBT, the primary dealkylation metabolite of TBT, and it is of note that a close resemblance exists between the effects of various tri- and dialkyltins on the thymus (see section 1.6.4).

Histopathological findings in the thymus after TBT or DBT exposure have commonly been reported to be confined to a reduction in the cortical/medullary ratio; as a result of cortical thymocyte depletion, and the loss of a distinct corticomedullary junction (Snoeij et al., 1987; Krajnc-Franken et al. 1990). Signs of widespread cell destruction and inflammatory change are characteristically absent during the course of cortical thymocyte depletion. There has been one report of large scale thymocyte pyknosis and karyorrhexis, associated with diminished cell viability, in rats after 3-20 days feeding with 320 ppm, though this level caused signs of generalised toxicity (Vos et al., 1984a). Attention has also focused on in vitro experiments which indicate that triorganotins are very cytotoxic to isolated thymocytes (Vos et al., 1984a; Snoeij et al., 1986a). However, on balance, there is very little direct evidence to support cell killing by *necrosis* as a lymphocytotoxic mechanism in organotin-induced thymic involution in rodent species. Based on toxicokinetics data, it seems unlikely that concentrations of TBT associated in vitro with necrotic cell death (see chapter 3) would occur at these target cells in vivo. In a similar vein, no overt cytotopathic effects on thymic epithelial cells have been noted after administration of TBTO (De Waal et al., 1991; De Waal et al., 1993).

Early reports indicated that TBT compounds such as TBTO when administered to rats at high acute doses (100 mg/kg) or for protracted periods at lower levels (6-12 mg/kg/day for 13-26 weeks) could cause pituitary and adrenal hypertrophy (Funahashi et al., 1980), though these treatments were poorly tolerated. Since endocrine or metabolic disturbances may cause indirect depression of the thymus-dependent immune system, further investigations of such parameters have been conducted in parallel with assessments of TBT immunotoxicity (Krajnc et al., 1984; Vos et al., 1985; Wester et al., 1990). By means of immunocytochemistry, Krajnc et al. demonstrated that feeding rats with up to 80 ppm (8 mg/kg/day) for 6 weeks produced no effect on pituitary cells secreting either ACTH or somatotropin (growth hormone; a thymotrophic substance). In connection with the latter finding the observation that, in contrast to hypophysectomy-induced thymic atrophy, the involution produced by organotin compounds cannot be reversed by administration of comparable amounts of growth hormone (Penninks et al., 1990) may also be of relevance. TBTO can depress thyroid function, resulting in diminished thyroid stimulating hormone and thyroxine levels, but no evidence exists to suggest a consequent effect on T cell proliferation (Vos et al., 1985). The same workers indicate that hyperglycaemia or

hypoinsulinaemia, both of which can severely affect the thymus, are not mechanistically important since glucose levels were unaffected by TBTO treatment and serum insulin depression did not correlate with thymic involution. Involvement of stress-induced glucocorticoid lymphocytolysis as a mechanism for TBT or dialkyltin-mediated thymic atrophy has now been substantially discounted for a number of reasons. Neither adrenal weight or adrenal cortex histology were affected after exposure of rats to moderate doses of TBTC (Snoeij et al., 1985), TBTO (Vos et al., 1985) or dialkyltin compounds (Seinen and Willems, 1976). Thymic weight was reduced equally in adrenalectomised and sham-operated rats fed TBTC (Snoeij et al., 1985) or DOTC (Seinen and Willems, 1976). Corticosterone levels in rats exposed repeatedly to moderate concentrations of TBTO were unaltered (Vos et al., 1985). Notwithstanding these conclusions, there is ample evidence to suggest that a pituitary-adrenal axis effect has been an important confounding factor in some previous badly designed studies of organotin immunotoxicity.

Based on measurements of ^{3}H-thymidine incorporation into DNA, all lipophilic triorganotin compounds, including TBT, exhibit marked antiproliferative effects when introduced into ex vivo thymocyte cultures at concentrations greater than 50 nM (Snoeij et al., 1986a and b). There is data to suggest that in fractionated cell populations, the small non-proliferating thymocytes are most affected compared to proliferating subpopulations (Snoeij et al., 1986c). It should be noted that none of these investigations considered the possibility that depression of DNA synthesis might also partly be a consequence of the activation of apoptosis (see 1.2.2). Persistent effects on thymocyte DNA synthesis have also been recorded during in vivo studies with TBTC (Snoeij et al., 1988a) and in investigations of T cell mitogen-induced ^{3}H-thymidine incorporation after TBTO exposure (Vos et al., 1985). Due to their biochemical effects, triorganotins are likely to disturb a number of key cellular processes including energetics, cell division and Ca^{2+} signal transduction (see 5.1.3). Dialkyltin compounds, e.g. DBTC and di-n-octyltin dichloride also exert considerable antiproliferative effects on isolated thymocytes (Vos and Penninks 1987) and also in vivo (Volsen et al., 1989; Snoeij et al., 1989). The in vitro EC_{50} for this effect has been determined to be approximately 50 nM (Dr. A Penninks, personal communication). Snoeij et al. (1988a) observed that a single oral dose of TBTC or DBTC caused a severe reduction in the proliferating activity of thymocytes and in the number of large proliferating thymoblasts (*sic*) within 24 h. They proposed that such an antiproliferative effect could, in tandem with physiological thymocyte death, cause thymic atrophy. The sequence by which thymocyte CD markers become diminished during this process, i.e. CD2, CD8, CD4 and then CD5, resembles the appearance of these antigens in the process of ontogeny (Kampinga et al., 1990), suggesting that the disturbance occurred at an early developmental stage. During a review of relevant work it was concluded that the organotins disturb thymocyte differentiation at, or just preceding, the beginning of the $CD4^{+}CD8^{+}$ developmental stage (Penninks et al., 1991). In the case of the dialkyltins, it

has been proposed that their high affinity for cellular dithiol groups could be a molecular basis for an antiproliferative action (Vos and Penninks 1987). However, to what extent direct antiproliferative effects or more subtle disturbances of cell-cell interaction feature in organotin-induced thymic atrophy is presently unclear.

Snoeij et al. (1988a) compared the toxicodynamics of the action of TBTC and DBTC on the thymus of juvenile male Wistar rats. The log dose-effect relationship of thymic involution following a single p.o. dose of the two compounds was linear and parallel over the range 5-60 mg/kg. In addition, their effects on thymic weight, cell count and precursor incorporation into DNA, RNA or protein were qualitatively similar and occurred over equivalent timeframes. They calculated that TBTC was about 40% less effective in molal dose terms than DBTC in reducing thymus weight. Taking into account the correspondence in cortical thymocyte depletion, the differential dose-response data on thymic weight and the kinetics of cell loss, it was postulated that TBTC-mediated thymus atrophy results from the action of its metabolic dealkylation product DBT. Since mono-n-butyltin trichloride was completely ineffective in producing atrophy at up to 180 mg/kg, the conclusion was made that the ultimate dealkylation product monobutyltin has no thymus-directed activity. In previous unpublished experiments (Snoeij, 1987) it had been shown that, in contrast to DBTC, when TBTC was given as a single i.v. injection (0.5-2.5 mg/kg) to rats it did not produce thymic atrophy. Taken in context with the above study, this seems to provide persuasive evidence for the 'bioactivation' hypothesis, whereby the mechanism of tri- and dialkyltin thymotoxicity is a common one; metabolism of ingested TBT results in formation of DBT, which then exerts a primary antiproliferative effect on critical proliferating thymocyte subsets (Snoeij et al., 1988a). Whilst this idea has merit in terms of many of the known effects of organotins, a number of possible objections to its validity are apparent:

(i) The only available plasma clearance rate data for TBT show that it is very rapidly removed following i.v. administration (Humpel et al., 1986), with a first process half-time measured in minutes, and therefore thymus perfusion concentrations will not be equivalent to the sustained levels recorded via the oral route. Since an intravenous dose of only 6 mg/kg TBT has been found to cause 100% mortality in rats within minutes (Snoeij, 1987), it is not possible to experimentally generate persistent blood concentrations in the range associated with thymic atrophy. In addition, the distribution of TBT and DBT compounds differs, with the former rapidly entering biomembranes and tissues with a high lipid content—this may account for the lethality seen by the i.v. route, since acute effects related to haemolysis and entry into the central nervous system may occur.

(ii) The site and extent of metabolism of TBT are poorly defined. However, the small difference in quantitative cell loss data between TBTC and DBTC reported by Snoeij et al. (1988a) does not support the conclusion that this loss could be due entirely to the predicted amount of DBT formed.

(iii) Given the high antiproliferative activity of both TBT and DBT in vitro, it is doubtful whether there is a basis for a selective action on thymocytes in vivo. In a later publication, the same group of researchers point out that the differential effects seen for TBT and DBT on the proliferation of various thymocyte subpopulations are not in keeping with the effects observed in vivo (Penninks et al., 1990).

Interference of organotins with bone marrow stem cells has been considered as a prospective mechanism, though there is some contention regarding this possibility. Using ex vivo marrow cells, TBT (TBTO or TBTC) and DBT have been variously reported as being moderately cytotoxic (Vos et al., 1984a; Snoeij et al., 1986a), or in the case of the latter compound as having very little effect on marrow cell viability or mitotic index (Penninks et al., 1985). Since organotin-induced atrophy occurs after 2-4 days, it has been pointed out that if, as it is currently thought, prothymocytes mature in the thymus for several days before proliferating, this would preclude an effect on cell traffic or thymic entry being of importance (Penninks et al., 1991). It is also still a matter of conjecture as to whether a disturbance of the intrinsic thymic humoral function could be involved in organotin toxicity. Vacuolation of epithelial cells has been described for dialkyltins and TBT (De Waal et al., 1993), though the significance of reports of increased numbers of secretory granules is debated (Penninks et al., 1990). The key role of various intrinsic polypeptide hormones in thymus physiology (Ritter and Crispe, 1992) represents a potentially critical and complex target for toxicant action.

In conclusion, presently there are divided opinions regarding the importance of the various prospective mechanisms underlying TBT thymotoxicity. Some workers favour a hypothesis in which antiproliferative effects on certain key thymocyte subsets occur only after dealkylation of TBT to an active DBT metabolite (Penninks et al., 1990). Others focus more on its cytolethality as a primary effect (Boyer, 1989; De Waal et al., 1993).

6.1.3 The question of the possible role of apoptosis in the toxicodynamics of TBT

The mode of cell death known as apoptosis is an essential process in the regulation of the developing thymic T lymphocyte repertoire and the deletion of autoreactive cells (Ritter and Crispe, 1992). Due to their primed state, thymocytes readily undergo apoptosis in vitro after exposure to a variety of exogenous stimuli including glucocorticoids and radiation (see Chapter 1), resulting in characteristic endonucleolytic degradation of genomic DNA followed by cell death. There is increasing recognition that similar non-necrotic cell killing is also involved in certain toxic effects in vivo, and that agents such as 7,12-dimethylbenz[*a*]anthracene (Burchiel et al., 1992), thioacetamide (Barker and Smuckler, 1973) and colchicine (Afanas'ev et al., 1988) can exert their toxicity to lymphoid cells by this means. TBT is particularly effective in stimulating apoptosis in isolated thymocytes at concentrations which are thought to be relevant to those causing

thymus atrophy in vivo (see Chapter 3-5; Aw et al., 1990; Raffray and Cohen, 1991). Although it was hypothesised that these observations might be relevant to the in vivo situation, their actual significance was uncertain. Therefore the subsequent studies were designed to investigate this possibility using TBTO as the prototype TBT compound. Since the anionic group present in organotins is thought to have limited influence on their biological activity (refer to section 1.6.1; Blunden and Chapman, 1982), any findings on TBTO should have general applicability to TBT compounds.

The investigations reported here formed the basis of the following publication:

Raffray M, Cohen GM (1993) Thymocyte apoptosis as a mechanism for tributyltin-induced thymic atrophy in vivo. Arch Toxicol 67: 231-236

6.2 METHODS

6.2.1 Materials

TBTO was obtained from Fluka (Glossup, England) and repurified (section 2.14). DBTC (CAS no. 683-18-1), purity in excess of 97%, was from Aldrich (Gillingham, England). Materials and reagents employed for cell viability assessment, production of resin sections and TEM preparations, assay of DNA fragmentation (colorimetric method) and conduct of neutral agarose gel electrophoresis were as given in section 2.2.2, 2.4.1.2, 2.5.2, 2.6.2 and 2.8.2, respectively. Materials for the quantitation of DNA content by H33258 fluorescence were as in section 2.7.2, whilst those used for preparatory hypotonic cellular lysis and differential centrifugation stages are detailed in 2.6.2. Other items, not mentioned in the appropriate methods section (chapter 2), were from BDH Ltd (Poole, England).

6.2.2 Animal husbandry, study design and dosing procedures

Juvenile male Wistar rats (4-5 weeks of age) were obtained from the breeding colony at the School of Pharmacy. Prior to study commencement, animals were gang housed by proposed treatment group and allowed a 1 week acclimatisation period during which they were handled every day. Experimental rooms were maintained at 21 ± 2^{o} with a relative humidity of $55\pm10\%$, under a 12 h constant light/dark cycle. Drinking water and diet (Expanded Maintenance Diet, Bantin and Kingman, Hull, U.K.) were provided *ad libitum*. Animals received a single dose of 30 or 60 mg/kg TBTO dissolved in ethanol/corn oil (5/95, v/v), by oral intubation at a dosage volume of 5 ml/kg. This equated to dose levels of 100 or 200 μmol/kg TBT, respectively. An equal number of rats, closely pair matched by bodyweight, received the ethanol/corn oil vehicle alone at equivalent dosage volumes. Clinical signs observations were performed at hourly intervals for 3 h after dosing and then once each morning and evening until termination.

In the main study, three animals per treated (60 mg/kg) or control group were sacrificed at

18, 36 or 48 h after dosing. A single group received 30 mg/kg TBTO and was sacrificed 48 h later. Satellite studies, which followed the same experimental protocol, were performed with additional animals (two per group) in order to compare the histopathology of the thymus by conventional means.

6.2.3 Terminal procedures

The final bodyweight of each animal was obtained immediately prior to its euthanasia by diethyl ether anaesthesia followed by cervical dislocation. Thymi were rapidly dissected free of lymph nodes and connective tissue and weighed, prior to being placed separately in ice-cold unsupplemented Krebs Henseleit buffer (pH 7.4). All subsequent manipulations involving live thymic material were performed at 4°. The spleen and adrenals were then excised and weighed. Any macroscopic findings evident upon necropsy were recorded.

Thymic cell suspensions were prepared by slicing thymi using a McIlwain tissue chopper (Mickle Laboratory Engineering, Gomshall, UK), followed by extensive disaggregation through a 100 mesh nylon sieve. As far as practicable, these manipulations were precisely standardised for each thymus processed. Cell counts were performed in triplicate on samples from each animal using a haemocytometer (see section 2.3). Cell viability was assessed in triplicate by the trypan blue dye exclusion technique described in section 2.2.

6.2.4 Determination of DNA fragmentation

Aliquots of thymic cell suspensions were reserved for cytopathology studies, and the remainder of the cell mass was harvested by centrifugation at 200 x *g*. A known number of cells was subjected to lysis and differential centrifugation as described in section 2.6.3, using a lysis buffer addition of 3.5-5 ml. The supernatant fractions arising from this procedure were separated, samples taken for analysis and the remainder stored at -80°. After a tenfold dilution in TE buffer (to give an approximate DNA concentration of 2 $\mu g\ ml^{-1}$), the DNA content of triplicate supernatant aliquots were determined by the fluorimetric method detailed in section 2.7. Following application of appropriate dilution factors, the DNA content values obtained were standardised by reference to the original cell number contained in each lysis sample (μg DNA/10^8 cells).

6.2.5 DNA electrophoresis

3ml aliquots (corresponding to between 450-600 x 10^6 cells) of the supernatant fraction derived from the thymic cell preparations were gently thawed. After initial concentration by extraction with butan-2-ol/chloroform and ethanol precipitation, the samples were resolubilised in 1 ml TE buffer and SDS to 0.5%, and then serially extracted with equal volumes of phenol, phenol:chloroform (1:1) and chloroform according to the procedure given in section 2.8.3. Electrophoresis was performed at 15-18 mA for 6-8 h in 1.5% neutral agarose gels using a running buffer containing 89 mM Tris, 89 mM boric acid,

2 mM EDTA, pH 8.0, according to the protocol described in 2.8.5. Within experimental sets, the volumes of the purified DNA samples loaded onto the gel were matched to equivalence on the basis of original cell number in the lysis sample derived from each animal. DNA visualisation was as described in section 2.8.6.

6.2.6 Cytopathology studies and histopathology

0.2 ml aliquots of thymic cell suspensions (15-20 x 10^6 cells) obtained from animals in the main study were suspension fixed in 2.5% glutaraldehyde in 0.1 M sodium cacodylate buffer at 4° and pelleted by centrifugation at 170 x *g*. Semi-thin epoxy resin sections (0.5 μm) were stained with toluidine blue as described in section 2.4.1.4. Wherever possible, the sections were obtained from equivalent regions in each cell pellet. The number of activated mononuclear phagocytic cells (MPc), containing recognisable apoptotic bodies, was estimated in fifteen contiguous fields by light microscopy using a Nikon Microphot FXA microscope (Nikon Corporation, Tokyo, Japan) fitted with an internal graticule. At a standard magnification of x 900 under oil immersion the total area of the counted region was calculated to be approximately 1 mm^2. MPc without identifiable inclusion bodies were excluded; all counts were unadjusted for total cell numbers. Selected regions of pellet sections were processed for further morphological study by transmission electron microscopy according to the protocol given in section 2.5.

Thymus samples obtained from animals in the satellite study were processed whole (without disaggregation). These tissues were fixed in 10% neutral buffered formalin, dehydrated and embedded in paraffin. Sections (6 μm) were stained with haematoxylin-eosin prior to examination by light microscopy.

6.2.7 In vitro studies

Thymocytes were isolated from 3-5 week old Wistar rats (see section 2.1), and incubated in RPMI-1640 medium supplemented with 10% foetal bovine serum. Organotin compounds (DBTC or TBTO) were diluted in ethanol immediately prior to use such that when added to cell suspensions, the cultures contained a final concentration of 0.2% ethanol. An equivalent vehicle addition was introduced into control plates. Thymocyte viability was determined after 0, 1, 2, 4, 6 and 24 h according to the method detailed in section 2.2. DNA fragmentation (colorimetric method), and morphological studies were performed after 6 h, as described in 2.6 and 2.4.1 respectively.

6.2.8 Statistical analysis

All results are presented as the mean (arithmetic) $\pm$ 1 SE unless otherwise stated. For in vivo experiments, where reference is made to sample size this relates to the number of animals in each experimental group. Comparisons were made, versus controls only, using

an unpaired two-tailed t-test and accepting a statistical significance for p of less than 0.05, preceded by analysis of data distribution and homogeneity of variance as appropriate.

6.3 RESULTS

6.3.1 Preterminal observations

No deaths occurred in animals that received a single oral dose of 30 or 60 mg/kg TBTO. Overt clinical signs were not observed during the course of the study; the animals maintained good general condition and were considered to exhibit a normal activity profile. Control bodyweights showed a gradual increase over the 2 day post-dosing period, whereas bodyweight gain in treated animals was suppressed to an equivalent extent at both dosage levels (Table 6.1).

6.3.2 Necropsy findings, organ weights and thymic cell counts

At necropsy, macroscopic alteration of the thymus was noted for most treated rats, with the organ appearing shrunken, pale and diffuse. The severity of this finding was considered to increase with the advance of the post-dosing interval. Other macroscopic findings were unremarkable and age consistent.

TBTO treatment caused a progressive, dose-related, and statistically significant decrease in thymus weight (Table 6.1) which was evident from the 18 h timepoint onwards. By 48 h, relative thymus weights with reference to the mean control value approximated to 66% at 30 mg/kg and 43% at 60 mg/kg. Spleen weights of treated rats were also decreased in a manner that correlated well with the effect on the thymus. Adrenal weights were apparently unaffected by treatment.

The diminished thymus weights recorded in animals at both TBTO dosage levels were associated with statistically significant decreases in thymic cellularity (Table 6.1). At 60 mg/kg TBTO, the group mean cell count was reduced to only 36% of the control by 48 h. Thymic cell viability, as determined by trypan blue dye exclusion, exceeded 95% for suspensions prepared from either control or treated animals (Table 6.1) at all timepoints.

6.3.3 DNA fragmentation and gel electrophoresis

In order to study the extent of DNA fragmentation in thymic cell suspensions obtained during the terminal procedures, aliquots of cells were subjected to hypotonic lysis and differential centrifugation, followed by fluorimetric analysis of the content of low molecular weight DNA retained in the supernatant fractions. The fluorimetric technique used gave superior sensitivity and precision compared to traditional colorimetric methodologies for DNA estimation. Due to the difficulty in solubilising pellet fractions from the differential centrifugation stage, the results were standardised by means of relating the absolute supernatant DNA values obtained to original cell number. An improvement over this

TABLE 6.1 Effect of a single oral dose of TBTO on organ weights and thymocyte counts of male rats.

Parameter	18 h[a] Control	18 h[a] TBTO 60 mg/kg	36 h[a] Control	36 h[a] TBTO 60 mg/kg	48 h[a] Control	48 h[a] TBTO 30 mg/kg	48 h[a] TBTO 60 mg/kg
Bodyweight change (g)[b]	4±1	1±2	6±3	-1±2	7±2	-1±2	-2±3
Absolute thymus weight (mg)	297±19	262±4	339±34	195±13*	332±27	216±25*	136±18*
Relative thymus weight (%)	0.32±0.01	0.28±0.01*	0.36±0.06	0.21±0.02*	0.35±0.03	0.23±0.04*	0.15±0.02*
Absolute spleen weight (mg)	331±7	257±21*	332±59	240±10	346±41	277±37	228±19*
Relative spleen weight (%)	0.36±0.01	0.28±0.02*	0.35±0.08	0.26±0.02	0.37±0.08	0.30±0.09	0.25±0.04*
Absolute adrenal weight (mg)[c]	26±1	25±1	24±2	24±1	26±1	28±2	25±0
Relative adrenal weight (%)[c]	0.029±0.001	0.027±0.002	0.025±0.001	0.025±0.001	0.028±0.001	0.030±0.002	0.027±0.001
Thymic cell count (x 10^6)[d]	842±88	634±27*	964±23	521±68*	962±75	544±105*	350±42*
Thymic cell viability (%)	97±0.8	98±0.9	98±0.6	98±0.3	97±0.7	96±0.8	96±0.3

Animals received a single p.o. dose of TBTO according to the procedures described in section 6.2.2 and were sacrificed at the indicated times after dosing. Organ weights, thymic cell count and viability were determined by the methods detailed in sections 6.2.3, 2.3 and 2.2 respectively. Results are group means ± SE (n=3). * Significantly different from control value, $p < 0.05$ (Student's t-test). Note: [a] Time of sacrifice; [b] Difference between terminal and pre-dosing bodyweight; [c] Weight of organ pair; [d] Total number of nucleated cells isolated from thymus.

methodology might have been to sonicate samples of hypotonic buffer cell lysate and supernatant fraction, and report relative DNA fragmentation as the ratio of DNA content in the supernatant to the lysate (Kizaki et al, 1989).

Fragmentation values obtained for the controls remained consistently low at all timepoints examined (Fig. 6.1a) Administration of 60 mg/kg TBTO produced a significant elevation in detected DNA fragmentation, which increased with the progression of the post-dosing period (Fig. 6.1a). The mean value obtained for this group at 48 h after dosing was 380% of the respective control. A less pronounced increase was also apparent at this timepoint for the group that received 30 mg/kg TBTO (270% of the control mean).

Isolates of highly concentrated purified DNA were separated by agarose gel electrophoresis in order to examine the characteristics of the TBTO-stimulated degradation process. The majority of samples from TBTO-treated rats exhibited faint but discernible fragmentation patterns corresponding to the occurrence of internucleosomal cleavage, i.e. a multimeric series of scission products with an integer repeat of approximately 200 base pairs (Fig. 6.1b; lane 2). This marker was detectable in some animals from 18 h after dosing. Comparable DNA cleavage patterns were either absent or only very faintly present in control samples (Fig. 6.1b; lane 1 and 3). It was noted that a relatively high degree of non-specific cleavage was also evident in a few samples, giving the appearance of a smear superimposed on the nucleosomal ladder (Fig. 6.1b; lane 4).

6.3.4 Cytopathology and histopathology

Microscopic examination of whole thymus sections revealed a dose-related depletion of cortical thymocytes in treated rats, which was in agreement with previously reported findings on tributyltin (Krajnc-Franken et al. 1990). The effect was considered to be progressive in severity from the 18 h to 48 h timepoints. Histological findings in these animals were otherwise unremarkable, and in particular signs of widespread thymocyte pyknosis or karyorrhexis were absent. Most previous toxicological studies of organotin action on lymphoid tissue have relied on conventional histopathology of haematoxylin-eosin stained wax embedded sections. Though they were included in the experimental protocols to allow for equivalent comparison of any findings, it should be noted that whole tissue resin embedding techniques confer significant advantages in the evaluation of morphological criteria of cell death.

Comparative cytopathology assessments were also performed on toluidine blue stained resin sections of suspension-fixed thymic cells isolated at necropsy. Preparations from TBTO-treated rats showed no evidence of an elevation in the relative number of unassociated thymocytes bearing the morphological markers of necrosis or apoptosis. However it was noted that TBTO treatment caused a statistically significant increase in the

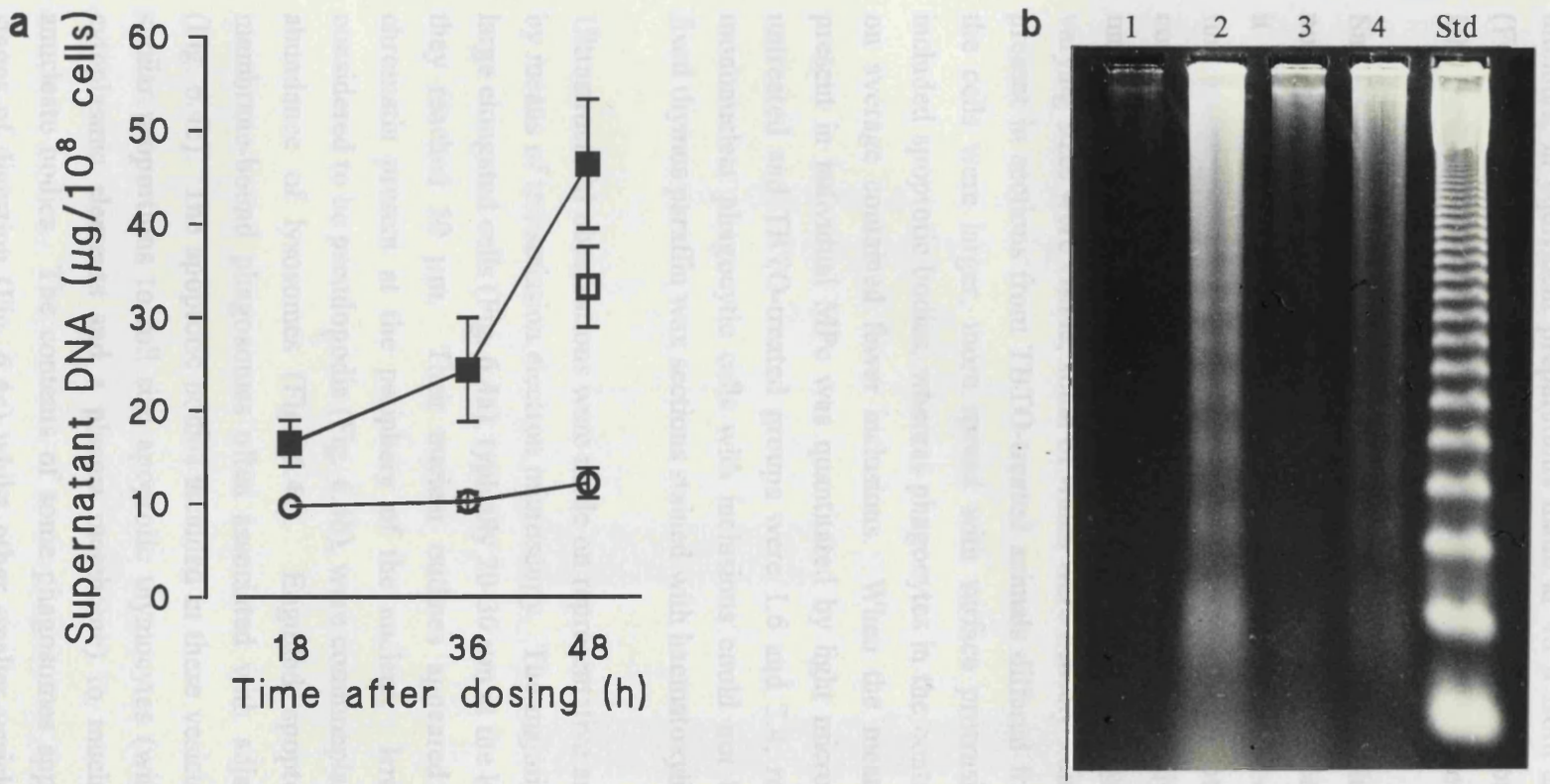

FIGURE 6.1 Effect of TBTO administration on a) thymic cell DNA fragmentation and b) electrophoretic appearance of DNA isolates.

a) Results are expressed as the total DNA that resisted sedimentation at 27 000 x *g*, normalised for the respective total cell number of each isolate (as described in section 6.2.4). Points represent the mean ± SE (n=3) of supernatant aliquots prepared from animals at the stated timepoints after administration of 30 mg/kg (□) or 60 mg/kg (■) TBTO, or vehicle control (○).

b) Animals were sacrificed 18 h after receiving a single p.o. dose of 60 mg/kg TBTO, and DNA isolates were derived from thymic cell lysates (as detailed in 6.2.5) and electrophoresed. Gel tracks shown relate to unpooled isolates from individual animals. Lanes 1 and 3, control; lane 2 and 4, TBTO-treated; Std, DNA molecular weight calibration standard corresponding to an integer repeat of 123 bp.

incidence of mononuclear phagocytic cells (MPc) containing inclusion bodies (Fig. 6.2). Quantification of this effect showed it to be maximal by 36 h after dosing for the group that received 60 mg/kg TBTO. Such cells were also present, in significantly elevated numbers, in equivalent preparations made at 48 h from animals given 30 mg/kg TBTO (Fig. 6.2). Absolute MPc counts for individual animals correlated well with the extent of DNA fragmentation present in the respective cell lysates (results not shown).

Since immunocytochemical markers were not evaluated, the phenotype of the MPc could not be unequivocally established, but on the basis of nuclear and cytoplasmic morphology it was initially concluded that they were macrophages (see also the ultrastructural study findings presented later in this section). Engulfed apoptotic bodies with large, highly condensed nuclear chromatin structures were commonly present either singly or as multiple aggregates (Fig. 6.3 b and c), whilst in other phagocytes smaller cell remnants of varying sizes were visible, some of which were densely stained. The character of the MPc present in sections from TBTO-treated animals differed from the controls; in the former the cells were larger, more spread with surface protrusions and a greater number of included apoptotic bodies, whereas phagocytes in the controls were smaller, rounded and on average contained fewer inclusions. When the mean number of apoptotic bodies present in individual MPc was quantitated by light microscopy at 36 h, the values for untreated and TBTO-treated groups were 1.6 and 3.4, respectively. It was noted that mononuclear phagocytic cells with inclusions could not be reliably visualised in whole fixed thymus paraffin wax sections stained with haematoxylin and eosin.

Ultrastructural observations were made on representative areas of sections containing MPc by means of transmission electron microscopy. The majority of MPc with inclusions were large elongated cells (Fig. 6.4a), typically 20-30 μm at the longest axis, though on occasion they reached 50 μm. Their nuclear outlines appeared convoluted with considerable chromatin present at the periphery of the nucleus. Irregular cytoplasmic projections, considered to be pseudopodia (Fig. 6.4b), were commonplace and cells contained a relative abundance of lysosomes (Fig. 6.4c). Engulfed apoptotic bodies were localised in membrane-bound phagosomes often associated with adjacent electron-dense lysosomes (Fig. 6.4c). The apoptotic bodies included in these vesicles ranged in size from those of similar proportions to full size apoptotic thymocytes (with large densely stained nuclei, cytoplasmic elements and a plasma membrane) to much smaller chromatin masses or anucleate bodies. The contents of some phagosomes appeared to be at more advanced stages of digestion (Fig. 6.4c) whilst other smaller vesicles, with amorphous inclusions, were considered to represent residual bodies (Fig. 6.4b). Considered collectively, these morphological features provide further corroborative evidence to support the supposition that the MPc in sections derived from TBTO-treated animals were tissue derived macrophages.

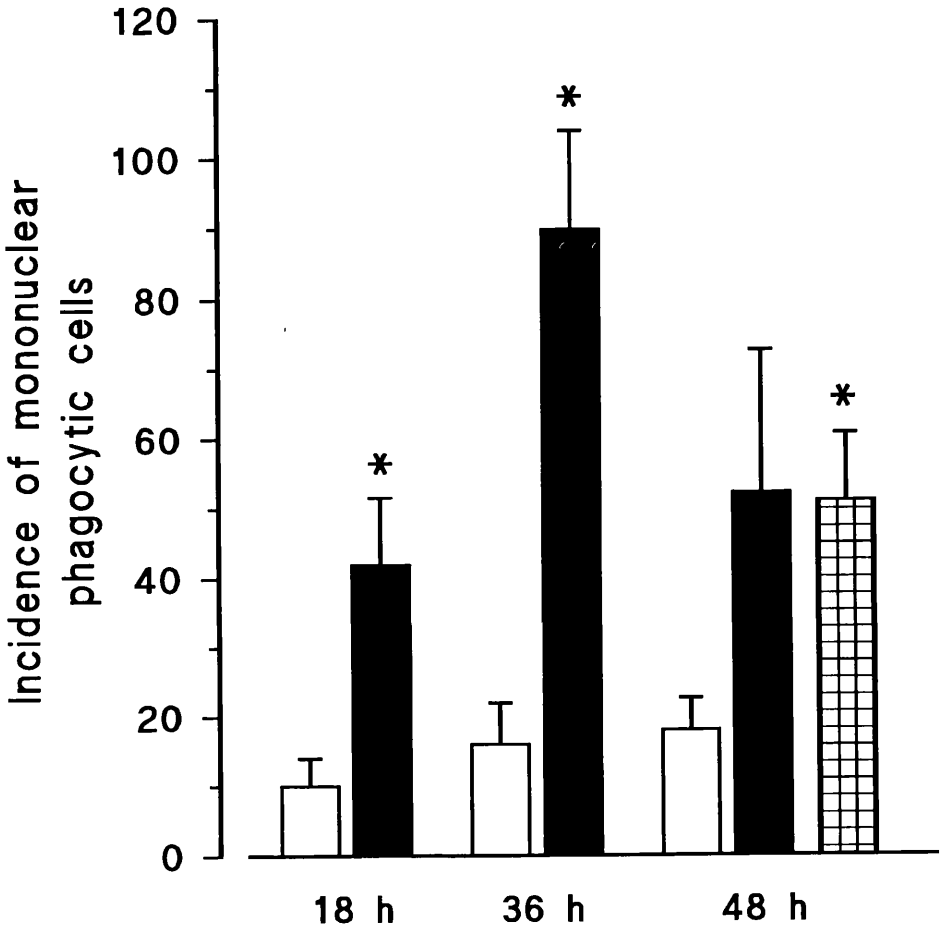

FIGURE 6.2 Effect of TBTO treatment on the incidence of mononuclear phagocytic cells.

Results are means ± SE (n=3) for each timepoint, and are expressed as the number of phagocytic cells with inclusions present in 15 contiguous fields within standard areas of semi-thin resin sections. Treatment groups: control (*open bars*), 60 mg/kg (*closed bars*) and 30 mg/kg (*hatched bars*). Detail of the methodology employed is given in section 6.2.6. * Result significantly different from control value, $p < 0.05$ (Student's t-test).

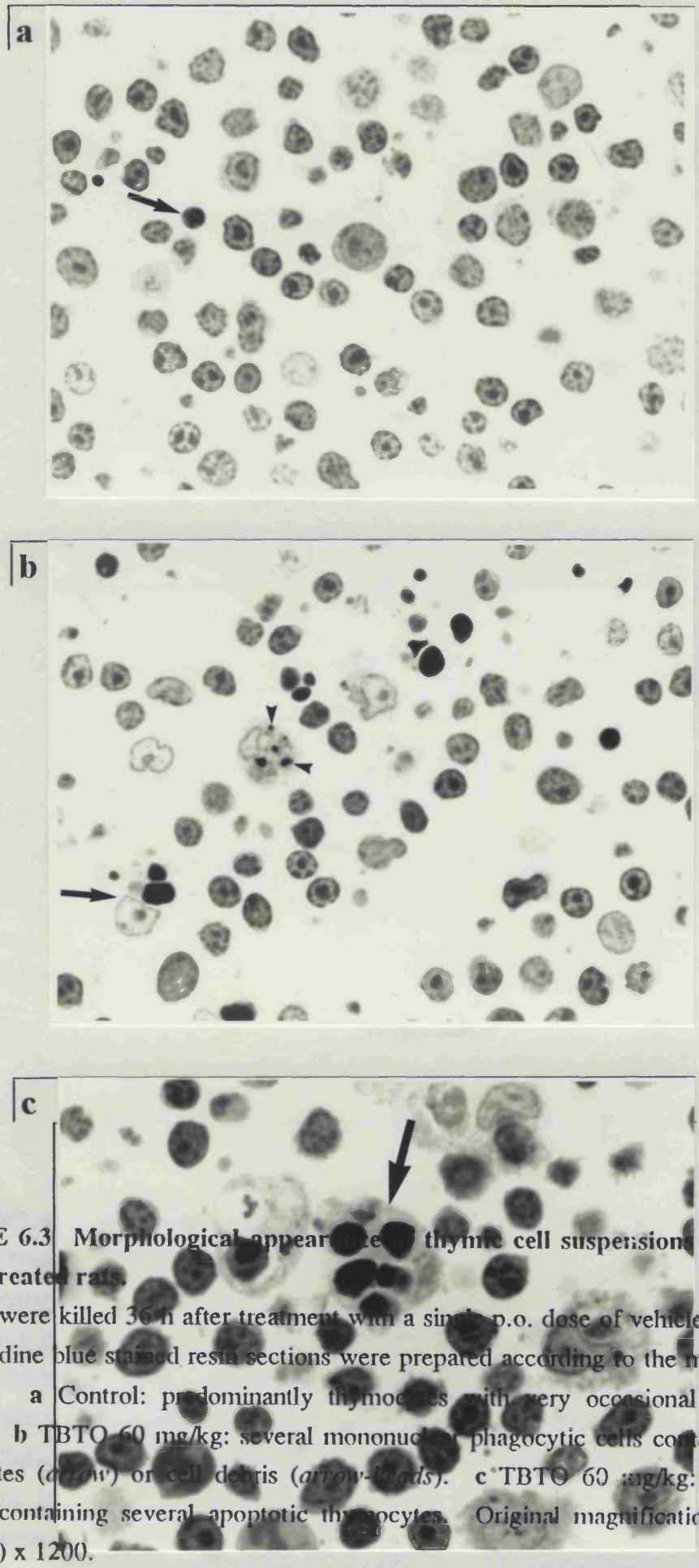

FIGURE 6.3 Morphological appearance of thymic cell suspensions prepared from TBTO-treated rats.

Animals were killed 36 h after treatment with a single p.o. dose of vehicle only or TBTO, and toluidine blue stained resin sections were prepared according to the method described in 6.2.6. **a** Control: predominantly thymocytes with very occasional apoptotic cells (*arrow*). **b** TBTO 60 mg/kg: several mononuclear phagocytic cells containing apoptotic thymocytes (*arrow*) or cell debris (*arrow-heads*). **c** TBTO 60 mg/kg: phagocytic cell (*arrow*) containing several apoptotic thymocytes. Original magnifications: (a) and (b) x 900, (c) x 1200.

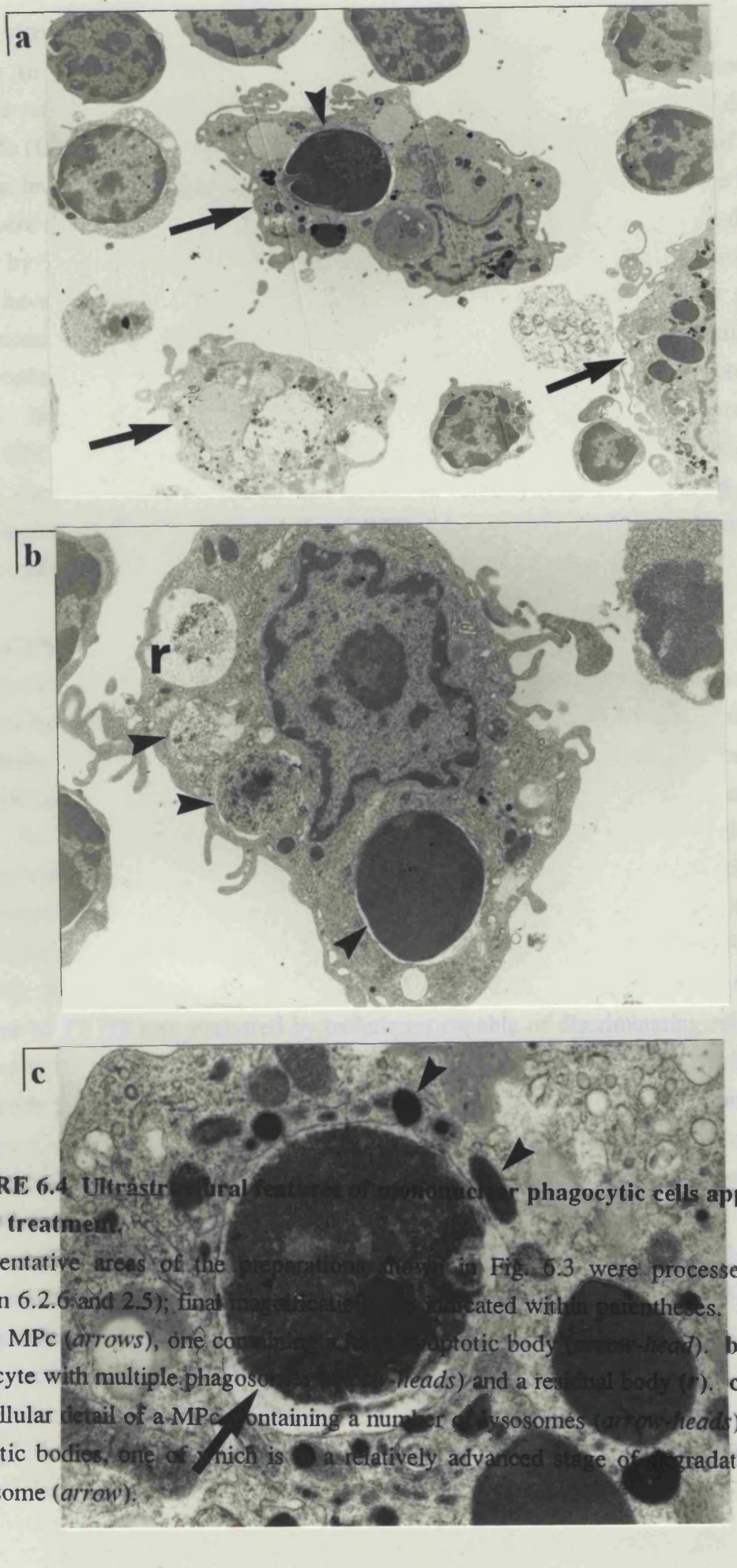

FIGURE 6.4 Ultrastructural features of mononuclear phagocytic cells apparent after TBTO treatment.

Representative areas of the preparations shown in Fig. 6.3 were processed for TEM (section 6.2.6 and 2.5); final magnifications are indicated within parentheses. **a** (x 7 000): several MPc (*arrows*), one containing a single apoptotic body (*arrow-head*). **b** (x 10 000): Phagocyte with multiple phagosomes (*arrow-heads*) and a residual body (*r*). **c** (x 27 000): Intracellular detail of a MPc containing a number of lysosomes (*arrow-heads*) and several apoptotic bodies, one of which is at a relatively advanced stage of degradation within a phagosome (*arrow*).

6.3.5 In vitro studies

In order to investigate the mode of dibutyltin cytotoxicity, isolated thymocytes from immature rats were exposed in vitro to graded concentrations (1-10 μM) of di-n-butyltin dichloride (DBTC). Prior to 6 h, no decline in viability was apparent at any of the DBTC treatment levels. Only slight increases in DNA fragmentation (less than twice the control value) were apparent by 6 h at 1 or 2 μM DBTC (Fig. 6.5), whilst subsequent decreases in viability by 24 h were correspondingly limited. Comparable cytolethality dose-response profiles have previously been recorded by Seinen and co-workers (Seinen et al., 1977a). Higher concentrations of DBTC appeared to be even less effective in stimulating DNA fragmentation, such that the values obtained equated to, or were below that detected in the controls. In contrast, treatment of cells with 2 μM TBTO resulted in the production of marked DNA fragmentation (325% of the respective control mean) in these comparator cultures, together with a substantial late decline in viability (Fig. 6.5). During preliminary morphological studies it was noted that DBTC did not cause significant elevations in the incidence of necrotic cells at the concentrations tested.

6.4 DISCUSSION

The detection of apoptosis following toxic injury to a tissue such as the thymus is hampered by a number of factors. Apoptosis typically occurs non-synchronously in single cells usually surrounded by normal neighbours, whilst the apoptotic bodies formed have a short half-life prior to their presence being masked by phagocytosis (Kerr and Harmon, 1991). In addition, at the light microscope level, certain cytopathological changes observed such as pyknosis and nuclear segregation are also common to necrotic cell death. Biochemical markers, e.g. internucleosomal DNA cleavage may also be difficult to detect in unseparated cell populations even when the incidence of apoptosis is high (Facchinetti et al., 1991). In this study, thymic material derived from rats previously treated with a single oral dose of TBTO was evaluated by techniques capable of discriminating relatively small increases in the number of apoptotic cells. Equivalent treatment regimens with tributyltin compounds produce the greatest depletion of cortical thymocytes in young male rats after 3-4 days (Snoeij, 1987), and therefore emphasis was placed on investigating the period preceding maximal involution of the thymus. Based on available toxicokinetic data (Humpel et al. 1986; Snoeij, 1987), the doses administered (30-60 mg/kg) were calculated to give sustained plasma TBTO levels approaching 1 μM by 24 h after dosing—these should equate to a 2 to 3 fold higher total blood concentration. The intention was that predicted tissue perfusion levels of unmetabolised TBTO should be of a similar order to the plate concentrations employed in the in vitro experiments reported in previous chapters.

Although the disaggregation technique employed was purposely more aggressive than that used to release the lymphoid compartment for the in vitro studies, a visible stromal residue

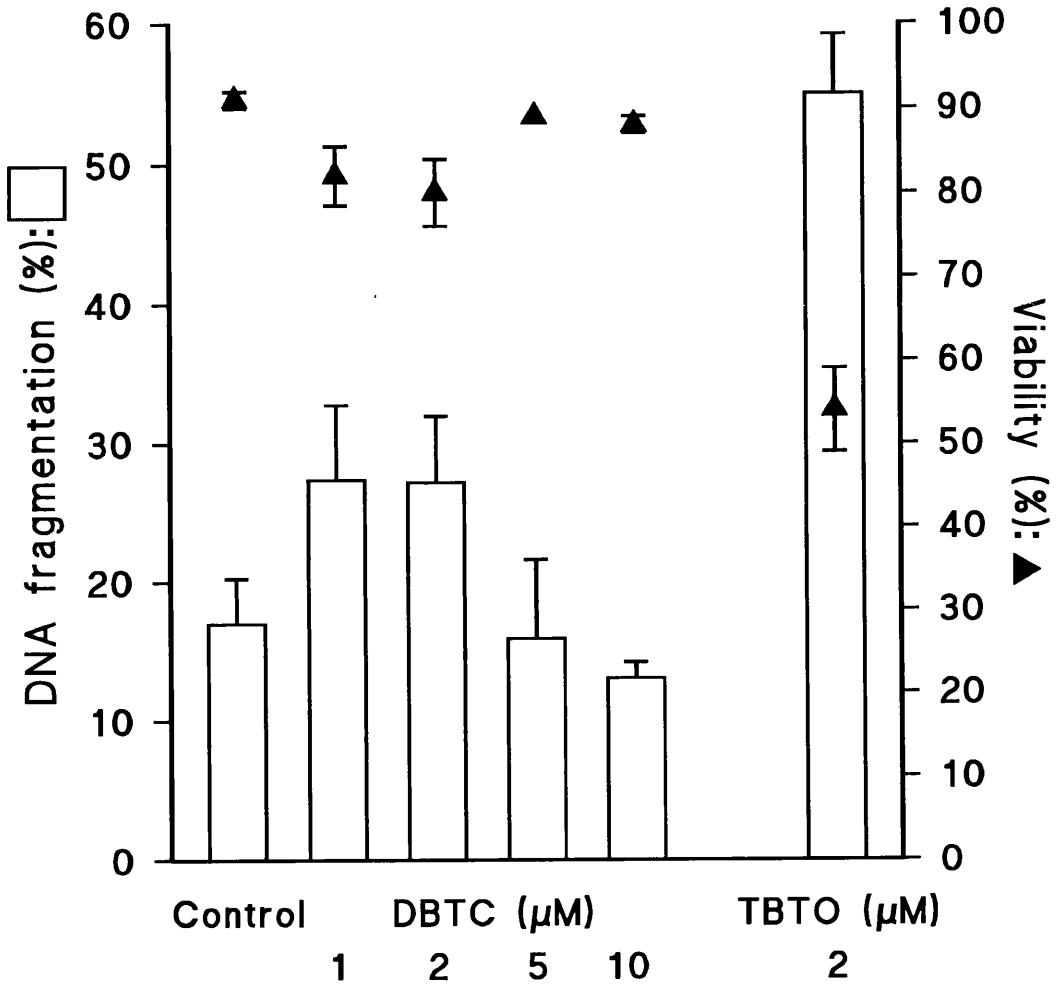

FIGURE 6.5 DNA fragmentation and thymocyte viability after in vitro exposure to DBTC or TBTO.

Estimation of DNA fragmentation (*open bars*) was performed after 6 h incubation with the agents as indicated; results represent the percentage of total DNA resisting sedimentation at 27 000 x *g*; means ± SE from three separate experiments. Viability assessment was conducted at 24 h (▲); means ± SE from at least three separate experiments. DNA fragmentation was determined as described in section 2.6, and viability was estimated by trypan blue dye exclusion as described in section 2.2.

did remain on the separation sieve. Given this, and based on morphological criteria discussed later, it is likely that the resulting thymic cell suspension was principally composed of thymocytes together with a minor MPc population. Small numbers of epithelial cells, erythrocytes and other cell phenotypes must inevitably have been present, but in view of the high lymphoid to stromal cell ratio of the thymus it is improbable that this had a major confounding influence on the DNA degradation and cytopathology observations.

Increased DNA fragmentation, which was temporally progressive in extent and apparently dose-dependent, was noted for TBTO-treated animals (Fig. 6.1a). This contrasted with the low levels of DNA degradation found for the controls which were considered to be consistent with the detection of physiological thymocyte apoptosis in these preparations. The accompanying internucleosomal chromatin cleavage patterns observed after electrophoretic analysis of samples from the majority of rats that received TBTO (Fig. 6.1b) matched that previously described as a cardinal identifier for the occurrence of apoptosis (Wyllie 1980). Further secondary DNA degradation, visualised as 'smearing' in some gel tracks, had no discernible pattern and may have been due either to secondary acid hydrolase action or to artefactual damage arising from the intensive DNA isolation procedures employed. Some commentary is pertinent here regarding the commonly used neutral agarose gel electrophoretic technique, coupled to ethidium bromide visualisation, for the identification of apoptotic internucleosomal DNA cleavage. The relative insensitivity of this method has been widely recognised (Facchinetti et al., 1991; Huang and Plunkett, 1992). The latter investigators cite a reliable detection limit of approximately 25 μg DNA/lane using ethidium bromide fluorescence of nucleosomal ladders. In my hands, 5-10 μg DNA/lane was the lowest achievable value; although this was not routinely obtained, and photographic reproduction of such low intensity fluorescence was unsatisfactory. Therefore in preliminary studies of the action of TBTO in vivo, an attempt was made to use Southern blot analysis of gels, coupled to an enhanced chemiluminescence detection method to try to increase resolution sensitivity. The hybridisation probe utilised, dUTP-fluorescein labelled DNA, was prepared using a commercially available kit (RPN3040 Random prime system; Amersham International plc, Bucks, UK) according to a method adapted from that of Feinberg and Vogelstein (1983). But despite considerable effort, unresolved methodological difficulties prevented application of this approach to these investigations. Whilst accepting the above limitations, the electrophoretic findings in concert with the DNA fragmentation results gave the first indication that TBTO administration produced a supra-physiological incidence of apoptosis in the thymus.

Although there was biochemical evidence for an in vivo stimulation of apoptosis by TBTO, careful examination of both whole thymus sections and cell suspensions failed to reveal a corresponding increase in the incidence of unassociated apoptotic thymocytes. However,

statistically significant elevations in the number of phagocytes containing cell remnants categorised as apoptotic bodies were noted in treated rats (Fig. 6.2; Fig. 6.3 b and c). The occurrence of this phenomenon correlated well with the DNA fragmentation values obtained for individual animals. Ultrastructural examination revealed that the apoptotic bodies resident in the cytoplasm of phagocytes were retained within phagosomes surrounded by lysosomes (Fig. 6.4 a-c). Very similar observations have previously been associated with the resolution phase of apoptosis in a variety of physiological and pathological states (Searle et al., 1975; Pipan and Sterle 1979; also reviewed by Saunders, 1966; Kerr et al., 1972; and Wyllie, 1987). Therefore, the phagocytosis of apoptotic bodies by resident macrophages, parenchymal or neoplastic cells is considered to be a highly reliable diagnostic indicator for the existence and rate of apoptosis (see also section 1.2). Based on morphological assessments, it was concluded that the MPc were macrophages, although the possibility cannot be excluded that a proportion of these cells were of epithelial phenotype. Use of an immunocytochemical technique based on monoclonal antibodies with reactivity to thymic cortical and medullary macrophage populations, e.g. ED-1, ED-2 and ED-7/ED-8 (Van Loveren et al., 1991) would provide valuable information on this issue. It would also be of value to confirm that the phagocytosed apoptotic cells were indeed immature cortical thymocytes.

A number of investigators have previously observed increases in thymic macrophage numbers and activity following administration of TBTO. Administration of a single p.o. dose of 100 mg/kg TBTO to immature rats caused thymic atrophy with cortical cell death and macrophage involvement (Funahashi et al., 1980), but this was preceded by adrenal hypertrophy and elevated cortisol levels indicative of a stress glucocorticoid-mediated effect. Repeated dietary intake of TBTO at 320 ppm (equivalent to approximately 32 mg/kg/day) by young Wistar rats for 4 weeks produced thymocyte depletion accompanied by pyknosis and karyorrhexis, and an increase in the number of lipofuscin-loaded macrophages (Kranjc et al., 1984). Interpretation of this result is complicated by the fact that the treatment level bordered on overt toxicity and therefore, in the absence of contrary biochemistry findings, may have also been stress-induced—similar pathological changes were not evident at 80 ppm. A subsequent study performed in weanling rats by the same group (Vos et al., 1984a) reproduced this result after only 3 days treatment with 320 ppm TBTO demonstrating diminished cell counts and, in contrast to the findings given here, dramatically reduced thymocyte viability. A study by Snoeij and co-workers (Snoeij et al., 1985) which controlled for stress-related effects by using adrenalectomised rats, showed that administration of 100 ppm TBTC for 4 weeks (approximating to 16 mg/kg/day) caused thymic involution in the absence of severe cytotoxicity. Although unreported by them, examination of a published photomicrograph of a methacrylate-embedded section of thymus from a treated animal is suggestive of increased apoptosis with macrophage activity (see page 279 of Snoeij et al., 1985). Two

recently published reports may be of particular relevance. In the first, juvenile male Wistar rats received a single p.o. dose of either 30 or 90 mg/kg TBTO (De Waal et al., 1993); a 4-fold increase in "starry-sky" (*sic*) cortical macrophages was evident by 4 days post-treatment (coincident with diminution of thymic cortical weight). This order of enhancement in phagocyte activity is very similar to that observed in this experiment. In another study, histopathological and TEM examination of the thymic involution produced when young female Balb/c mice received 200 ppm TBTC (25 mg/kg/day) in the diet showed raised numbers of phagocytes present at 2 days (Kempston et al., 1993) In neither case was the potential significance of the finding recognised by the investigators. Considered in the context of my findings, there is now a growing body of evidence indicating a prominent role for MPc action in cortical thymocyte deletion after TBT administration to rodents.

Compared to examination of tissue sections, the technique employed to disaggregate the thymus facilitated the identification of MPc involved in the removal of apoptotic cells. However, for a number of reasons, caution is required in the interpretation of the derived quantitative assessments (Fig. 6.2). The actual phagocyte numbers present in vivo were probably underestimated due to incomplete disruption of the thymic stroma, isolation losses, counting omissions due to plane of section and also difficulties in visualising small apoptotic bodies. Another criticism is that the proportion of MPc released from each organ is liable to relate to the extent of processing; though it is notable that inter-sample variability within experimental groups was never extreme. Furthermore, given the dynamic nature of the process under study, over-reliance on only three timepoints after dosing for conclusions on the course of MPc involvement would be unwise. The diminution in phagocyte number observed between 36-48 h at 60 mg/kg TBTO is interesting (Fig. 6.2). It could be speculated that this related to a resolution phase after an initial cytotoxic event.

Widespread thymic apoptosis in situ, with many clearly identifiable unphagocytosed thymocytes, can be produced in vivo by certain toxic agents, e.g. etoposide (X M Sun and Dr. G M Cohen, unpublished results). In other reports with toxins such as colchicine (Bumbaserivec et al., 1985) and ricin (Griffiths et al., 1987) a more complex situation exists with apoptotic cells in the thymus or other lymphoid tissues together with extensive macrophage uptake of apoptotic bodies. The findings presented here for TBTO are rather atypical, in that whilst the incidence of apoptosis was stimulated by treatment, free apoptotic thymocytes were very rarely observed. This may simply reflect the relatively small absolute increment in apoptosis combined with the limitations of the counting technique, but it is also possible that MPc might have a particularly high avidity for TBT-injured cells given the membrane directed nature of this toxicant.

In view of the previously detailed constraints relating to detection of apoptosis in vivo, it is perhaps unsurprising that signs of non-necrotic thymocyte death have not been reported in previous investigations of TBT-mediated thymic atrophy. Kerr et al. (1972) were the first to point out that the detection of even relatively low levels of apoptotic markers could indicate that extensive cell deletion was taking place within a tissue. It has been calculated that only an increase to 4-8% in the point prevalence of apoptosis in a tissue such as the thymus, could account for an involution in organ mass by 50% over a period as short as three days (Arends and Wyllie 1991). This should be considered in the context of the differential increases in DNA fragmentation and incidence of mononuclear phagocytes reported here. In order to assess whether apoptosis could possibly account partially or *in toto* for the cell deletion component of TBT-mediated thymic involution, a kinetics calculation was performed. It must be stressed that due to the large number of assumptions implicit in the model fitted to the experimental data, and the small study size, the resulting evaluation is highly tentative. Without confirmation as to its validity it can only be viewed as indicative of the order of magnitude for the deletion process. Details of the model, intrinsic assumptions and details of the calculation are given in Figure 6.6. The most critical factor involved is the duration selected for the span of visibility of apoptotic bodies; it is now widely accepted that the initial phase of apoptosis takes only a matter of minutes (Wyllie, 1985), whilst the ensuing degradative process within phagocytic vacuoles has a half time of hours (Moore, 1987). Good data are available for some normal vertebrate cell types including liver cells, in which a duration of about 3 h is typical (Bursch et al., 1990b), and senescent neutrophils for which a clearance time of 1-2 h has been established (Dr. J Savill, personal communication). Other estimates of apoptotic body duration range from 4-9 h (Arends and Wyllie, 1991). In the absence of definitive published kinetics data for rodent thymocytes in vivo, timescales bounding 2 to 6 h were arbitrarily selected as a best estimate. Clearly this model can be criticised on a number of counts, including the following: (i) during the course of the TBT mediated thymotoxicity it is highly unlikely that the rate constant for apoptosis will be invariant; (ii) in some cases a single apoptotic thymocyte may generate several apoptotic bodies, therefore with reference to assumption '4' there will be an overestimate of the incidence of apoptosis; (iii) not all MPc will have been extracted from the stroma and made available for counting, hence this will lead to an underestimation error. Notwithstanding these objections, it may be seen that the projected cell loss figures due to apoptosis are close to the actual cell mass lost in the involuting thymi.

To sum up thus far, increases seen in stereotypical DNA degradation after TBTO treatment, allied with the previously detailed cytopathology findings, provide adequate evidence to conclude that apoptosis is a major cause of thymocyte elimination from the involuting thymus. Kinetics estimates support the idea that the incidence of this process is sufficient to account for a large proportion, or perhaps all, of the cortical cell loss.

Assumptions

1. By 36 h after administration of a p.o. dose of 60 mg/kg TBTO, the thymic involution approximates to 50% of normal cell mass. (Refer to total cell count data; sub-assumption that the cell loss is essentially composed of thymocytes). This treated group is typical of the TBTO-mediated process.
2. The incidence of mononuclear phagocytic cells (MPc) containing apoptotic bodies (AB) is directly proportional to the extent of involution, i.e. no other major cell deletion mechanism exists.
3. The cell elimination rate constant is invariable over the course of thymic involution, and therefore point prevalence calculations are applicable, e.g. at the observational mid-point of 18 h.
4. Each AB contained in the MPc represents the deletion of a single apoptotic thymocyte.
5. The clearance time of included AB, equates to their duration of visibility and lies between the bounds of 2 to 6 h.
6. All MPc in thymic tissue made available for counting, these are uniformly distributed, and the sections viewed are representative of the total derived cell population.
7. Subtraction of control mean MPc no. from treated group mean will correct for spontaneous background apoptosis.

Calculation

Treated group: mean AB inclusions in MPc = 3.4

Treated group: mean no. MPc at median timepoint after dosing (18 h) = 40

$\therefore$ No. AB in 15 contiguous fields = 40 x 3.4 = 136

Control group: mean AB inclusions in MPc = 1.6

Control group: mean no. MPc at median timepoint after dosing (18 h) = 10

$\therefore$ Subtracting spontaneous background (control value) = 136 - (10 x 1.6) = 120

Average no. cells observed in 15 fields of cell preparations = ~ 2600

Treated group mean total cells available in thymic isolate (18 h) = ~ 600×10^6

$\therefore$ Theoretical maximal AB yield due to treatment (18 h) = $(600 \times 10^6/2600) \times 120$

$= 28 \times 10^6$

$\therefore$ Total cells eliminated by 36 h for a range of clearance times spanning 2 to 6 h:

2 h = $18 \times (28 \times 10^6)$ = ~ 500×10^6

6 h = $6 \times (28 \times 10^6)$ = ~ 170×10^6

Actual differential in mean thymic cell counts between treated and controls at 36 h

= ~ 430×10^6

FIGURE 6.6 TBT thymotoxicity: kinetics of apoptosis estimate.

The calculation is based on data derived from the experimental group which received a single p.o. dose of 60 mg/kg TBTO (see section 6.2). Assumptions made in the calculation are applied without the use of weighting factors.

It will be apparent from the preceding introduction to this chapter, that to date, there is no consensus about the fundamental cellular effect underlying the depletion of cortical thymocytes by triorganotins. Some of the controversy undoubtedly comes from the tendency to oversimplify an experimental system in the search for a single unifying mechanism. For example, in any consideration of the prospective mechanism of TBT thymotoxicity, the inevitable presence of the highly active dealkylation metabolite DBT militates against a postulate of a single mode of action. Although my work may be more pertinent to identification of the mode of cell deletion rather than the underlying mechanisms, some consideration of the latter is appropriate at this juncture. To aid in the overview of the various possibilities, some important candidate mechanisms are summarised in Figure 6.7, together with ones newly emergent from these experiments.

As detailed in section 6.1.2, several bases for action for the triorganotins, in particular TBT, have now been discounted. These include severe cytotoxicity involving necrosis and inflammatory change, disturbance of extrinsic thymus-directed hormones, metabolic alterations causing secondary immunosuppression, and overt damage of the thymic epithelium. Whilst TBT compounds are cytotoxic to isolated bone marrow cells, they have only limited effects on marrow cellularity in vivo which become apparent after prolonged administration (Vos et al., 1985). Therefore it has been surmised that depletion of precursor thymocyte stem cells is unlikely. It should be noted that prothymocytes represent a small fraction of the bone marrow cell population and therefore their differential sensitivity is not yet properly established. Similarly, there is no evidence to suggest that a major efflux or redistribution of thymocytes occurs after organotin treatment.

In contrast to the dialkyltins, TBTO does affect cells of the mononuclear phagocyte system (Seinen et al., 1977b; Vos et al., 1984a), since slight inhibition of splenic and peritoneal macrophage action has been observed. Taken in isolation, the cytopathology findings reported in section 6.3.4 are not wholly inconsistent with the possibility of a direct action of TBTO on thymic macrophages causing abnormal activation of phagocytosis, or a reduced clearance of physiologically-derived apoptotic thymocytes. However, this cannot account for increased cortical thymocyte loss, and it is difficult to find a realistic rationale for a primary involvement of MPc dysfunction.

Thymic involution is quite a common non-specific finding in rodent experimental toxicology studies at or near the maximally tolerated dose (Stefanski et al., 1990). Hence stress-induced lymphocytolysis mediated by glucocorticoids is an important possible confounding factor of particular relevance to investigations of organotin thymotoxicity. It has brought into doubt the conclusions from a number of previous reports where dose level selection was inappropriately high, or generalised toxicity was observed (Snoeij, 1987). Whilst stress-related thymocyte killing has been reported to occur when TBT has been

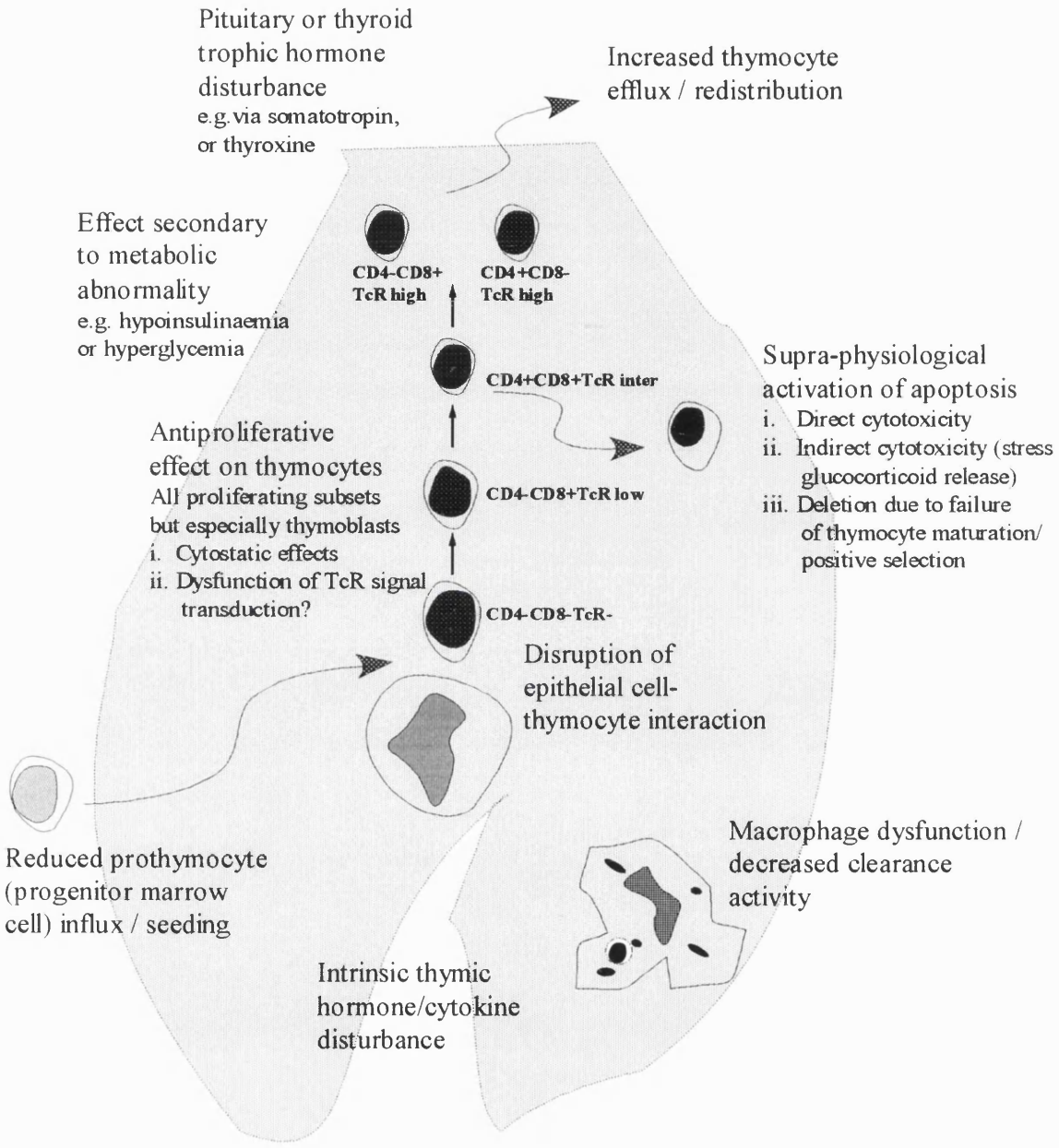

FIGURE 6.7 Candidate mechanisms for the in vivo thymotoxicity of TBT.
The rodent thymus is depicted in stylised fashion, with thymocyte ontogeny and interaction shown in a much simplified form.

administered at relatively high doses or for protracted periods, often resulting in adrenal hypertrophy, I have discounted the involvement of a similar mechanism in this study for several reasons. Firstly, free apoptotic cells were present in sections from treated animals and controls at a similarly low incidence, and the signs of widespread cell destruction and viability loss reported to occur after indirect or direct glucocorticoid action (Vos et al. 1985; Compton and Cidlowski 1986) were notably absent. In a closely comparable study performed by Snoeij et al. (1988a) the thymic atrophy caused by intubation of single doses of TBTC was linear over the range 5-60 mg/kg, and stress-related histopathological changes in the thymus were not reported. Additionally, in common with our findings, no changes in adrenal weight were recorded by these investigators; contrary to this, Funahashi et al. (1980) observed that with an overtly toxic dose of 100 mg/kg TBTO, increases in adrenal mass occurred rapidly (by 12 h) and persisted until thymus changes developed. The observation that thymic weight reduction was equivalent in adrenalectomised and non-adrenalectomised rats fed with moderately high levels of TBTC (Snoeij et al., 1985) is also of relevance. In connection with my work, it is recognised that serum corticosterone investigations in satellite treatment groups, or the use of adrenalectomised animals would have provided additional security to the above reasoning. However, at the time these techniques were unavailable.

Some investigators are convinced that the prior metabolic dealkylation of triorganotins to give active dialkyltin analogues is crucial to the subsequent cortical thymocyte loss (IPCS 1990; and see 6.1.2). In terms of a mechanism, this could involve cytotoxic or cytostatic (antiproliferative) mechanisms. Since there had only been a single limited negative report of the potential of DBT to activate thymocyte apoptosis (Aw et al., 1991), I performed a more extensive in vitro study on DBTC, using TBTO as a comparator agent. Exposure of rat thymocytes in vitro to low concentrations of TBT resulted in considerable fragmentation of genomic DNA and a subsequent decline in cell viability, indicating that thymocyte apoptosis had been significantly activated by this treatment (see chapter 3 and Fig. 6.5). This was at variance with the finding that equimolar concentrations of DBT were relatively ineffective in stimulating thymocyte apoptosis (Fig. 6.5). In addition, for reasons that are not clear, at higher DBTC levels (5 or 10 μM) there was a reversal in even this moderate degree of cytotoxicity. Plate concentrations of DBTC below 1 μM were not examined. Shortly after completion of these experiments, a study by Comment et al. (1992) assessed the effect of DBTC in the concentration range 0.1-1 μM. They found LC_{50} values of 0.2-0.3 μM for isolated mouse and rat thymocytes after 18 h incubation, and attributed the cytolethality to activation of apoptosis. A number of methodological discrepancies and apparently anomalous results are evident in their report: (i) though DNA fragmentation at 0.5-0.7 μM DBTC was 49% after 6 h, the control value was very high (approximately 30%); (ii) morphological markers had a quantitatively poor correlation with the extent of DNA degradation; (iii) concurrent necrotic cell death was evident at

'apoptotic' concentrations of DBTC; (iv) patterns of internucleosomal DNA cleavage were grossly inconsistent compared to indicated DNA fragmentation levels. In vitro exposure of rat thymocytes to DBTC (1 or 5 μM) for 10 minutes has recently been shown to disturb forward light scatter and side scatter in $CD4^+CD8^+$ subsets when evaluated by flow cytometry 22 h later (Pieters, 1992)—this was interpreted as an increase in apoptosis. On balance, DBT must be assumed to have some potential to cause apoptotic killing of thymocytes. Although less potent in this respect than TBT, this may have bearing on cytocidal effects in vivo given the relatively higher target tissue levels of DBT accruing after metabolism of TBT compounds. DBT seems to possess significantly lower potential to activate apoptosis than TBT, but it is impossible to completely discount the alternate hypothesis that the former is alone the proximate toxicant. In view of the very high biological activity of TBT such a simplistic explanation seems implausible.

Due to demonstrations of potent antiproliferative effects both in vitro and in vivo, (refer to 6.1.2), a fashionable hypothesis until quite lately was that dialkyltins administered directly, or formed by dealkylation, produced thymic involution by direct cytostatic actions on developing thymocytes (Snoeij et al., 1987). Since neither the antiproliferative effects of di- or tributyltins can account for their selectivity towards thymocytes, a new postulate is that more subtle disruptions occur to thymic T-cell maturation involving disordered epithelial cell signalling (Penninks et al., 1990). This focuses on the transition of the immature $CD4^-CD8^-$ to $CD4^+CD8^+$ subsets as a critical phase. Some preliminary but interesting data shows that DBTC did not affect spontaneous in vitro differentiation *per se*, but does decrease the number of thymocytes bound to thymic epithelial cells and also enhances Ca^{2+} fluxes associated with TcRαβ signal transduction processes (Pieters et al., 1993).

In conclusion, the involvement of rapidly resolved thymocyte apoptosis is consistent with both the previously described histopathology and reversibility of the thymic atrophy described following exposure to TBT. My work provides a different perspective on the cellular events involved in the thymus-dependent immunotoxicity of TBT. A plausible hypothesis is that a composite mechanism is involved in cortical thymocyte deletion, involving (i) TBT cytotoxicity, with a possible contribution from DBT, resulting in activation of apoptosis, and (ii) complex antiproliferative or antidevopmental effects predominantly due to DBT. The latter may involve multiple sub-components including disturbed interaction of thymocytes with epithelial cells and altered TcRαβ-signal transduction. Since disruption of thymocyte maturation in itself is likely to provoke apoptotic deletion, if it interferes with positive selection, the end result of both effects may be indistinguishable.

CHAPTER 7
FINAL DISCUSSION AND CONCLUSIONS

The objective of this chapter is to overview major findings and conclusions, to indicate areas of uncertainty, and possible future directions for experimental investigation.

7.1 Recent publications

At the point this thesis was completed, two separate reports relevant to TBT-stimulated thymocyte apoptosis were published. Firstly, Zucker and co-workers (1994) confirmed the protein synthesis independency of TBT apoptotic killing, and observed mutually antagonistic effects between TBT and dexamethasone activated apoptosis. Taken in tandem with the apparent rapidity of action of TBT, they concluded that different initiation mechanisms were involved in triorganotin and glucocorticoid apoptosis. Where areas of investigation overlap (see Chapter 3 and 5), my results are broadly in concordance with their findings. However, even with due allowance for methodological differences between the respective studies, TBTO stimulation of DNA degradation and the appearance of apoptotic markers appears to be slower than they describe for TBT methoxide. In the second publication, Chow and Orrenius (1994) reported that TBT very rapidly depolymerised the rat thymocyte F-actin microfilament cytoskeleton by a mechanism predominantly involving thiol modification, with only a limited contribution from Ca^{2+} fluxes. Triphenyltin or DBT, both of which are immunotoxic and have at least some potential to cause apoptosis, had similar effects whereas non-immunotoxic organotins did not. This data complements my finding of the profound effect of TBT on the thymocyte microtubular cytoskeleton (chapter 5). Though Chow and Orrenius propose that cytoskeletal alterations could be important in the actuation of apoptosis, both myself and their group have observed that initiation of TBT-mediated apoptosis is a Ca^{2+}-dependent process (Chow et al., 1992; chapter 3) whereas cytoskeleton disruption appears not to be fundamentally linked to $[Ca^{2+}]_i$ alterations. In addition, my data (see sections 5.3.4 and 5.4) suggest that microtubule disruption is not directly connected to non-necrotic cell killing by TBT. Therefore unless microfilament depolymerisation is responsible for nuclear level events such as chromatin decondensation, cytoskeletal changes are probably not pivotal events in thymocyte apoptosis. This does not preclude the possibility that organotin-mediated cytoskeletal dysfunction could have very significant influence on the functional capability of immune system cells. An interesting correlation exists between the microfilament-disrupting efficiency of various organotins (Chow and Orrenius, 1994) and their propensity to cause apoptosis, i.e. TBT>TPhT>DBT, which merits further investigation.

7.2 Activation of thymocyte apoptosis by TBT

In vitro studies demonstrated that exposure to low concentrations of TBTO activated non-necrotic death in thymocytes isolated from immature rats. A number of features provided secure evidence that the mode of cell killing involved was apoptosis. Key criteria were the appearance of stereotypic morphological markers followed by delayed loss of membrane

integrity (chapter 3); extensive internucleosomal DNA fragmentation (chapter 3) which was Ca^{2+}-dependent (chapter 4); and the inhibitory effects of Zn^{2+} (chapter 4) on these processes. In these respects, cell killing by TBTO was comparable to that induced by control compounds with established propensity to cause thymocyte apoptosis. These were the glucocorticoid MPS (chapter 3) and the cation ionophore A23187 (chapter 3).

An intriguing aspect of the in vitro work was the nature of the biphasic cytotoxicity response, whereby low concentrations of TBTO (< 5 μM) caused apoptosis, whereas higher levels evoked necrosis (chapter 3). Thus TBTO itself provided the means to confirm the contrast between apoptotic and necrotic death modes, without recourse to the use of another comparator agent. This finding also confirmed the postulate that apoptosis can be induced in susceptible cells by injurious stimuli of lesser amplitude to those causing necrosis (Kerr et al., 1972; Wyllie, 1987b). The abrupt concentration-effect transition from maximally effective apoptotic levels of TBTO (Fig. 3.5) of around 2 μM, to those producing necrosis (3.5-5 μM), paralleled that observed for A23187 (Fig. 3.4b). Such a steep concentration-effect curve suggests the existence of one, or a few, critical cellular targets with a minimum integrity or activity requirement to allow apoptosis. The alternative of a specific locus instigating the transition to necrosis appears much less plausible. My studies were not designed to probe mechanistic aspects of the apoptotic-necrotic threshold, though this is clearly now a fundamentally important question in toxicology (e.g. see Lennon et al., 1991). With respect to TBT, it is unlikely that a critical delineating $[Ca^{2+}]_i$ is involved, but plasmalemmal Na^+/K^+-translocating ATPase function may be a critical biochemical target (see section 3.4).

My findings on TBTO, together with reports that TBTC (Aw et al., 1990) and TBT methoxide (Zucker et al., 1994) both markedly stimulate thymocyte apoptosis support the theory that the anionic substituent of such organotins is of limited consequence at the cellular level (Penninks et al., 1990). The relative biological activity of the TBT cation (TBT^+), and another physiologically relevant species, e.g. TBT hydroxide or chloride, is currently unestablished.

Possible future research directions (utilising the isolated thymocyte model unless otherwise stated) are given below:

1. Extend the data on low concentrations (< 1 μM) of TBTO, to investigate the EC_{01} for TBT apoptosis in vitro. Establish critical product value (CPV) functions on the basis of concentration and exposure time. Examine the reversibility of TBT cytotoxicity.
2. Investigate in vitro the effect of other triorganotin and diorganotin homologues. Some doubts still remain in respect of the propensity of DBT to cause thymocyte apoptosis (see section 6.3.5; Aw et al., 1990; Comment et al., 1992). Establish the relationship of lipophilicity and also anionic substituent nature to apoptotic potency.

3. Use CD identification or fractionation techniques to determine the relative sensitivity of thymocyte subpopulations to TBT-activated apoptosis.
4. Investigate the relationship of parameters such as Na^+/K^+-ATPase inhibition, univalent cation homeostasis, and $[Ca^{2+}]_i$ to the mode of cell death effected by TBT.
5. Perform bridging studies to enable better linkage with the in vivo work discussed later. The study of TBT thymotoxicity by means of fetal thymic lobe explant culture, to more closely mimic the in vivo situation, and avoid artefactual disruption of the thymic microenvironment might be one such avenue.
6. Examine TBT cytolethality modes in other cells, e.g. mature T cells; CEM human T-lymphoblastoid cell lines; murine erythroleukemic cells; HL-60 cells; and lower order vertebrate and invertebrate systems of relevance to TBT ecotoxicity. Use thymocytes from clinical thymectomy to establish the relevance of the in vitro findings to human cells.

7.3 Nocodazole also causes thymocyte apoptosis

Nocodazole, a specific antimicrotubular agent, had previously been shown to cause apoptosis in myeloid cells (Martin and Cotter, 1990). The studies reported in chapter 5 were the first demonstration that this compound could also activate this death mode in rat thymocytes (section 5.3.3). The initiation mechanism appeared to relate to disruption of the microtubular cytoskeleton, since microtubule loss preceded cell death, and the microtubular stabilising agent taxol A was cytoprotective (section 5.3.4).

The following further work is proposed:

1. An in depth evaluation of the importance of the cytoskeleton in the cytotoxicity of various agents with specific or non-specific effects on this locus. To include investigation of cation ionophore A23187; reversibility experiments using nocodazole; and the action of sulphydryl group reactive compounds.
2. Application of more sophisticated techniques such as quantitative immunofluorescence flow cytometry, ultrastructural immunocytochemistry assessment, and radiolabelled colchicine competitive binding assays.
3. Determination of the role of Ca^{2+} fluxes in cytotoxic agent disruption of microtubules.

7.4 Mechanisms in TBT-stimulated apoptosis

Apoptosis still occurred in isolated thymocytes exposed to concentrations of TBTO causing rapid and maximal inhibition of protein synthesis (Chapter 5; Fig. 5.2). The protein synthesis independency of this phenomenon was confirmed using the translational inhibitor cycloheximide (Fig. 5.3), a finding recently confirmed by other investigators (Zucker et al., 1994). As discussed in chapter 5, this challenges the long standing axiom that thymocyte apoptosis is dependent on de novo protein synthesis. Apart from heat shock (Sellins and Cohen, 1991; Migliorati et al., 1992) and gliotoxin (Waring, 1990), equivalent observations

have now been reported for the intracellular zinc chelator TPEN (McCabe et al., 1993). It seems implausible that such disparate agents could share a common mechanism of action, and the tenet of obligate macromolecular synthesis dependency in apoptosis is now discredited even in the thymocyte model. Three inferences can be drawn from my work: (i) the proteins required for TBT apoptosis are constitutively present in thymocytes, and are not in rapid turnover; (ii) no de novo synthesis is required for the activation of involved effector proteins; (iii) it is possible that repressor protein loss, i.e. a *release* model of apoptosis (Cohen, 1993; Jacobson et al., 1994), could be operational. However, there is currently no direct evidence to support the latter hypothesis, and the rapidity of TBT-mediated apoptosis, and the generally poor correlation between macromolecular synthesis inhibition and apoptosis (see 1.3.3) militate against this idea.

Figure 7.1 summarises certain other possible initiation mechanisms for apoptosis following cellular injury with TBT. Cytoskeleton disruption does not seem to be directly implicated (chapter 5; section 7.1). Energetics failure in thymocytes at apoptotic concentrations of TBT is incomplete (chapter 5), and FCCP which produces similar oxidative phosphorylation inhibition does not cause apoptosis (section 5.3.2). On the contrary, it is interesting that non-necrotic cell killing can still proceed when cellular ATP pools are severely depressed (chapter 5). At least in thymocytes, there is no evidence for cell cycle blockade as a death program trigger (chapter 5). Though intracellular acidification can activate effector enzymes such as DNase II (Barry and Eastman, 1992; 1993), the postulate that lactate and inorganic phosphate accumulation in TBT-intoxicated cells (section 5.4) could be relevant remains to be investigated. Membrane fixation and marked Na^+/K^+-ATPase inhibition are likely to be effects of more significance at necrotic concentrations of TBT. The possibility of direct relaxation of high order chromatin superstructure by TBT, thereby facilitating nuclease attack, was not fully addressed in these studies, but preliminary data (section 5.4) did not suggest this was the case.

Ample evidence exists to implicate Ca^{2+} fluxes in thymocyte apoptosis (chapter 4), and the simplest model is that low level TBT exposure causes a moderate and sustained elevation in $[Ca^{2+}]_i$ which leads to chromatin degradation and cell death. The data presented in chapter 4 relating to the protective effects of intracellular chelators support this postulate, and are in line with other more detailed studies (Aw et al., 1990; Chow et al., 1992). TBT circumvention of a protein synthesis requirement for apoptosis could relate to direct Ca^{2+} fluxes which obviate the need for porter proteins (McConkey et al., 1992), and therefore act at a downstream point of a single death pathway (Martin, 1993). If this is so, then the mechanism of action of Ca^{2+} ionophores requires reconsideration, since these agents do show macromolecular synthesis dependency in the thymocyte model (Wyllie et al., 1984a; McConkey et al., 1989a). Intranuclear Ca^{2+} increases can activate constitutive Ca^{2+}/Mg^{2+}-dependent endonucleases, and also cause chromatin unfolding, especially

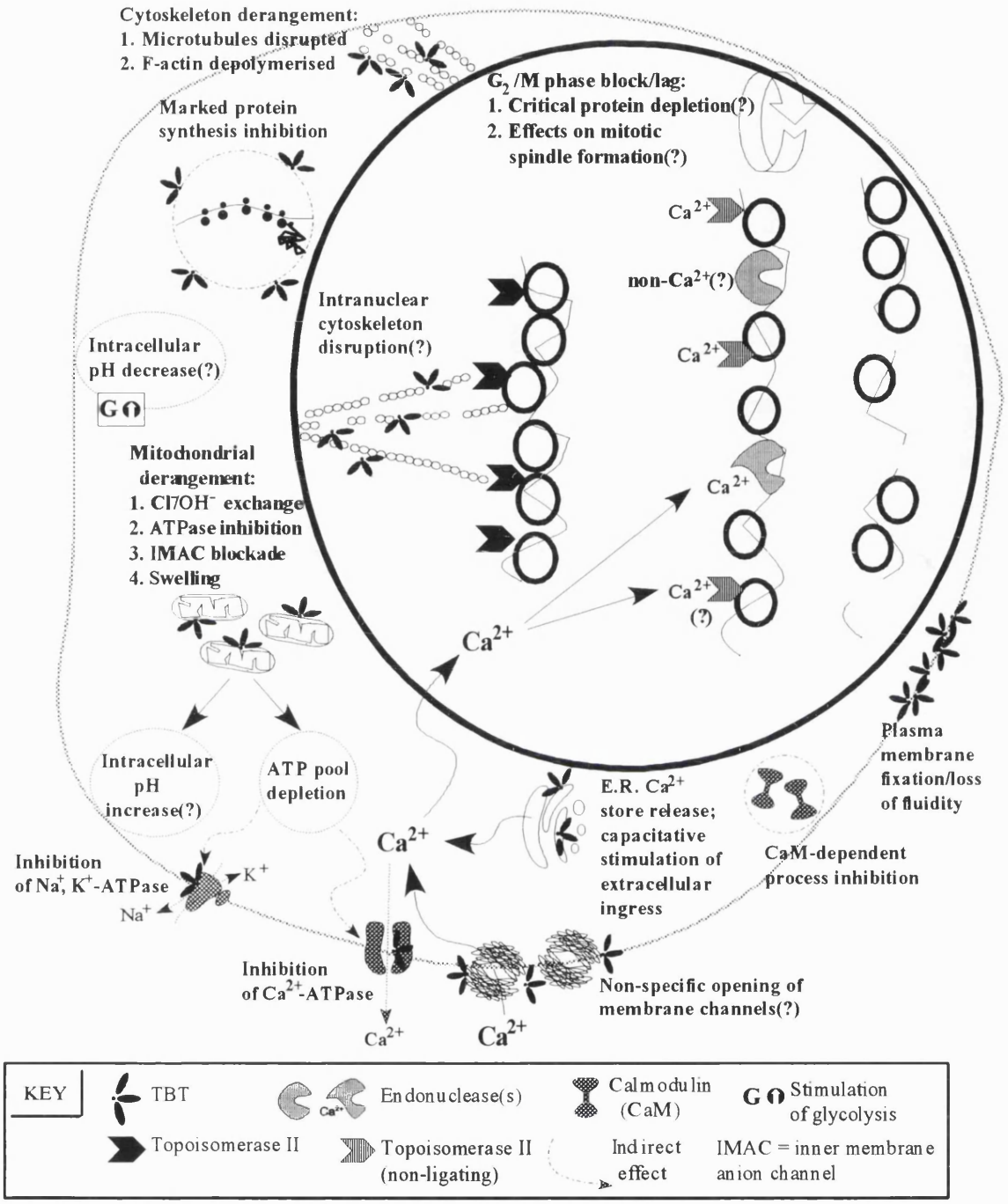

FIGURE 7.1 Known or proposed cytopathic and biochemical effects of TBT.
An overview of key effects (some with potential relevance to apoptotic mechanisms) is shown in the context of a notional cell; general applicability to all cell types is not necessarily inferred. (?) indicates a hypothesised effect, or one lacking adequate experimental substantiation.

in circumstances of elevated pH (McCabe et al., 1992). Paradoxic to the prior statement regarding the possibility of cellular pH drop in TBT-treated cells, because of triorganotin inhibition of proton pumping, there is also the potential for extra-mitochondrial pH increase (section 5.4).

The data presented in chapter 4 reveal that Zn^{2+} can protect TBT-exposed rat thymocytes from internucleosomal DNA cleavage, certain major morphological apoptotic stigmata, and delayed viability loss. Ancillary findings support the notion that multiple DNA degradative processes exist in thymocyte apoptosis (Cohen et al., 1992; Brown et al., 1993; Sun and Cohen, 1994), and that the inhibitory action of Zn^{2+} is restricted to endstage events.

Topoisomerases may be implicated in early chromatin changes in apoptosis (section 1.3.4 and 1.3.5), and it is also possible that chromatin relaxation in TBT-injured cells could be in part due to the action of topoisomerase II. In such circumstances, elevated Ca^{2+} and depleted ATP levels could trap the enzyme in a form which cleaves but does not religate DNA (section 4.4). This possibility remains speculative; further work, including studies with minor groove ligands such as H33258, should be performed.

There have been contradictory reports on the modulation of T cell apoptosis by PKC stimulation via the use of phorbol esters (chapter 4). Based on my results, there is no good case to support the unbalanced signalling hypothesis (McConkey et al., 1990c) in pathologically initiated thymocyte apoptosis.

Certain of the modulator experiments described in chapter 4 are suggestive of differential inhibition of thymocyte apoptosis. For example, cyclosporin A is known to block activation-induced cell death (Shi et al., 1989) but did not protect against glucocorticoid or TBT-mediated apoptosis (section 4.3.6), and although phorbol esters were similarly ineffective they did substantially reduce levels of spontaneous DNA fragmentation in the controls (Fig. 4.10). Apart from these data, there is evidence for the existence of multiple interlinked signal transduction pathways involved in the initiation of apoptosis in immature T cells. Cation ionophores antagonise cell killing by glucocorticoids, but not CD3 ligation (Iseki et al., 1993), and heat shock protects thymocytes against apoptosis caused by dexamethasone, TPA or A23187 (Migliorati et al., 1992). Most recently, it has been demonstrated that TBT and glucocorticoids may use different apoptotic pathways since they mutually antagonise each others action (Zucker et al., 1994). It is also notable that *bcl-2* inhibits the death program activated in murine thymocytes during negative selection but is not protective against the effects of glucocorticoids, irradiation, ionophores, phorbol esters or anti-CD3 antibody (Sentman et al., 1991; Strasser et al., 1991). Furthermore, thymocyte apoptosis can occur both by macromolecular synthesis dependent or independent mechanisms (section 5.4). As intimated in section 4.4, even various

'sub-pathways' probably exist, e.g. multiple entry points in Ca^{2+}-modulated transduction systems. Some of the data fit an alternate hypothesis of a single pathway with multiple trigger points, of which only the early stages are protein synthesis dependent (Martin, 1993). However, the weight of evidence indicates that, at least in thymocytes, several essentially separate signal transduction systems operate with interlinks that permit 'cross-talk' between them. Figure 7.2 provides a partial overview of known major pathways.

In summary, TBT is an unusual and interesting probe for mechanistic investigation of thymocyte apoptosis. However, the plethora of biochemical and cellular effects it elicits complicates study design.

The following further work is proposed:

1. Use ^{35}S-methionine labelling and PAGE to confirm that TBT apoptosis proceeds without specific de novo protein synthesis.
2. Intracellular pH measurements (including compartmentalisation) following TBT exposure, using fluorescent probes and digitised video microscopy.
3. Studies of DNA fragments obtained during TBT-mediated apoptosis, e.g. to assess cleaved end character.
4. Thymocyte nuclei isolation experiments could be employed to investigate the characteristics of effector enzyme(s) whose activity is upregulated by TBT.
5. The observations relating to taxol as an inhibitor of apoptosis caused by microtubular disruption require replication and extension. Investigate the relevance of cytoskeletal disruption to functional deficits induced by triorganotins in immune system cells.
6. Clarify whether triorganotin compounds possess protein thiol reactivity.
7. Several potential lines for the investigation of signal transduction processes in TBT cytotoxicity exist. One specific is the differentiation of the relative importance of the various components of the TBT-mediated $[Ca^{2+}]_i$ increase, e.g. modulation of intracellular stores, and activity profiling of the plasma membrane Ca^{2+}-translocase.
8. Investigate the role of topoisomerase II in thymocyte apoptosis.
9. Pathways central to positive and negative signalling in thymocyte apoptosis are poorly understood; there is ample scope for further study, including examination of 'cross-talk' mechanisms, and the applicability of protein synthesis dependency.

7.5 TBT thymotoxicity in vivo

The findings detailed in chapter 6, constitute the first report that TBT thymotoxicity in vivo involves apoptosis as a cellular elimination mechanism. This conclusion was based on observations of elevated absolute DNA fragmentation values, supra-physiological levels of internucleosomal DNA cleavage, and increased incidence of mononuclear phagocytes (MPc) containing apoptotic bodies following acute administration of TBTO to immature

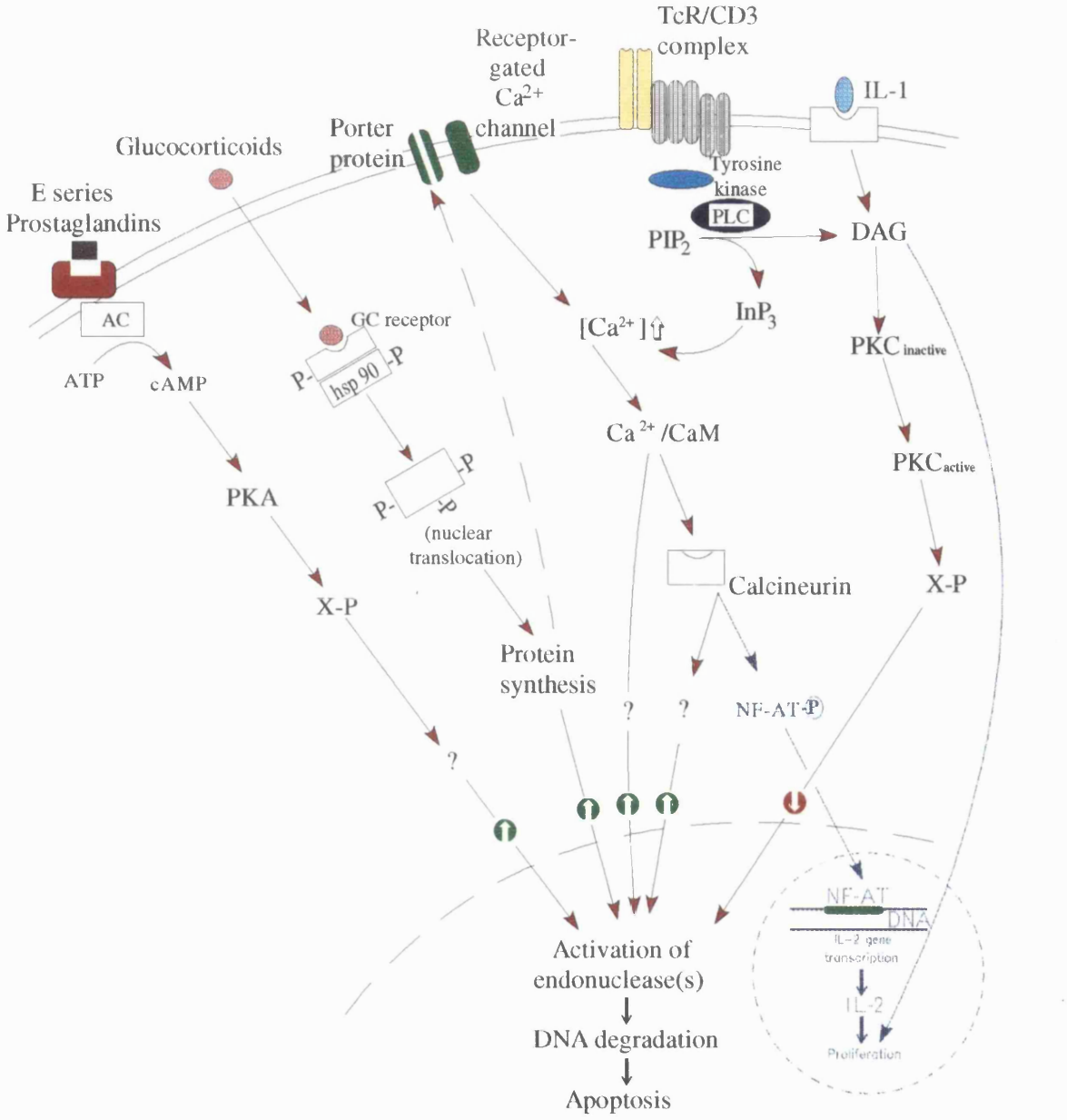

FIGURE 7.2 Thymocyte signal transduction pathways of importance in apoptosis. The schematic (greatly simplified) shows pathways which are thought to be stimulatory (⇧), or suppressive (⇩) in nature. Elements shown in feint shading are proximately related T cell activation pathways. Refer to section 4.1 and 4.4 for further discussion of these mechanisms. Abbreviations: AC = adenylate cyclase; hsp = heat shock protein; X-P indicates an unknown protein phosphorylation; ? indicates a presently undefined process or target. See main abbreviations index for other definitions.

Wistar rats. Cell loss kinetics estimates indicated that the apoptotic index under such circumstances was sufficiently high to account for the thymic cortical involution (Fig. 6.6). In view of the dealkylation pattern of TBT metabolism (section 6.1.1), and the known high biological activity of the parent compound and also DBT (section 6.1.2), it is considered very unlikely that a single underlying effect provokes TBT thymotoxicity (section 6.4). A plausible hypothesis is that a composite mechanism is involved in cortical thymocyte deletion. TBT cytotoxicity, with a possible contribution from DBT, results in activation of apoptosis, and secondly, complex antiproliferative or antidevelopmental effects predominantly due to DBT cause cytostasis. As disturbance of thymocyte maturation itself is likely to precipitate apoptotic deletion, the end result of both effects may be indistinguishable.

The following experimental investigations are suggested:

1. Repeat the study described in chapter 6 using increased group sizes to improve statistical power. Extend the timeframe of experimentation and increase the number of sacrifice points (to include the point of maximal thymic involution and recovery).
2. Study and quantitate MPc cell occurrence in situ. Confirm these cells are tissue macrophages. Use quantitative histocytochemistry, e.g. acid hydrolase indicators and macrophage cell surface markers to assess MPc incidence.
3. Confirmatory experiments to exclude the possibility that equivalent TBTO treatment regimens to those described in chapter 6 cause stress-related thymic involution. This could focus on blood corticosterone level measurements, or utilise adrenalectomised animals.
4. Blood, plasma and thymic tissue toxicokinetics following oral administration, in order to establish levels of TBT and its dealkylation metabolites, and allow relation of this data to in vitro experiments.
5. Distribution and elimination studies subsequent to i.v. administration of TBTO, including blood, plasma and thymus levels of TBT.
6. Design a study to assess whether DBT causes thymocyte apoptosis in vivo.
7. Develop a high sensitivity apoptosis assay for use in vivo studies.
8. Develop a method to sort mononuclear phagocytes containing apoptotic bodies.
9. Confirm and extend evaluations of the potential of DBT to cause apoptosis in vitro.

REFERENCES

A

Adachi Y, Kas E, Laemmli UK (1989) Preferential, cooperative binding of DNA topoisomerase II to scaffold-associated regions. EMBO J 8: 3997-4006

Afanas'ev VN, Korol' BA, Mantsygin YA, Nelipovich PA, Pechatnikov VA, Umansky SR (1986) Flow cytometry and biochemical analysis of DNA degradation characteristic of two types of cell death. FEBS Lett. 194: 347-350

Afanas'ev VN, Korol' BA, Matylevich NP, Pechatnikov VA, Umanskii SR (1988) The features of colchicine induced death of lymphoid cells. Tsitologiya 30: 1108-1116

Akbar AN, Salmon M, Savill J, Janossy G (1993) A possible role for *bcl-2* in regulating T-cell memory - a 'balancing act' between cell death and survival. Immunol Today 14: 526-532

Alajouaine T, Derobert L, Thieffry S (1958) Etude clinique d'ensemble de 210 cas d'intoxication par les sels organiques d'etain. revue Neurologique 98: 85-96 (translation)

Alberts B, Bray D, Lewis J, Raff M, Roberts K, Watson JD (1989) Molecular biology of the cell, Garland, New York

Aldridge WN, Cremer JE (1955) The biochemistry of organotin compounds: Diethyltin dichloride and triethyltin sulphate. Biochem J 61: 406-418

Aldridge WN, (1958) The biochemistry of organotin compounds. Trialkyltins and oxidative phosphorylation. Biochem J 69: 367-376

Aldridge WN, Street BW (1964) Oxidative phosphorylation: biochemical effects and properties of trialkyltins. Biochem J 91:287-297

Aldridge WN (1976) The influence of organotin compounds on mitochondrial functions. In: Zuckermann JJ (ed) Organotin compounds: new chemistry and applications, American Chemical Society, Washington, pp 186-196

Allan DJ, Harmon BV, Kerr JFR (1987) Cell death in spermatogenesis. In: Potten CS (ed) Perspectives on mammalian cell death, Oxford University Press, Oxford, pp 229-258

Allen TD (1987) Ultrastructural aspects of cell death. In: Potten CS (ed) Perspectives on mammalian cell death, Oxford University Press, Oxford, pp 39-65

Alles A, Alley K, Barrett JC, Buttyan R, Columbano A, Cope FO, Copelan EA, Duke RC, Farel PB, Gerschenson LE, Goldgaber D, Green DR, Honn KV, Hully J, Isaacs JT, Kerr JFR, Krammer PH, Lockshin RA, Martin DP, McConkey DJ, Michaelson J, Schulte-Hermann R, Server AC, Szende B, Tomei LD, Tritton TR, Umansky SR, Valerie K, Warner HR (1991) Apoptosis: a general comment. FASEB J 5: 2127-2128

Alnemri ES, Litwack G (1989) Glucocorticoid-induced lymphocytolysis is not mediated by an induced endonuclease. J Biol Chem 264: 4104-4111

Alnemri ES, Litwack G (1990) Activation of internucleosomal DNA cleavage in human CEM lymphocytes by glucocorticoid and novobiocin. J Biol Chem 265: 17323-17333

Anilkumar TV, Sarraf CE, Alison MR (1992) The biology and pathology of programmed cell death. Vet Hum Toxicol 34: 251-254

Arends MJ, Morris RG, Wyllie AH (1990) Apoptosis: The role of the endonuclease. Am J Pathol 136: 593-608

Arends MJ, Wyllie AH (1991) Apoptosis: Mechanisms and roles in pathology. Int Rev Exp Pathol 32: 223-254

Aw TY, Nicotera P, Manzo L, Orrenius S (1990) Tributyltin stimulates apoptosis in rat thymocytes. Arch Biochem Biophys 283: 46-50

B

Bachvaroff RJ, Ayvazian JH, Skupp S, Rapaport FT (1977) Specific restriction endonuclease degradation of DNA as a consequence of immunologically mediated cell damage. Transplant Proc 9: 807-812

Bancroft JD, Cook HC (1984) Manual of histological techniques. Churchill Livingstone, Edinburgh

Bansal N, Houle A, Melnykovych G (1991) Apoptosis: mode of cell death induced in T cell leukemia lines by dexamethasone and other agents. FASEB J 5: 211-216

Barbieri D, Troiano L, Grassilli E, Agnesini C, Cristofalo EA, Monti D, Capri M, Cossarizza A, Franceschi C (1992) Inhibition of apoptosis by zinc: A reappraisal. Biochem Biophys Res Comm 187: 1256-1261

Barker EA, Smuckler EA (1973) Nonhepatic thioacetamide injury. I. Thymic cortical necrosis. Am J Path 71: 409-418

Barnes JM, Stoner HB (1958) Toxic properties of some dialkyl and trialkyl tin salts Brit J Ind Med 15: 15-23

Baron C, Penit C (1990) Study of the thymocyte cell cycle by bivariate analysis of incorporated bromodeoxyuridine and DNA content. Eur J Immunol 20: 1231-1236

Barry MA, Behnke CA, Eastman A (1990) Activation of programmed cell death (apoptosis) by cisplatin, other anticancer drugs, toxins and hyperthermia. Biochem Pharmacol 40: 2353-2362

Barry MA, Eastman A (1992) Endonuclease activation during apoptosis: The role of cytosolic Ca^{2+} and pH. Biochem Biophys Res Comm 186: 782-789

Barry MA, Eastman A (1993) Identification of deoxyribonuclease II as an endonuclease involved in apoptosis. Arch Biochem Biophys 300: 440-450

Batel R, Bihari N, Rinkevich B, Dapper J, Schacke H, Schroder HC, Muller WEG (1993) Modulation of organotin-induced apoptosis by the water pollutant methyl mercury in a human lymphoblastoid tumor cell line and a marine sponge. Mar Ecol Prog Ser 93: 245-251

Bellomo G, Perotti M, Taddei F, Mirabelli F, Finardi G, Nicotera P , Orrenius S (1992) Tumor-necrosis factor α induces apoptosis in mammary adenocarcinoma cells by an increase in intranuclear free Ca^{2+}. Cancer Res 52: 142-1346

Bicknell GR, Snowden RT, Cohen GM (1994) The induction of apoptosis by cycloheximide and Actinomycin D in a human pro-monocytic cell line (U937). Human and Exp Toxicol 13: 201

Blackman M, Kappler J, Marrack P (1990) The role of the T cell receptor in positive and negative selection of developing T cells. Science 248: 1335-1341

Blunden SJ, Chapman AH (1982) The environmental degradation of organotin compounds--a review. Environ Tech Letters 3: 267-272

Boe R, Gjertsen BT, Vintermyr OK, Houge G, Lanotte M, Doeskeland SO (1991) The protein phosphatase inhibitor okadaic acid induces morphological changes typical of apoptosis in mammalian cells. Exp Cell Res 195: 237-246

Bokranz A, Plum H (1975) Industrial manufacture and use of organotin compounds. Schering AG, Germany (company report)

Bondy SC, Hall DL (1986) The relation of the neurotoxicity of organic tin and lead compounds to neurotubule disaggregation. Neurotoxicology 7: 51-56

Boobis AR, Fawthrop DJ, Davies DS (1989) Mechanisms of cell death. Trends Pharmacol Sci 10: 275-280

Bouldin TW, Goines ND, Bagnell CR, Krigman MR (1981) Pathogenesis of trimethyltin neuronal toxicity. Ultrastructural and cytochemical observations. Am J Pathol 104: 237-249

Bowen ID (1981) Techniques for demonstrating cell death. In: Bowen ID, Lockshin RA (eds) Cell death in biology and pathology, Chapman and Hall, London, pp 379-444

Bowen ID, Bowen SM (1990) Programmed cell death in tumours and tissues. Chapman and Hall, London

Boyer IJ (1989) Toxicity of dibutyltin, tributyltin and other organotins to humans and to experimental animals. Toxicology 55: 253-298

Bressa G, Hinton RH, Price SC, Isbir M, Ahmed RS, Grasso P (1991) Immunotoxicity of tri-n-butyltin oxide (TBTO) and tri-n-butyltin chloride (TBTC) in the rat. J Appl Toxicol 11: 397-402

Brown DG, Sun XM, Cohen GM (1993) Dexamethasone-induced apoptosis involves cleavage of DNA to large fragments prior to internucleosomal fragmentation. J Biol Chem 268: 3037-3039

Brune B, Hartzell P, Nicotera P, Orrenius S (1991) Spermine prevents endonuclease activation and apoptosis in thymocytes. Exp Cell Res 195: 323-329

Brunk CF, Jones KC, James TW (1979) Assay for nanogram quantities of DNA in cellular homogenates. Anal Biochem 92: 497-500

Bumbasirevic V, Lackovic V, Japundzic M (1985) Enhancement of apoptosis in lymphoid tissue by microtubule disrupting drugs. ICRS Med Sci 13: 1257-1258

Burchiel SW, Davis DP, Ray SD, Archuleta MM, Thilsted JP, Corcoran, GB (1992) DMBA-induced cytotoxicity in lymphoid and nonlymphoid organs of B6C3F1 mice: relation of cell death to target cell intracellular calcium and DNA damage. Toxicol Appl Pharmacol 113: 126-132

Bursch W, Dusterberg B, Schulte-Hermann R (1986) Growth, regression and cell death in rat liver as related to tissue levels of the hepatomitogen cyproterone acetate. Arch Toxicol 59: 221-227

Bursch W, Kleine L, Tenniswood M (1990a) The biochemistry of cell death by apoptosis. Biochem Cell Biol 68: 1071-1074

Bursch W, Paffe S, Putz B, Barthel G, Schulte-Hermann R (1990b) Determination of the length of the histological stages of apoptosis in normal liver and in altered hepatic foci of rats. Carcinogenesis 11: 847-852

Bursch W, Oberhammer F, Schulte-Hermann R (1992a) Cell death by apoptosis and its protective role against disease. Trends Pharmacol Sci 13: 245-251

Bursch W, Fesus L, Schulte-Hermann R (1992b) Apoptosis ('Programmed' cell death) and its relevance in liver injury and carcinogenesis. In: Dekant W, Neumann HG (eds) Tissue-specific toxicity: biochemical mechanisms, Academic Press, London, pp 95-115

Burton K (1956) A study of the conditions and mechanism of the diphenylamine reaction for the colorimetric estimation of deoxyribonucleic acid. Biochem J 62: 315-323

Butterfield DA, Schneider AM, Rangachari A (1991) Electron paramagnetic resonance studies of the effects of tri-n-butyltin on the physical state of proteins and lipids in erythrocyte membranes. Chem Res Toxicol 4: 141-143

Buttyan R (1991) Genetic response of prostate cells to androgen deprivation: Insights into the molecular mechanism of apoptosis. In: Tomei LD, Cope FO (eds) Apoptosis: The molecular basis of cell death, Cold Spring Harbor Laboratory Press, New York, pp 157-173

Byington KH, Yeh RY, Forte LR (1974) The hemolytic activity of some trialkyltin and triphenyltin compounds. Toxicol Appl Pharmacol 27: 230-240

C

Cain K, Inayat-Hussain SH, Wolfe JT, Cohen GM (1994) DNA fragmentation into 200-250 and/or 30-50 kilobase pair fragments in rat liver nuclei is stimulated by Mg^{2+} alone and Ca^{2+}/Mg^{2+} but not by Ca^{2+} alone. FEBS Lett 349: 385-391

Calbiochem Biochemical Datasheet (1990) Antibiotic A23187. Novabiochem (UK) Ltd.

Cameron JA, Kodavanti PRS, Pentyala SN, Desaiah D (1991) Triorganotin inhibition of rat cardiac adenosine triphosphatases and catecholamine binding. J Appl Toxicol 11: 403-409

Carafoli E (1987) Intracellular calcium homeostasis. Ann Rev Biochem 56: 395-433

Caron-Leslie LAM, Schwartzman RA, Gaido ML, Compton MM, Cidlowski JA (1991) Identification and characterization of glucocorticoid-regulated nuclease(s) in lymphoid cells undergoing apoptosis. J Steroid Biochem 40: 661-671

Casida JE, Kimmel EC, Holm B, Widmark G (1971) Oxidative dealkylation of tetra-, tri- and dialkyltin and tetra- and trialkylleads by liver microsomes. Acta Chemica Scandinavica 25: 1497-1499

Chang MP, Bramhall J, Graves S, Bonavida B, Wisnieski BJ. (1989) Internucleosomal DNA cleavage precedes diphtheria toxin-induced cytolysis. J Biol Chem 264: 15261-15267

Chow SC, Kass GEN, McCabe MJR Jr., Orrenius S (1992) Tributyltin increases cytosolic free calcium concentration in thymocytes by mobilizing intracellular calcium, activating a calcium entry pathway, and inhibiting calcium efflux. Arch Biochem Biophys 298: 143-149

Chow SC, Orrenius S (1994) Rapid cytoskeletal modification in thymocytes induced by the immunotoxicant tributyltin. Toxicol Appl Pharmacol 127: 19-26

Christmas SE, Moore M (1987) Immunologically-mediated cell death. In: Potten CS (ed) Perspectives on mammalian cell death, Oxford University Press, Oxford, pp 259-294

Clipstone NA, Crabtree GR (1992) Identification of calcineurin as a key signalling enzyme in T-lymphocyte activation. Nature 357: 695-697

Cochrane BJ, Irby RB, Snell TW (1991) Effects of copper and tributyltin on stress protein abundance in the rotifer Brachionus plicatilis. Comp Biochem Physiol 98C: 385-390

Cohen GM, Sun XM, Snowden RT, Dinsdale D, Skilleter DN (1992) Key morphological features of apoptosis may occur in the absence of internucleosomal DNA fragmentation. Biochem J 286: 331-334

Cohen GM, Sun XM, Snowden RT, Ormerod MG, Dinsdale D (1993) Identification of a transitional preapoptotic population of thymocytes. J Immunol 151: 566-574

Cohen JJ, Duke RC (1984) Glucocorticoid activation of a calcium-dependent endonuclease in thymocyte nuclei leads to cell death. J Immunol 132: 38-42

Cohen JJ (1993) Overview: Mechanisms of apoptosis. Immunol Today 14: 126-130

Collins RJ, Harmon BV, Souvlis T, Pope JH, Kerr JFR (1991) Effects of cycloheximide on B-chronic lymphocytic leukaemic and normal lymphocytes in vitro: induction of apoptosis. Br J Cancer 64: 518-522

Comment CE, Blaylock BL, Germolec DR, Pollock PL, Kouchi Y, Brown HW, Rosenthal GJ, Luster MI (1992) Thymocyte injury after in vitro chemical exposure: potential mechanisms for thymic atrophy. J Pharmacol and Exp Therapeutics 262: 1267-1273

Compton MM, Cidlowski JA (1986) Rapid in vivo effects of glucocorticoids on the integrity of rat lymphocyte genomic deoxyribonucleic acid. Endocrinology 118: 38-45

Compton MM, Caron LM, Cidlowski JA (1987) Glucocorticoid action on the immune system. J Steroid Biochem 27: 201-208

Compton MM (1991) Development of an endonuclease assay. DNA and Cell Biol 10: 133-141

Compton MM (1992) A biochemical hallmark of apoptosis: Internucleosomal degradation of the genome. Cancer Metastasis Rev 11: 105-119

Corcoran GB, Ray SD (1992) The role of the nucleus and other compartments in toxic cell death produced by alkylating hepatotoxicants. Toxicol Appl Pharmacol 113: 167-183

Costa LG (1985) Inhibition of γ-[^{3}H]aminobutyric acid uptake by organotin compounds in vitro. Toxicol Appl Pharmacol 79: 417-479

Cotter TG, Lennon SV, Glynn JM, Martin SJ (1990) Cell death via apoptosis and its relationship to growth, development and differentiation of both tumour and normal cells. Anticancer Res 10: 1153-1160

Cotter TG, Lennon SV, Glynn JM, Green DR (1992) Microfilament-disrupting agents prevent the formation of apoptotic bodies in tumour cells undergoing apoptosis. Cancer Res 52: 997-1005

Crabtree GR (1989) Contingent genetic regulatory events in T lymphocyte activation. Science 243: 355-361

Crissman H, Mullaney PF, Steinkamp JA (1975) Methods and applications of flow systems for analysis and sorting of mammalian cells. In: Prescott DM (ed) Methods in cell biology, vol 9, Academic Press, New York, pp 179-246

D

Darzynkiewicz Z (1986) Cell growth and division cycle. In Dethlefsen LA (ed) Cell cycle effects of drugs, Permagon Press, Oxford, pp 1-65

De Brabander MJ, Van de Veire RML, Aerts FEM, Borgers M, Janssen PAJ (1976) The effects of methyl [5-(2-thienylcarbonyl)-1*H*-benzimidazol-2-yl]carbamate, (R 17934; NSC 238159), a new synthetic antitumoral drug interfering with microtubules, on mammalian cells cultured in vitro. Cancer Res 36: 905-916

De Brabander MJ, Geuens G, Nuydens R, Willebrords R, De Mey J (1980) The microtubule nucleating and organising activity of kinetochores and centrosomes in living PtK_2 cells. In: De Brabander M, De Mey J (eds) Microtubules and microtubule inhibitors 1980, Elsevier Science Publishers, Amsterdam, pp 255-268

Deeg HJ, Bazar LS (1991) Apoptosis in T lymphocytes after ultraviolet (UV) B or γ irradiation: repair requires Ca^{2+} and protein synthesis. Exp Haematol 19: 498

Deenen GJ, Van Balen I, Opstelten D (1990) In rat B lymphocyte genesis sixty percent is lost from the bone marrow at the transition of nondividing pre-B cell to surface IgM-positive B lymphocyte, the stage of Ig light chain gene expression. Eur J Immunol 20: 557-564

De Waal EJ, Rademakers LHPM, Schuurman HJ, Van Loveren H, Vos JG (1991) Atrophy of the rat thymus. Effects of 2,3,7,8-tetrachlorodibenzo-p-dioxin on the epithelial microenvironment assessed at the ultrastructural level: A comparison with bis(tri-n-butyltin) oxide. In: Imhof BA, Berrih-Aknin S, Ezine S (eds) Lymphatic tissues and in-vivo immune responses; Tenth International Conference on lymphatic tissues and germinal centres in immune reactions, Marcel-Decker, New York, pp 117-121

De Waal EJ, Schuurman HJ, Rademakers LHPM, Van Loveren H, Vos JG (1993) The cortical epithelium of the rat thymus after in vivo exposure to bis(tri-n-butyltin) oxide (TBTO). An (immuno)histochemical and ultrastructural study. Arch Toxicol 67: 186-192

Dive C, Hickman JA (1991) Drug-target interactions: only the first step in the commitment to a programmed cell death? Br J Cancer 64: 192-196

Douglas K (1994) Making friends with death-wish genes. New Scientist No. 1936: 30-34

Duke RC, Chervenak R, Cohen JJ (1983) Endogenous endonuclease-induced DNA fragmentation: An early event in cell-mediated cytolysis. Proc Natl Acad Sci 80: 6361-6365

Duke RC, Sellins KS (1989) Target cell nuclear damage in addition to DNA fragmentation during cytotoxic T lymphocyte-mediated cytolysis. Prog Leukocyte Biol 9: 311-314

Duke RC (1991) Apoptosis in cell-mediated immunity. In: Tomei LD, Cope FO (eds) Apoptosis: The molecular basis of cell death, Cold Spring Harbor Laboratory Press, New York, pp 209-226

Durant S, Homo F, Duval D (1980) Calcium and A23187-induced cytolysis of mouse thymocytes. Biochem Biophys Res Comm 93: 385-391

Duvall E, Wyllie AH, Morris RG (1985) Macrophage recognition of cells undergoing programmed cell death (apoptosis). Immunology 56: 351-358

Duvall E, Wyllie AH (1986) Death and the cell. Immunology Today 7: 115-119

Dykes TA, McCall C, Weimer L, Duke R, Cohen JJ (1987) Purification and characterization of the endogenous endonuclease involved in programmed cell death of developing thymocytes. Clin Res 35: 139

Dyson JED, Simmons DN, Daniel J, McLaughlin JM, Quirke P and Bird CC (1986) Kinetic and physical studies of cell death induced by chemotherapeutic agents or hyperthermia. Cell Tissue Kinet 19: 311-324

E

Eastman A (1990) Activation of programmed cell death by anticancer agents: Cisplatin as a model system. Cancer Cells 275-280

Eldeiry WS, Tokino T, Velculescu VE, Levy DB, Parsons R, Trent JM, Lin D, Mercer WE, Kinzler KW, Vogelstein B (1993) *WAF1*, a potential mediator of *p53* tumor progression. Cell 75: 817-825

Ellis RE, Yuan J, Horvitz HR (1991) Mechanisms and functions of cell death. Annu Rev Cell Biol 7: 663-698

Epe B, Mutzel P, Adam W (1988) DNA damage by oxygen radicals and excited state species: A comparative study using enzymatic probes in vitro. Chem Biol Interactions 67: 149-165

Evan GI, Wyllie AH, Gilbert CS, Littlewood TD, Land H, Brooks M, Waters CM, Penn LZ, Hancock DC (1992) Induction of apoptosis in fibroblasts by *c-myc* protein. Cell 69: 119-128

Evans WH, Cardarelli NF, Smith DJ (1979) Accumulation and excretion of [1-^{14}C]bis(tri-n-butyltin) oxide in mice. J Toxicol Environ Health 5: 871-877

F

Facchinetti A, Tessarollo L, Mazzocchi M, Kingston R, Collavo D, Biasi G (1991) An improved method for the detection of DNA fragmentation. J Immunol Methods 136: 125-131

Farber JL (1990) The role of calcium ions in toxic cell injury. Env Health Perspect 84: 107-111

Fawthrop DJ, Boobis AR. Davies DS (1991) Mechanisms of cell death. Arch Toxicol 65: 437-444

Fernandes G, Nair M, Onoe K, Tanaka T, Floyd R, Good RA (1979) Impairment of cell-mediated immunity functions by dietary zinc deficiency in mice. Proc Natl Acad Sci 76: 457-461

Feinberg AP, Vogelstein B (1983) A technique for radiolabelling DNA restriction endonuclease fragments to high specific activity. Anal Biochem 132: 6-13

Fesus L, Thomazy V, Autuori F, Ceru MP, Tarcsa E, Piacentini M (1989) Apoptotic hepatocytes become insoluble in detergents and chaotropic agents as a result of transglutaminase action. FEBS Lett 245: 150-154

Fesus L, Davies PJA, Piacentini M (1991) Apoptosis: molecular mechanisms in programmed cell death. Eur J Cell Biol 56: 170-177

Filipski J, Leblanc J, Youdale T, Sikorska M, Walker PR (1990) Periodicity of DNA folding in higher order chromatin structures. EMBO J 9: 1319-1327

Finkel TH, Kubo RT, Cambier JC (1991) T-cell development and transmembrane signalling: Changing biological responses through an unchanging receptor. Immunol Today 12: 79-85

Fish RH, Kimmel EC, Casida JE (1976) Bioorganotin chemistry: biological oxidation of organotin compounds. In: Zuckermann JJ (ed) Organotin compounds: new chemistry and applications, American Chemical Society, Washington, pp 197-203

Fish RH (1984) Bioorganotin chemistry: a commentary on the reactions of organotin compounds with a cytochrome P-450 dependent monooxygenase enzyme system. Neurotoxicology 5: 159-162

Fisher TC, Milner AE, Gregory CD, Jackman AL, Aherne GW, Hartley JA, Dive C, Hickman JA (1993) *bcl-2* modulation of apoptosis induced by anticancer drugs: Resistance to thymidylate stress is independent of classical resistance pathways. Cancer Res 53: 3321-3326

Fraker PJ, DePasquale-Jardieu P, Zwicki CM, Luecke RW (1978) Regeneration of T-cell helper function in zinc-deficient adult mice. Proc Natl Acad Sci 75: 5660-5664

Fruman DA, Mather PE, Burakoff SJ, Bierer BE (1992) Correlation of calcineurin phosphatase activity and programmed cell death in murine T cell hybridomas. Eur J Immunol 22: 2513-2517

Funahashi N, Iwasaki I, Ide G (1980) Effects of bis(tri-n-butyltin) oxide on endocrine and lymphoid organs of male rats. Acta Pathol Jpn 30:955-966

G

Gaal JC, Smith KR, Pearson CK (1987) Cellular euthanasia mediated by a nuclear enzyme: a central role for nuclear ADP-ribosylation in cellular metabolism. Trends Biol Sci 12: 129-130

Gabai VL, Mosin AF, Poverenny AM (1990) Increase in free calcium concentration in γ-irradiated thymocytes may induce their death. Radiobiologiya 30: 837-839 (translation)

Gao E, Lo D, Cheney R, Kanagawa O, Sprent J (1988) Abnormal differentiation of thymocytes in mice treated with cyclosporin A. Nature 336: 176-179

Gaido ML, Cidlowski JA (1991) Identification, purification, and characterization of a calcium-dependent endonuclease (NUC 18) from apoptotic rat thymocytes. J Biol Chem 266: 18580-18585

Galili U, Leizerowitz R, Moreb J, Gamliel H, Gurfel D, Polliack A (1982) Metabolic and ultrastructural aspects of the in vitro lysis of chronic lymphocytic leukemia cells by glucocorticoids. Cancer Res 42: 1433-1440

Gerschenson LE, Rotello RJ (1992) Apoptosis: a different type of death. FASEB J 6: 2450-2455

Ghoneum M, Hussein AE, Gill G, Alfred LJ (1990) Suppression of murine natural killer cell activity by tributyltin: In vivo and in vitro assessment. Environ Res 52: 178-186

Giannakis C, Forbes IJ, Zalewski PD (1991) Ca^{2+}/Mg^{2+}-dependent nuclease: Tissue distribution, relationship to inter-nucleosomal DNA fragmentation and inhibition by Zn^{2+}. Biochem Biophys Res Comm 181: 915-920

Gietzen K, Sadorf I, Bader H (1982) A model for the regulation of the calmodulin dependent enzymes erythrocyte calcium transport ATPase and brain phosphodiesterase by activators and inhibitors. Biochem J 207: 541-548

Giroir BP, Brown T, Beutler B (1992) Constitutive synthesis of tumor necrosis factor in the thymus. Proc Natl Acad Sci 89: 4864-4868

Glaister JR (1986) Principles of toxicological pathology. Taylor and Francis, London

Glucksmann A (1951) Cell deaths in normal vertebrate ontogeny Biol Rev 26: 59-86

Goldstein P, Ojcius DM, Young JD. (1991) Cell death mechanisms and the immune system. Immunol Rev 121: 29-65

Golovenko NYA, Galkin BN, Filoppova TO (1986) Catalytic properties of monooxygenases from isolated immunocompetent cells. Biokhimiya 51: 51-58

Goya RG (1986) Role of programmed cell death in the ageing process. Gerontology 32: 37-42

Gray BH, Porvaznik M, Lanfong H L, Flemming C (1986) Inhibition of tributyltin mediated hemolysis by mercapto compounds. J Appl Toxicol 6: 363-370

Gray BH, Porvaznik M, Flemming C, Lanfong H L (1987) Tri-n-butyltin: A membrane toxicant. Toxicology 47: 35-54

Griffiths GD, Leek MD, Gee DJ (1987) The toxic plant proteins ricin and abrin induce apoptotic changes in mammalian lymphoid tissues and intestine. J Pathol 151: 221-229

Groux H, Torpier G, Monte D, Mouton Y, Capron A, Ameisen JC (1992) Activation-induced death by apoptosis in $CD4^+$ T cells from human immunodeficiency virus-infected asymptomatic individuals. J Exp Med 175: 331-340

H

Hall LW and Pinkney AE (1985) Acute and sublethal effects of organotin compounds on aquatic biota: an interpretative literature evaluation. CRC Toxicol 14: 159-209

Hallick RB, Chelm BK, Gray PW, Orozco EM Jr. (1977) Use of aurintricarboxylic acid as an inhibitor of nucleases during nucleic acid isolation. Nucleic Acids Res 4: 3055-3064

Hamasaki T, Sato T, Nagase H, Kito H (1993) The mutagenicity of organotin compounds as environmental pollutants. Mutation Res 300: 265-271

Hardwick SJ, Wilson JW, Fawthrop DJ, Boobis AR, Davies DS (1992) Paracetamol toxicity in hamster isolated hepatocytes: the increase in cytosolic calcium accompanies, rather than precedes, loss of viability. Arch Toxicol 66: 408-412

Harper JW, Adami GR, Wei N, Keyomarsi K, Elledge SJ (1993) The p21 CDK-interacting protein CIP1 is a potent inhibitor of G1 cyclin-dependent kinases. Cell 75: 805-816

Henschler D (1991) Occupational toxicants: critical data evaluation for MAK values and classification of carcinogens Vol. 1, VCH Publishers, New York, pp 315-333

Hengartner MO, Ellis RE, Horvitz HR (1992) *Caenorhabditis elegans* gene ced-9 protects cells from programmed cell death. Nature 356: 494-499

Hesketh JE (1984) Microtubule assembly in rat brain extracts. Further characterization of the effects of zinc on assembly and cold stability. Int J Biochem 16: 1331-1339

Hewish DR, Burgoyne LA (1973) Chromatin substructure. The digestion of chromatin at regularly spaced sites by a nuclear deoxyribonuclease. Biochem Biophys Res Comm 52: 504-510

Hickman JA (1992) Apoptosis induced by anticancer drugs. Cancer Metastasis Rev 11: 121-139

Hickman JA, Beere HM, Wood AC, Waters C, Parmar R (1992) Mechanisms of cytotoxicity caused by antitumour drugs. Toxicol Lett 64/65: 553-561

Hockenbery D, Nunez G, Milliman C, Schreiber RD, Korsmeyer (1990) Bcl-2 is an inner mitochondrial membrane protein that blocks programmed cell death. Nature 348: 334-336

Hockenbery DM, Oltvai ZN, Yin XM, Milliman CL, Korsmeyer SJ (1993) BCL-2 functions in an antioxidant pathway to prevent apoptosis. Cell 75: 241-251

Holden JA, Rolfson DH, Wittwer CT (1990) Human DNA topoisomerase II evaluation of enzyme activity in normal and neoplastic tissues. Biochemistry 29: 2127-2134

Horwitz SB, Schiff PB, Parness J, Manfredi JJ, Mallado W, Samar SN (1986) Taxol: a probe for studying the structure and function of microtubules. In: Clarkson TW, Sager PR, Syversen TLM (eds) The cytoskeleton, a target for toxic agents, Plenum Press, New York, pp 53-65

Hotz MA, Traganos F, Darzynkiewicz Z (1992) Changes in nuclear chromatin related to apoptosis or necrosis induced by the DNA topoisomerase inhibitor fostriecin in MOLT-4 and HL-60 cells are revealed by altered DNA sensitivity to denaturation. Exp Cell Res 201: 184-191

Huang P, Plunkett W (1992) A quantitative assay for fragmented DNA in apoptotic cells. Anal Biochem 207: 163-167

Hume WJ (1987) A pathologist's view of cell death. In: Potten CS (ed) Perspectives on mammalian cell death, Oxford University Press, Oxford, pp 66-92

Humpel M, Kuhne G, Tauber U, Schulze PE (1986) Studies on the kinetics of bis(tri-n-butyl-^{113}tin) oxide (TBTO). In: Toxicology and analytics of the tributyltins--the present status, ORTEP, Berlin, pp 122-142

Hunt SV (1987) Preparation of lymphocytes and accessory cells. In: Klaus GGB (ed) Lymphocytes: A practical approach, IRL press, Oxford, pp 1-34

I

Ijiri K (1989) Apoptosis (cell death) induced in mouse bowel by 1,2-dimethylhydrazine, methylazoxymethanol acetate, and γ-rays. Cancer Res 49: 6342-6346

Iseki R, Mukai M, Iwata M (1991) Regulation of T lymphocyte apoptosis. Signals for the antagonism between activation- and glucocorticoid-induced death. J Immunol 147: 4286-4292

Ishaaya I, Engel JL, Casida JE (1976) Dietary triorganotins affect lymphatic tissues and blood composition of mice. Pestic Biochem Physiol 6: 270-279

Iwai H, Wada O, Arakawa Y (1981) Determination of tri-, di- and monobutyltin and inorganic tin in biological materials and some aspects of their metabolism in rats. J Anal Toxicol 5: 300-306

IPCS, International Programme on Chemical Safety (1990) Environmental Health Criteria 116: Tributyltin compounds. WHO, Geneva.

J

Jacobson MD, Burne JF, Raff MC (1994) Programmed cell death and Bcl-2 protection in the absence of a nucleus. EMBO J 13: 1899-1910

Jensen KG, Andersen O, Ronne M (1991) Direct and indirect assessment of the aneuploidy-inducing potency of organotin compounds. ATLA 19: 214-218

Jones DP, McConkey DJ, Nicotera P, Orrenius S (1989) Calcium-activated DNA fragmentation in rat liver nuclei. J Biol Chem 264: 6398-6403

K

Kaiser N, Edelman IS (1977) Calcium dependence of glucocorticoid-induced lymphocytolysis. Proc Natl Acad Sci 74: 638-642

Kaiser N, Edelman IS (1978) Further studies on the role of calcium in glucocorticoid-induced lymphocytolysis. Endocrinology 103: 936-942

Kamb A, Gruis NA, Weaverfeldhaus J, Liu QY, Harshman K (1994) A cell-cycle regulator potentially involved in genesis of many tumor types. Science 264: 436-440

Kammer GM (1988) The adenylate cyclase-cAMP-protein kinase A pathway and regulation of the immune response. Immunol Today 9: 222-229

Kampinga J, Aspinall R (1990) Thymocyte differentiation and thymic microenvironment in the fetal rat thymus: An immunohistological approach. In: Kendall MD, Ritter MA (eds) Thymus update Vol. 3, Harwood Academic Publishers, London, pp 149-186

Kanetoshi A (1983) The metabolism of butyltin compounds in isolated viable rat hepatocytes. J Hyg Chem (Eisei Kagaku) 29: 303-311

Kaufmann SH (1989) Induction of endonucleolytic DNA cleavage in human acute myelogenous leukemia cells by etoposide, camptothecin, and other cytotoxic anticancer drugs: A cautionary note. Cancer Res 49: 5870-5878

Keith CH, Bajer AS, Ratan R, Maxfield FR, Shelanski ML (1985) In: De Brabander M, De Mey J (eds) Microtubules and microtubule inhibitors 1985, Elsevier Science Publishers, Amsterdam, pp 89-96

Kempston D, Earl JR, Bressa G, Grasso P, Hubbard R, Eales LJ, Hinton RH (1993) The development of thymic changes in female mice following ingestion of diets containing tributyltin chloride. Human and Exp Toxicol 12: 430-431

Kerr JFR (1965) A histochemical study of hypertrophy and ischaemic injury of rat liver with special reference to changes in lysosomes. J Pathol Bacteriol 90: 419-435

Kerr JFR (1971) Shrinkage necrosis: A distinct mode of cellular death. J Pathol 105: 13-20

Kerr JFR, Wyllie AH, Currie AR (1972) Apoptosis: A basic biological phenomenon with wide-ranging implications in tissue kinetics. Br J Cancer 26: 239-257

Kerr JFR, Searle J, Harmon BV, Bishop CJ (1987) Apoptosis. In: Potten CS (ed) Perspectives on mammalian cell death, Oxford University Press, Oxford, pp 93-128

Kerr JFR, Harmon BV (1991) Definition and incidence of apoptosis: A historical perspective. In: Tomei LD, Cope FO (eds) Apoptosis: The molecular basis of cell death, Cold Spring Harbor Laboratory Press, New York, pp 5-29

Kisielow PH, Bluthmann H, Staerz UD, Stainmez M, Von Boehmer H (1988) Tolerance in transgenic mice involves deletion of nonmature $CD4^{+}8^{+}$ thymocytes. Nature 333: 742-746

Kimmel EC, Fish RH, Casida JE (1977) Bioorganotin chemistry: Metabolism of organotin compounds in microsomal monooxygenase systems and in mammals. J Agric Food Chem 25: 1-9

Kizaki H, Shimada H, Ohsaka F, Sakurada T (1988) Adenosine, deoxyadenosine and deoxyguanosine induce DNA cleavage in mouse thymocytes. J Immunol 141: 1652-1657

Kizaki H, Tadakuma T, Odaka C, Muramatsu J, Ishimura Y (1989) Activation of a suicide process of thymocytes through DNA fragmentation by calcium ionophores and phorbol esters. J Immunol 143: 1790-1794

Klassen NV, Walker PR, Ross CK, Cygler J, Lach B (1993) Two-stage cell shrinkage and the OER for radiation-induced apoptosis of rat thymocytes. Int J Radiat Biol 64: 571-581

Koizumi T, Waalkes MP (1990) Effects of zinc on the binding of cadmium to DNA: Assessment with testicular interstitial cell and calf thymus DNA. Toxic in vitro 4: 51-55

Kolber MA, Broschat KO, Landa-Gonzalez B (1990) Cytochalasin B induces cellular DNA fragmentation. FASEB J 4: 3021-3027

Korsmeyer SJ (1992) Bcl-2: a repressor of lymphocyte death. Immunol Today 13: 285-288

Koury MJ, Bondurant MC (1990) Erythropoietin retards DNA breakdown and prevents programmed cell death in erythroid progenitor cells. Science 248: 378-381

Kraft AS, Anderson WB (1983) Phorbol esters increase the amount of Ca^{2+}, phospholipid dependent protein kinase associated with plasma membrane. Nature 301: 621-623

Krajnc EI, Wester PW, Loeber JG, Van Leeuwen FXR, Vos JG, Vaessen HAMG, Van der Heijden CA (1984) Toxicity of bis(tri-n-butyltin)oxide in the rat I. Short-term effects on general parameters and on the endocrine and lymphoid systems. Toxicol Appl Pharmacol 75: 363-386

Krajnc-Franken MAM, Van Loveren H, Schuurman HJ, Vos JG (1990) The immune system as a target for toxicity: A tiered approach to testing, with special emphasis on histopathology. In: Dayan AD, Hertel RF, Heseltine E, Kazantis G, Smith EM, Van der Venne MT (eds) Immunotoxicology of Metals and Immunotoxicology, Plenum Press, New York, pp 241-264

Krammer PH, Behrmann I, Bier V, Daniel P, Dhein J, Falk MH, Garcin G, Klas C, Knipping E, Lucking-Famira KM, Matzku S, Oehm A, Richards S, Trauth BC, Bornkamm GW, Falk W, Moller P, Debatin KM (1991) Apoptosis in the APO-1 system. In: Tomei LD, Cope FO (eds) Apoptosis: The molecular basis of cell death, Cold Spring Harbor Laboratory Press, New York, pp 87-99

Krebs HA, Henseleit K (1932) Untersuchungen uber die Hamstoffbildung im Tierkorper. Zeitschrift fur Physiol Chemie 210: 33-66

Krowke R, Bluth U, Neubert D (1986) In vitro studies on the embryotoxic potential of bis(tri-n-butyltin)oxide in a limb bud organ culture system. Arch Toxicol 58: 125-129

Khromenkov YUI, Likov VF, Tagirova AK, Ukhaskaya OV, Saprin AN (1984) Cytochrome P-450 activity in subpopulations of immunocompetent cells. Immunologiya 4: 29-32

Kupfer G, Bodley AL, Liu LF (1987) Involvement of intracellular ATP in cytotoxicity of topoisomerase II-targetting antitumour drugs. Natl Cancer Inst Monogr 4: 37-40

Kure S, Tominaga T, Yoshimoto T, Tada K, Narisawa (1991) Glutamate triggers internucleosomal DNA cleavage in neuronal cells. Biochem Biophys Res Comm 179: 39-45

Kyprianou N, English HF, Isaacs JT (1988) Activation of a Ca^{2+}-Mg^{2+}-dependent endonuclease as an early event in castration-induced prostatic cell death. Prostate 13: 103-118

L

Lane DP (1993) A death in the life of p53. Nature 362: 786-787

La Pushin RW, de Harven E (1971) A study of gluco-corticoid-induced pyknosis in the thymus and lymph node of the adrenalectomised rat. J Cell Biol 50: 583-597

Larrick JW, Wright SC (1990) Cytotoxic mechanism of tumour necrosis factor-α. FASEB J 4: 3215-3223

Laughlin RB, Guard HE, Coleman WM (1986) Tributyltin in seawater: Speciation and octanol-water partition coefficient. Environ Sci Technol 20: 201-204

Ledda-Columbano GM, Coni P, Faa G, Manenti G, Columbano A (1992) Rapid induction of apoptosis in rat liver by cycloheximide. Am J Pathol 140: 545-549

Lemasters JL, Hackenbrock CR (1978) Firefly luciferase assay for ATP production by mitochondria. In: Methods in Enzymology, vol 57, Academic Press, London, pp 36-50

Lemasters JJ, DiGuiseppi J, Nieminen AL, Herman B (1987) Blebbing, free Ca^{2+} and mitochondrial membrane potential preceding cell death in hepatocytes. Nature 325: 78-81

Lennon SV, Martin SJ, Cotter TG (1991) Dose-dependent induction of apoptosis in human tumour cell lines by widely diverging stimuli. Cell Prolif 24: 203-214

Leow ACT, Anderson R, Little RA, Leaver DD (1979) A sequential study of changes in the brain and cerebrospinal fluid of the rat following triethyltin poisoning. Acta Neuropathol 47: 117-121

Lipetz PD, Galsky AG, Stephens RA (1982) Relationship of DNA tertiary and quarternary structure to carcinogenic processes. Adv Cancer Res 36: 165-210

Liu LF (1989) DNA topoisomerase poisons as antitumour drugs. Annu Rev Biochem 58: 351-375

Lockshin RA, Beaulaton J (1974) Programmed cell death. Life Sci 12: 1549-1565

Lockshin RA, Zakeri-Milovanovic Z (1984) Nucleic acids in cell death. In: Davies I, Sigee DC (eds) Cell Ageing and Cell Death, Cambridge University Press, Cambridge, pp 243-268

Lockshin RA, Zakeri Z (1991) Programmed cell death and apoptosis. In: Tomei LD, Cope FO (eds) Apoptosis: The molecular basis of cell death, Cold Spring Harbor Laboratory Press, New York, pp 47-60

Lowe SW, Schmitt EM, Smith SW, Osborne BA, Jacks T (1993) p53 is required for radiation-induced apoptosis in mouse thymocytes. Nature 362: 847-852

M

MacDonald HR, Lees RK (1990) Programmed death of autoreactive thymocytes. Nature 343: 642-644

Maguire RJ, Carey JH, Hale EJ (1983) Degradation of the tri-n-butyltin species in water. J Agric Food Chem 31: 1060-1065

Maguire RJ (1987) Environmental aspects of tributyltin. Appl Organomet Chem 1: 475-498

Majno G, Lagattuta M, Thompson T (1960) Cellular death and necrosis; chemical, physical and morphological changes in rat liver Virchow Arch [Pathol Anat] 333: 421-465

Manes C, Menzel P (1982) Spontaneous release of nucleosome cores from embryoblast chromatin. Dev Biol 92: 529-538

Manfredi JJ, Horwitz SB (1986) Taxol: An antimitotic agent with a new mechanism of action. In Dethlefsen LA (ed) Cell cycle effects of drugs, Permagon Press, Oxford, pp 287-333

Maniatis T, Fritsch EF, Sambrook J (1989) Molecular cloning: A laboratory manual, Cold Spring Harbour Laboratory, New York

Marinovich M, Viviani B, Galli CL (1990a) Reversibility of tri-n-butyltin-chloride-induced protein synthesis inhibition after ATP recovery in HEL-30 cells. Toxicol Lett 52: 311-317

Marinovich M, Sanghvi A, Colli S, Tremoli E, Galli CL (1990b) Cytoskeletal modifications induced by organotin compounds in human neutrophils. Toxic in vitro 4: 109-113

Maro B, Marty M, Bornens M (1982) In vivo and in vitro effects of the mitochondrial uncoupler FCCP. EMBO J 11: 1347-1352

Marrack P, Blackman M, Burgert HG, McCormack JM, Cambier J, Finkel TH, Kappler J (1989) T-cell repertoire and thymus. Cold Spring Harbor Symp Quant Biol 54: 105-110

Martin DP, Johnson EM Jr. (1991) Programmed cell death in the peripheral nervous system. In: Tomei LD, Cope FO (eds) Apoptosis: The molecular basis of cell death, Cold Spring Harbor Laboratory Press, New York, pp 247-261

Martin SJ, Lennon SV, Bonham AM, Cotter TG (1990) Induction of apoptosis (programmed cell death) in human leukemic HL-60 cells by inhibition of RNA or protein synthesis. J Immunol 145: 1859-1867

Martin SJ, Cotter TG (1990) Disruption of microtubules induces an endogenous suicide pathway in human leukaemia HL-60 cells. Cell Tissue Kinet 23: 545-559

Martin SJ, Mazdai G, Strain JJ, Cotter TG, Hannigan BM (1991) Programmed cell death (apoptosis) in lymphoid cell lines during zinc deficiency. Clin Exp Immunol 83: 338-343

Martin SJ (1993) Apoptosis: suicide, execution or murder? Trends in Cell Biol 3: 141-144

Matter A (1979) Microcinematographic and electron microscopic analysis of target cell lysis induced by cytotoxic T lymphocytes. Immunology 36: 179-190

Matylevich NP, Korol' BA, Nelipovich PA, Afanas'ev VN, Umanskii SR (1991) Inhibition by heavy water of the interphase death of lymphocytes. Radiobiologiya 31: 27-32 (translation)

Mazzei GJ, Schatzman RC, Turner RS, Volger WR, Kuo JF (1984) Phospholipid sensitive calcium dependent protein kinase inhibition by R-24571 calmidazolium, a calmodulin antagonist. Biochem Pharmacol 33: 125-130

McCabe MJ Jr., Orrenius S (1992) Deletion and Depletion: The involvement of viruses and environmental factors in T-lymphocyte apoptosis. Lab Invest 66: 403-406

McCabe MJ Jr., Nicotera P, Orrenius S (1992) Calcium-dependent cell death. Role of the endonuclease, protein kinase C, and chromatin conformation. Ann New York Acad Sci 663: 269-278

McCabe MJ Jr., Jiang SA, Orrenius S (1993) Chelation of intracellular zinc triggers apoptosis in mature thymocytes. Lab Invest 69: 101-110

McConkey DJ, Hartzell P, Duddy SK, Hakansson H, Orrenius S (1988a) 2,3,7,8-tetrachlorodibenzo-p-dioxin kills immature thymocytes by Ca2+-mediated endonuclease activation. Science 242: 256-259

McConkey DJ, Hartzell P, Nicotera P, Wyllie AH, Orrenius S (1988b) Stimulation of endogenous endonuclease activity in hepatocytes exposed to oxidative stress. Toxicol Lett 42: 123-130

McConkey DJ, Hartzell P, Nicotera P, Orrenius S (1989a) Calcium-activated DNA fragmentation kills immature thymocytes. FASEB J 3: 1843-1849

McConkey DJ, Nicotera P, Hartzell P, Bellomo G, Wyllie, AH, Orrenius S (1989b) Glucocorticoids activate a suicide process in thymocytes through an elevation of cytosolic Ca^{2+} concentration. Arch Biochem Biophys 269: 365-370

McConkey DJ, Hartzell P, Amador-Perez JF, Orrenius S, Jondal M (1989c) Calcium-dependent killing of immature thymocytes by stimulation via the CD3/T cell receptor complex. J Immunol 143: 1801-1806

McConkey DJ, Hartzell P, Jondal M, Orrenius S (1989d) Inhibition of DNA fragmentation in thymocytes and isolated nuclei by agents that stimulate protein kinase C. J Biol Chem 264: 13399-13402

McConkey DJ, Orrenius S, Jondal M (1990a) Agents that elevate cAMP stimulate DNA fragmentation in thymocytes. J Immunol 145: 1227-1230

McConkey DJ, Hartzell P, Orrenius S (1990b) Rapid turnover of endogenous endonuclease activity in thymocytes: effects of inhibitors of macromolecular synthesis. Arch Biochem Biophys 278: 284-287

McConkey DJ, Orrenius S, Jondal, M (1990c) Cellular signalling in programmed cell death (apoptosis). Immunol Today 11: 120-121

McConkey DJ, Chow SC, Orrenius S, Jondal M (1990d) NK cell induced cytotoxicity is dependent on a Ca^{2+} increase in the target. FASEB J 4: 2661-2664

McConkey DJ, Hartzell P, Chow SC, Orrenius S, Jondal M (1990e) Interleukin 1 inhibits T cell receptor-mediated apoptosis in immature thymocytes. J Biol Chem 265: 3009-3011

McConkey DJ, Orrenius S (1991) Cellular signalling in thymocyte apoptosis. In: Tomei LD, Cope FO (eds) Apoptosis: The molecular basis of cell death, Cold Spring Harbor Laboratory Press, New York, pp 227-246

McConkey DJ, Aw TY, Orrenius S (1992) Role of Ca^{2+}-mediated endonuclease activation. In: Dekant W, Neumann HG (eds) Tissue-specific toxicity: biochemical mechanisms, Academic Press, London, pp 1-14

McConkey DJ, Orrenius S, Okret S, Jondal, M (1993) Cyclic AMP potentiates glucocorticoid-induced endogenous endonuclease activation in thymocytes. FASEB J 7: 580-585

Merritt AJ, Potten CS, Kemp CJ, Hickman JA, Balmain A, Lane DP, Hall PA (1994) The role of *p53* in spontaneous and radiation-induced apoptosis in the gastrointestinal tract of normal and p53-deficient mice. Cancer Res 54: 614-617

Migliorati G, Nicoletti I, Crocicchio F, Pagliacci C, D' Adamio F, Riccardi C (1992) Heat shock induces apoptosis in mouse thymocytes and protects them from glucocorticoid-induced cell death. Cell Immunol 143: 348-356

Miura M, Zhu H, Rotello R, Hartweig EA, Yuan J (1993) Induction of apoptosis in fibroblasts by IL-1-β-converting enzyme, a mammalian homolog of the *C.elegans* cell death gene *ced-3*. Cell 75: 653-660

Moore GE, Woods LK (1976) Culture media for human cells RPMI-1630, RPMI-1634, RPMI-1640 and GEM-1717. Tissue Cult Assoc Man 3: 503-509

Moore JV (1987) Death of cells and necrosis of tumours. In: Potten CS (ed) Perspectives on mammalian cell death, Oxford University Press, Oxford, pp 295-325

Morimoto RI, Abravaya K, Mosser D, Williams GT (1990) Cellular stress response. In Santoro MG, Garaci E (eds) Stress proteins, Springer-Verlag, Berlin, pp 1-17

Morris RG, Hargreaves AD, Duvall E, Wyllie AH (1984) Hormone-induced cell death: 2. Surface changes in thymocytes undergoing apoptosis. Am J Pathol 115: 426-436

Munck A, Crabtree GR (1981) Glucocorticoid-induced lymphocyte death. In: Bowen ID, Lockshin RA (eds) Cell death in biology and pathology, Chapman and Hall, London, pp 329-359

N

Nagle WA, Soloff BL, Moss AJ, Henle KJ (1990) Cultured Chinese hamster cells undergo apoptosis after exposure to cold but nonfreezing temperatures. Cryobiology 27: 439-451

Nelipovich PA, Nikonova LV, Umansky SR (1988) Inhibition of poly(ADP-ribose) polymerase as a possible reason for activation of Ca^{2+}/Mg^{2+}-dependent endonuclease in thymocytes of irradiated rats. Int J Radiat Biol 53: 749-765

Ng J, Fredholm BB, Jondal M, Andersson T (1988) Regulation of receptor-mediated calcium influx across the plasma membrane in a human leukemic T-cell line: evidence of its dependence on an initial calcium mobilisation from intracellular stores. Biochim Biophys Acta 971: 207-214

Nicoletti I, Migliorati G, Pagliacci C, Grignani F, Riccardi C (1991) A rapid and simple method for measuring thymocyte apoptosis by propidium iodide staining and flow cytometry
J Immunol Methods 139: 271-279

Nicotera P, Hartzell P, Davis G, Orrenius S (1986) The formation of plasma membrane blebs in hepatocytes exposed to agents that increase cytosolic Ca^{2+} is mediated by the activation of a non-lysosomal proteolytic system. FEBS Lett 209: 139-144

Nicotera P, McConkey DJ, Jones DP, Orrenius S (1989) ATP stimulates Ca^{2+} uptake and increases the free Ca^{2+} concentration in isolated rat liver nuclei. Proc Natl Acad Sci 86: 453-457

Nicotera P, Bellomo G, Orrenius S (1990) The role of Ca^{2+} in cell killing. Chem Res Toxicol 3: 484-494

Nicotera P, Bellomo G, Orrenius S (1992) Calcium-mediated mechanisms in chemically induced cell death. Annu Rev Pharmacol Toxicol 32: 449-470

Nieto MA, Lopez-Rivas A (1989) IL-2 protects T lymphocytes from glucocorticoid-induced DNA fragmentation and cell death. J Immunol 143: 4166-4170

Nikonova LV, Nelipovich PA, Umansky SR (1982). The involvement of nuclear nucleases in rat thymocyte DNA degradation after γ-irradiation. Biochem. Biophys. Acta 699: 281-289

Nikonova LV, Beletsky IP, Umansky SR (1993). Properties of some nuclear nucleases of rat thymocytes and their changes in radiation-induced apoptosis. Eur J Biochem 215: 893-901

Nishida E (1978) Effects of solution variables on the calcium sensitivity of the microtubule assembly system. J Biochem. 84: 507-512

Nishloka W, Welsh R (1991) Inhibition of CTL-induced DNA fragmentation, but not target cell lysis by inhibitors of DNA topoisomerase I and II. Am Soc Exp Biol 5: 601

O

Oberhammer F, Fritsch G, Schmied M, Pavelka M, Printz D, Purchio T, Lassmann H, Schulte-Hermann R (1993a) Condensation of the chromatin at the membrane of an apoptotic nucleus is not associated with activation of an endonuclease. J Cell Science 104: 317-326

Oberhammer F, Wilson JW, Dive C, Morris ID, Hickman JA, Wakeling AE, Walker PR, Sikorska M (1993b) Apoptotic death in epithelial cells: cleavage of DNA to 300 and/or 50 kb fragments prior to or in the absence of internucleosomal fragmentation. EMBO J 12: 3679-3684

Ojcius DM, Zychlinsky A, Zheng LM, Young JD-E (1991) Ionophore-induced apoptosis: Role of DNA fragmentation and calcium fluxes. Exp Cell Res 197: 43-49

Orrenius S, McConkey DJ, Bellomo G, Nicotera P (1989) Role of Ca^{2+} in toxic cell killing. Trends Pharmacol Sci 10: 281-285

Osheroff N, Zechiedrich EL (1987) Calcium-promoted DNA cleavage by eukaryotic topoisomerase II: trapping the covalent enzyme-DNA complex in an active form. Biochemistry 26: 4303-4315

Owens GP, Hahn WE, Cohen JJ (1991) Identification of mRNAs associated with programmed cell death in immature thymocytes. Mol Cell Biol 11: 4177-4188

P

Patterson DJ, Green JR, Jeffries WA, Puklavec M, Williams AF (1987) The MRC OX-44 antigen marks a functionally relevant subset among rat thymocytes. J Exp Med 165: 1-13

Pechatnikov VA, Afanasyev VN, Korol' BA, Korneev VN, Rochev YU, Umansky SR (1986) Flow cytometry analysis of DNA degradation in thymocytes of γ-irradiated or hydrocortisone treated rats. Gen Physiol Biophys 5: 273-284

Peitsch MC, Muller C, Tschopp J (1993a) DNA fragmentation during apoptosis is caused by frequent single-strand cuts. Nucleic Acids Res 21: 4206-4209

Peitsch MC, Polzar B, Stephan H, Crompton T, MacDonald HR, Mannherz HG, Tschopp J (1993b) Characterisation of the endogenous deoxyribonuclease involved in nuclear degradation during apoptosis (programmed cell death). EMBO J 12: 371-377

Penninks AH, Kuper F, Spit BJ, Seinen W (1985) On the mechanism of dialkyltin-induced thymus involution. Immunopharmacology 10: 1-10

Penninks AH, Snoeij NJ, Pieters RHH, Seinen W (1990) Effect of organotin compounds on lymphoid organs and lymphoid functions: An overview. In: Dayan AD, Hertel RF, Heseltine E, Kazantis G, Smith EM, Van der Venne MT (eds) Immunotoxicology of Metals and Immunotoxicology, Plenum Press, New York, pp 191-207

Penninks AH, Pieters RHH, Snoeij NJ, Seinen W (1991) Organotin-induced thymus atrophy. In: Kendall MD, Ritter MA (eds) Thymus update Vol. 4: The thymus in immunotoxicology, Harwood Academic Publishers, London, pp 57-80

Penninks AH (1993) The evaluation of data-derived safety factors for bis(tri-n-butyltin)oxide. Food Addit and Contaminants 10: 351-361

Perotti M, Toddei P, Mirabelli F, Vairetti M, Bellomo G, McConkey DJ, Orrenius S (1990) Calcium-dependent DNA fragmentation in human synovial cells exposed to cold shock. FEBS Lett 259: 331-334

Perotti M, Toddei P, Mirabelli F, Vairetti M, Bellomo G (1991) In vitro models for biochemical investigations on programmed cell death. ATLA 19: 71-76

Pfeifer RW, Irons RD (1983) Alteration of lymphocyte function by quinones through a sulfhydryl-dependent disruption of microtubule assembly. Int J Immunopharmac 5: 463-470

Piacentini M, Fesus L, Farrace MG, Ghibelli L, Piredda L, Melino G (1991) The expression of tissue transglutaminase in two human cancer cell lines is related with the programmed cell death apoptosis. Eur J Cell Biol 54: 246-254

Pieters RHH (1992) Cellular and molecular aspects of organotin-induced thymus atrophy. PhD thesis, University of Utrecht

Pieters RHH, Bol M, Punt P, Seinen W, Penninks AH (1993) Organotin-induced thymus atrophy: close to the mechanism? Human and Exp Toxicol 12: 73-74

Pipan N, Sterle M (1979) Cytochemical analysis of organelle degradation in phagosomes and apoptotic cells of the mucoid epithelium of mice. Histochem 59: 225-232

Poenie M, Tsien RY, Schmitt-Verhulst AM (1987) Sequential activation and lethal hit measured by $[Ca^{2+}]_i$ in individual cytolytic T cells and targets EMBO J 6: 2223-2232

Porvaznik M, Gray BH, Mattie D, Jackson AG, Omlor RE (1986) The ultrastructural localisation of tri-n-butyltin in human erythrocyte membranes during shape transformation leading to hemolysis. Lab Invest 54: 254-267

Potten CS, Merrit A, Hickman J, Hall P, Faranda A (1994) Characterization of radiation-induced apoptosis in the small intestine and its biological implications. Int J Radiat Biol 65: 71-78

Pounds JG, Rosen JF (1988) Cellular Ca^{2+} homeostasis and Ca^{2+}-mediated cell processes as critical targets for toxicant action: Conceptual and methodological pitfalls. Toxicol Appl Pharmacol 94: 331-341

Powers MF, Beavis AD (1991) Triorganotins inhibit the mitochondrial inner membrane anion channel. J Biol Chem 266: 17250-17256

Pressman BC (1976) Biological applications of ionophores. Ann Rev Biochem 45: 501-530

Pritchard DJ, Butler WH (1989) Apoptosis--the mechanism of cell death in dimethylnitrosamine-induced hepatotoxicity. J Pathol 158: 253-260

R

Raff MC (1992) Social controls in cell survival and cell death. Nature 356: 397-400

Raffray M, Cohen GM (1991) Bis(tri-n-butyltin) oxide induces programmed cell death (apoptosis) in immature rat thymocytes. Arch Toxicol 65: 135-139

Ray SD, Sorge CL, Raucy JL, Corcoran GB (1990) Early loss of large genomic DNA in vivo with accumulation of Ca^{2+} in the nucleus during acetaminophen-induced liver injury. Toxicol Appl Pharmacol 106: 346-351

Revillard JP (1990) The immune system: An integrated overview. In: Dayan AD, Hertel RF, Heseltine E, Kazantis G, Smith EM, Van der Venne MT (eds) Immunotoxicology of Metals and Immunotoxicology, Plenum Press, New York, pp 19-28

Reinhardt CA, Schawalder H, Zbinden G (1982) Cell detachment and cloning efficiency as parameters for cytotoxicity. Toxicology 25: 47-52

Ribeiro JM, Carson DA (1993) Ca^{2+}/Mg^{2+}-Dependent endonuclease from human spleen: Purification, properties and role in apoptosis. Biochemistry 32: 9129-9136

Rice CD, Weeks BA (1989) Influence of tributyltin on in vitro activation of oyster toadfish macrophages. J Aquat Animal Health 1: 62-68

Rigler R (1969) Acridine orange in nucleic acid analysis. Ann NY Acad Sci 157: 211-216

Ritter MA, Crispe IN (1992) The thymus. Oxford University Press, New York

Robinson G, Gray T (1990) Electron microscopy: Tissue preparation, sectioning and staining. In: Bancroft JD, Stevens A (eds) Theory and practice of histological techniques, Churchill Livingstone, Edinburgh, pp 525-562

Robertson AMG, Bird CC, Waddell AW, Currie AR (1978). Morphological aspects of glucocorticoid-induced cell death in human lymphoblastoid cells. J Pathol 126: 181-187

Rothenberg EV (1990) Death and transfiguration of cortical thymocytes: a reconsideration. Immunol Today 11: 116-119

RTECS (1993) Registry of Toxic Effects of Chemical Substances datafile on TBTO (RTECS no. JN8750000), National Institute of Occupational Safety and Health database, Dialog On-line Services, California

Russell SW, Rosenau W, Lee JC (1972) Cytolysis induced by human lymphotoxin. Am J Pathol 69: 103-118

Russell JH, White CL, Loh DY, Meleedy-Rey P (1991) Receptor-stimulated death pathway is opened by antigen in mature T cells. Proc Natl Acad Sci 88: 2151-2155

S

Sager PR, Syversen TLM, Clarkson TW, Cavanagh JB, Elgsaeter A, Guldberg HC, Lee SD, Lichtman MA, Mottet K, Olmsted JB (1984) Structure and function of the cytoskeleton. In: Clarkson TW, Sager PR, Syversen TLM (eds) The cytoskeleton, a target for toxic agents, Plenum Press, New York, pp 3-21

Saunders JW (1966) Death in embryonic systems. Death of cells is the usual accompaniment of embryonic growth and differentiation. Science 154: 604-612

Savill JS, Wyllie AH, Henson JE, Walport MJ, Henson PM, Haslett C (1989) Macrophage phagocytosis of ageing neutrophils in inflammation. Programmed cell death in the neutrophil leads to its recognition by macrophages. J Clin Invest 83: 865-875

Savill JS, Dransfield I, Hogg N, Haslett C (1990) Vitronectin receptor-mediated phagocytosis of cells undergoing apoptosis. Nature 343: 170-173

Schiff PB, Fant J, Horwitz SB (1979) Promotion of microtubule assembly in vitro by taxol. Nature 277: 665-667

Schmid N, Behr JP (1991) Location of spermine and other polyamines on DNA as revealed by photoaffinity cleavage with polyaminobenzenediazonium salts. Biochemistry 30: 4357-4361

Schrantz J (1990) TBT marine paint under EPA scrutiny. Industrial Finishing 66: 58-61

Schulte-Hermann R, Bursch W (1990) Cell death through apoptosis and its relationship to carcinogenesis. In: Volans GN, Sims J, Sullivan FM, Turner P (eds) Basic science in toxicology: the proceedings of the 5th International Congress of Toxicology, Brighton, UK, 16-21 July 1989, Taylor and Francis, London, pp 669-678

Schwartzman RA, Cidlowski JA (1991) Internucleosomal DNA cleavage activity in apoptotic thymocytes: Detection and endocrine regulation. Endocrinology 128: 1190-1197

Scollay R, Wilson A, D'Amico A, Kelly K, Egerton M, Pearse M, Wu L, Shortman K (1988) Developmental status and reconstitution potential of subpopulations of murine thymocytes. Immunol Rev 104: 81-120

Sealey PG, Southern EM (1990) Gel electrophoresis of DNA. In: Rickwood D, Hames BD (eds) Gel electrophoresis of nucleic acids: A practical approach, IRL press, Oxford, pp 51-99

Searle J, Lawson TA, Abbott PJ, Harmon B, Kerr JFR (1975) An electron-microscope study of the mode of cell death induced by cancer-chemotherapeutic agents in populations of proliferating normal and neoplastic cells. J Pathol 116: 129-138

Searle J, Kerr JFR, Bishop CJ (1982) Necrosis and apoptosis: Distinct modes of cell death with fundamentally different significance. Pathol Annu 17: 229-259

Seinen W, Willems MI (1976) Toxicity of organotin compounds. I. Atrophy of thymus and thymus-dependent lymphoid tissue in rats fed di-n-octyltindichloride. Toxicol Appl Pharmacol 35: 63-75

Seinen W, Vos JG, Van Spanje I, Snoek M, Brands R, Hooykaas H (1977a) Toxicity of organotin compounds. II. Comparative in vivo and in vitro studies with various organotin and organolead compounds in different animal species with special emphasis on lymphocyte cytotoxicity. Toxicol Appl Pharmacol 42: 197-212

Seinen W, Vos JG, Van Krieken R, Penninks A, Brands R, Hooykaas H (1977b) Toxicity of organotin compounds. III. Suppression of thymus dependent immunity in rats by di-n-butyltindichloride and di-n-octyltindichloride. Toxicol Appl Pharmacol 42: 213-224

Seinen W, Penninks AH (1979) Immune suppression as a consequence of a selective cytotoxic activity of certain organometallic compounds on thymus and thymus-dependent lymphocytes. Ann N Y Acad Sci 320: 499-517

Sellins KS, Cohen JJ (1987) Gene induction by γ-irradiation leads to DNA fragmentation in lymphocytes. J Immunol 139: 3199-3206

Sellins KS, Cohen JJ (1991a) Hyperthermia induces apoptosis in thymocytes. Radiat Res 126: 88-95

Sellins KS, Cohen JJ (1991b) Cytotoxic T lymphocytes induce different types of DNA damage in target cells of different origins. J Immunol 147: 795-803

Selwyn MJ, Dawson AP, Stockdale M, Gains N (1970) Chloride-hydroxide exchange across mitochondrial, erythrocyte and artificial membranes mediated by trialkyl- and triphenyltin compounds. Eur J Biochem 14: 120-126

Selwyn MJ (1976) Triorganotin compounds as ionophores and inhibitors of ion translocating ATPases. In: Zuckermann JJ (ed) Organotin compounds: new chemistry and applications, American Chemical Society, Washington, pp 204-226

Sentman CL, Shutter JR, Hockenberry D, Kanagawa O, Korsmeyer SJ (1991) Bcl-2 inhibits multiple forms of apoptosis but not negative selection in thymocytes. Cell 67: 879-888

Server AC, Mobley WC (1991) Neuronal cell death and apoptosis. In: Tomei LD, Cope FO (eds) Apoptosis: The molecular basis of cell death, Cold Spring Harbor Laboratory Press, New York, pp 263-278

Servomaa K, Rytomaa T (1988) Suicidal death of rat chloroleukemia cells by activation of the long interspersed repetitive DNA element (*L1Rn*). Cell Tissue Kinet 21: 33-43

Shen W, Kamendulis LM, Ray SD, Corcoran GB (1992) Acetaminophen-induced cytotoxicity in cultured mouse hepatocytes: Effects of Ca^{2+}-endonuclease, DNA repair, and glutathione depletion inhibitors on DNA fragmentation and cell death. Toxicol Appl Pharmacol 112: 32-40

Shi Y, Sahai BM, Green DR (1989) Cyclosporin A inhibits activation-induced cell death in T-cell hybridomas and thymocytes. Nature 339: 625-626

Shi Y, Szalay, MG, Paskar L, Boyer M, Bhagirath S, Green DR (1990) Activation-induced cell death in T cell hybridomas is due to apoptosis. J Immunol 144: 3325-3333

Shimizu T, Kubota M, Tanizawa, A, Sano H, Kasai Y, Hashimoto H, Akiyama Y, Mikawa H (1990) Inhibition of both etoposide-induced DNA fragmentation and activation of poly(ADP-ribose) synthesis by zinc ion. Biochim Biophys Res Comm 169: 1172-1177

Skalka M, Matyasova J, Cejkova M (1976) DNA in chromatin of irradiated lymphoid tissues degrades in vivo into regular fragments. FEBS Lett 72: 271-274

Smeyne RJ, Vendrell M, Hayward M, Baker SJ, Miao GG, Schilling K, Robertson LM, Curran T, Morgan JI (1993) Continuous *c-fos* expression precedes programmed cell death in vivo. Nature 363: 166-169

Smialowicz RJ, Riddle MM, Rogers RR, Luebke RW, Copeland CB (1989) Immunotoxicity of tributyltin oxide in rats exposed as adults or pre-weanlings. Toxicology 57: 97-111

Smith CA, Williams GT, Kingston R, Jenkinson EJ, Owen JJT (1989) Antibodies to CD3/T-cell receptor immune complex induce death by apoptosis in immature T cells in thymic cultures. Nature 377: 181-184

Smith PJ, Bell SM, Dee A, Sykes H (1990) Involvement of DNA topoisomerase II in the selective resistance of a mammalian cell mutant to DNA minor groove ligands: ligand-induced DNA--protein crosslinking and responses to topoisomerase poisons. Carcinogenesis 11: 659-665

Snoeij NJ, Van Iersel AAJ, Penninks AH, Seinen W (1985) Toxicity of triorganotin compounds: comparative in vivo studies with a series of trialkyltin compounds and triphenyltin chloride in male rats. Toxicol Appl Pharmacol 81: 274-286

Snoeij NJ, Van Iersel AAJ, Penninks AH, Seinen W (1986a) Triorganotin-induced cytotoxicity to rat thymus, bone marrow and red blood cells as determined by several in vitro assays. Toxicology 39: 71-83

Snoeij NJ, Punt PM, Penninks AH, Seinen W (1986b) Effects of tri-n-butyltin chloride on energy metabolism, macromolecular synthesis, precursor uptake and cyclic AMP production in isolated rat thymocytes. Biochim Biophys Acta 852: 234-243

Snoeij NJ, Van Rooijen HJM, Penninks AH, Seinen W (1986c) Effects of various inhibitors of oxidative phosphorylation on energy metabolism, macromolecular synthesis and cyclic AMP production in isolated rat thymocytes. Biochim Biophys Acta 852: 244-253

Snoeij NJ (1987) Triorganotin compounds in immunotoxicology and biochemistry. PhD thesis, University of Utrecht

Snoeij NJ, Penninks AH, Seinen W (1987) Biological activity of organotin compounds—an overview. Environ Res 44: 335-353.

Snoeij NJ, Penninks AH, Seinen W (1988a) Dibutyltin and tributyltin compounds induce thymus atrophy in rats due to a selective action on thymic lymphoblasts. Int J Immunopharmac 10: 891-899

Snoeij NJ, Bol-Schoenmakers M, Penninks AH, Seinen W (1988b) Differential effects of tri-n-butyltin chloride on macromolecular synthesis and ATP levels of rat thymocytes obtained by centrifugal elutration. Int J Immunopharmac 10: 29-37

Snoeij NJ, Penninks AH, Seinen W (1989) Thymus atrophy and immunosuppression induced by organotin compounds. Arch Toxicol Suppl 13: 171-174

Snyder RD (1989) Polyamine depletion is associated with altered chromatin structure in HeLa cells. Biochem J 260: 697-704

Sorenson CM, Barry MA, Eastman A (1990) Analysis of the events associated with cell cycle arrest at G_2 phase and cell death induced by cisplatin. J Natl Cancer Inst 82: 749-754

Stefanski S, Elwell MR, Stromberg PC (1990) Spleen, lymph nodes and thymus. In: Boorman GA, Eustis SL, Elwell MR, Montgomery CA, MacKenzie FW (eds) Pathology of the Fischer Rat. Reference and Atlas, Academic Press, New York, pp 369-393.

Stokke T, Steen HB (1985) Multiple binding modes for Hoescht 33258 to DNA. J Histochem Cytochem 33: 333-338

Strasser A, Harris AW, Cory S (1991) *bcl-2* Transgene inhibits T cell death and perturbs thymic self-censorship. Cell 67: 889-899

Strickland D, Fraser MJ, Pittman S, Ireland C (1992) Altered expression of tubulin during apoptosis. Proc Am Assoc Cancer Res Annu Meet 33: 95

Sun XM, Cohen GM (1994) Mg^{2+}-dependent cleavage of DNA into kilobase pair fragments is responsible for the initial degradation of DNA in apoptosis. J Biol Chem 269: 14857-14860

Swat W, Ignatowicz L, Von Boehmer H, Kisielow P (1991) Clonal deletion of immature $CD4^{+}8^{+}$ thymocytes in suspension culture by extrathymic antigen-presenting cells. Nature 351: 150-153.

Syversen TLM, Sager PR, Clarkson TW, Cavanagh JB, Elgsaeter A, Guldberg HC, Lee SD, Lichtman MA, Mottet K, Olmsted JB (1984) The cytoskeleton as a target for toxic agents. In: Clarkson TW, Sager PR, Syversen TLM (eds) The cytoskeleton, a target for toxic agents, Plenum Press, New York, pp 25-34

T

Tan LP, Ng ML, Kumar Das VG (1978) The effect of trialkyltin compounds on tubulin polymerisation. J Neurochem 31: 1035-1041

Tanphaichitr N, Chalkley R (1976) Production of high levels of phosphorylated F-1 histone by zinc chloride. Biochemistry 15: 1610-1614.

Taylor MK, Cohen JJ (1992) Cell-mediated cytotoxicity. Curr Opin Immunol 4: 338-343

Taylor MV, Metcalfe JC, Hesketh TR, Smith GA, Moore JP (1984) Mitogens increase phosphorylation of phosphoinositides in thymocytes. Nature 312: 462-465

Telford WG, King LE, Fraker PJ (1991) Evaluation of glucocorticoid-induced DNA fragmentation in mouse thymocytes by flow cytometry. Cell Prolif 24: 447-459

Tempel KH, Ignatius A (1993) Toxicological studies with primary cultures of chick embryo cells: DNA fragmentation under the influence of DNase I-inhibitors. Arch Toxicol 67: 318-324

Thornthwaite JJ, Sugarbaker EO, Temple WJ (1980) Preparation of tissues for DNA flow cytometric analysis. Cytometry 1: 229-337

Timbrell JA (1991) Principles of biochemical toxicology, Taylor and Francis, London

Tomei LD (1991) Apoptosis: A program for death or survival? In: Tomei LD, Cope FO (eds) Apoptosis: The molecular basis of cell death, Cold Spring Harbor Laboratory Press, New York, pp 279-316

Traganos F, Darzynkiewicz Z, Sharpless T, Melamed MR (1977) Simultaneous staining of ribonucleic and deoxyribonucleic acids in unfixed cells using acridine orange in a flow cytofluorometric system. J Histochem Cytochem 25: 46-56

Trump BF, Berezesky IK, Osornio-Vargas AR (1981) Cell death and the disease process. The role of calcium. In: Bowen ID, Lockshin RA (eds) Cell death in biology and pathology, Chapman and Hall, London, p 209-242

Trump BF, Berezesky IK (1984) The role of sodium and calcium regulation in toxic cell injury. In: Mitchell JR, Homing MG (eds) Drug metabolism and drug toxicity, Raven Press, New York, pp 261-300

Trump BF, Berezesky IK (1992) The role of Ca^{2+} in cell injury, necrosis and apoptosis. Current Opinion in Cell Biology 4: 227-232

Truneh A, Albert F, Golstein P, Schmitt-Verhulst AM (1985) Early steps of lymphocyte activation bypassed by synergy between calcium ionophores and phorbol ester. Nature 313: 318-320

Tsien RY (1980) New calcium indicators with high selectivity against magnesium and protons: Design, synthesis and properties of prototype structures. Biochemistry 19: 2396-2404

Tsien RY (1981) A nondisruptive technique for loading calcium buffers and indicators into cells. Nature 290: 527-528

U

Umansky SR, Korol' BA, Nelipovich PA (1981) In vivo DNA degradation in thymocytes of irradiated or hydrocortisone-treated rats. Biochim Biophys Acta 655: 9-17

Umansky SR (1991) Apoptotic process in the radiation-induced death of lymphocytes. In: Tomei LD, Cope FO (eds) Apoptosis: The molecular basis of cell death, Cold Spring Harbor Laboratory Press, New York, pp 193-208

V

Vanderbilt JN, Bloom KS, Anderson JN (1982) Endogenous nuclease: Properties and effects on transcribed genes in chromatin. J Biol Chem 257: 13009-13017

Van der Kerk GJM, Luijten JGA (1954) Investigations of organotin compounds. III. The biocidal properties of organotin compounds. J Appl Chem 4: 314-319

Van der Kerk GJM (1976) Organotin chemistry: past, present and future. In: Zuckermann JJ (ed) Organotin compounds: new chemistry and applications, American Chemical Society, Washington, pp 1-25

Van Haelst U (1967) Light and electron microscope study of the normal and pathological thymus of the rat. II. Acute thymic involution. Z Zellforsch Mikrosk Anat 80: 153-182 (translation)

Van Loveren H, Schuurman HJ, Kampinga J, Vos JG (1991) Reversibility of thymic atrophy induced by 2,3,7,8-tetrachlorodibenzo-p-dioxin (TCDD) and bis(tri-n-butyltin) oxide (TBTO). Int J Immunopharmac 13: 369-377

Vedeckis WV, Bradshaw HD Jr. (1983) DNA fragmentation in S49 lymphoma cells killed with glucocorticoids and other agents. Mol Cell Endocrinol 30: 215-227

Verdier E, Virat M, Schweinfurth H, Descotes J (1991) Immunotoxicity of bis(tri-n-butyltin)oxide in the rat. J Toxicol Environ Health 32: 307-317

Verschuuren HG, Kroes R, Vink HH, Van Esch GJ (1966) Short-term toxicity studies with triphenyltin compounds in rats and guinea pigs. Food Cosmet Toxicol 4: 35-45

Verschuuren HG, Ruitenberg F, Peetoom F, Helleman PW, Van Esch GJ (1970) Influence of triphenyltin acetate on lymphatic tissue and immune responses in guinea pigs. Toxicol and Appl Pharmacol 16: 400-410

Volsen SG, Barrass N, Scott MP, Miller K (1989) Cellular and molecular effects of di-n-octyltin dichloride on the rat thymus. Int J Immunopharmac 11: 703-715

Voris BP, Young DA (1981) Glucocorticoid-induced proteins in rat thymus cells. J Biol Chem 256: 11319-11329

Vos JG, de Klerk A, Krajnc EI, Kruizinga W, Van Ommen B, Rozing J (1984a) Toxicity of bis(tri-n-butyltin)oxide in the rat II. Suppression of thymus-dependent immune responses and of parameters of nonspecific resistance after short-term exposure. Toxicol Appl Pharmacol 75: 387-408

Vos JG, Van Logten MJ, Kreeftenberg JG, Kruizinga W (1984b) Effect of triphenyltin hydroxide on the immune system of the rat. Toxicology 29: 325-336

Vos JG, Krajnc EI, Wester PW (1985) Immunotoxicity of bis(tri-n-butyltin)oxide. In: Dean JH, Luster MI, Munson AE, Amos H (eds) Immunotoxicity and immunopharmacology, Raven Press, New York, pp 327-340

Vos JG, Penninks AH (1987) Dioxin and organotin compounds as model immunotoxic chemicals. In: De Matteis F, Lock EA (eds) Selectivity and Molecular Mechanisms of Toxicity, Macmillan, London, pp 85-102

Vos JG, De Klerk A, Krajnc EI, Van Loveren H, Rozing J (1990) Immunotoxicity of bis(tri-n-butyltin)oxide in the rat: Effects on thymus-dependent immunity and on nonspecific resistance following long-term exposure in young versus aged rats. Toxicol and Appl Pharmacol 105: 144-155

W

Walker PR, Smith C, Youdale T, Leblanc J, Whitfield JF, Sikorska M (1991) Topoisomerase II-reactive chemotherapeutic drugs induce apoptosis in thymocytes. Cancer Res 51: 1078-1085

Waring P (1990) DNA fragmentation induced in macrophages by gliotoxin does not require protein synthesis and is preceded by raised inositol triphosphate levels. J Biol Chem 265: 14476-14480

Waring P, Egan M, Braithwaite A, Mullbacher A, Sjaarda A (1990) Apoptosis induced in macrophages and T blasts by the mycotoxin sporidesmin and protection by Zn^{2+} salts. Int J Immunopharmac 12: 445-447

Waring P, Kos FJ, Mullbacher A, (1991) Apoptosis or programmed cell death. Medicinal Res Rev 11: 219-236

Watanabe-Fukunaga R, Brannan CI, Copeland NG, Jenkins NA, Nagata S (1992) Lymphoproliferation disorder in mice explained by defects in Fas antigen that mediates apoptosis. Nature 356: 314-317

Watson PF, Morris GJ (1987) Cold shock injury in animal cells. In: Bowler K, Fuller BJ (eds) Temperature and animal cells, Society for Experimental Biology, Cambridge, pp 311-340

Wester PW, Krajnc EI, Van Leeuwen FXR, Loeber JG, Van der Heijden CA, Vaessen HAMG, Helleman PW (1990) Chronic toxicity and carcinogenicity of bis(tri-n-butyltin)oxide (TBTO) in the rat. Fd Chem Toxic 28: 179-196

WHO (1980) Tin and Organotin compounds. A preliminary review. Environmental Health Criteria 15, WHO, Geneva

Widom J, Baldwin RL (1980) Cation-induced toroidal condensation of DNA. Studies with $Co^{3+}(NH_3)_6$. J Mol Biol 144: 431-453

Wielckens K, Delfs T (1986) Glucocorticoid-induced cell death and poly[adenosine diphosphate (ADP)-ribosyl]ation: Increased toxicity of dexamethasone on mouse S49.1 lymphoma cells with the poly(ADP-ribosyl)ation inhibitor benzamide. Endocrinology 119: 2383-2392

Wielckens K, Delfs T, Muth A, Freese V, Kleeberg H (1987) Glucocorticoid-induced lymphoma cell death: The good and the evil. J Steroid Biochem 27: 413-419

Wilcock C, Chahwala SB, Hickman JA (1988) Selective inhibition by bis(2-chloroethyl)methylamine (nitrogen mustard) of the $Na^+/K^+/Cl^-$ cotransporter of murine L1210 leukemia cells. Biochim Biophys Acta 946: 368-378

Williams GT, Smith CA, Spooncer E, Dexter TM, Taylor DR (1990) Haemopoietic colony stimulating factors promote cell survival by suppressing apoptosis. Nature 343: 76-79

Williams JR, Little JB, Shipley WU (1974) Association of mammalian cell death with a specific endonucleolytic degradation of DNA. Nature 252: 754-755

Wood AC, Waters CM, Garner A, Hickman JA (1994) Changes in c-myc expression and the kinetics of dexamethasone-induced programmed cell death (apoptosis) in human lymphoid leukemia cells. Br J Cancer 69: 663-669

Woynarowski JM, Sigmund RD, Beerman TA (1989) DNA minor groove binding agents interfere with topoisomerase II mediated lesions induced by epipodophyllotoxin derivative VM-26 and acridine derivative m-AMSA in nuclei from L1210 cells. Biochemistry 28: 3850-3855

Wulf RG, Byington KH (1975) On the structure-activity relationships and mechanism of organotin induced, nonenergy dependent swelling of liver mitochondria. Arch Biochem Biophys 167: 176-185

Wyllie AH (1980) Glucocorticoid-induced thymocyte apoptosis is associated with endogenous endonuclease activation. Nature 284: 555-556

Wyllie AH, Kerr JFR, Currie AR (1980) Cell death: the significance of apoptosis. Int Rev Cytol 68: 251-306

Wyllie AH (1981) Cell death: a new classification separating apoptosis from necrosis. In: Bowen ID, Lockshin RA (eds) Cell death in biology and pathology, Chapman and Hall, London, pp 9-34

Wyllie AH, Morris RG (1982) Hormone induced cell death: Purification and properties of thymocytes undergoing apoptosis after glucocorticoid treatment. Am J Pathol 109: 78-87

Wyllie AH, Morris RG, Smith AL, Dunlop D (1984a) Chromatin cleavage in apoptosis: association with condensed chromatin morphology and dependence on macromolecular synthesis. J Pathol 142: 67-77

Wyllie AH, Duvall E, Blow JJ (1984b) Intracellular mechanisms in cell death in normal and pathological tissues. In: Davies I, Sigee DC (eds) Cell Ageing and Cell Death, Cambridge University Press, Cambridge, pp 269-294

Wyllie AH (1985) The biology of cell death in tumours. Anticancer Res 5: 131-136

Wyllie AH (1986) What is apoptosis? Histopathology 10: 995-998

Wyllie AH, Morris RG, Arends MJ (1986) Nuclease activation in programmed cell death. In: Clayton RM, Truman DES (eds) Co-ordinated regulation of gene expression, Plenum Press, London, pp 33-44

Wyllie AH (1987a) Apoptosis: Cell death in tissue regulation. J Pathol 153: 313-316

Wyllie AH (1987b) Apoptosis: Cell death under homeostatic control. Arch Toxicol Suppl 11: 3-10

Wyllie AH, Walker SW, Evans I, Hogg RM, Milner SW, Morris RG (1988) Purification of an endonuclease implicated in thymocyte apoptosis. J Pathol 155: 348

Wyllie AH (1992) Apoptosis and the regulation of cell numbers in normal and neoplastic tissues: an overview. Cancer Metastasis Rev 11: 95-103

Y

Yamada T, Ohyama H, Kinjo Y, Watanabe M (1981) Evidence for the internucleosomal breakage of chromatin in rat thymocytes irradiated in vitro. Radiat Res 85: 544-553

Yallapragada PR, Vig PJS, Desaiah D (1990) Differential effects of triorganotins on calmodulin activity. J Toxicol Environ Health 29: 317-327

Yallapragada PR, Vig PJS, Kodavanti PRS, Desaiah D (1991) In vivo effects of triorganotins on calmodulin activity in rat brain. J Toxicol Environ Health 34: 229-237

Young JDE, Liu CC (1988) Multiple mechanisms of lymphocyte-mediated killing. Immunol Today 5: 140-144

Yuan J, Shaham S, Ledoux S, Ellis HM, Horvitz HR (1993) The *C.elegans* cell death gene *ced-3* encodes a protein similar to mammalian interleukin-1-β-converting enzyme. Cell 75: 641-652

Z

Zhang H, Liu AYC (1992) Tributyltin is a potent inducer of the heat shock response in human diploid fibroblasts. J Cell Physiol 153: 460-466

Zheng LM, Zychlinsky A, Liu C, Ojcius DM, Young JD (1991) Extracellular ATP as a trigger for apoptosis or programmed cell death. J Cell Biol 112: 279-288

Zhivotovsky B, Nicotera P, Bellomo G, Hanson K, Orrenius S (1993) Ca^{2+} and endonuclease activation in radiation-induced lymphoid cell death. Exp Cell Res 207: 163-170

Zimmer C, Wahnert U (1986) Nonintercalating DNA-binding ligands: specificity of the interaction and their use as tools in biophysical, biochemical and biological investigations of genetic material. Prog Biophys Mol Biol 47: 31-112

Zubiaga AM, Munoz E, Huber BT (1992) IL-4 and Il-2 selectively rescue T_h cell subsets from glucocorticoid-induced apoptosis. J Immunol 149: 107-112

Zucker RM, Elstein KH, Easterling RE, Ting-Beall HP, Allis JW, Massaro EJ (1988) Effects of tributyltin on biomembranes: Alteration of flow cytometric parameters and inhibition of Na^+/K^+-ATPase two-dimensional crystallisation. Toxicol Appl Pharmacol 96: 393-403

Zucker RM, Elstein KH, Easterling RE, Massaro EJ (1989) Flow cytometric comparison of the effects of trialkyltins on the murine erythroleukemic cell. Toxicology 58: 107-119

Zucker RM, Massaro EJ, Elstein KH (1992) The reversibility of tributyltin-induced toxicity in vitro as a function of concentration and duration of exposure (C x T). Environ Res 57: 107-116

Zucker RM, Elstein KH, Thomas DJ, Rogers JM (1994) Tributyltin and dexamethasone induce apoptosis in rat thymocytes by mutually antagonistic mechanisms. Toxicol Appl Pharmacol 127: 163-170

Zwelling LA, Chan D, Hinds M, Mayes J, Silberman LE, Blick M (1988) Effect of phorbol ester treatment on drug-induced, topoisomerase II-mediated DNA cleavage in human leukemia cells. Cancer Res 48: 6625-6633

Zychlinsky A, Zheng LM, Liu C, Young JD (1991) Cytolytic lymphocytes induce both apoptosis and necrosis in target cells. J Immunol 146: 393-400

APPENDIX

Formulation and physico-chemical characteristics of media

RPMI-1640	g/l		g/l
Sodium chloride	6.000	L-Arginine (free base)	0.200
Potassium chloride	0.400	L-Asparagine (anhydrous)	0.050
Magnesium sulphate		L-Aspartic acid	0.020
(anhydrous)	0.04884	L-Cystine dihydrochloride	0.0652
Sodium hydrogen carbonate	2.000	L-Glutamic acid	0.020
Calcium nitrate	0.100	L-Glutamine	0.300
Sodium phosphate dibasic		Glycine	0.010
(anhydrous)	0.400	L-Histidine (free base)	0.015
		Hydroxy-L-proline	0.020
D-Biotin	0.0002	L-Isoleucine	0.050
Choline chloride	0.003	L-Leucine	0.050
Folic acid	0.001	L-Lysine hydrochloride	0.040
myo-Inositol	0.035	L-Methionine	0.015
Niacinamide	0.001	L-Phenylalanine	0.015
p-Aminobenzoic acid	0.001	L-Proline	0.020
D-Pantothenic acid	0.00025	L-Serine	0.030
Pyridoxine hydrochloride	0.001	L-Threonine	0.020
Riboflavin	0.0002	L-Tryptophan	0.005
Thiamine hydrochloride	0.001	L-Tyrosine, sodium salt	
Vitamin B12	0.000005	(dihydrate)	0.02883
		L-Valine	0.020
D-Glucose	2.000		
Glutathione (reduced form)	0.001		
Phenol red, sodium salt	0.0053		
pH at 25°C	7.3±0.3		
Osmolality (mOsm/kg H_2O)	279±5%		

A statement was received from the supplier to the effect that zinc ion was not present as an intentional ingredient in the formulation.

DMEM	g/l		g/l
Sodium chloride	6.400	L-Arginine hydrochloride	0.084
Potassium chloride	0.400	L-Cystine dihydrochloride	0.0604
Magnesium sulphate		L-Glutamine	0.584
(heptahydrate)	0.200	Glycine	0.030
Sodium hydrogen carbonate	3.700	L-Histidine hydrochloride	0.042
Calcium chloride (dihydrate)	0.265	L-Isoleucine	0.105
Sodium phosphate dibasic		L-Leucine	0.105
(dihydrate)	0.141	L-Lysine hydrochloride	0.146
Ferrous nitrate (nonahydrate)	0.0001	L-Methionine	0.030
		L-Phenylalanine	0.066
Choline chloride	0.004	L-Serine	0.042
Folic acid	0.004	L-Threonine	0.095
myo-Inositol	0.007	L-Tryptophan	0.016
Niacinamide	0.004	L-Tyrosine, sodium salt	
D-Calcium pantothenoate	0.004	(dihydrate)	0.089
Pyridoxine hydrochloride	0.004	L-Valine	0.094
Riboflavin	0.0004		
D-Glucose	4.500		
Glutathione (reduced form)	0.001		
Phenol red	0.015		
Sodium pyruvate	0.110		
pH at 25°C	7.3±0.3		
Osmolality (mOsm/kg H_2O)	330±5%		

A statement was received from the supplier to the effect that zinc ion was not present as an intentional ingredient in the formulation.